

INVESTIGATIONS  
OF  
FLOW THROUGH BOILER SPACES AND TUBE BANKS  
WITH  
SPECIAL REGARD TO THE INFLUENCE  
OF  
SECOND ROW TUBES.

ProQuest Number: 13850444

All rights reserved

INFORMATION TO ALL USERS

The quality of this reproduction is dependent upon the quality of the copy submitted.

In the unlikely event that the author did not send a complete manuscript and there are missing pages, these will be noted. Also, if material had to be removed, a note will indicate the deletion.



ProQuest 13850444

Published by ProQuest LLC (2019). Copyright of the Dissertation is held by the Author.

All rights reserved.

This work is protected against unauthorized copying under Title 17, United States Code  
Microform Edition © ProQuest LLC.

ProQuest LLC.  
789 East Eisenhower Parkway  
P.O. Box 1346  
Ann Arbor, MI 48106 – 1346

PREFACE.  
BY PROFESSOR WILLIAM KERR.

Mr. Mohamed entered upon the official period of his Research Studentship in May, 1942, but for some months before that he was associated with a confidential inquiry into certain boiler tube failures. These failures occurred only in the second row tubes of a large four row bank and in this respect, and in their rapid development, they presented striking and unusual features.

The thesis which Mr. Mohamed is presenting derives from the investigation of these tube troubles. The explanation originally advanced was based on the idea, supported by published small scale experimental work on the flow across tube arrangements, that the conditions around the second row elements were exceptional. In an actual boiler, however, the flow is not purely transverse; the angle of attack varies widely; and the baffle arrangements confuse the conditions considerably.

It was thought desirable to study the second row effects more thoroughly and Mr. Mohamed took up this line of investigation after completing the work he had been doing on behalf of the inquiry. His thesis presents the results of his various investigations.

In Section I. an account is given of the boiler tube failures, and in the preparation of this Mr. Mohamed has, of course, had the advantage of access to the confidential report on the problem. He has, however, arranged the treatment in his own way and kept it as clear and straightforward as possible by leaving out a good deal of confusing detail and by extending the discussion on the experimental side somewhat.

His main experimental work is presented in Section II. and deals in succession with water tank, wind tunnel and high speed trunk investigations. In all these cases, a great deal of preliminary work was done which is not included. The water tank work was undertaken mainly to obtain the best possible photographic results for second row actions in cross flow. The wind tunnel experiments allowed of the study of inclined tube bank models with and without baffles. The small trunk apparatus was specially designed by Mr. Mohamed so that higher speeds of flow could be used.

All this experimental work was done at a time of considerable departmental difficulty when the assistance possible both in the preparation of apparatus and in the running of tests was slight. Mr. Mohamed had frequently to make, erect and adjust gear and run experiments without help, and his indefatigable efforts as an investigator are worthy of special remark.

The second row features established by the experimental work led Mr. Mohamed to adopt a suggestion to study the pressure distributions given theoretically by ideal two-dimensional flow analysis. The results of this intensely laborious work are given in Section III. It is shown that this line of attack does not explain the phenomena, but it thereby gives added value to the conclusion reached that the uniqueness of the second row in staggered arrangements is due to the wake vortices of the first.

It had been Mr. Mohamed's intention to carry the subject further and enter upon an investigation into the friction and heat transmission aspects of the problem but time has not permitted of more than a start on this by the examination of lift and drag forces on the models and some friction loss measurements. What has been done in these directions has been given in appendices while others show the wide range of experimental data and theoretical calculation by tabulation.

The thesis represents an interesting combination of an engineering inquiry, fundamental experiment and theoretical analysis carried out under conditions of difficulty not the least of which is perhaps that the author has had to write in what is, to him, a foreign language.

Department of Civil & Mechanical Engineering & Applied Mechanics  
The Royal Technical College,  
Glasgow.

CONTENTS.PAGE.

PREFACE .....	BY PROFESSOR WILLIAM KERR.	ii
<u>SECTION I.</u>	<u>BOILER TUBE FAILURES.</u>	1
<u>PART I.</u>	<u>CHARACTERISTICS OF FAILURES.</u>	1
(a)	Arrangement of Tubes .....	1
(b)	The First Failure .....	1
(c)	Subsequent Failures .....	5
(d)	General Features of Failures.....	7
<u>PART 2.</u>	<u>EXAMINATION OF TUBES.</u>	8
(a)	Conditions of Materials .....	8
(b)	External Slags .....	9
(c)	Internal Scales .....	10
(d)	Summary of Conditions .....	10
<u>PART 3.</u>	<u>CONSIDERATION OF SECOND ROW EFFECTS.</u>	12
(a)	Significance of the Second Row .....	12
(b)	Cross Flow Conditions .....	13
(c)	Second Row in Cross Flow .....	13
<u>PART 4.</u>	<u>EXPLANATION OF FAILURES.</u>	17
(a)	The Slagging Conditions .....	17
(b)	The Wall Effects .....	17
(c)	The Internal Effects .....	18
<u>SECTION II.</u>	<u>EXPERIMENTAL FLOW INVESTIGATION.</u>	20
<u>PART I.</u>	<u>INTRODUCTORY.</u>	20
(a)	Aim of Experiments .....	20
(b)	Experimental Plan .....	21
<u>PART 2.</u>	<u>WATER TANK EXPERIMENTS.</u>	23
(a)	Previous Methods .....	23
(b)	Small Tank Arrangement .....	23
(c)	Large Tank Arrangement .....	26
(d)	Photographic Results .....	26
(e)	The Second Row Enlargement .....	32
<u>PART 3.</u>	/	

	<u>PAGE.</u>
<u>PART 3.</u> <u>WIND TUNNEL EXPERIMENTS.</u> .....	39
(a) Experimental Lay-out. ....	39
(b) Range and Procedure .....	43
(c) Influence of Position .....	46
(d) Influence of Setting .....	46
(e) Influence of Baffles .....	47
(f) Experimental Results .....	48
(g) Discussion of Results .....	49
(h) Features of Second Row Curves .....	57
 <u>PART 4.</u> <u>SMALL HIGH SPEED TRUNK EXPERIMENT.</u> ...	 64
(a) Description of Plant .....	64
(b) Single Tube Readings .....	71
(c) Multi Tube Readings .....	71
(d) Angled Tube Readings .....	73
(e) Smoke Tests .....	78
(f) Discussion of Results .....	82
 <u>SECTION III. HYDRODYNAMIC ANALYSIS.</u> .....	 89
 <u>PART I.</u> <u>INTRODUCTORY</u> .....	 89
(a) Purpose of Analysis .....	89
(b) Ideal Flow across Single Tube .....	90
 <u>PART 2.</u> <u>SINGLE ROW CASE.</u> .....	 93
(a) Flow across Limited Single Row .....	93
(b) Calculations and Collected Results ....	94
(c) Contrast with Experimental Curve .....	94
 <u>PART 3.</u> <u>DOUBLE ROW CASE.</u> .....	 97
(a) Extension of Theory for Two Rows .....	97
(b) Calculation and Collected Results .....	97
(c) Contrast with Experimental Curves .....	100
 <u>PART 4.</u> <u>THREE AND FOUR ROW CASES.</u> .....	 102
(a) Further Extensions of Formula .....	102
(b) Calculations and Collected Results ....	102
(c) Contrast with Experimental Curves .....	102
 <u>PART 5.</u> <u>INFLUENCE OF WAKE VORTICES.</u> .....	 112
(a) Turbulent Action in Wake Vortices .....	112
(b) Features of Vortex Pairs .....	114
(c) Change of Strength in Wake Vortices ...	114
 <u>ACKNOWLEDGEMENT.</u> .....	 115

	<u>PAGE.</u>
<u>APPENDIX - I.</u>	117
Wind Tunnel Experiments for Lift and Drag on Bank of Tubes.	
<u>APPENDIX - II.</u>	130
Resistance to Stream Flow through Tube Banks and Friction Measurement.	
<u>APPENDIX - III.</u>	135
Tabulated Results of Wind Tunnel Experiments.	
<u>APPENDIX - IV.</u>	154
Tabulated Results of Small High Speed Trunk Tests.	
<u>BIBLIOGRAPHY .</u>	168
List of References:	

SECTION I.

# SECTION I - BOILER TUBE FAILURES.

## PART 1 - CHARACTERISTICS OF FAILURES.

- (a) Arrangement of Tubes : The tube bank in the boiler was arranged as shown in the pictorial sketch, Plate No.1, which gives an impression of the scheme of baffles and the general direction of flow of the gases. The manner in which the tubes are pitched is shown in Plate No.2, Fig.1.

The boiler generates steam at about 450°F, the superheater raising the final temperature to about 825°F. All failures, however, were in the screen bank where the lower temperatures would apply.

The screen bank tubes are in four rows of 48 tubes per row, see Plate No.2, Fig.1, and were  $2\frac{1}{4}$  ins. external diameter, No.7 L.S.G. thickness. They were bent to a large radius in the upper portion of their length. All failures took place in second row tubes and below the bend.

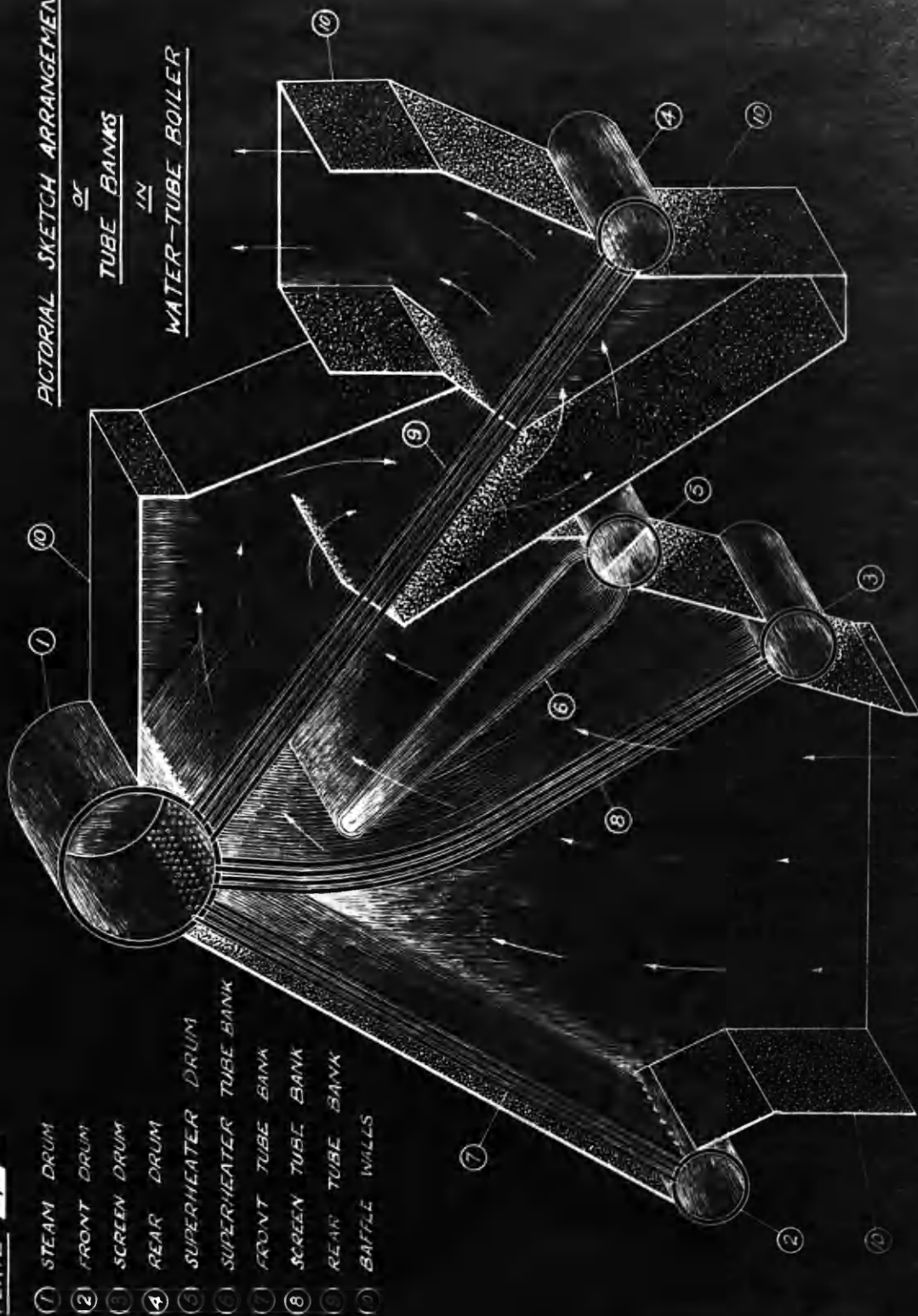
- (b) The First Failure : The first failure occurred in the second tube of the second row a short time after the boiler went into service. The perforation took place at the lower end of the bend. It was also found at this time that the first tube of the row was badly corroded.

The perforation occurred on the front of the tube. An attempt was made in Plate No.3 to picture the conditions. The hole is in the centre of an area of severe working on the inside. This area shows signs of violent action and rapid corrosion. General corrosion is fairly marked over the length below and above the perforation. It starts at the terminus of the length of rough internal scale which is especially heavy in the front inside and tapers to a thin deposit on the rear.

The scale deposit gave an eccentric bore and a rough surface at the approach to the area near the perforation. At the other places on the tube the scale was thin.

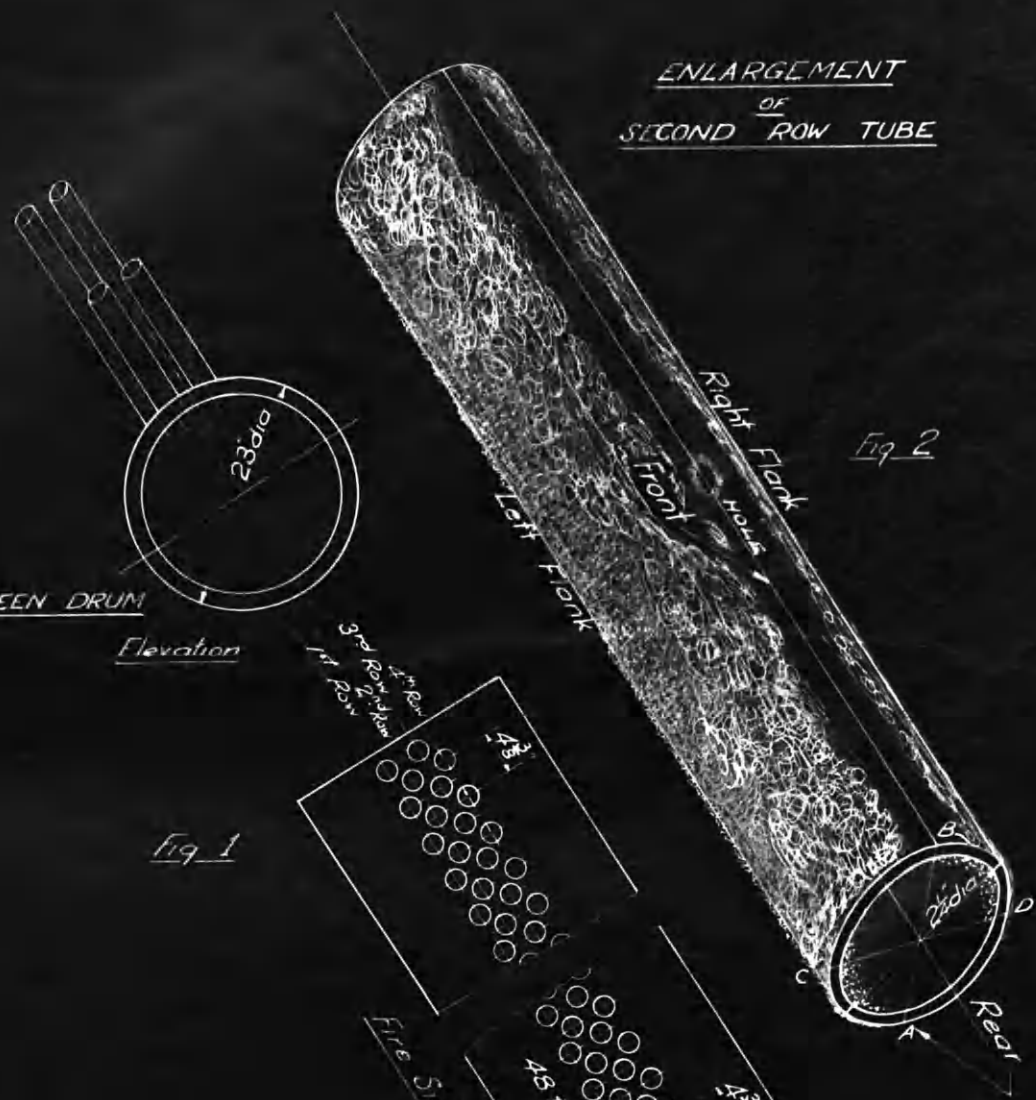
Externally the conditions were peculiar. A narrow band along the front in which the perforation occurred and in which the internal scaling was permanent, was clear and/

PICTORIAL SKETCH ARRANGEMENT  
OF  
TUBE BANKS  
IN  
WATER-TUBE BOILER



ENLARGEMENT  
OF  
SECOND ROW TUBE

Fig 2



SCREEN DRUM

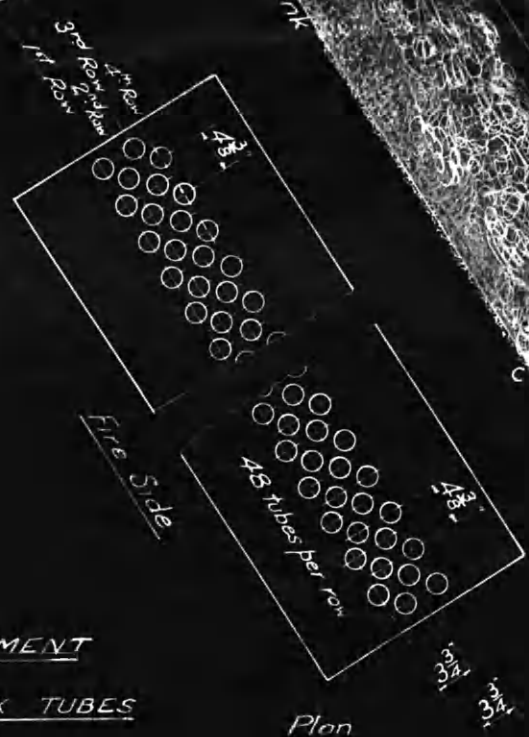
Elevation



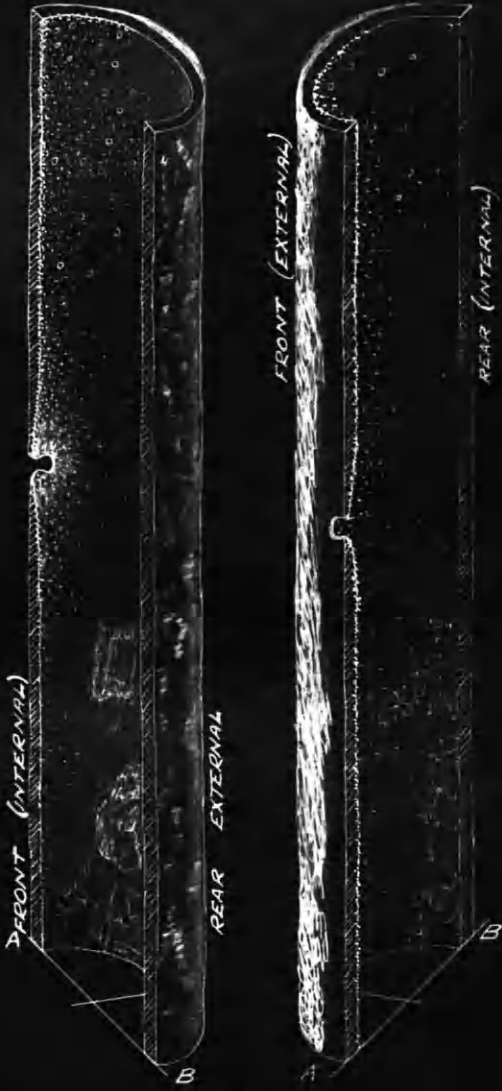
Fig 1

ARRANGEMENT  
OF  
SCREEN BANK TUBES

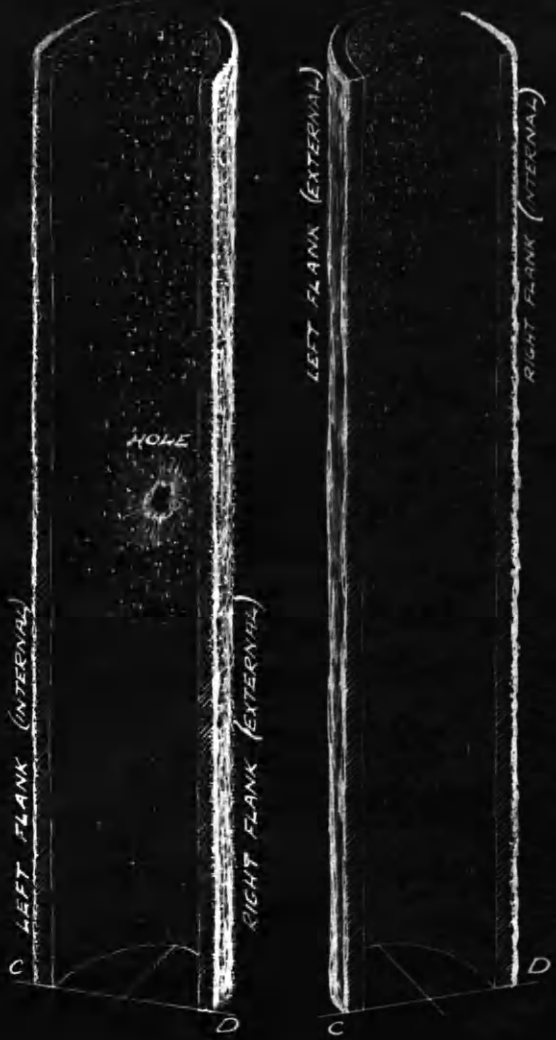
Plan



PICTORIAL SKETCH  
OF  
2<sup>ND</sup> ROW TUBE FAILURES



SECTION AT AB



SECTION AT CD

INTERNAL

-  SCALE
-  CORROSION
-  MAGNETITE

EXTERNAL

-  SCALE
-  FLAKY COATING
-  POWDERY DEPOSIT

/and free from slag deposit. At a short distance round from the front slag formation started. This continued right round but attained considerable thickness on the lateral diameter. The general appearance, therefore, was of clear metal on the front and slag bulges on the flanks. In the vicinity of the perforated part the slag was hard, rough and strongly adherent.

Stereo-photographs were taken of the inside area around the hole and gave a very clear impression of the violent corrosive action that had taken place. The form and marking gave the idea of a vortex swirling around the perforation as centre. By cutting longitudinally the effect of the corrosion on the thickness could be gauged. In the region of the hole it was less than 1/16 in. thick. Above the corrosion pit the metal thickened slowly to normal in a length of about 6 in. while below the centre it tapered more quickly.

Samples from a tube of the front row of the bank close to the perforated tube of the second row, showed a fairly similar external condition but not so acute. There was slag all round, heavier on the sides than on the front and patchy on rear. Internally there was a layer of scale all round.

A part of the burst tube, cut from a position well below the point of failure, showed external condition much the same as at the holed part but the front was broader. The layer of scale inside was thin and uniform.

- (c) Subsequent Failures : The second failure was in the third tube of the second row at the left hand end. There were two perforations in this case at roughly the same level as in the first case. The conditions are pictured in Plate No.4, Fig.1, and the general features are closely similar to what has been described.

The failure was followed by another in the first tube of the second row at the same end. The perforation here was more of the order of a rupture over a weakened length but was as broad and at the centre of a deeply corroded part. This case is represented on Plate No.4, Fig.2.

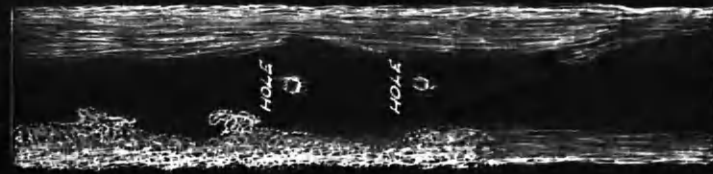
At the same time a slight depression was found at a point on the tenth tube of the second row and on removal was found to be coincident with a corroded part inside. It was clear that a failure had been developing. Again the narrow clear band of metal on the front was to be seen.

2ND ROW TUBES

Fig 1 2<sup>ND</sup> Failure



SECTIONAL ELEV

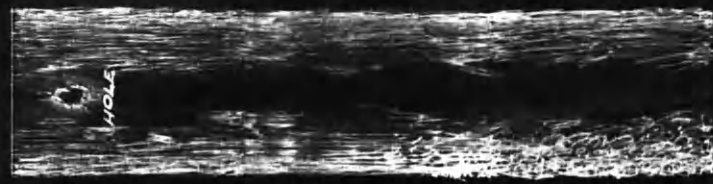


FRONT ELEV

Fig 2 3<sup>RD</sup> Failure



SECTIONAL ELEV



FRONT ELEV



Further failures occurred on the sixth tube at the left hand of the second row and the tenth tube from the other end, but, as these showed the same features as the previous case, they were not specially investigated.

- (d) General Features of the Failures : The main aspect of these failures are striking. All occurred in second row tubes and all in tubes placed within a quarter of the boiler length from the ends.

In every case the perforation was at the centre of a corroded part which appeared to have developed rapidly. It was exactly on the tubes' front centre line and in a narrow band of metal practically free from external slag.

On the flanks of the tubes and starting a little way round from the hole, the slagging was relatively heavy, creating what were in effect side bulges. Slag might or might not be prominent on the rear surfaces.

Internally the corroded part was relatively small and deep. It was always on the front of the tubes and the wastages of metal tapered off fairly rapidly above and below. Below the corrosion zone there was a definite scaled area which was particularly heavy on the front.

Below the corrosion zone internally the tube bore was made eccentric by the scaling, with the maximum thickness on the front. In the vicinity of perforation the tubes external form was made oval by the slag concentrations on the flanks.

These features were all very marked where actual failure took place. In general, similar conditions were shown by second row tubes and, in a less well defined fashion, by tubes of the other rows. But although scale could be drawn from other tubes, there was no case of failure in any but the second row tubes, and no case of failure at all except when there was a narrow clear band on the front with slag bulges on the sides and with the perforation in the centre of the clear front area.

PART 2 - EXAMINATION OF TUBES.

- (a) Conditions of Materials : The usual mechanical tests were made on the tube material, showing yield and maximum tensile stress, elongation, percentage and impact value. The properties of the material were all that could be expected and very uniform showing that the material at failure, whether scaled or corroded, was not in any way different from elsewhere.

Hounsfield specimens were used. These being obtained from very small specimens are generally somewhat different from what would be given by tests on a full scale machine, but they provide consistent results of sound guidance and are competent in showing up any serious differences. The results were in good agreement with the requirements of B.S.S. No.512 - 1934, if some allowance is made for scale effect.

Impact specimens were tested. These were 1/8 in. square and were notched 1/32 in. deep by fine saw cuts. The tests were carried out on a light type of Izod machine of 20 in.lb. capacity for which the 1/8 in. square specimens have been found suitable.

For the metallurgical examination, pieces were cut from the middle section of the defective tube and submitted to microscopical examination. In no case was the steel found to be dirty or suffering from any defect such as overheating, although, as would be expected, the outer front side of the tube was decarbonized to a small extent. The tubes were made of low carbon steel and showed direction of working, a feature characteristic of such material.

The inner surfaces of the tubes were, in general, marked by slight uniform pitting. In none of these cases, however, could severe corrosion have developed quickly and, if judged by those above, the life of the tubes should have been of many years duration. The scale of magnetic oxide was dense and adherent.

In the zones of marked corrosion where failures actually occurred the conditions were different. There was here a loose scale slightly adherent and porous. At the edge of the metal, beside a perforation, the microscope examination showed loss of carbon. This suggests that/

/that hydrogen had perforated the porous scale. Steam would probably accelerate the oxidation acting on the iron to give hydrogen and successive oxidation and reductions would help to keep the scale porous.

The cause of these local areas of corrosion does not, therefore, be in the quality of the steel but in some external factor, causing an abnormal type of scale and so permitting severe attack on the metal.

The metallurgical investigations support the mechanical tests to the effect that the metal has not been at fault initially and has not deteriorated in use. Besides this, there is no sure proof of overheating.

- (b) External Slags : The slags were fully analysed. The main constituents were ferrous and ferric iron, aluminium, calcium, magnesium, sodium sulphate, phosphate and ash. These were present in all. The main constituents were present but varied somewhat between the samples.

All samples gave an acid reaction although in varying degrees. This is attributed to the use of a coal rich in sulphur relative to alkalies.

The softening temperatures of various slags were determined. A soft micro-crystalline slag from the rear part of a tube began to soften at  $780^{\circ}\text{C}$ . This represents the softening temperature of impure sodium sulphate. A fused slag from another tube commenced to soften at  $1150^{\circ}\text{C}$ , but it cannot be expected that an already fused slag will again soften at the original temperature.

The slag attack on the metal was in no place serious. In the rear slags, numerous small patches of magnetite and ferric oxide occurred at the tube-slag interface. In the corresponding position on the tube, small black patches containing sulphide and magnetite were found. This type of attack is quickly credited to sodium sulphate and it is necessary then to assume that the particles removed fused long enough to react with the metal. A temperature of  $800^{\circ}\text{C}$  would, therefore, be required to soften the slag.

Due to radiation effect and to the internal scale, fire side temperatures would seemingly be somewhat higher and consequently oxidation attacks by fused sulphate had to be expected.

But the presence of sodium pyrosulphate/

/pyrosulphate provides an alternative explanation. This melts at  $400^{\circ}\text{C}$  and by reversal of reaction begins to liberate  $\text{SO}_3$  at  $460^{\circ}\text{C}$  and up to  $700^{\circ}\text{C}$ . Consequently, with fluctuating temperatures and changing concentrated  $\text{SO}_3$  in the gases, there would be alternate absorption and liberation of this in the range of  $460^{\circ}$  to  $700^{\circ}\text{C}$ . It is suggested that the slag attack is due to  $\text{SO}_3$  at the point of liberation and experiment showed that iron can be attacked by fused pyrosulphate at a little above  $460^{\circ}\text{C}$ . This would seem to be the minimum temperature possible.

Some of the slags showed various colourings. These were probably due to the action of moisture, or when water was sprayed on the acid slag from a perforation. The cause of the probable reactions is not clear but some of the colour coatings are consistent with a temperature of about  $500^{\circ}\text{C}$ .

- (c) Internal Scales : Fairly complete analysis of water samples from boiler, condenser and make-up supply was made and served to show that the feed water generally contained a slight margin of alkalinity, whilst the boiler water was different in alkalinity. The boiler water was, therefore, slightly corrosive.

Examination of the internal scale was made. To establish the connection between magnesium salts in the water and the corrosion produced, samples of the magnetite from the tubes were examined for the  $\text{CaO}/\text{MgO}$  ratios and observations showed that the magnesium salts were associated with the production of the corrosion product.

The scale generally could be classified as of two distinct types. The first was extensive, uniform and crystalline with hard, smooth magnetite next the tube and indicating uniform general corrosion below. This corrosion varied in degree from tube to tube.

The second was a rough irregular scale having thin patches of calcium sulphate crystals over magnetite and much exposed magnetite of irregular thickness and soft texture. This type is intimately associated with deep pitting and perforation of the tubes.

- (d) Summary of Conditions : It has been proved, both by mechanical tests and by metallurgical investigation, that the material of the tubes was sound and, apart from slight evidence of a/

/a minor degree of overheating on the front side of the parts perforated, not severely tried by the service conditions.

It appeared, as the result of analysis, that the boiler water possessed both scale forming and corrosive properties.

The study made of the slags indicated the use of a fuel fairly rich in sulphur and there was slight evidence of attack on the metal due to fusion of the slag. This was not serious and was mainly important as a pointer to temperature conditions.

The internal scales were of two types, one being of uniform and hard characteristics with general corrosion beneath, the other of rough texture with soft exposed magnetite. The latter is invariably associated with severe corrosion and perforation.

The study of slags and scales showed up the clear relationship between the inside scale and the clear areas externally on the tube front. It was deduced by chemical studies that the internal scaling and corrosion in the failure areas occurred simultaneously.

These characteristic slag, scale and corrosive features accompanied failures of the second row tubes. The slag was in heavy deposits on the flanks, while the corrosion and perforation were on the front. The scale in the zones of failure was of a particular type and present in quantity. Examination of parts where no failure occurred showed that one or more of these features was absent or modified.

PART 3 - CONSIDERATION OF SECOND ROW EFFECTS.

- (a) Significance of the Second Row : The previous sections have dealt with those aspects of the evidence that allowed investigation by tests and chemical analysis, but the detailed consideration of materials, slags, water and scales as substances involved in the failures, rather hide the more general and striking features of the trouble. Obviously, as the facts stand, they might apply to any tubes under the action of the same boiler water and boiler gases at similar conditions, but actual destruction has been confined to the second row tubes only. This demands particular attention.

The first row which normally one would expect to be the more severely tried is, in fact, only mildly affected. The signs of the same disease are not altogether absent but are definitely much less severe. Similarly with the other rows except the second. They are practically clear of the trouble.

In any consideration of a special significance attached to the second row, the feature of radiation effects naturally present themselves. But we reach at once the conclusion that the first row is at least equally liable and if radiation was the main cause, the inside rows of the front bank might be expected to show up to even greater disadvantage, since a large proportion of their duty will probably depend on their radiant heat absorbing powers.

Possibly the bend in the screen bank tubes may give special significance to the radiation factor over a length below the bend, where, in fact, the failures have occurred, but there is nothing in this point of view that can establish the second row as more liable to trouble than the first. It might be permissible to assume that the first and second rows were more prone to trouble than the other rows since their frontal pressures are higher, but this fails to meet the facts completely.

Attention must, therefore, be directed to the gas flow conditions. In general there will be a considerable longitudinal component of velocity. If the flow was wholly axial all the tubes in the group would be performing practically the same duty and the first two rows would be special only on account of radiation effects. But equally/

/equally strong radiation affects the front bank tubes where convection heating by axial flow will occur, and no failures occurred there. Consequently, no guidance of any value is obtained by consideration of this type of flow.

- (b) Cross Flow Conditions : Consideration of the arrangement gives the impression of strong cross flow in places. They would never be entirely free from axial components but these might, in certain rows, be low. The rush of gases from the combustion chamber would seem, naturally, to be mainly across the tubes at about the middle of the length. In particular this might be most marked towards the boiler ends where the longitudinal flow would probably be less active. This point of view gives the idea of strong cross currents near the middle of the tubes and towards the ends of the rows, and these are the places of failure in the second row tubes.

Examination of the characteristics of cross flow in staggered tube arrangement brings out a peculiar feature. The main work available for guidance is that by Wallis and White.<sup>(53)</sup> These investigators established the pressure variations all around the various tube walls in nests of tubes with both staggered and chain pitching. The pressure curves which they present and the comments which they make are of particular value and significance.

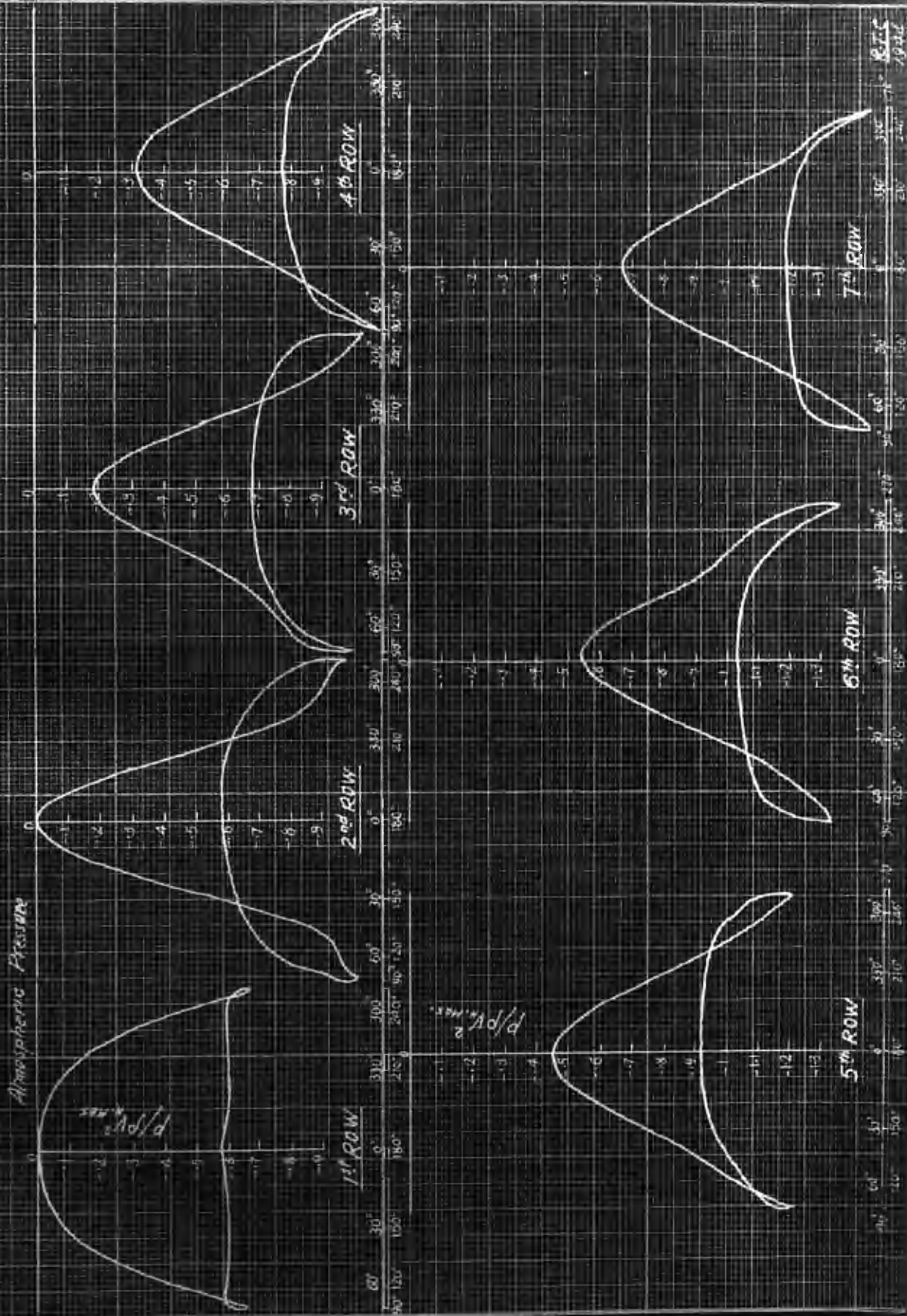
- (c) Second Row in Cross Flow : From model experiments on small vertical tubes with nests of seven rows in staggered arrangement, it was found that the pressure diagram for the first row had an area of approximately twice that of subsequent rows as shown in Plate No.5 and Plate No.6, Fig.1. On the upstream face the pressure distribution is almost identical in all experiments, whereas, in the second and subsequent rows, the pressure of the two adjacent tubes of the previous row causes much lower pressures in the region from 10 to 70 degrees.

The second row is said to be anomalous in the lowness of the pressure at 90 degrees, which, taking 0 degrees as datum, is nearly 50 per cent lower than in the 1<sup>st</sup> row or 25% lower than in the other rows. The cause of this is ascribed to the relatively large form drag of the first row which must be associated with a wake of low energy. Thus the stream, as it passes the constriction of the second row, contains a central core of fluid moving at low velocity which reduces the effective width of the gap and increases the speed of the two/

FORM DRAG DIAGRAMS FOR SEVEN ROWS STAGGERED

BY WALLIS & WHITE

(Engineering 1938)



FORM DRAG DIAGRAMS FOR TWO NESTS OF VERTICAL TUBES

Staggered & Chain Arrangement

RESULTS OF WALLIS & WHITE

(Engineering 1938)

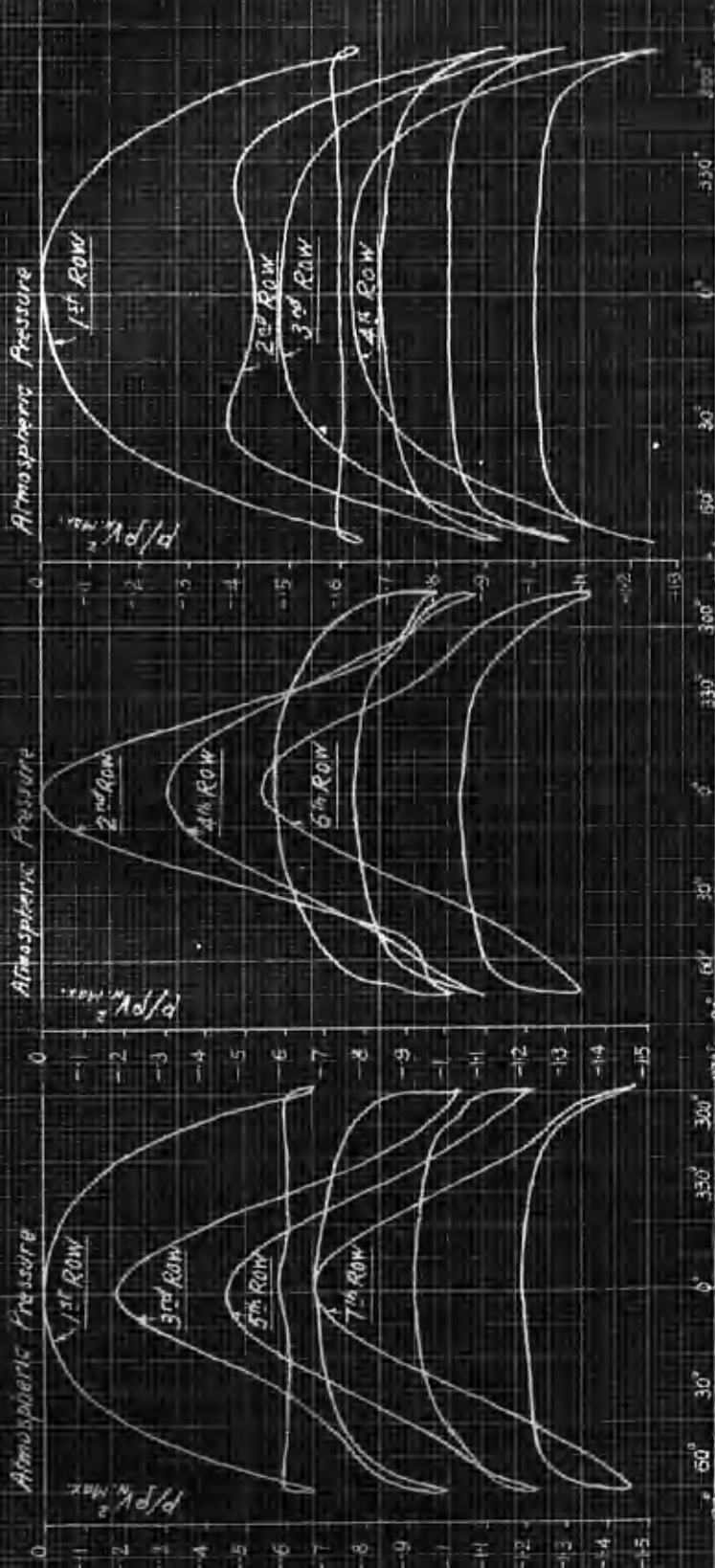


Fig 1 SEVEN ROWS STAGGERED

Mean Ordinate
1st Row 0.431
3rd " 0.170
5th " 0.191
7th " 0.215

Fig 2 FOUR ROWS CHAIN

Mean Ordinate
1st Row 0.435
2nd " 0.235
3rd " 0.260
4th " 0.278

/two parts of the main stream adjacent to the second tube.

In the nest of tubes each tube may be visualised as shedding a stream of low energy fluid which is large in the case of the first tube, small for the second tube and normal for the rest. Incidental to the low pressure at and before 90 degrees, the diagram exhibits two large negative loops which reduce greatly the total drag on the second row. The pressure recovered at the rear of this tube is considerable, being about 43 per cent of the drop from 0 degrees to 90 degrees.

The somewhat low drag of the third row is probably due to the abnormal first and second rows, which together have a resistance well above the average and which presumably shed correspondingly wide wakes.

The pressure curves for parallel rows, corresponding to those for the staggered arrangement, are given in Plate No.6, Fig.2. The differences are considerable and are also indicated by the fluid motions pictured in the paper. It is clear that the second row in the parallel scheme does not show the exceptional features of the staggered pitching.

Clearly these experimental results by Wallis and White makes it reasonable to claim that in cross flow through a staggered arrangement of tubes the pressure conditions around the second row have unique characteristics.

PART 4 - EXPLANATION OF FAILURES.

- (a) The Slagging Conditions : In view of the relationship between external slagging, internal scaling, corrosion and perforation that has already been fully established, it is certain that the conditions outside the holed tube have a high share of responsibility for the consequences. The remarkable feature of its concentration in the second row calls for some special feature in the flow there. This may quite possibly lie in the pressure curves for cross flow in such a case. It must be recognised that this argument is not invalidated by the presence of a minor axial component nor by the fact that the flow across a staggered bank is possibly diagonal.

It may, therefore, be assumed that the slagging characteristics on the tube walls are governed by pressure gradients rather than by precise temperature values, although, of course, the latter must still be favourable.

If the slagging is controlled by pressure gradients, then the curves for the first and second rows would imply a relatively broad, finely slagged, or clear area in the front of the first row and a relatively narrow clear one in the second; with a heavy flanking slag on the second row and a lighter one on the first. The demarcation lines between the clear and the slagged ones should be more definite in the second row than in the first. The conditions controlling slagging on the rear are difficult to deduce since, undoubtedly, the severe eddying that exists there will have an influence.

- (b) The Wall Effects : With the slags selecting the second row for preference and forming with small, clear frontal area and heavy tendencies on the flank, the tube wall temperatures undergo changes. With purely radial heat transmission, the clear wall temperature would remain unchanged and the slagged temperature would drop. As soon as this occurs, however, the clear area is called upon to transmit heat circumferentially and because of that it has to transmit more radially.

As the slag on the flanks increases, the temperature differences increase and the impression is given of a progressively overworked narrow frontal area. This state becomes still worse if the condition of short lengths of clear/

/clear front in considered, because the additional need to transmit heat axially is also imposed on the clear section.

This does not mean that the wall temperature in front becomes excessive because of the particular process. It merely becomes the peak point of the wall temperature curve. It supplies heat to the covered flanks but also transmits increased quantities direct.

- (c) The Internal Effects : This latter aspect now influences the conditions internally. If the water has scaling properties, deposits will start at this place. As the scaling proceeds, the wall temperatures again change, rising higher because of the internal deposits but still with the front temperature dominant.

The boiling behind this critical frontal area will be the most active and if the scale should not be fully protective or should, in part, become dislodged, the opportunity for severe or localized corrosion is provided. Should the scale not be able to remain on this very active length, but gather in quantity below it forming an eccentric bore, the disturbing effect of this on the water flow would further contribute to the rate of corrosion.

Every aspect of this idea of the events indicates that they will accelerate rapidly. The tendency to the uneven slagging increases with the slagging. This reduces the amount of front clear surface and, together with the internal scaling, increases those temperature differences that set up the peak condition. The zone of the violent action thus narrows and becomes more violent and once a corrosion hollow is started it intensifies until perforation occurs.

SECTION II.

SECTION II - EXPERIMENTAL FLOW  
INVESTIGATION.

PART 1 - INTRODUCTORY.

- (a) Aim of Experiments : The preceding section has given in its concluding part the reasoning which tries to explain the peculiar second row failures in a bank of staggered row boiler tubes. The reasoning hinges definitely on the results of cross-flow experiments which are applicable to the boiler tube bank case without much change.

The conditions in a boiler bank, however, are not so simple as in a direct cross-flow arrangement as set up for pressure experiments. The influences of axial components of flow might be considerable. Since the line of argument rests on pressure distribution it would be necessary to demonstrate that these are not altered greatly in character by the more complex condition of flow set up in an inclined tube bank. Actual data of pressures in such a case appear to be invaluable and experimental work is necessary. If the features established by pure cross-flow experiments should require excessive modification in the more general case the line of thought that had been followed would be weakened. It was important to know about this and, therefore, the chief aim of the experimental work was to investigate the pressure distribution in banks of tubes inclined to the general line of flow.

This main line of experiments raised quite a number of secondary points and in particular, the influences of baffle arrangement beyond the tubes and their effect on flow characteristics and pressures. The scheme of baffles used in practice vary widely and no attempt could be made to represent any particular arrangement. It was considered sufficient to investigate whether simple baffles deflecting the flow would upset the conditions seriously.

In addition attention had to be given to the pitching and setting of the tubes to see how these altered existing conditions of flow. However, it may be taken that the chief aim of the experimental work dealt with in this section was to examine the flow conditions, and, in particular, the tube wall pressure conditions in a tube bank when the fluid did not have previous cross-flow characteristics. It was of special importance to examine second row conditions/

/conditions and determine whether the unique features shown in cross-flow work persisted under more complex influences.

- (b) Experimental Plan : The examination of flow by water tank experiment, in which aluminium powder is used to show up the lines and eddies of flow, is now well established. Ahlborn<sup>(57)</sup> first used this method and it has been even more successfully used by Wallis and White.<sup>(52)</sup> It is essentially a method for photographic work under pure cross-flow conditions and does not give data for pressure effects. This method hardly meets the requirements of this experimental scheme except for the possibility of studying the second row effect particularly, and for the examination of the effect of baffles.

It was decided to undertake the water tank experiments even although this meant a repetition of other investigators work. This gave the opportunity for developing the technique relative to the second row tube effects, of baffle influences, size of tube and pitch of rows. A considerable amount of preliminary work was done and eventually investigation was made with two sizes of tanks, this range being the subject of Part 2 of this section.

The main work on inclined tube flow had to be carried out in a wind tunnel with proper arrangement for pressure measurement. No photography of flow was undertaken here, the essential requirements being the tube wall pressures under widely varied conditions. The preliminary experimental work was done to establish the best conditions of working, control and setting. Part 3 of this section gives the results obtained for the experiment planned after preliminary tests were completed and represents an important range of the scheme of experiment.

It was found generally, with baffles in use, that the pressures recorded were very low and consideration of the question of getting higher speeds led to the development of a small high speed tunnel served by air discharged from a nozzle. This meant small spaces and small parts and it was thought that the scale might introduce errors that would be prohibitive. On the other hand, if it could be shown that under such conditions the main feature of flow persisted, the more important aspect of the investigation would be established with greater assurance. This method also provided a means whereby tests using smoke introduced in the air flow could be carried out. With these points in view the special apparatus, as described in Part 4 of this section, was designed and set up as described in this section.

The experimental plan was, therefore, threefold. Firstly, water tank experiment for photographic purposes on the second row features and baffle effects; secondly, main wind tunnel work for tube wall pressure investigations on inclined banks with and without baffles; and thirdly, by the use of high air speeds on a small specially designed trunk for pressure distribution tests under various conditions and for smoke tests.

PART 2 - WATER TANK EXPERIMENTS.

- (a) Previous Methods : Ahlborn's discovery in 1900 had been appreciated in his time, and his method - sprinkled powder on the surface of fluid renders its motion visible - has been used in aerodynamics and civil engineering research works. Though several methods have been used yet Ahlborn's method still stands out for its easy application, and, by uniform illumination on models under test, good photographs could be produced.

Dr. Wallis,<sup>(54)</sup> in a paper given before the Institution of Mechanical Engineers, 1939, used moving fluid and fixed models. The method is as simple and easy to use as Ahlborn's. However, in both cases care is essential when taking the photographs. Dr. Wallis used a shallow tank and a sprinkler for distributing the aluminium dust on the water and the tank was equipped with a diffusing device to avoid the unwanted disturbances at water inlet.

Professor Hele-Shaw used another method in his experiments on fluid motion. His apparatus consisted of two glass plates separated from each other by cardboards one to two hundredths of an inch thick. The model is arranged between the plates and the water under pressure is applied from one end. Small jets of colour are introduced well in front of the model and before the fluid is sensibly deflected. The colouring matter in his experiments was Nestle's Milk.

These will form a basis of comparison with the more extensive investigation which is given in this thesis.

- (b) Small Tank Arrangement : The first tank used was 30 inches long by 15 inches wide and 15 inches deep, Plate No. 7. The height of the water was controlled by an adjustable weir at the end of the tank. Aluminium powder was distributed evenly by using a tray made of copper wire gauze. This tray extended across the tank and was 4 inches broad. It was found that only a very slight agitation gave to the water a uniform layer of the aluminium powder which floated on the surface of the water in the tank.

PLATE - 7 -



- ① STEEL TANK
- ② INLET PIPE
- ③ PLYWOOD PLATES
- ④ ALUMINIUM TRAY
- ⑤ WOODEN TRESTLE
- ⑥ GLASS PLATE
- ⑦ STEEL BAFFLES
- ⑧ MODEL TUBES
- ⑨ DIVISION WALL
- ⑩ ADJUSTABLE WEIR

Fig 1

SMALL TANK ARRANGEMENT

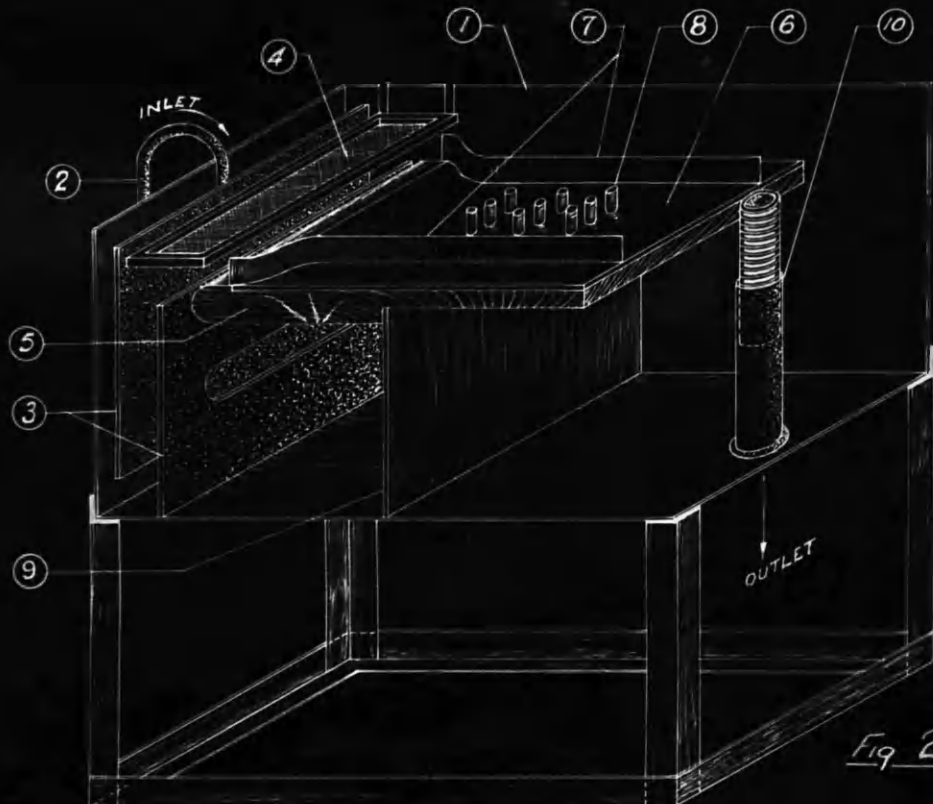


Fig 2

It was noted that with the afore mentioned tank the disturbances of the water flowing around the models was much too violent to give time for fluid flow to steady. After making a considerable number of experiments it was necessary to put two baffle plates made from plywood at the entrance of the tank about two inches apart. By experiment it was found that good results could be obtained with one baffle raised 2 inches from the bottom of the tank as shown in Plate No.7, Fig.2.

The complete arrangement of the apparatus for the small tank experiments is shown on Plate No.7, Figs.1 & 2. It will be seen that the models were supported on a trestle board extending across the tank. Indented into the wood is a thick glass plate about  $\frac{1}{4}$  inch thick. In order to make the back ground more suitable for photographic purposes a black piece of cloth was placed under the glass plate. The sketch of the arrangement does not show how the light is projected on to the surface of the moving water as it passes along the tank. It was found that two 500 Watt lamps were satisfactory. The camera was fixed to the side of the tank and could be set to the desired exposure and height above the models.

The other points to be mentioned concerning the arrangement is the position of the water inlet. This was placed near to the surface of the models which are in the vertical position. It was found that the surface of the fluid must be kept in one plane in order to obtain clear photographs, free from distortion and shadows.

The speed of the flow required careful investigation and regulation. It was found that speeds of one to two inches per second gave good results and at these speeds a level surface could be maintained.

The models used were cut from 2 inch diameter tubes about  $\frac{1}{8}$  inch thick. The length of the model tubes was kept at 2 diameters length. Solid models,  $\frac{5}{8}$  and 1 inches diameter by 2 diameters long, were also used so that the ratio of diameter and length was kept constant throughout the tests.

The models were arranged in various orders, chain and staggered pitches being used. These gave by grouping, nine different model positions.

The photograph and outline arrangement show the baffles in position. These baffles had to be bent to suit the model position required and were kept about  $\frac{1}{8}$  inch above the top of the models and, therefore, also at the/

/the same height above the surface of the flowing water.

- (c) Large Tank Arrangement : It was found that the 30 inch long tank did not permit of all the tests being carried out. A much longer tank about 20 feet long, which had been used for model ship tests, was adapted to suit requirements of all tests. This tank, which was also broader and shallower, gave a much better form for experimental purposes. Outlet and inlet disturbances were reduced to a minimum. Plate No.8 shows the general arrangement of tank.

To suit this tank a steel template of the pitches of the models was made. The template was  $1/16$  inch thick and  $\frac{1}{4}$  inch holes were bored at the required pitches, thus standardizing the model formations. A projection of  $1/16$  inch long and  $\frac{1}{4}$  inch diameter was made at the bottom of the one inch models-to fit into the perforated plate which formed a jig for the models assuring constant pitches for various arrangements, see Plate No.8, Fig.2.

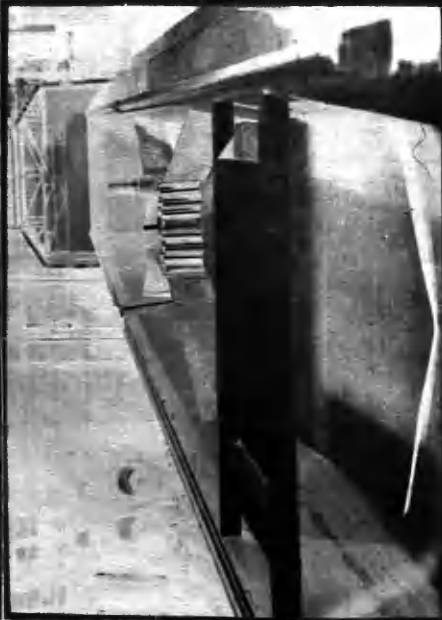
The tray used to spread the aluminium powder on the surface of the water was carried on four wheels. The wheels ran on a track along the sides of the tank. It was found that the motion of the wheels gave quite enough vibration to the tray and spread the powder very evenly on the surface of the water. No further agitation was required.

One arrangement of the baffle plates with the large tank just described is shown in Plate No.8, Fig.2. As will be seen, the larger tank lends itself to a more efficient arrangement of the baffle plates. These plates could be altered to suit requirements and were as far as possible bent to conform to boiler practice.

At first, half plate photographs were taken but, owing to the difficulty in obtaining a full supply of material, it was decided to go in for enlargements from smaller plates. All work had to be carried out with great care in order that the special features of fluid flow would appear in clear undistorted detail.

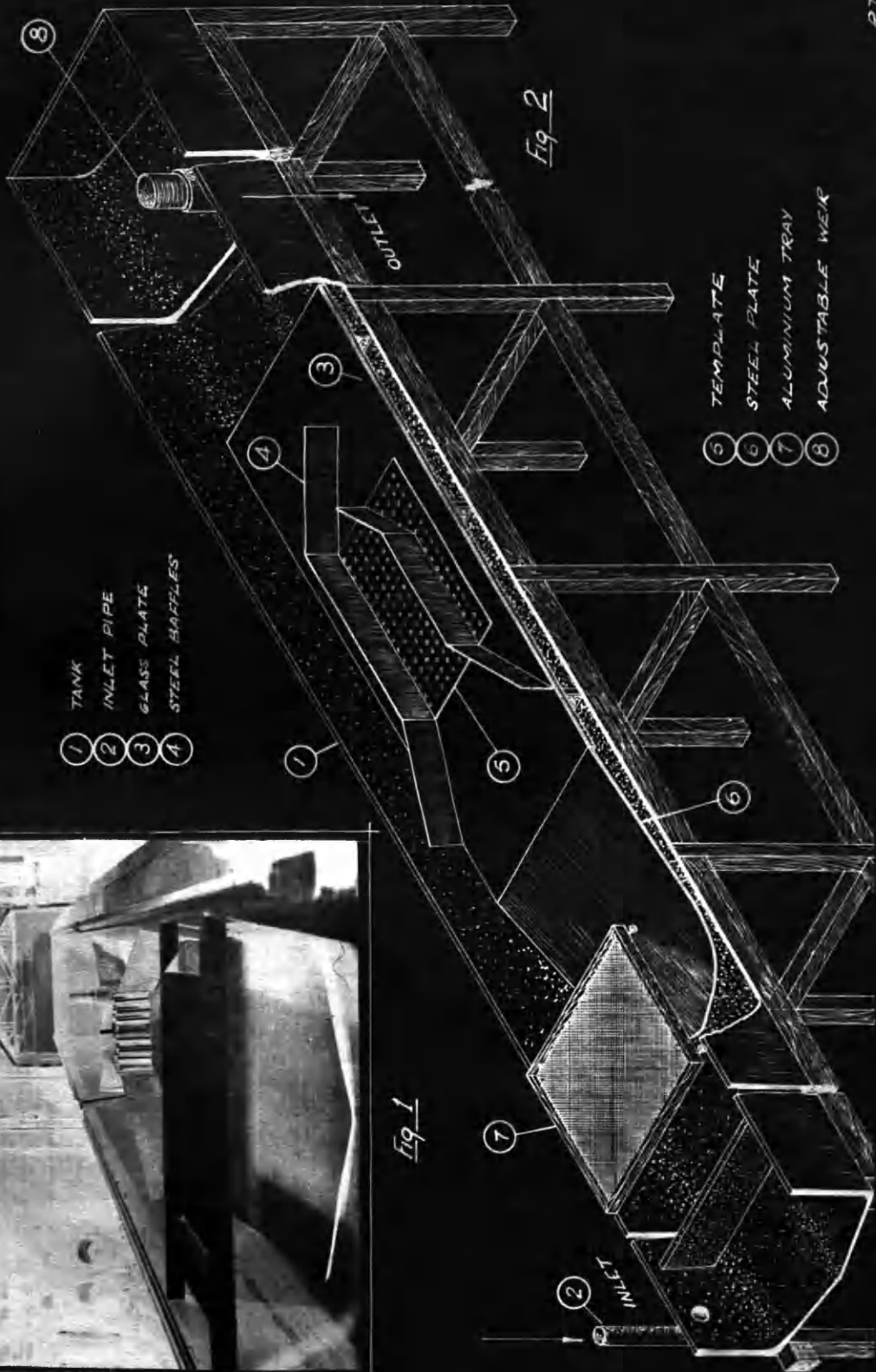
- (d) Photographic Results : The first series of experiments were carried out with the model tubes set in staggered pitch formation. Experiment was made on three different diameters of tubes and three different pitches for each tube. Adjustments of conditions were made and photographs taken for each speed of flow and model diameter.

LARGE TANK ARRANGEMENT



- 1 TANK
- 2 INLET PIPE
- 3 GLASS PLATE
- 4 STEEL BAFFLES

Fig 1



- 5 STEEL PLATE
- 6 TEMPLATE
- 7 ALUMINIUM TRAY
- 8 ADJUSTABLE WEAR

Fig 2

Plate No.9, Figs.1 & 2, shows how the flow is divided into two equal sections with a large area of dead water behind the model tubes. A reduction in pitch of the models altered the quantity of still water. It might be stated here that Dr. Wallis, when using staggered elliptical tubular models, found that the marked regions of dead water were those just at the rear of the last row of tubes and in the side pockets where half tubes would be necessary to complete the pattern.

An examination of these photographs show clearly the wake behind each row of tubes, see Plate No.10, Figs.1 & 2. The comparison between the pictures of the flow when the pitch is altered can be traced out, and intensity of the flow is shown up by the number of apparent lines of flow, see Plate No.9.

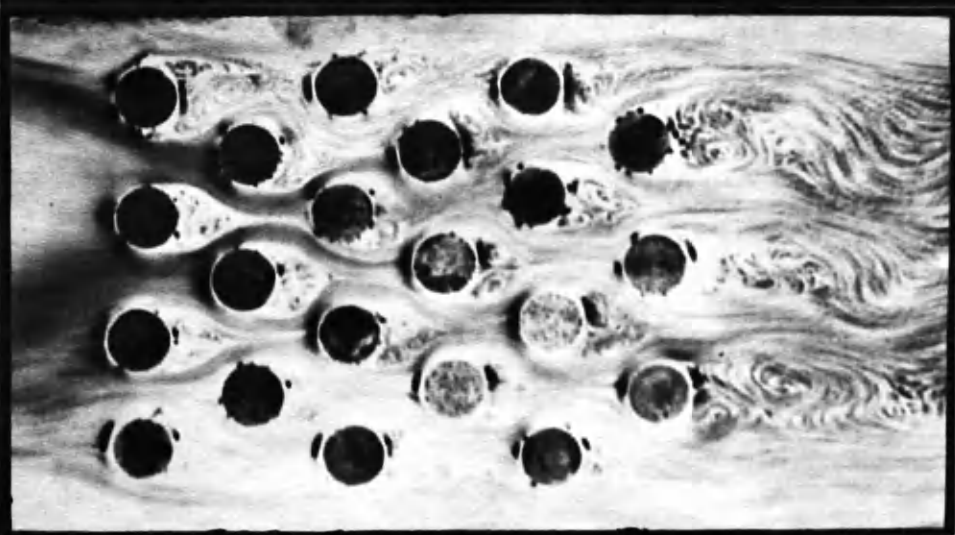
The same experiments were carried out with the tubes in chain formation and photographs were taken. These could be compared and may in some cases be of interest, but, since the staggered pitch is used more in boilers and heaters, this has been given full consideration.

With the chain arrangement, Plate No.11, Figs.1 & 3, shows how the water flows between the tubes and also the eddy form between the rows of tubes. The eddies, as shown by the photographs, are violent in form caused by vigorous swirling motion. In some of the photographs it can be clearly seen that the turbulent state gradually fades away. This stilling effect may be caused by the steady flow of the central piece of fluid (a dragging effect).

The position of the baffles is shown in Plate No.11, Fig.1, which is a six row tube test. The baffles are angled and it will be noticed that the effect is to cause swirling of flow with the chain arrangement. Comparing this with Fig.3, which is also for chain arrangement of tubes, the baffles here are straight and parallel. The stream-line flow has been enclosed by the baffles or guide plates and very slight swirling effect appears, if any. It will be seen that the swirling becomes more serious after the first two rows in Fig.1 while in Fig.3 there is a steady stream up to the last row.

Fig.2 shows the angled baffles used with the staggered tube arrangement for seven rows. There is a decided tendency for the baffles to have an effect on the flow form of those tubes in the second row. The effect of this is to break up the pockets of wake in the second and third rows.

In order to study the effect on the flow the tube bank is removed and a photographic study made. This/



SMALL TANK EXPERIMENT  
 (6 rows staggered arrgt.)  
 3/8 dia tubes pitch 3.3d x 2.1d



LARGE TANK EXPERIMENT  
 (4 rows staggered arrgt.)  
 1/2 dia tubes pitch 4d x 2.1d

PLATE - 10 -



LARGE TANK EXPERIMENT  
 (4 rows staggered arrgt.)  
 1" dia. tubes                      pitch 3.8d x 2.3d  
 without baffles



LARGE TANK EXPERIMENT  
 (4 rows staggered arrgt.)  
 1" dia. tubes                      pitch 3.8d x 2.3d  
 with baffles

R.T.C.  
 1944



*Fig 1 - Angled Baffles*



*Fig 2 - Angled Baffles*

↑  
*direction of flow*

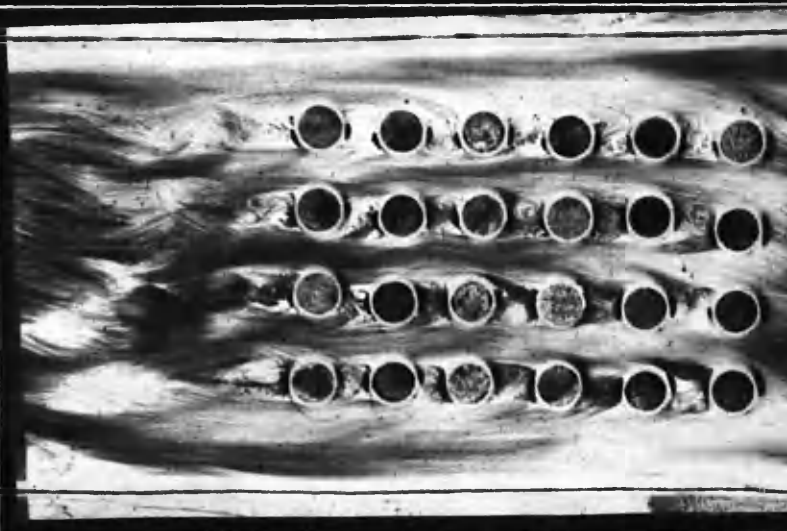


*Fig 3 - Parallel Baffles*

FLOW THROUGH NEST OF TUBES  
*(chain & staggered)*

/This is illustrated in Plate No.12. Fig.1 has straight baffles enclosing straight angled bends. Fig.2 has the same type of baffle plates but in this case the corners were carefully rounded. Fig.3 shows the effect of streamlined baffle plates.

The effect on the stream-line for these different shapes of baffles can be seen and will be considered when acting along with the test banks. It might be stated here that the baffles cause pockets of wake which may or may not all disappear when the banks of tubes are placed in position. The stream-line flow and pocket of wake are shown clearly on Plate No.12, Figs.1, 2 & 3.

- (e) The Second Row Enlargement : In order to examine the flow conditions at the second row more closely, enlargements were made of parts of the photographs for staggered row arrangements. These are reproduced in Plates No.13 to 16.

It is seen that the flowing fluid approaches the first row of tubes very steadily until it reaches the outside diameter. At this point the space closes in and there appears an accelerating effect as the same quantity attempts to pass through the smaller space. Up to this point of the first set of restrictions, the water appears to be free of turbulence.

On the width of the spacing depends the steadiness of flow from the first row. Again this holds at the second row but with altered conditions where there is a mixture of turbulent and stable flow. This goes on for all the rows but the acceleration becomes less towards the back rows.

The points where the boundary layer loses its motion, just where the stream flow separates from the tubular models, are shown quite clearly. These are shown on the curves which will appear later in the thesis. The position of the breakaway points as regards the second row has been given special attention on account of the lower drag effect. Pockets of dead water are left behind each tube in the row.

Consider the four enlarged photographs. The first, Plate No.13, shows the intensive sharp line of flow caused by the first row changing the stream-line form. The wake at the back of the first row is not much altered from that of a single row tube, but certainly is altered by the fluid flow being pressed into the stilled region. The wake at the first row could be readily seen in the tests as the/

PLATE- 12 —

FLOW THROUGH  
STRAIGHT & CURVED BAFFLES



*Fig. 1*



*Fig. 2*



*Fig. 3*

- 1 Straight baffles
- 2 Combination of st. & curved baffles
- 3 Curved baffles

PLATE - 13 -



SECOND ROW ENLARGEMENT

1" dia tubes pitch 4d x 2.1d

Parallel Baffles

R.T.C.  
1944



SECOND ROW ENLARGEMENT

1/2 inch tubes pitch 2.9d x 1.73d

Angled Baffles

R.T.C.  
1944

PLATE - 15 -



SECOND ROW ENLARGEMENT

1" dia tubes pitch 38d x 23d

Parallel Baffles

R.T.C.  
1944



SECOND ROW ENLARGEMENT  
 1" dia tubes pitch 3.8d x 2.3d  
Angled Baffles

R.T.C.  
 1944

/the aluminium powder remained compact and moved steadily with the surface of the water. It is also clearly seen that the speed of flow is faster as it strikes the frontal area of the second row. The break away points are readily seen on the second row and are earlier than on the first row. At the back of the second row there is a decidedly different appearance in the wake region. This has the appearance of great swirling with the effect of raising the negative pressure, while the side of tubes at the 90 degree region is relieved of pressure.

Plate No.14 illustrates the stream-line flow of the same tube arrangement as No.13 but is of smaller pitch and with ~~pitch~~ baffle plates in use. The effect of the smaller pitch on the wake area is readily seen in the photograph. The frontal area of the second row is subjected to intensive pressure and the wake, although keeping the same appearance, is naturally smaller. The appearance of side-sway towards the right in No.14 is caused by the baffles.

In the photographs, Plates No.15 and 16, with and without baffles the pitches are the same, the speed of water is constant and is the same in each test, but this speed is lower than that used when taking Plates No.13 and 14. At this slow speed the stream lines show clearly the features and behaviour of the water pressure on the tubes. This is very pronounced at the side region of the second row tubes. The side-sway of line of flow in Plate No.16 is caused by the baffle plates.

In the case of the front row tubes the break away point is at about 85 degree rotation from the frontal area. The second row tubes have this break away point much earlier. The photographs show this about 60 degrees and when compared with the pressure distribution curves, plotted from experimental data, is found to be almost exactly at this point. All the four photographic plates show the second row tubes to be undergoing more severe working than that of the other rows.

### PART 3 - WIND TUNNEL EXPERIMENTS.

- (a) Experimental Layout : These experiments were undertaken to study the distribution of pressure along banks of tubes arranged in staggered formation. The models in this case were inclined to the flow, and similar to those in a steam boiler. The Wind Tunnel at the Royal Technical College is a 5 foot diameter open-jet, closed-circuit Wind Tunnel. This tunnel has a speed range of zero to 100 m.p.h. and can be set to run constantly at any speed within that range by means of an electrical pressure balance. The maximum speed variation possible when the balance is in operation is  $\pm \frac{1}{2}$  per cent. There are slots round the bell-mouth of the collector to prevent the stagnant air, picked up by the jet in crossing the gap, from being drawn into the air-stream. Plate No.17, Fig.1 shows the arrangement and position of the model tubes.

The dimensions of the tubes were  $\frac{1}{2}$  inch diameter,  $\frac{3}{16}$  inch thick. The number of tube models in each bank was 90 and 58, and the length was 4 and 2 feet respectively. The tubes were kept together by end blocks or headers which were fixed on to two side plates, thus forming a trunk two feet wide as shown in Plate No.17, Fig.2.

The position of the model tubes in the space between the nozzle and the collector is about one foot in front of the nozzle. The back of the bank of tubes under test is inclined at an angle of 20 degrees to the axis of the wind tunnel. It will be seen that the baffle plate is also inclined to the same axis at 20 degrees, making an angle between model and baffle of 40 degrees. These angles are varied in first tests in order to get the best position for the model. Plates No.18 and 19 show outline diagrams for various settings. The setting 1B has been used throughout the remaining test, i.e. the centre line of the nozzle coincides with the end of the inclined bank of tubes where they enter the bottom header.

Seven holes  $\frac{1}{32}$  inch in diameter are bored in the test tubes at points 6 inches apart in a straight line along their lengths. The holes are used in turn, one at a time, and a dial arrangement for denoting the position of the holes is fixed at the top end. Thus various positions of rotation in the stream could be indicated for each of the seven holes through an angle of 360 degree by 10 degree increments.

ARRANGEMENT OF MODEL IN WIND TUNNEL

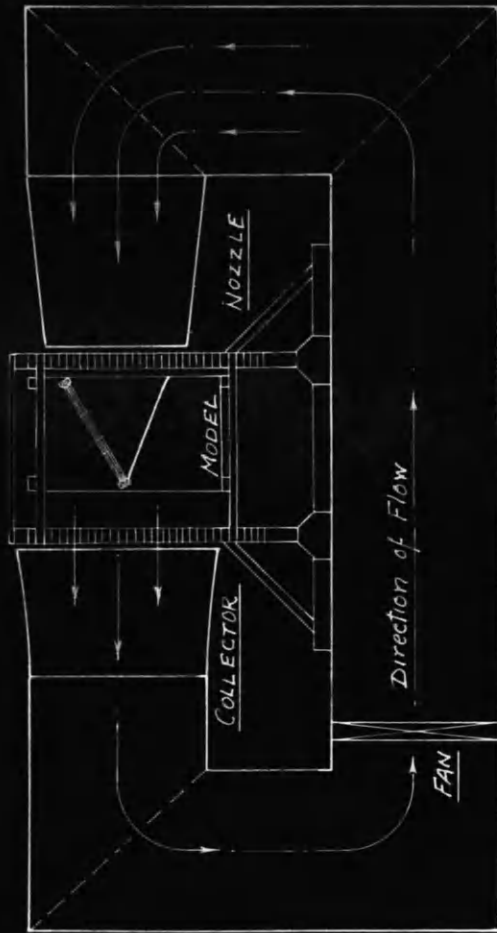


Fig 1 ELEVATION

DIAM. OF NOZZLE 5 FEET  
 SPEED OF JET 100 FT/Sec.

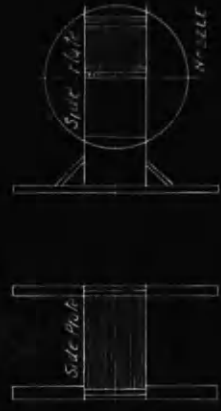


Fig 2 PLAN & SIDE VIEW of Model

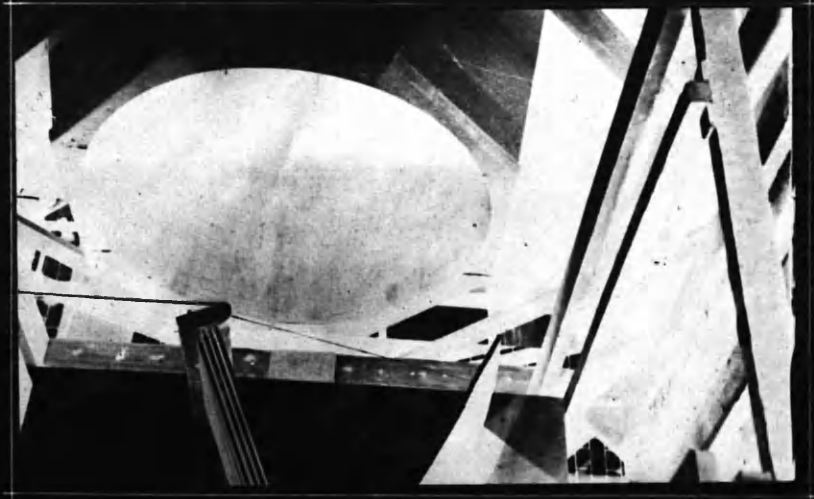
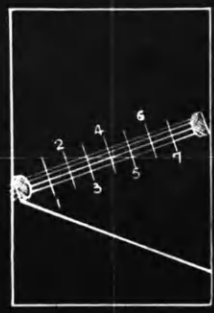
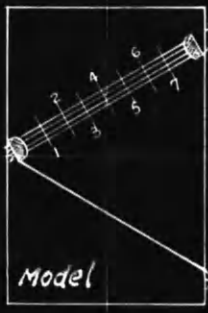


Fig 3

BAFFLE ARRANGEMENT



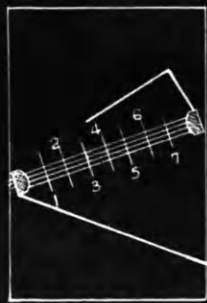
1 A



1 B

Direction  
of Flow

Fig 1 POSITION 1



2 A

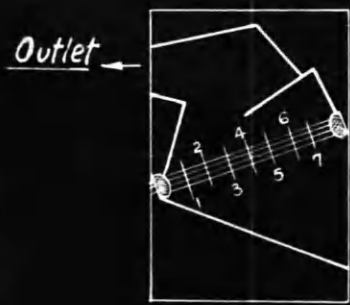


2 B



2 C

Fig 2 POSITION 2



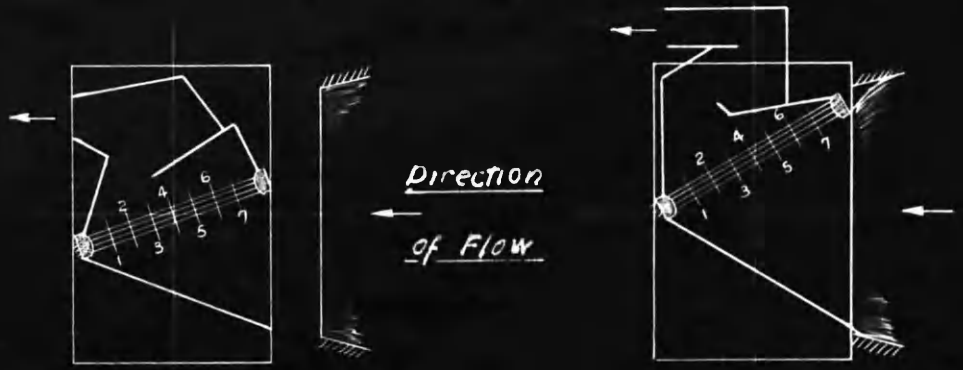
3 A



3 B

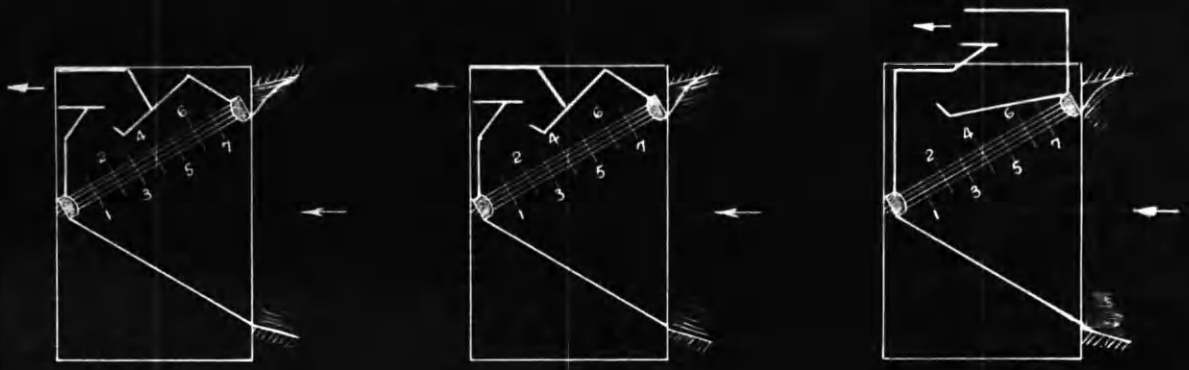
Fig 3 POSITION 3

BAFFLE ARRANGEMENT (Cont.)



3 A

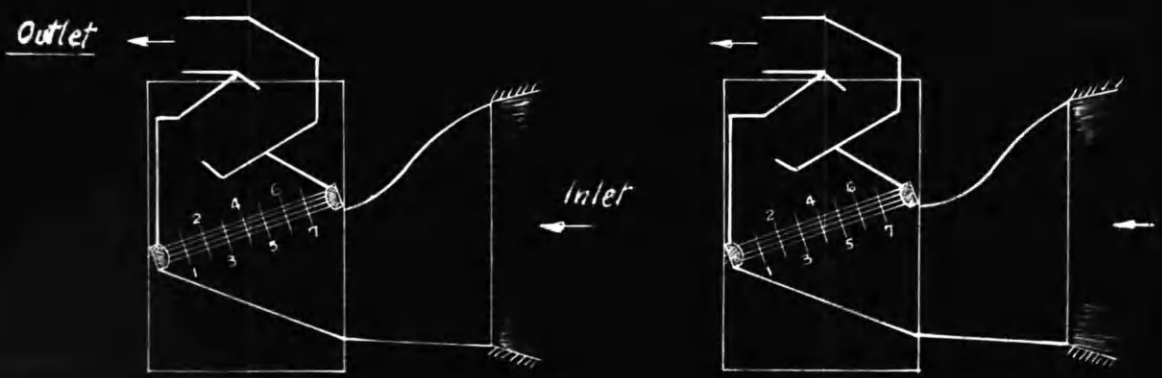
3 C



3 B<sub>1</sub>

3 B<sub>2</sub>

3 D



3 E<sub>1</sub>

3 E<sub>2</sub>

POSITION 3

In the actual tests a bank of ten tubes could be taken at one time and the readings obtained for these, i.e. three readings in first and third rows and two in second and fourth rows of the staggered tubes. Plate No.20, Fig.3 shows the arrangement of tubes and protractor dial. The tubes were arranged with diagonal pitches and proportional to those in an actual water tube boiler design. The boiler tubes were  $2\frac{1}{4}$  inches diameter and the model  $\frac{1}{2}$  inch diameter from which the scale of the model dimensions were found to be  $4\frac{1}{2}$  to 1. The bank of model tubes used consisted of four rows as in boilers.

As the angle of the bank of tubes is increased there is a tendency for the tubes to slide in the header. To guard against any change during the tests the pointer of the dial measuring arrangement was used to prevent the tubes from moving down and, therefore, the holes in the tubes were kept always in one plane when the tubes were turned through each 10 degree increment.

In order to measure the pressures a glass tube manometer, which could give readings up to thirty points at one time, was used. Coloured fluid was preferred as the medium so that photographs or blue print readings could be made. It was found that by using graph paper and a red line datum, graphs of the pressure could be plotted directly. The manometer tubes were carefully marked so that no mistakes in readings could be made. The marking was made in different colours - 1st row Green, 2nd row Red, 3rd row Blue and 4th row Orange. The arrangement of manometer, tubes and square paper plotting sheet for pressures is shown in Plate No.20, Fig.1, and was used in the vertical position as this gave more accurate intersection for the pressure lines. The plotting method avoided the more usual laborious and expensive photographic or blue print method.

In the tests for the 40 and 60 degrees angle included between tube rows and baffle, Plate No.18, the speed of air jet was kept at 100 ft./sec. This constant speed permitted of comparison without bringing in further variables.

Plate No.18, Figs.1 & 2, shows the position and form of the two baffle plate arrangement while Plate No.19 shows an arrangement of three baffle plates.

- (b) Range and Procedure : In the design of the apparatus, arrangement has been made to give a range of tests on banks of four rows. The headers have been arranged to take various pitches. At smallest pitch with staggered formation 90 tubes may be in use at one time. With the second length of tubes/

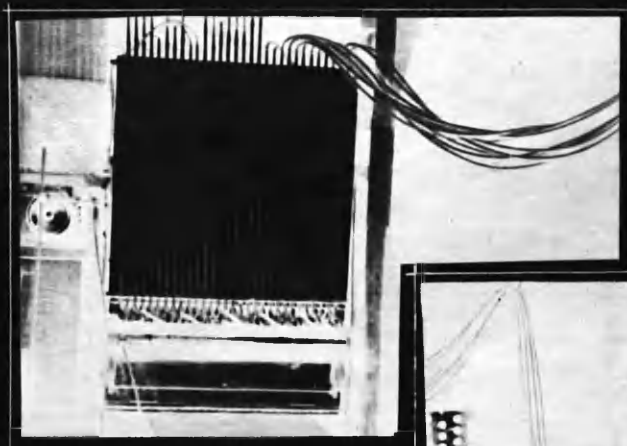


Fig 1 Monometer

direction  
of flow  
←

ARRANGEMENT OF BAFFLES  
IN  
5 FOOT WIND TUNNEL

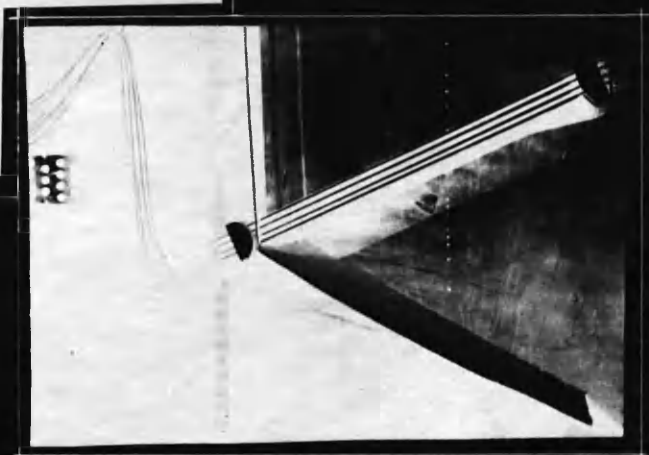


Fig 2 Position N° 1



Fig 3 Position N° 2



Fig 4 Position N° 3

RTC  
1944

/tubes a maximum of 58 could be used.

This gave a wide range of experiments which brought out the effect of lengths of tube and size or area of inlet to the model bank of tubes. The area was arranged to make certain of similar flow in each test.

The baffles were made adjustable and thus provided a means of regulated change of flow. At the same time the change of distance and direction of baffles were kept as near as possible to those pertaining in a water tube boiler. There are three different types of baffling. The side walls are kept constant while using the large and small model. The pressure readings could be taken at seven positions along the axis of the tubular models and each hole gave 36 positions of rotation (10 degrees). This held for each of the four rows of tubes in the bank so that over 250 readings could be made for each tube.

The procedure for carrying out each test and the method of using the test apparatus, had to be standardized in order to enable the great magnitude of data to be taken as close as possible to exact time and to constant conditions. After the flow had been stabilized the pressure readings were taken in ten tubes at one time. The manometer readings were plotted on graph paper, thus enabling a check to be made on conditions.

The velocity of air flow was kept constant at 100 feet per second by a regulator on the fan. A special velocity gauge gave the reading in feet per second. This was also checked by the pitot-tube reading of pressure, barometer and temperature which gave the velocity of flow by calculation.

After the desired conditions were reached the manner in which readings were taken were as follows:- The bottom hole in each of ten tubes was opened while the other six holes were kept closed by plugs. These plugs were such that no leakage could take place. When the readings had been taken of the ten pitot tubes a rotation movement of 10 degree increment was given. This was checked by the dial gauges at the top end of the tube banks. Then the bottom holes were plugged and the second lowest holes were opened in the ten tubes. The rotational movement was again given and pressure readings taken. This was carried out for second, third and fourth rows. Special attention was given to the second row readings which were checked and re-checked to ensure good average readings of pressures.

Another ten tubes along the front face/

/face of the bank of tubes and in each of the four rows were examined under the same flow conditions. The readings were again recorded as for the first set. This procedure was carried out until all the tubes had been brought under test.

- (c) Influence of Position. : It was found that the position of the model tube bank in the tunnel altered the condition of flow. The nozzle of the wind tunnel is five feet and the length of the model being four feet only certain longitudinal movements of model bank of tubes were available if all the air flowing had to pass through the model bank. Tests were carried out to determine the best position for the model. These test positions are shown in Plates No.18 & 19, Figs.1,2 & 3. It was found, however, that so long as the distance between the nozzle and the model did not exceed 12 inches there was no appreciable change in test results. It was thought at first to keep the model in a close up position in order to get the best results. The difficulty arose in the making of the various changes and then resetting accurately. But by experiment it was found that a clear space between nozzle and bank of 12 inches made no difference in the readings obtained.
- (d) Influence of Setting : In the water tank experiments the model tubes were kept in the vertical position. This is not the more common position for the water tube boiler has at least two inclined banks of tubes and it was considered that few tests had been carried out on the inclined tubes. It was, therefore, decided to carry out tests on banks of tubes inclined to horizontal position at various angles.

The angular setting was limited by the diameter of the Wind Tunnel. If tubes and the headers are to be in the air stream then the range of angular settings are limited to 30 degrees or 60 degrees between the bottom baffle plate and tubes under test. However, this angle could be reduced and tests were carried out with contained angle 40 degrees. Inspection of Plate No.20, Figs.2,3 & 4, which was shown in the description of apparatus, shows clearly the arrangement. The headers are kept outside the flow-stream. The best angular positions and settings having been found by preliminary test, it was therefore arranged to carry out complete test on two angular settings only. In the first the contained angle was 40 degrees. This was to conform to boiler practice and was similar to that in the boilers where failures had occurred. This was taken as the minimum angle and was increased to a maximum angle to suit the 5 foot wind tunnel.

The only change was in total pressure and these changes in pressure along the rows were found to be in same proportion throughout the bank of test tubes. This holds for chain and staggered tube arrangements. The same may be said for inclined tubes with different pitches. The staggered pitches were most closely examined for effects of inclination on the second row.

- (e) Influence of Baffles : The photographs of the test apparatus, Plate No.20, show clearly the position and arrangement of the baffles as used in the main tests. So far as possible the arrangement was similar to that used in the water tube boilers where failure of tubes had occurred.

Preliminary tests on the best positions for the bottom baffle were carried out and found to be as in Position 1. It was found that, when given the same inclination to the horizontal as the model bank of tubes, best results were obtained. The angle contained between test bank was kept constant and was equally divided on either side of the centre of the Wind Tunnel. The length of the bottom baffle was equal to the overall length of the tubes and headers. The angular position of tube banks and baffle could be altered but only two main test angles were used, namely 40 and 60 degrees.

The angular position of the first baffle was found to have little or no effect on the pressure readings. The surface of the "Seletex" baffle plate would be much the same as that used on the built up baffle in the water tube boiler. Experiments were carried out and readings taken when the first baffle plate was used alone.

The top right baffle, position 2, was of the form shown in Plate No.20, Fig.3. The baffle has been made Z form but an extension of the web was kept on so that further change might be made. The portion of the flange of the Z form, where it was attached to the header, was left of considerable length at first. This was done in order to determine the effect of the pressure on the tube due to the air trapped between the flange and web of the Z baffle.

The angle between the flange and web could also be changed and this was ultimately kept constant at 80 degrees which was found the most suitable. The flange length, which is really the distance of the baffle from the bank, was kept constant at 2 feet which also gave good results. The web length was then experimented on and was changed from 2 feet to 1 foot, that is, the web covered 1 foot length of tube bank length. The angle between flange and web of the/

/the Z form was ultimately fixed at  $120^{\circ}$ . The top flange of the Z form was necessary to guide the air out. The length of this was about 6 inches and again fixed at  $120$  degrees to the web.

The extension of the web plate was used to make a good form of outlet. This is also clearly shown in the photograph, Plate No.20, Fig.3. It might be stated here that this required careful designing and experiments had to be made. In the test results outline sketches will give each form and change made.

The top left hand baffle plates of Position 3, which are clearly shown by the photographs, Plate No.20, Fig.4, is of Z form. The upright supporting this baffle was at first inclined to the bank of tubes at the same angles -  $40$  and  $60$  degrees. After experimenting with this it was found better to keep this upright at  $90$  degrees to the stream line flow. It might be stated here that this is more in conformance with boiler practice.

The upright support for Position 3 was made hinged and could be carefully sealed against air leakage. The use of the hinged door was to permit changing the pitot tubes and the test holes.

The supports or fixings for the baffle plates were all kept free from the inside surface so that there could be no restriction or interference of air flow.

Further experiments were made using the above system of inclined banks of tubes and baffle arrangement but using an altered form of air inlet and outlet. On the 5 foot nozzle of the Wind Tunnel was placed a trunk piece changing from 5 feet diameter to rectangular sections to suit the space between the angle contained by Position 1. This trunk piece is about 3 feet long and the bottom face is horizontal and level with the bottom baffle. All the change in depth is made on the top face of this trunk extension. The bottom face was hinged and used as a manhole door through which changes and adjustments could be carried out. This is also shown in outline sketches, Plate No.19, Fig.3E.

- (f) Experimental Results : The test data required to make the complete set of form-drag diagrams was barometer conditions, temperature conditions, velocity of air flow and wind tunnel inlet pressure. As these are constant throughout one test, the barometer reading in Hg, the temperature in  $^{\circ}\text{F}$ , the velocity in feet per second and pressure in cms. of water were/

/were used and are given at the top of the various tables.

Tables No.1 to 5 show the collected results. Column 1 is the position of hole with  $0^\circ$  on the front face of each of the four rows of tubes. 1st, 2nd, 3rd and 4th row tubes have been allotted two columns - pressure  $p$  in centimetres of water and ratio of pressure  $p$  divided by product density  $\rho \times V^2/2$  (velocity ft/sec.)

From these tables "Form Drag Diagrams" have been plotted with  $p \div \rho V^2/2$  as ordinates and angle of turn of test hole in tube as base.

The first series of curves are without baffles, the second series are with one, two or three baffle plates. There are seventeen tables and ten plates for various graphs.

From the first set of graphs a second set of curves were plotted, pressure ratio - sine of angle of turn of test tube hole. The slope of the first curves was determined and plotted on angle base. This shows clearly the slope of the second row tube curves to be much steeper than in the first row and still greater than the third and fourth rows. This holds for all the data on the seventeen tables.

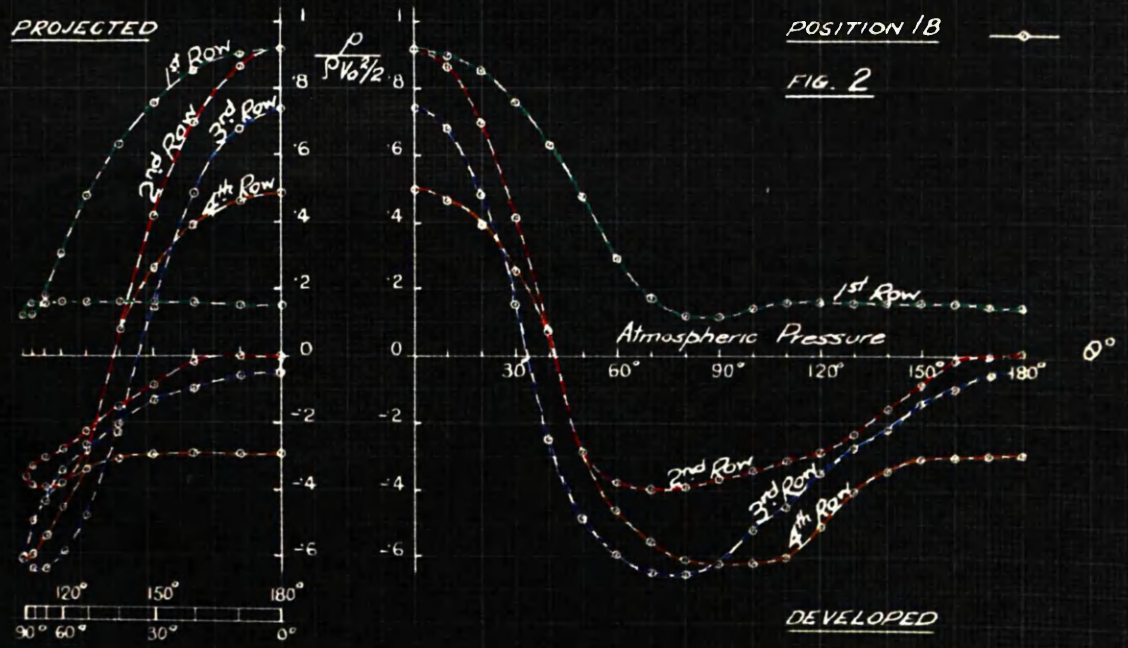
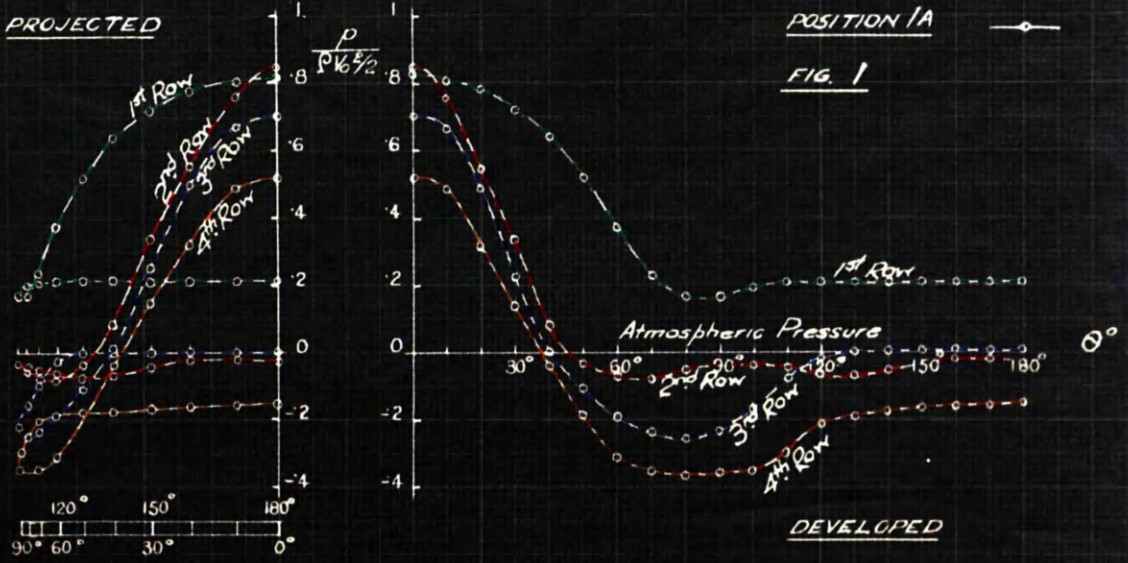
- (g) Discussion of Results : At first it was thought that an angle of turn of 180 degrees would bring out all the necessary features in the form-drag or pressure-distribution diagrams. The data from the tables was plotted, first as a projected diagram of  $p \div \rho V^2/2$  on a sine of angle base.

The diagrams all show a distinct loop of varying dimensions with the point of breakaway differing in row. It was thought that a developed curve of the same ordinates and on equal angle base might demonstrate the changes more clearly. In this case only one hole was taken so as to shorten these preliminary experiments and to get a comparison of results with those of other investigators.

The first row tube diagram keeps well above the atmospheric line which is taken as the datum level as shown in Plate No.21, Figs.1 and 2. In Fig.1 the second row comes close to the atmospheric line but below it, while the third and fourth row curves are well below. There is a slight difference in the curves in Fig.2 but all have a similarity.

The developed curves show the third row curve falling on the datum line close to the  $130^\circ$  angle/

FOUR ROWS PRESSURE DIAGRAMS  
 FOR  
 POSITIONS 1A AND 1B HOLE NO 4  
 100 ft/sec



/angle of tube turn, while the fourth row keeps well below. Figs.1 and 2 have differences which could not at first be accounted for. This led to the experiments being carried over both halves of the tubes, that is, angle of turn through 360 degrees.

A developed pressure-distribution diagram is shown in Plate No.22, Fig.1 for the first and second rows with hole No.2 in use in place of hole No.4. These curves show the same form but with a slight rise in pressure at the back of the second row tubes. When the curve is carefully examined it is found that the two halves differ. Pressures at 60 and 300 degree points of the top second row graph were almost exactly equal, but with the bottom second row curve there was quite a difference.

The projected curves are shown in Plate No.22, Fig.2 and these, while showing similarity, show also how necessary it is to complete the pressure curves over the whole circumference of the tubes under test. It was, therefore, seen how necessary the preliminary tests were, as it had always been taken for granted that both sides of the tubes would be the same. In all the remaining diagrams only the projected form of pressure distribution curves are used.

Returning to tests with hole No.4, the four rows are taken separately and two tests have been made on each row. The areas have been taken for different sets of readings and in each case an average was made. The maximum and minimum curves are shown. Curves drawn from average values over a number of tests with different angles of inclination of the tube bank are represented on Plate No.23 and the rows are shown separately. The test hole is in the centre of the bank of tubes or mid-way between the headers. The curves with highest pressure occur when the bank is at 30 degree angle of inclination in all four cases. The other angle is 20 degrees.

The front pressure on the first row is highest and remains high for a 30 degree angle of rotation of tube. The second row tubes are subjected to the highest front row pressures. The pressure at the sides of the tubes are greatest in the third and fourth rows. At the back of the tubes the second and third rows approach atmospheric or datum pressure. Comparing the first and fourth rows the pressures are positive and negative respectively at the back of the tubes.

At the sides where the diagrams show a pressure loop the stream-line flow round the tube varies in each row. The first row break in the flow round the tube takes place about 75 degrees from front central position./

FIRST ROW AND SECOND ROW PRESSURE DIAGRAMS  
Bank of four rows  
POSITIONS 1A & 1B HOLE NO 2

FIG 1 - DEVELOPED PRESSURE DIAGRAMS ON BASIS OF ANGLES

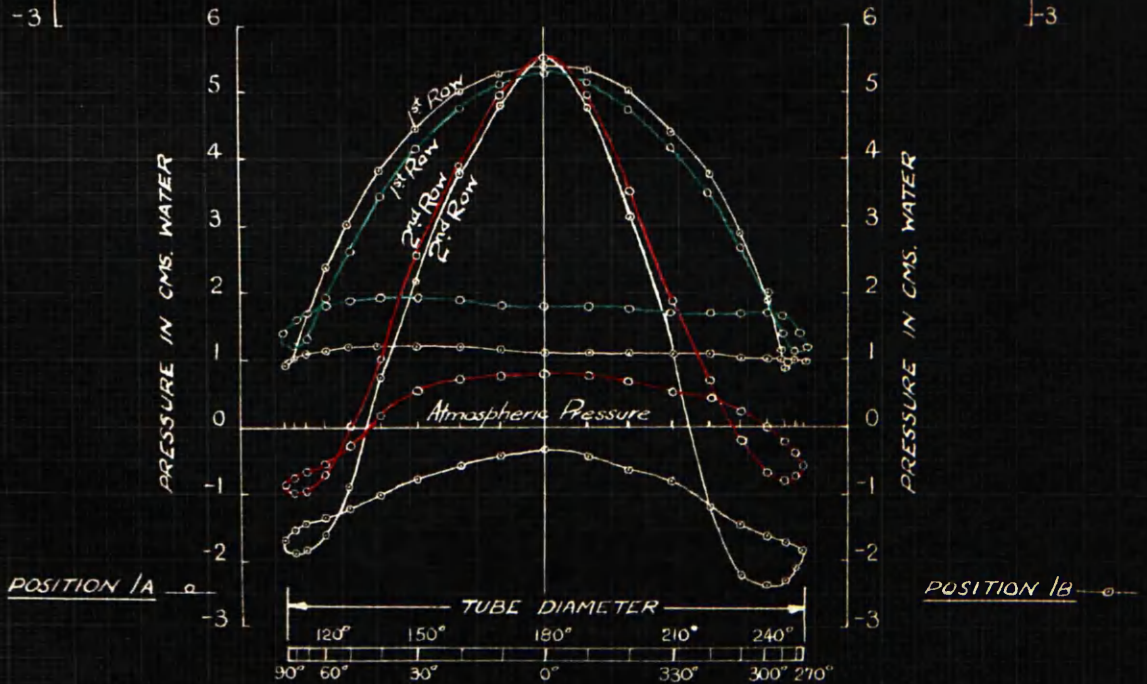
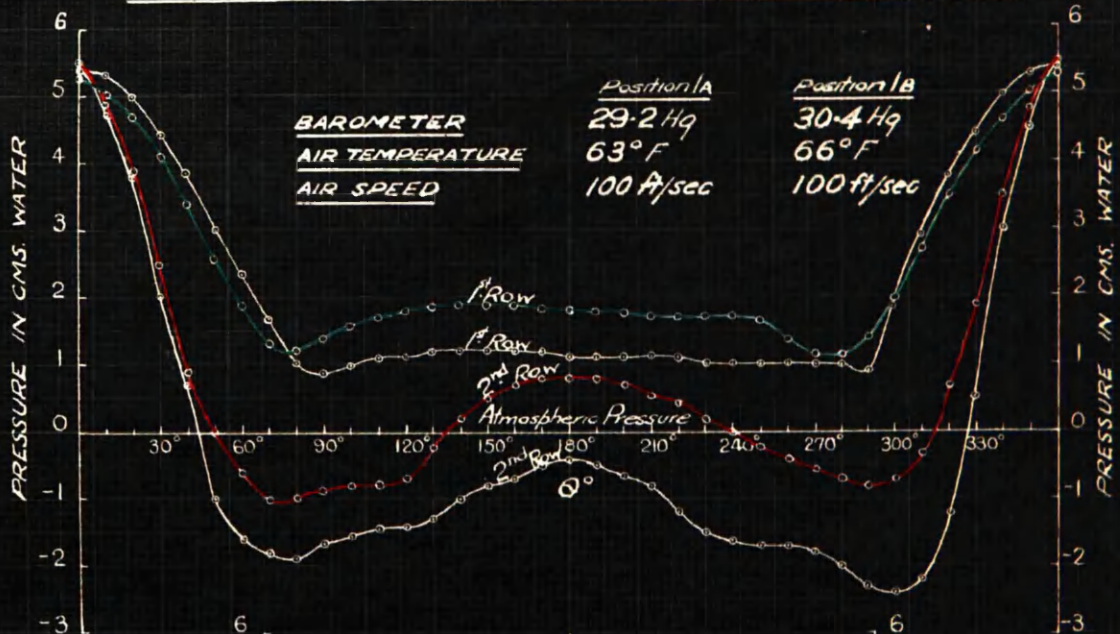


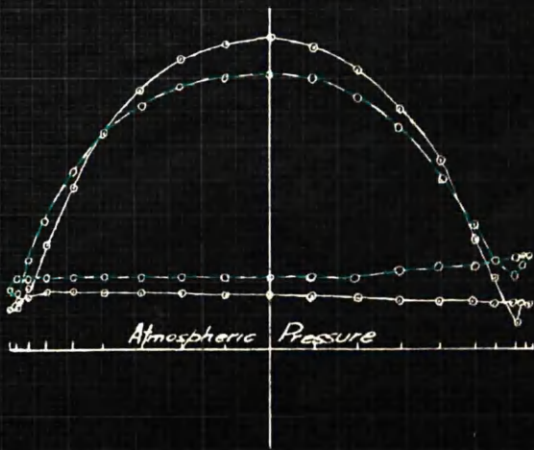
FIG 2 - PROJECTED PRESSURE CURVES ON BASIS OF SINES OF ANGLES

FIG - INFLUENCE OF TUBE RANK POSITION  
FORM DRAG DIAGRAMS

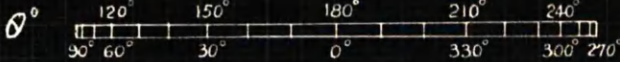
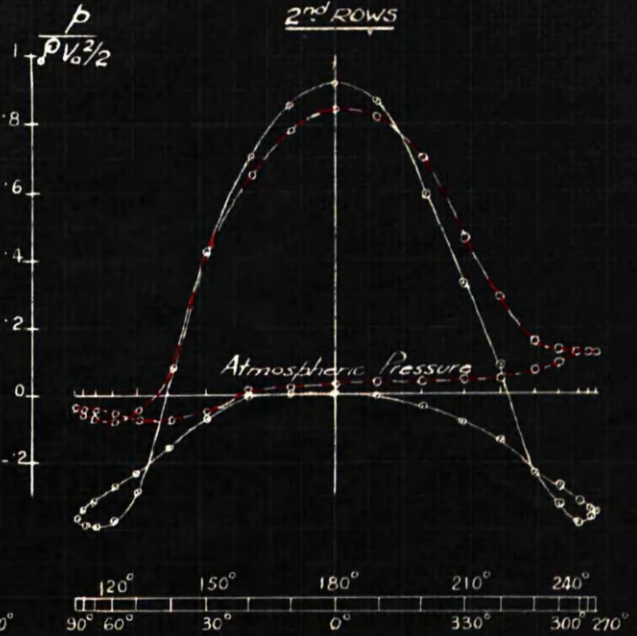
FOR  
POSITION 1A & 1B HOLE N°4

Without Baffles

1<sup>st</sup> ROWS

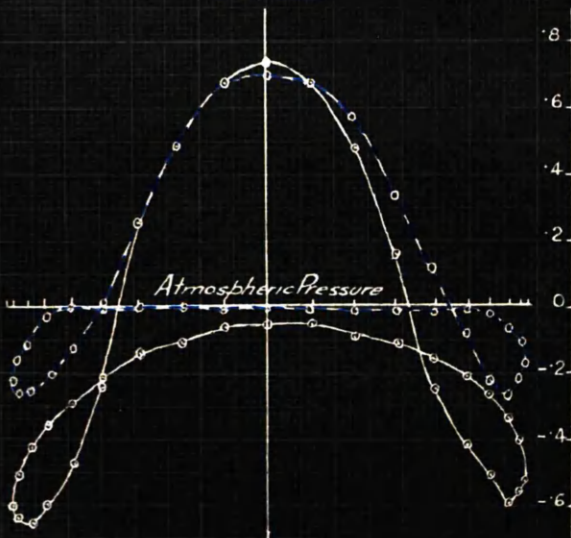


2<sup>nd</sup> ROWS

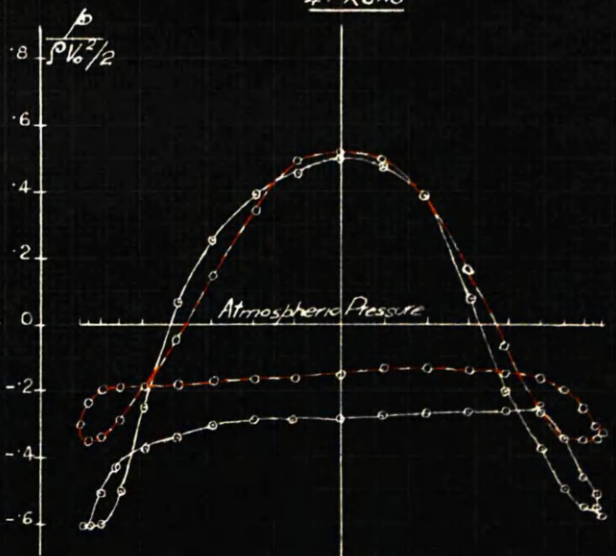


100 ft/sec

3<sup>rd</sup> ROWS



4<sup>th</sup> ROWS



POSITION 1A —○—

POSITION 1B -○-

/position. In the second row the band of pressure is released at about 50 degrees from the front central position, and it was in the zone from 50 degrees to 130 degrees that slag accumulated in the form of thick bulges in the boiler failure. The loop is a zone of falling and rising pressure with the third row the largest loop.

There is no doubt about the maximum front pressure in the inclined and vertical position of a bank of tubes. The second row has not only the maximum frontal pressure but it has also the minimum pressure at the back where drag takes place. The frontal pressure of the fourth row is the smallest and the diagram reverts back to the form-drag curve of the first row but with the pressure at 180 degrees greater than any of the other rows. This is readily understood as the stream flow returns to solid mass formation after leaving the fourth row.

In Plate No.24, for position 1B in which 30 degree inclination of bank was used, the pressure curves are shown for mid-position hole No.4 and for one hole No.2 below and No.6 above the central position. The test here is to show the pressures at different points along the tube models. The effect of the baffle plate is to make the frontal pressure at hole No.2 greater than the other two, but the total pressure in the bank is the same for all three curves, enclosed areas being equal.

It might be noted that No.2 hole would be slightly below the middle of the bend of the tube in the boiler, while hole No.4 is on the straight portion just below the bend. The pitch of the holes is one foot.

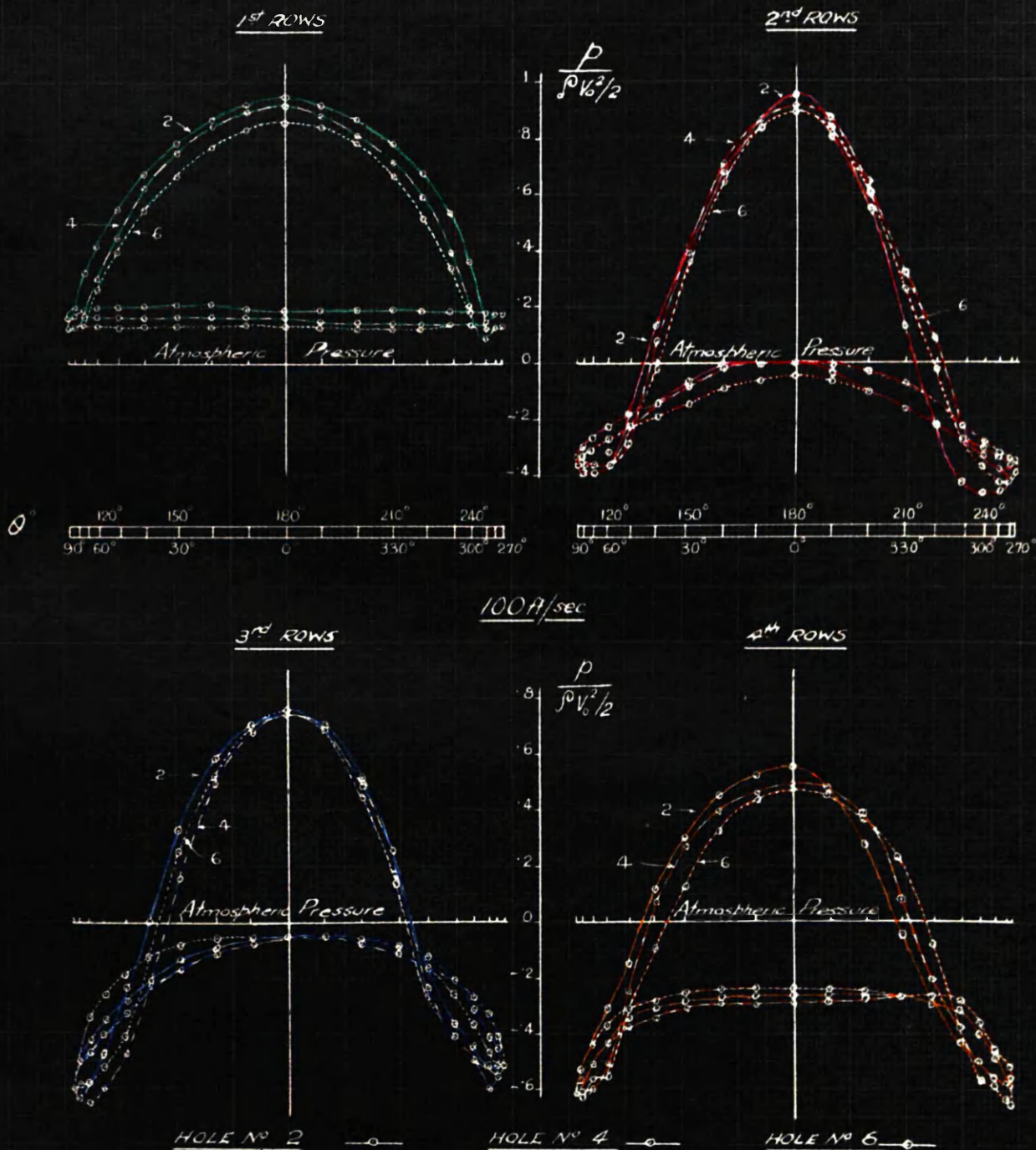
Consider now the influence of the baffles which are illustrated on Plate No.25. Curves have been drawn for position 2B and the bank inclination is retained at 30 degrees. The test holes are again No.2, 4 and 6. These positions are such that No.2 is absolutely clear of the top baffle, No.4 is just a little inside the baffle, while No.6 is enclosed entirely within the baffle plate influence.

The effect of this top baffle on the pressure distribution curves is clearly illustrated on Plate No.25. The rows are marked on each graph. The curves have the same characteristics but in each row and for all the three holes the back pressures at 180 degrees are above the atmospheric line. The pressure at the 180 degree point varies throughout the bank as they approach the datum line.

The total pressure throughout the bank is greatest at hole No.2 and has been tested for a hole nearer the bottom header since it was found that the pressure varied along the length of the tube.

FIG 1 - INFLUENCE OF TEST HOLE POSITION  
FORM DRAG DIAGRAMS  
FOR  
POSITION 1B HOLES N° 2, 4 & 6

Without Baffles

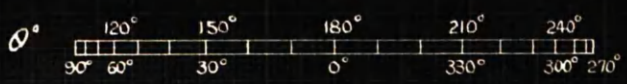
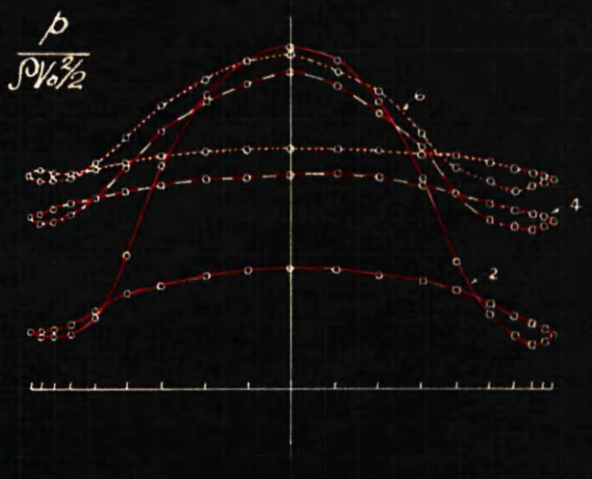
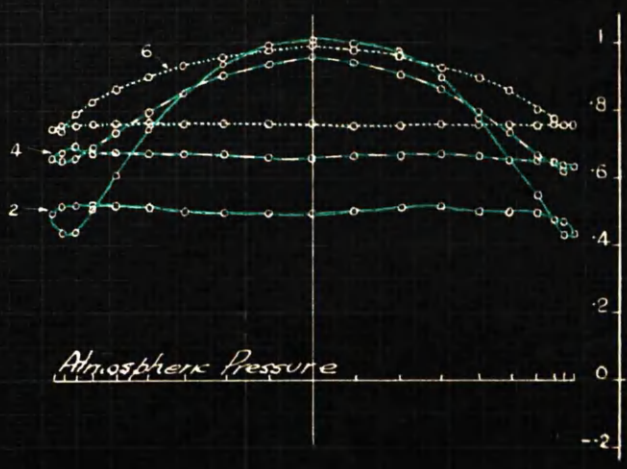


INFLUENCE OF TEST HOLE POSITION  
FORM DRAG DIAGRAMS  
 FOR  
POSITION 2B HOLES N° 2, 4, 6

With Two Baffles

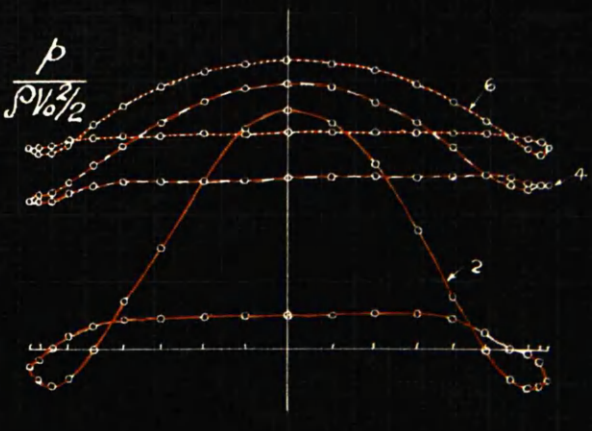
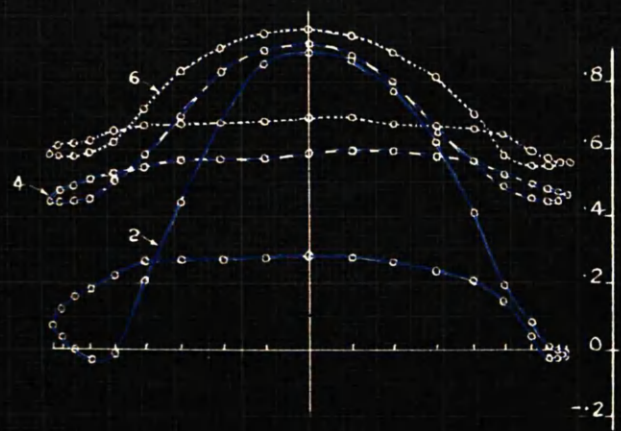
1st ROWS

2nd ROWS



3rd ROWS

4th ROWS



For comparison the tests have been plotted in four different sections on Plate No.26. Each set of curves is marked for the different rows. The top curve is with baffle plates and the bottom larger curve is without baffle plates. The change in back pressure is also clearly illustrated.

In order to compare the changes which the baffles make on the tests, one set of curves have been plotted from test data when all baffle plates are in use. Plate No.19 shows the position of baffles. The location of the baffles were changed and the effect of change of position is represented by the alteration to pressure distribution curves. Plate No.27 shows curves for all four rows with all baffles in use. Their position has been indicated with respect to tube bank.

The curves are shown for pressures taken at holes No.2, 4 and 6. It will be seen that all the curves conform to the usual characteristic but with all pressures above the datum or atmospheric line.

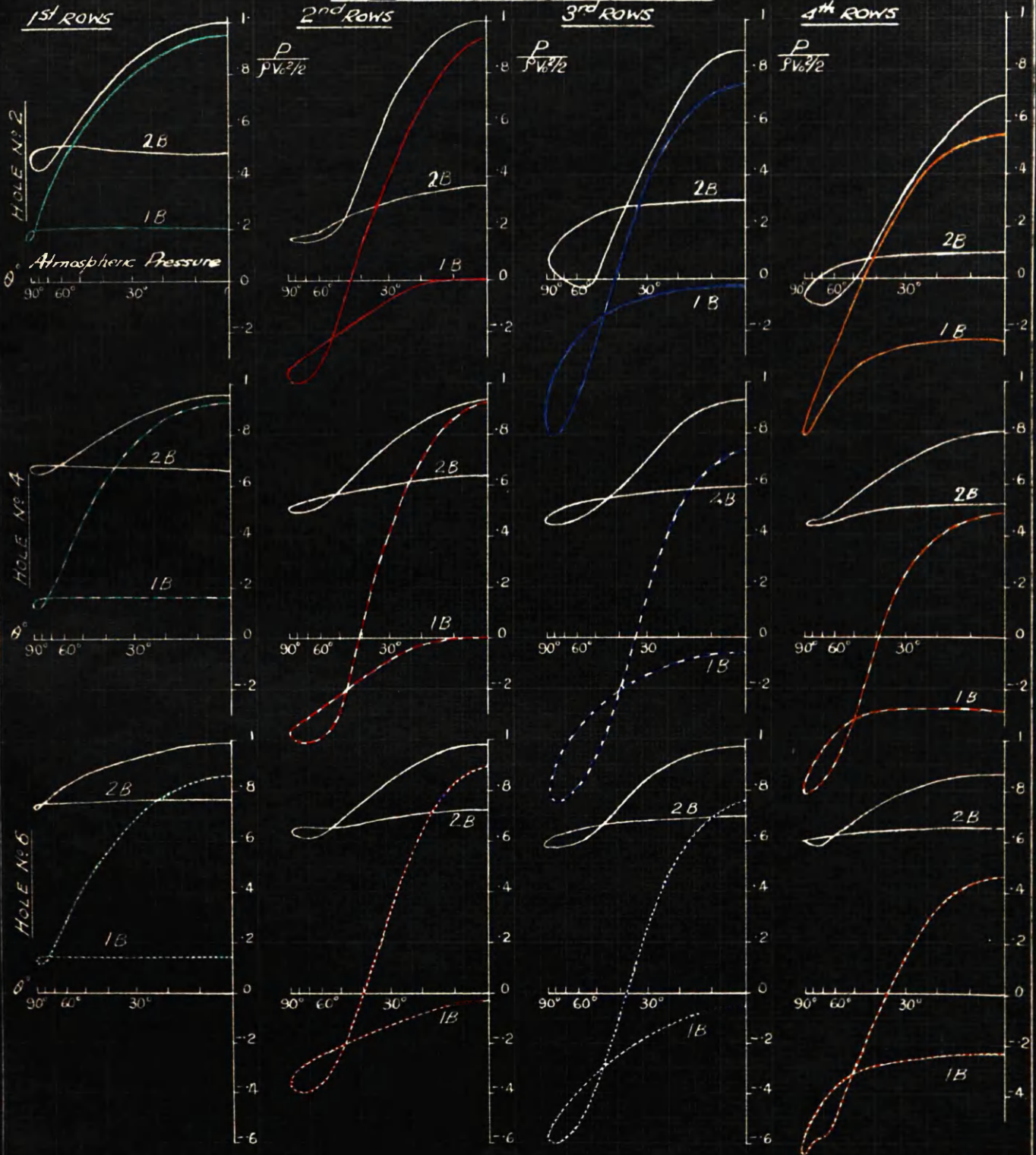
- (h) Features of Second Row Curves : Plates No.28 and 29 show a series of pressure distribution developed curves from 0 to 90 degrees. From these curves by differentiation the slope curves on Plate No.30 have been drawn for two positions on hole No.2. The gradient of the second row of tubes has the maximum value and occurs in the region of 30 to 40 degrees with and without baffles. The pressure is highest with the baffles at the point of maximum gradient. Consider the second row curves. It will be seen that the point of maximum gradient occurs without the baffles in use about 30 degrees, 1B, and with baffles at 35 degrees, 2B. On the developed pressure distribution curves these have been marked  $X_1$  and  $X_2$  and the pressures are  $0.35 p + \rho V_o^2/2$  and  $0.55 p + \rho V_o^2/2$  respectively. The point of minimum pressure is in the region of 75 degrees for baffled and unbaffled inclined banks of tubes under test

The pressure distribution curves show that in no case does the frontal pressure in the second row become lower than in any of the other rows. Some of the experiments show the second row frontal pressure to become slightly higher than that on the first row. In all cases the area of frontal pressure is less, giving a pressure per square inch of surface greater than in any of the other three rows.

The air stream breaks away from the face of the tube at an angle of 55 degrees from the front and connects up again at 125 degrees. These points on the front/

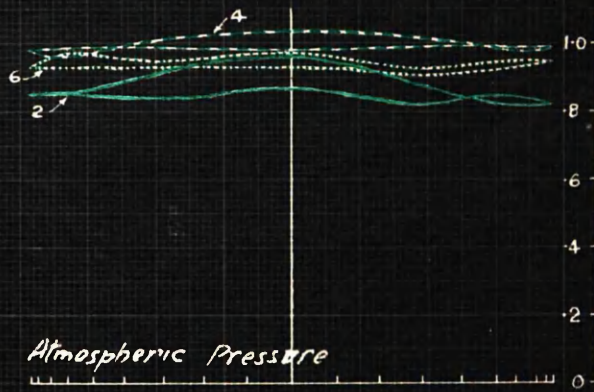
FORM DRAG DIAGRAMS

FOR POSITIONS 1B & 2B HOLES NO 2, 4 & 6

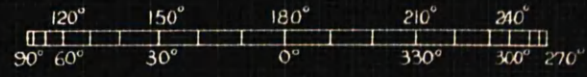
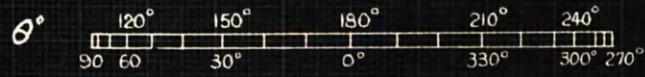
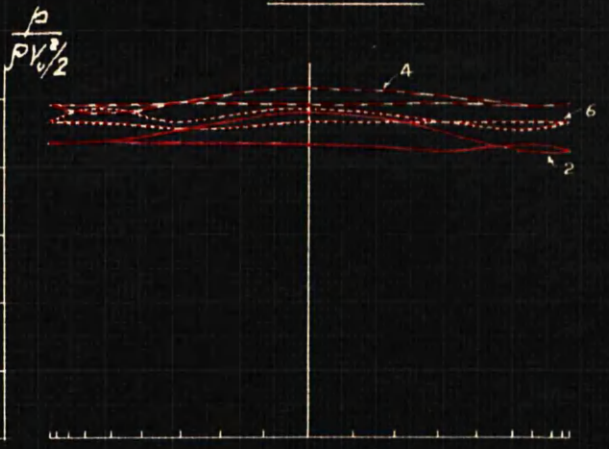


INFLUENCE OF TEST HOLE POSITION  
FORM DRAG DIAGRAMS  
FOR  
POSITION 3B HOLES N° 2,466  
With All Baffles

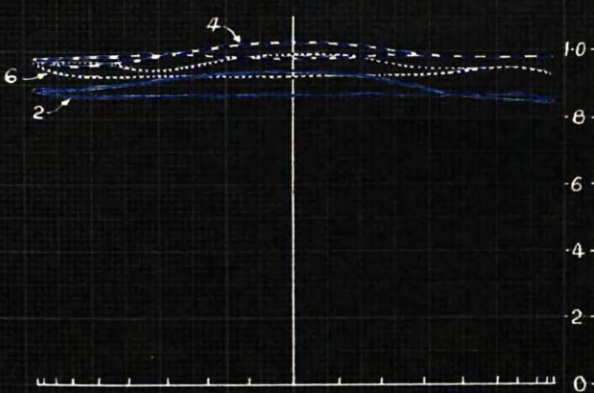
1<sup>st</sup> ROWS



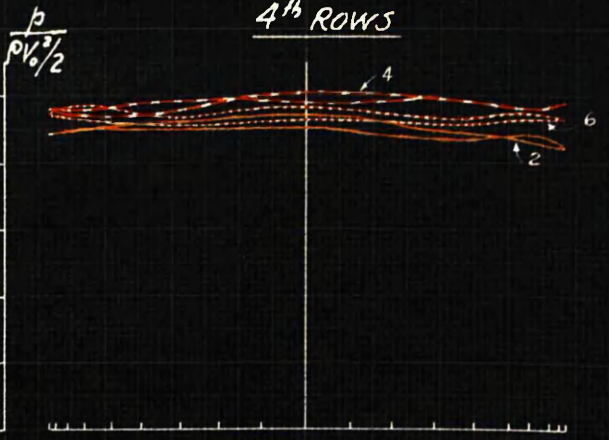
2<sup>nd</sup> ROWS



3<sup>rd</sup> ROWS



4<sup>th</sup> ROWS



PRESSURE DIAGRAMS  
from 0°-90°  
FOUR ROWS POSITION 1A & 1B

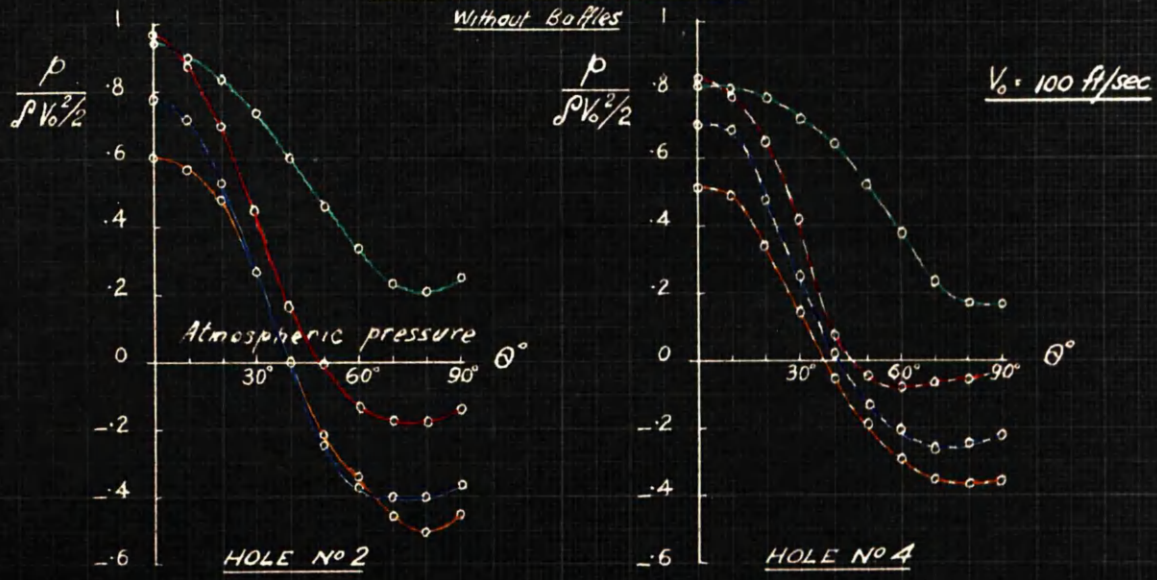


FIG 1 - POSITION 1A

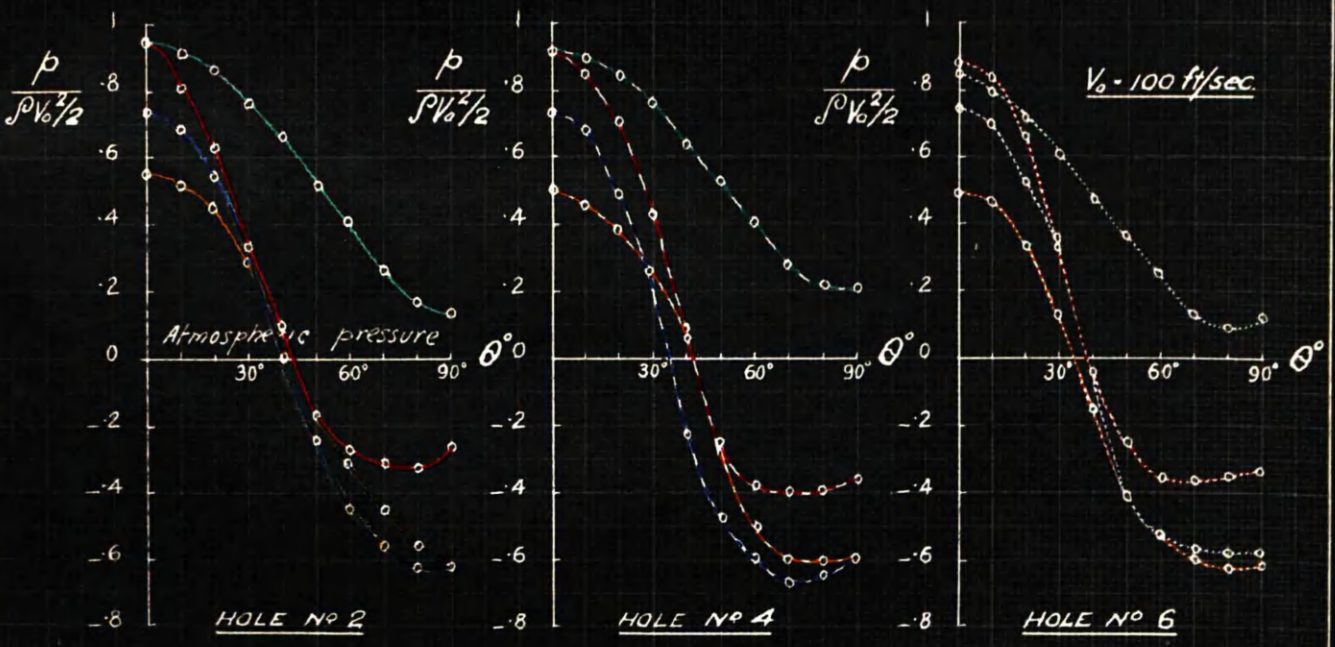
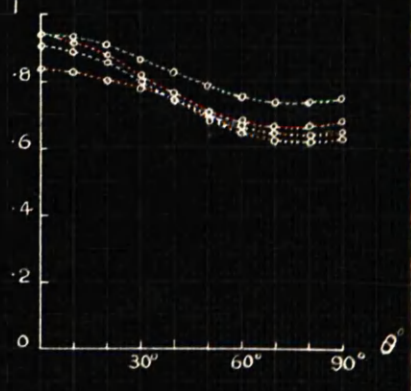
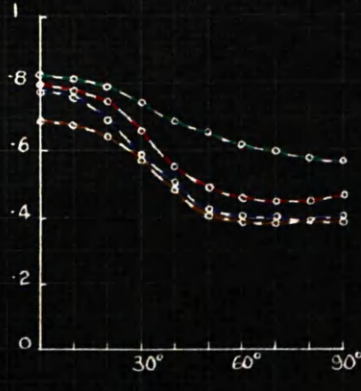
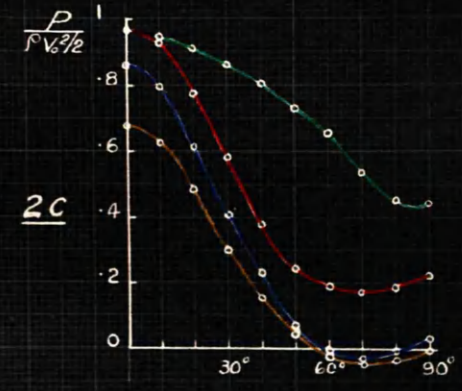
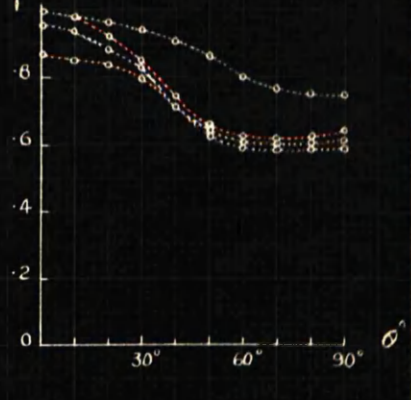
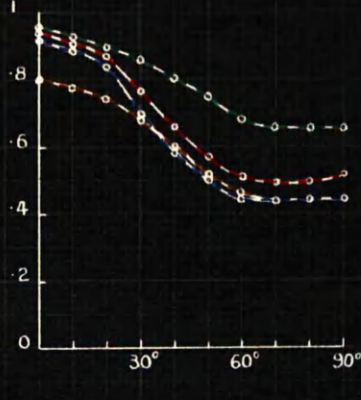
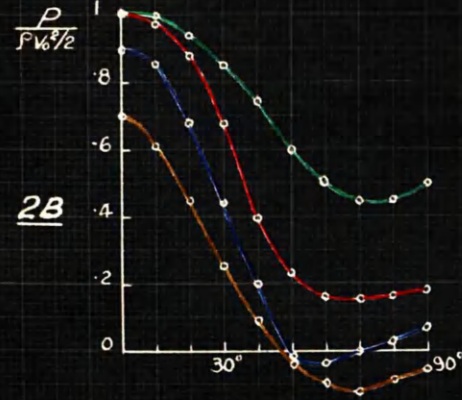
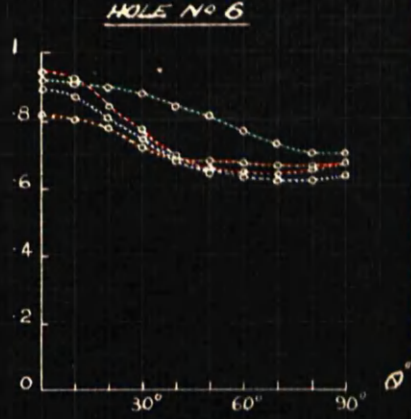
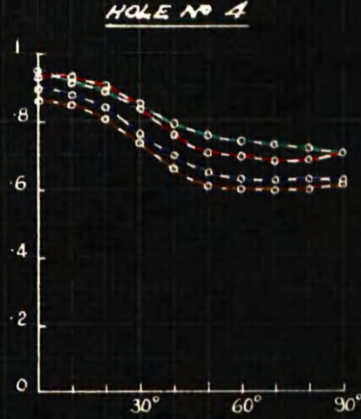
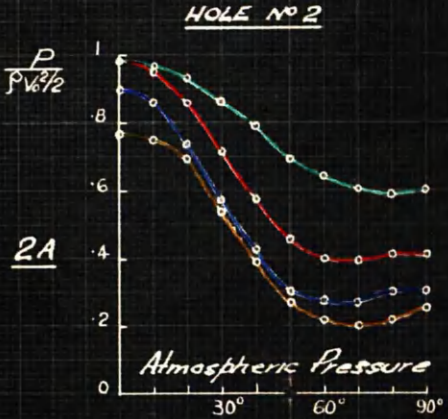
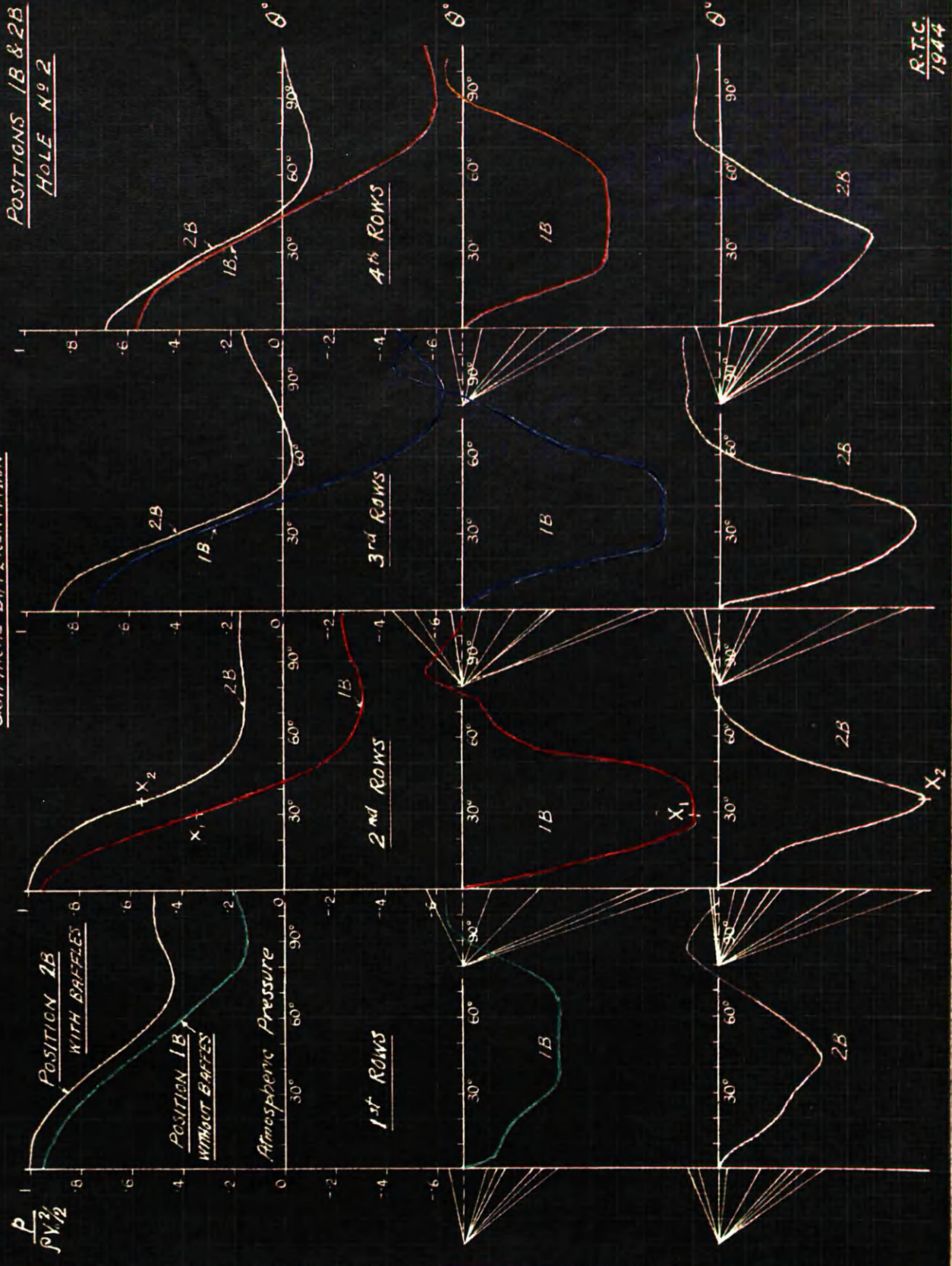


FIG 2 - POSITION 1B

PRESSURE DIAGRAMS  
FROM 0°-90°  
FOUR ROWS POSITIONS 2A, 2B & 2C  
With Two Baffles



GRADIENTS OF PRESSURE DIAGRAM  
GRAPHICAL DIFFERENTIATION



POSITIONS 1B & 2B  
HOLE N° 2

/front row are 80 to 100 degrees. In comparing the surface area of the front pressure on the third row it is found that , although the area is slightly less, the pressure on the second is much greater.

Comparing the pressure distribution on the second row tubes with and without baffles, it is found that the features of the curves are the same, but the baffles have the effect of increasing the pressure throughout the bank and the second row tubes are again the more severely worked. The gradient of the second row pressure distribution curves is always steeper than any of the others.

The tabulated results for the various tests carried out on the three positions, with and without baffles, are shown at the appendix.

Since the enclosed areas for the seven tests on the banks with all baffles in use were very small, indicating that the limitation of the tests in the large wind tunnel had been reached, it was decided to use a second wind tunnel designed for higher air speeds with adjustable baffles and smaller vertical tube models. This is fully illustrated and discussed in the next part of this section.

PART 4 - SMALL HIGH SPEED TRUNK EXPERIMENT.

- (a) Description of Plant : The small trunk employed in this series of experiments was arranged to use the air supply from a compressor. A large air receiver was available which could be supplied for either of two compressors, one steam driven, the other electrically driven. The trunk dimensions were determined so that, by the use of these machines, speed ranges up to 375 feet per second were possible.

The general arrangement is shown in Plate No.31, Fig.1. The supply from the receiver is regulated by the valve, the pressure before the valve being given on the gauge shown. An auxiliary valve was also fitted before the main valve for use in connection with smoke tests.

An enlargement view of the nozzle and trunk is shown on Plate No.32. The nozzle of rectangular form is only slightly smaller than the trunk into which it discharges, the nozzle dimensions being 2.5" x 0.3" and the trunk 3" x 0.5". The pressure drop through the nozzle is given by a manometer connected to the inlet and outlet positions indicated. The temperature before the nozzle and after the model tubes is measured by thermometer.

The trunk beyond the nozzle has a clear length of 9 inches. The experimental part is a box of the inner dimensions mentioned and outer dimensions 14" x 5" x  $\frac{1}{2}$ ". As the nozzle plate was bolted to a circular flange, the box could be placed vertically or horizontally as required. Single tubes or groups of several rows could be inserted in the box. Plate No.31, Fig.2 shows single tubes in vertical and angled positions, while groups are indicated in Plate No.31, Fig.3 and in Plate No.32.

The effective length of the tubes is  $\frac{1}{2}$  inch and the hole for the measurement of pressure is  $\frac{1}{32}$  inch diameter. The tubes are fitted with a dial arrangement at the top end which indicated the position in degrees.

In Plate No.33, Figs.1 to 4, a single row and two rows with different pitches of  $\frac{5}{8}$  inch to  $1\frac{1}{4}$  inches are shown. In Figs.5 to 8 the pitch is  $\frac{5}{8}$  inch and the arrangement is for a single, two, three and four rows. All the tests in this series were carried out without baffle plates.

PLATE - 31 -

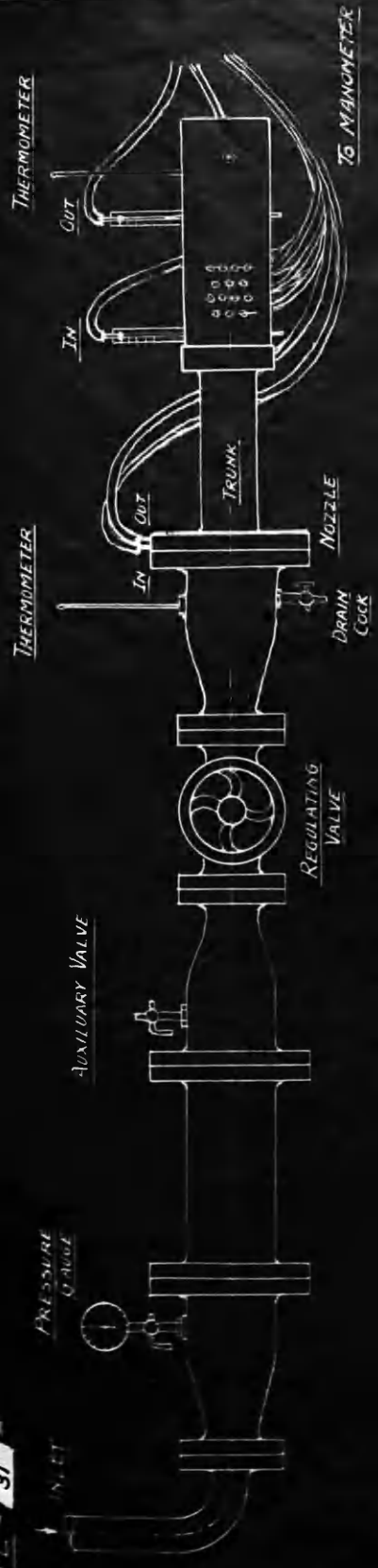


FIG. 1 SMALL HIGH SPEED TRUNK ARRANGEMENT



FIG. 2

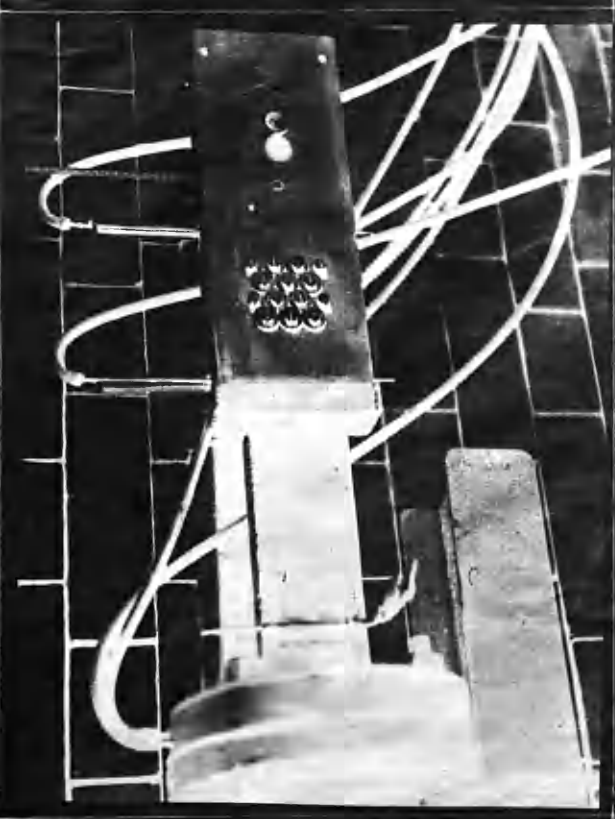
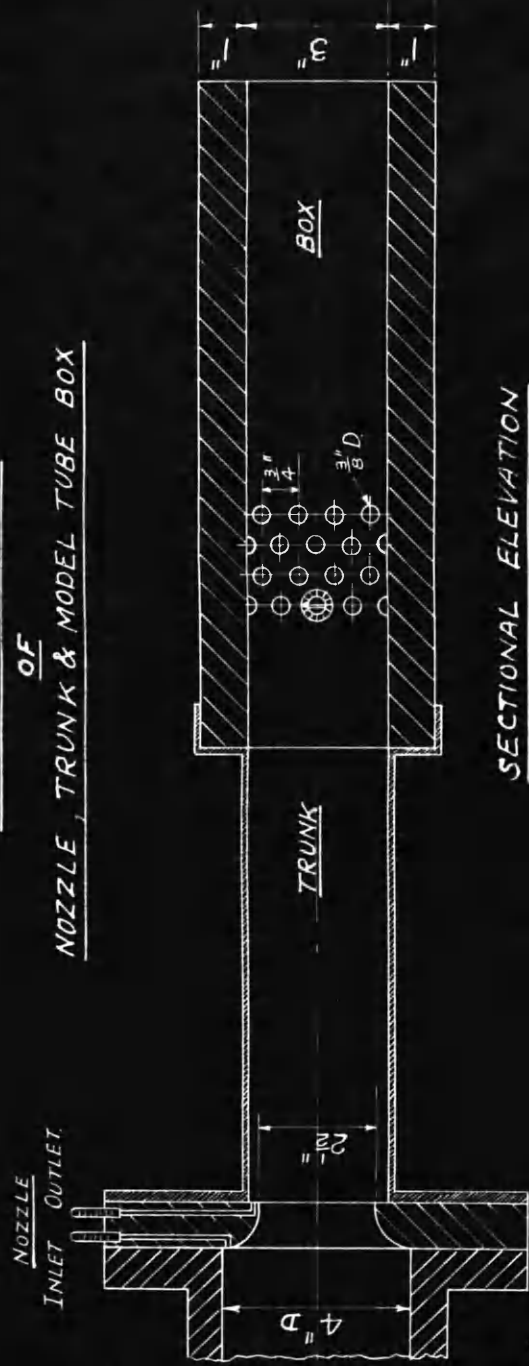


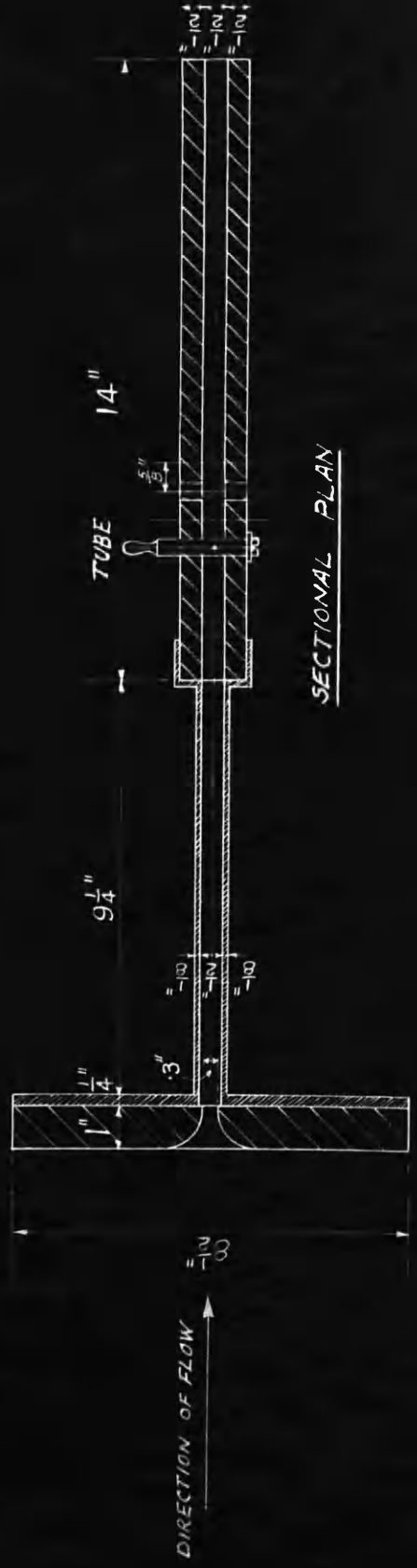
FIG. 3

ENLARGEMENT VIEW  
OF  
NOZZLE TRUNK & MODEL TUBE BOX



SIDE VIEW OF NOZZLE

SECTIONAL ELEVATION



SINGLE AND MULTIPLE TUBE ARRANGEMENT

TRANSVERSE PITCH  $\frac{3}{4}$ " THROUGHOUT



FIG. 1



FIG. 2



FIG. 3

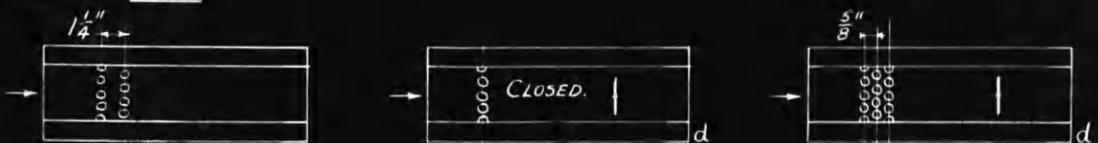


FIG. 4



FIG. 9



FIG. 11

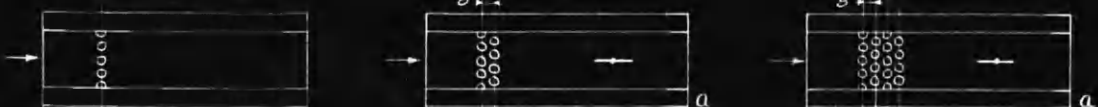


FIG. 5



FIG. 6

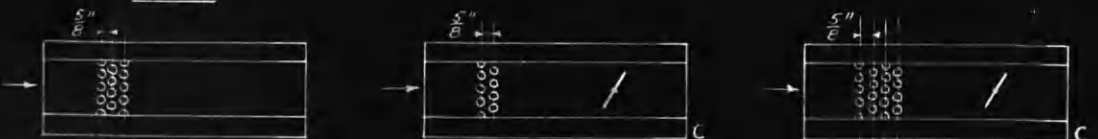


FIG. 7



FIG. 8



FIG. 10



FIG. 12

A baffle plate  $2\frac{1}{2}$ " x  $\frac{1}{2}$ " x  $\frac{1}{8}$ " is fitted in the next series of tests. The baffle plate could be easily turned by hand to the required opening. Figs. 9 to 12 show the tube arrangement for  $\frac{5}{8}$  inch staggered pitch. The position of the opening of the baffle is shown.

In Plate No. 34, Fig. 13 is shown the arrangement of two rows having staggered pitches of  $\frac{5}{16}$  to  $1\frac{1}{4}$  inches. Fig. 14 shows a two row arrangement with pitches  $\frac{1}{4}$  to  $2\frac{1}{2}$  inches. Fig. 15 is staggered arrangement for four rows with pitches  $\frac{5}{16}$  to  $\frac{15}{16}$  inch. Fig. 16 is a four row chain arrangement with pitches  $\frac{5}{8}$  to  $1\frac{1}{4}$  inches.

The tube models in these tests are  $\frac{3}{8}$  inch diameter and fitted into the box with the open end connected to the manometer tubes.

In Plate No. 34, Figs. 17a and 18a single tube arrangement for vertical and angled positions is used. In these tests  $\frac{1}{8}$  inch diameter tubes are used. The tubes have been placed parallel to the long side of the trunk. Figs. 17b and 18b are for multiple tube arrangement for vertical and angled positions for four staggered rows. The diameter of the model tubes in these tests is  $\frac{3}{16}$  inch and the inside dimensions of the box are  $3 \times \frac{3}{4}$  inches.

In running the experiments it was necessary in the case of the steam-driven air compressor to keep the number of revolutions as constant as possible. The steam stop valve opening had to be carefully adjusted during the long period tests as an alteration in steam pressure gave a higher air pressure with a corresponding higher air speed at nozzle. There was adjustment between the receiver and the nozzle so that constant pressure of air as it entered the trunk could be ensured.

The tubes were then joined to the manometer and pressure readings were obtained from which the velocities can be calculated. The size of the nozzle is  $2.5 \times 0.3$  inches, the coefficient of discharge is 0.963 obtained by calibration with a standard nozzle and the formula  $v = C\sqrt{Th/p}$  gives the velocities where T = absolute temperature °F.

h = difference between inlet and outlet across nozzle.

p = Outlet pressure of nozzle + barometer in Cms. Hg.

C = constant = 57.

STAGGERED AND CHAIN ARRANGEMENT

TRANSVERSE PITCH  $\frac{3}{4}$ " THROUGHOUT.

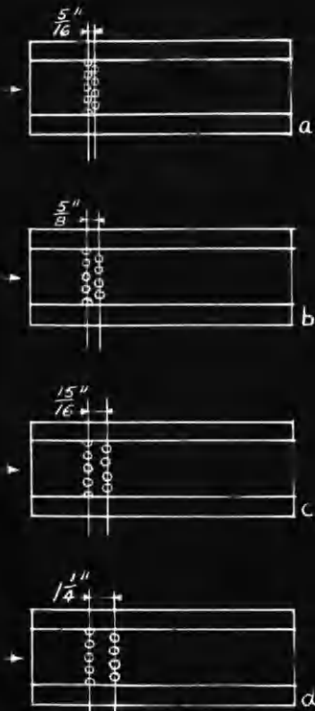


FIG. 13

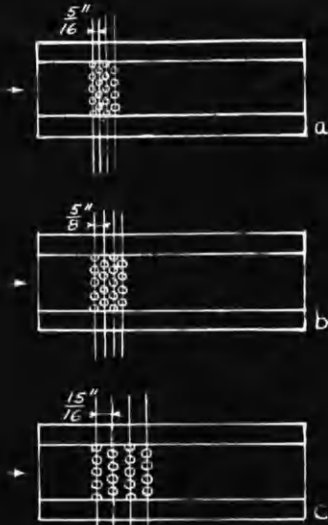


FIG. 15

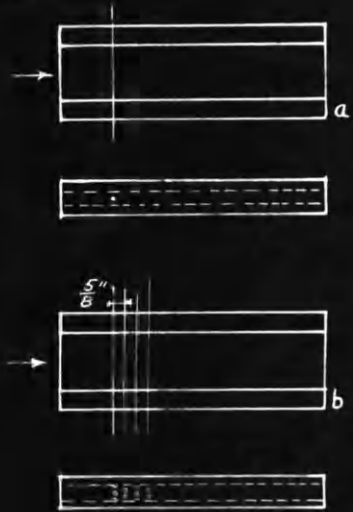


FIG. 17  
(VERTICAL)

STAGGERED  
(HORIZONTAL)

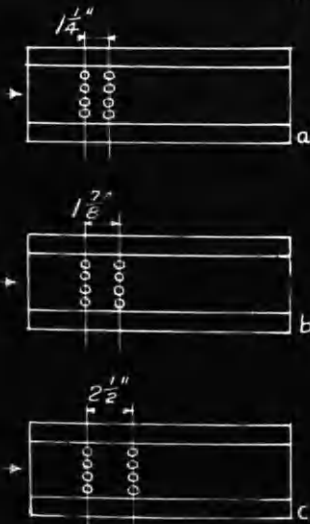


FIG. 14

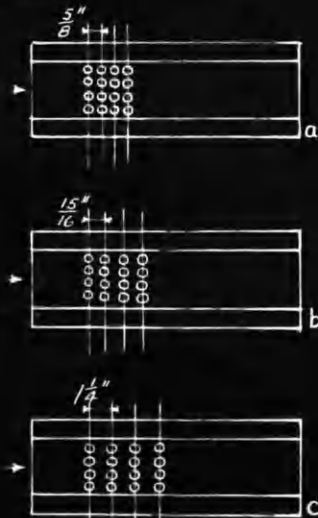


FIG. 16

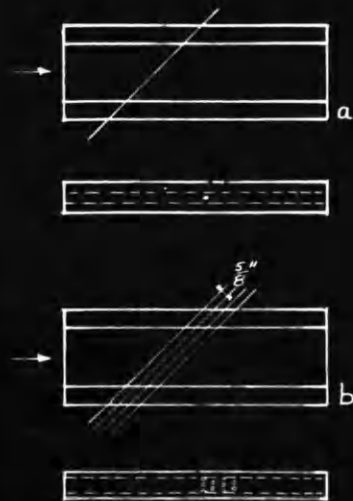


FIG. 18  
(ANGLED 45°)

CHAIN  
(HORIZONTAL)

- (b) Single Tube Readings : In the first set of tests a single tube was used in the box without baffle plate. A tube of 1/8 inch diameter was used for the vertical and inclined positions. Three test pressure holes are used as shown in Plate No.35, Figs.1 and 2. In the horizontal position a 3/8 inch diameter tube is used with a test pressure hole at centre as shown in Fig.3.

The model tubes can be turned at 30 degree intervals. Great care had to be taken to have these made tight in box after each angular rotation. The pressure readings were taken by two manometers, one using water and the other mercury according to the range of pressure readings.

The tables of pressure readings before the nozzle and at the test tube holes are shown at the appendix. Column (1) gives angular position of holes, with corresponding temperature T °F for pressures at the test holes which are taken at one time - first, 1 inch above the centre line, second, on the centre line and third, 1 inch below the centre line of the box. For example - 0° angle of turn readings are taken for the 1/8 inch diameter test model tube with 1/32 inch hole. These have been tabulated as 5 cms. Hg at entrance to nozzle with temperature 75.8°F, while exit pressure is -0.5 cm Hg below atmospheric pressure. The tube is in vertical position during this test and the pressure at the hole, 0 degree to 180 degrees, indicates a change from 2.8 to 1.5 cms. of Hg on the manometer. The pressure distribution curve of this reading is shown on Plate No.35, Fig.6, with hole 1 inch above centre.

Fig.4 shows the pressure curves for the four holes shown on the vertical tube in Fig.1. Two pressure curves are plotted in Fig5, one for a vertical tube and the other for a horizontal tube. Figs.6 and 7 show curves for vertical and inclined positions and are plotted with three test holes.

- (c) Multi Tube Readings : After completing the tests on the single vertical tube, banks of tubes were tested. The first was a two row arrangement with four tubes in front row but the walls of the box partitioned off the tube and gave only three full and two half tubes under test condition. The second row was staggered with four full tubes in this row. Readings of pressures and temperatures were taken as in single row experiments.

From the readings of angle of turn of tubes and pressures in cms. of Hg the curves have been plotted as shown for staggered and chain arrangement on Plate No.36, Figs.1 and 2, for pitches 5/16 to 1 1/4 inch and 5/8 to 2 1/2 inches/

SINGLE TUBE TESTS

ON VERTICAL, INCLINED & HORIZONTAL TUBES

FIG. 4  
Vertical Tube

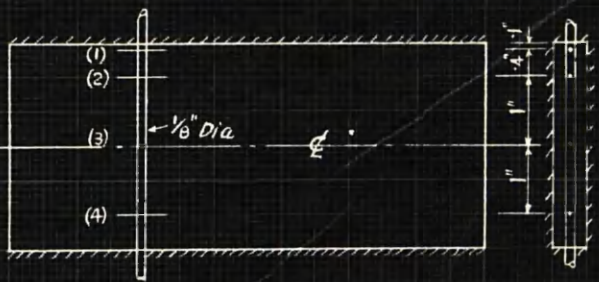


FIG. 1  
Vertical Tube

FIG. 5  
Vertical and Horizontal Tube

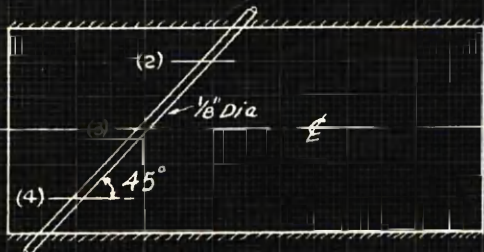
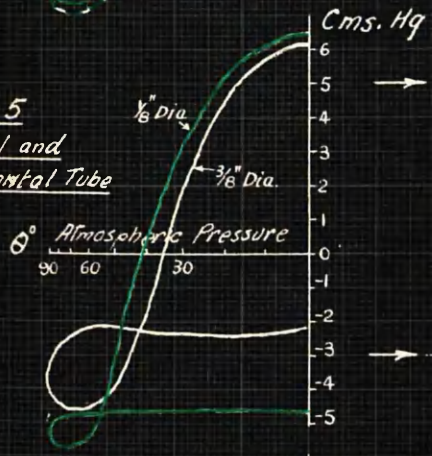


FIG. 2  
Inclined Tube

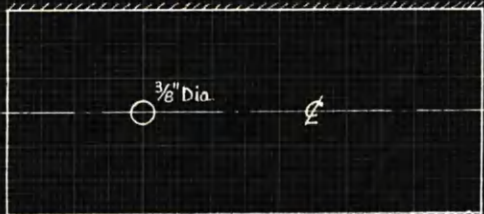


FIG. 3  
Horizontal Tube

FIG. 6  
Vertical Tube

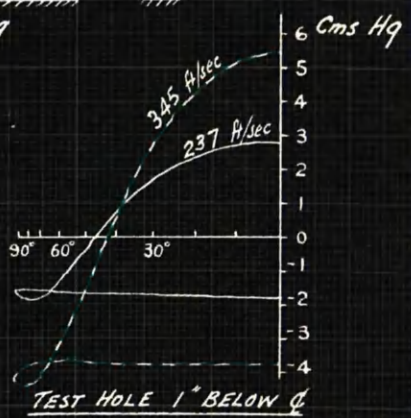
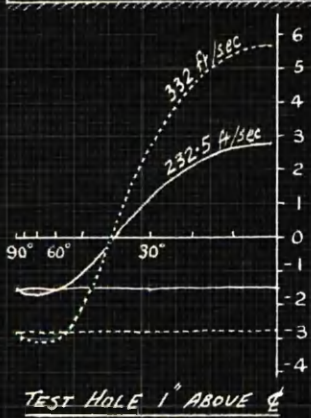
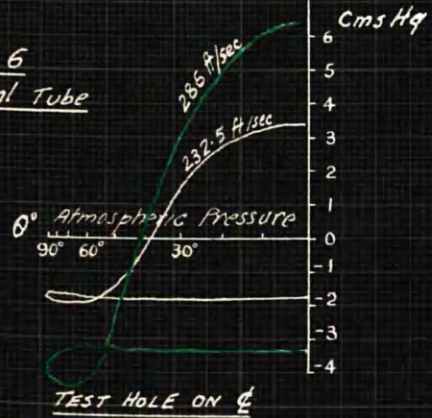
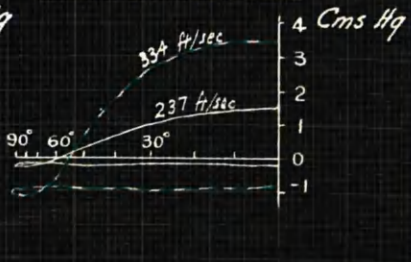
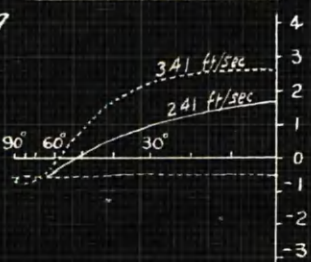
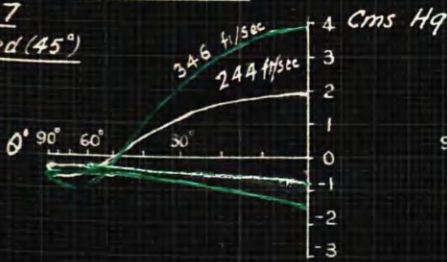


FIG. 7  
Inclined (45°)



FORM DRAG DIAGRAMS FOR TWO ROWS WITHOUT BAFFLE PLATE  
FOR STAGGERED & CHAIN - VARIOUS PITCHES

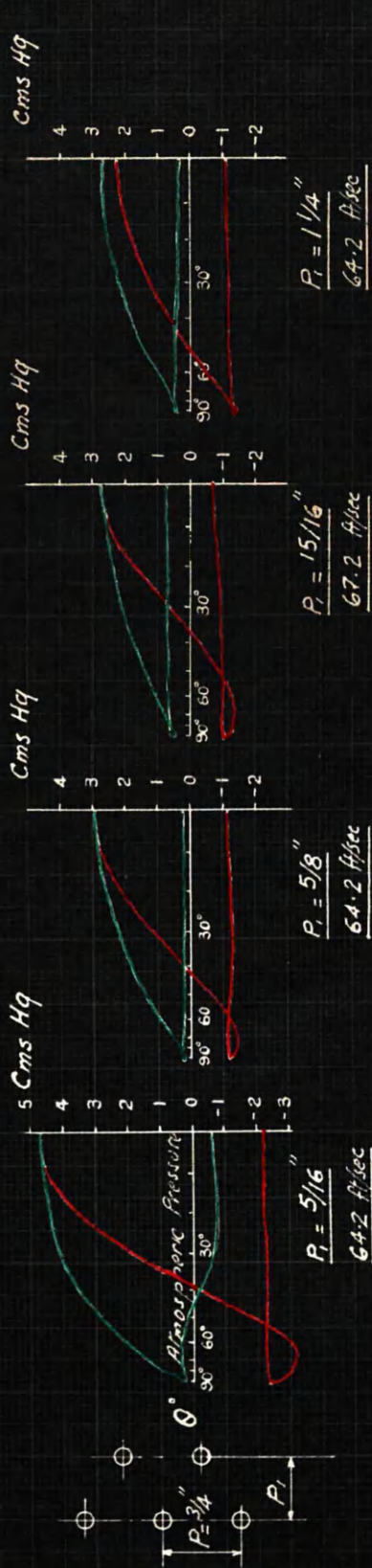


FIG. 1 - STAGGERED

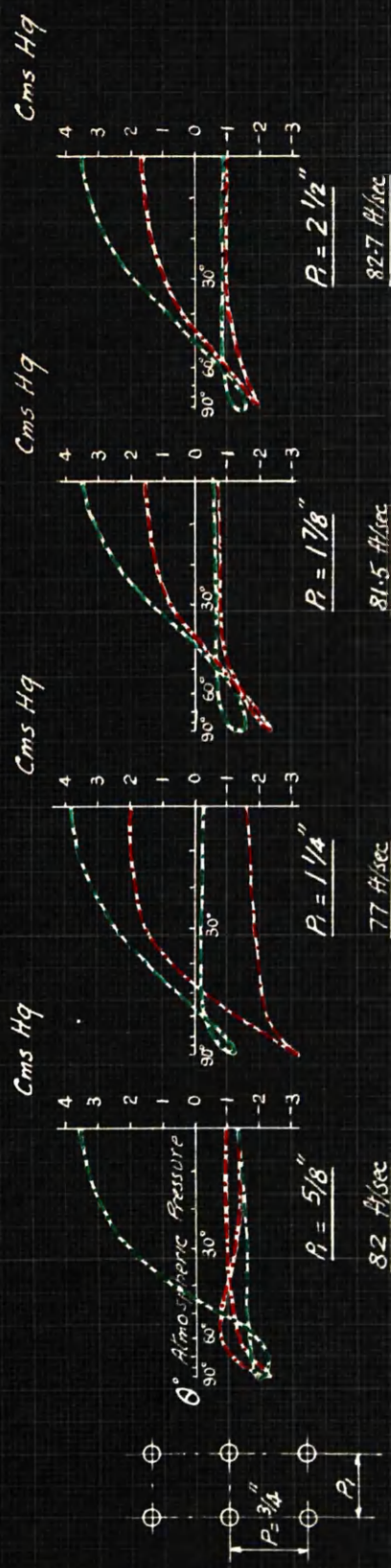


FIG. 2 - CHAIN

/inches respectively. These show similar features, the gradient of the second row being steeper than the first row, and the first row curves are similar in all respects to single row tests.

The same tests were made with staggered and chain arrangement of three and four rows in bank of model tubes. These tests were made without a baffle plate as shown in Plate No.34, Figs.13 to 16.

In the series of experiments with baffle plate, the pitch of tubes and arrangement of baffle have been kept in agreement with those of the Water Tube Boilers. This was done in order to get close co-ordination between small test laboratory experiments and workshop practice. From the pressure readings taken, curves have been plotted for first, second, third and fourth rows for four boxes fitted with one, two, three and four row banks. Plates No.37 and 38 show the pressure curves for this set of series.

With the trunk turned so that the long side is vertical, the effective length of tube is 3 inches and there are three test tube holes  $1/32$  inch diameter in the  $3/16$  inch diameter tube. In these series of experiments only two tubes are in each row. The tubes are again in staggered formation and four rows in bank as shown in Plate No.34, Fig. 17b.

A short series of tests were carried out on the vertical position but with tubes in chain arrangement. These are shown on Plates No.39 and 40, for comparison with practice with stay tubes in boilers.

- (d) Angled Tube Readings : In this set of experiments the banks of tubes were placed in an inclined position to the direction of flow of air. The angle of inclination was 45 degrees.

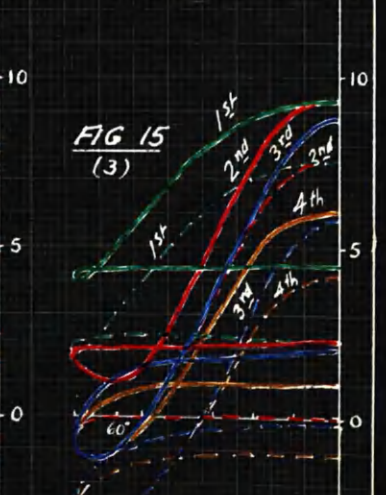
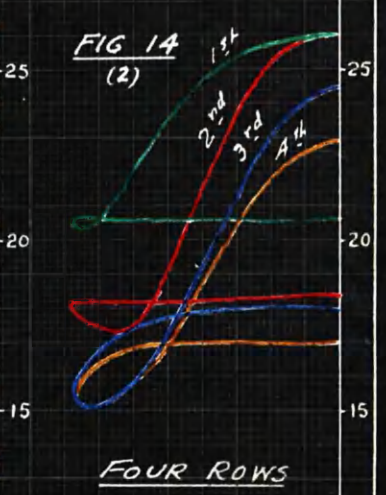
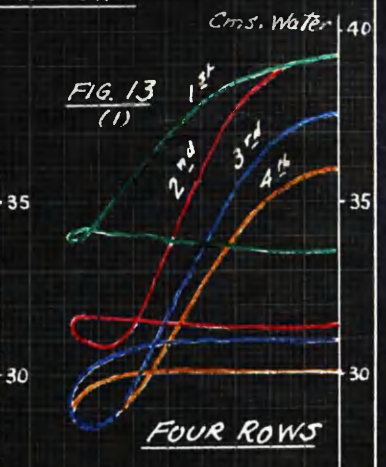
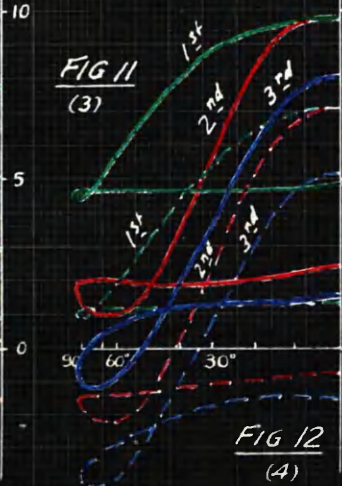
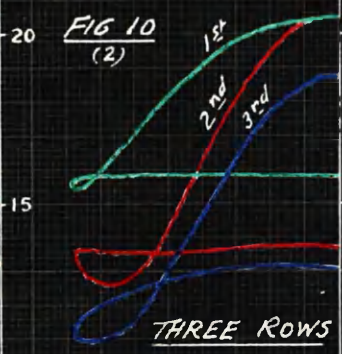
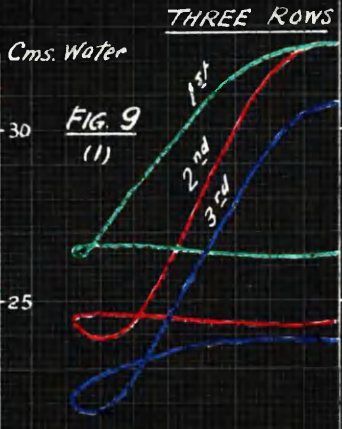
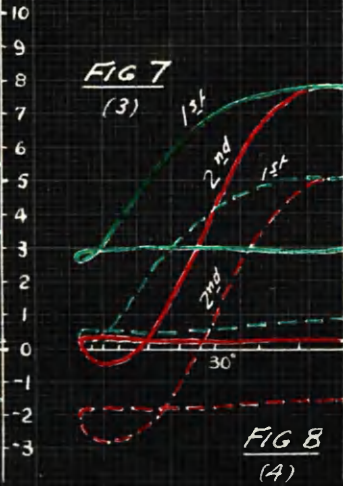
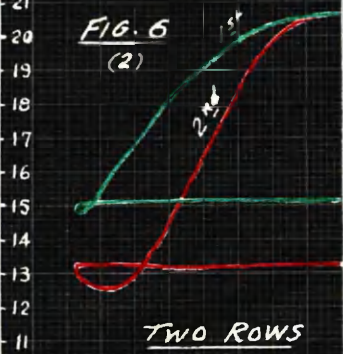
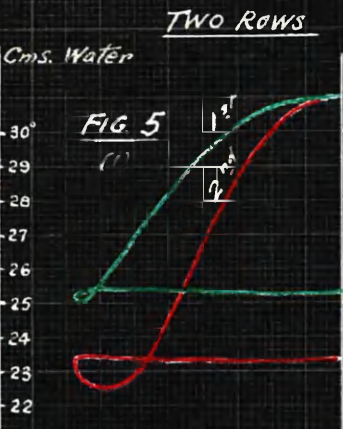
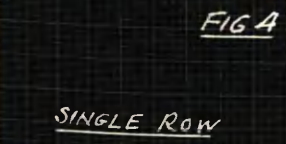
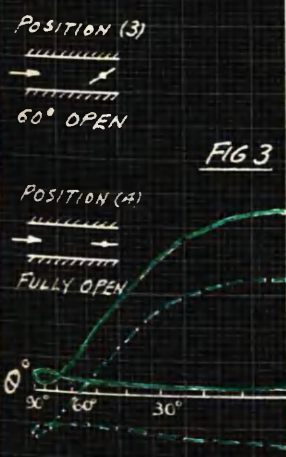
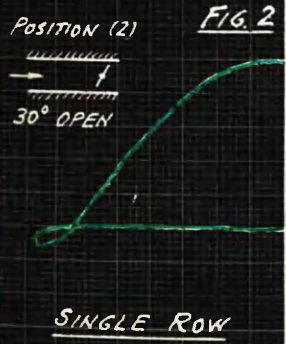
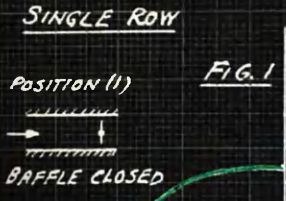
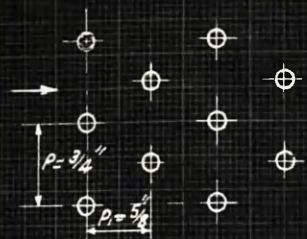
The readings taken are tabulated at the appendix for single and multi tube angled readings. The length of tubes under test was approximately  $4\frac{1}{4}$  inches long.

The first set of pressure readings was taken when the test holes were drilled at right angles to the axis of the tubes. The second set was obtained when the holes were drilled so as to lie along the trunk axis, that is, 45 degrees to axis of tube. No difference in the results were found.

In the inclined position of tube the/

FORM DRAG DIAGRAMS FOR SINGLE, TWO, THREE & FOUR ROWS  
FOR 5/8" PITCH - STAGGERED WITH BAFFLE  
PLATE IN FOUR DIFFERENT POSITIONS

ON  
ONE COMMON DATUM LINE



SINGLE ROW

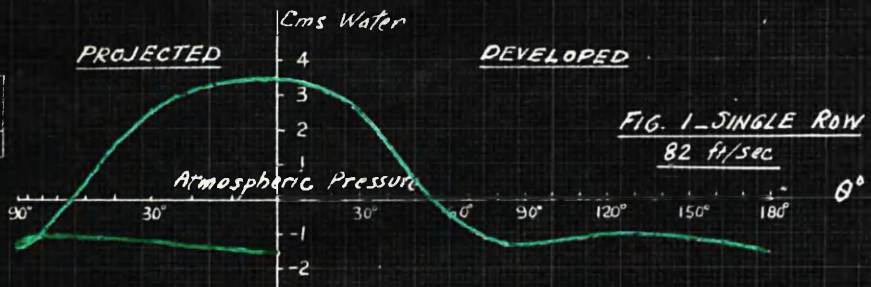
TWO ROWS

THREE ROWS

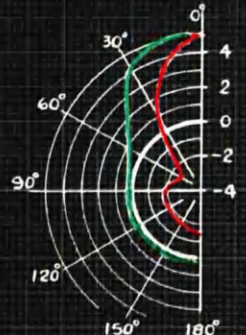
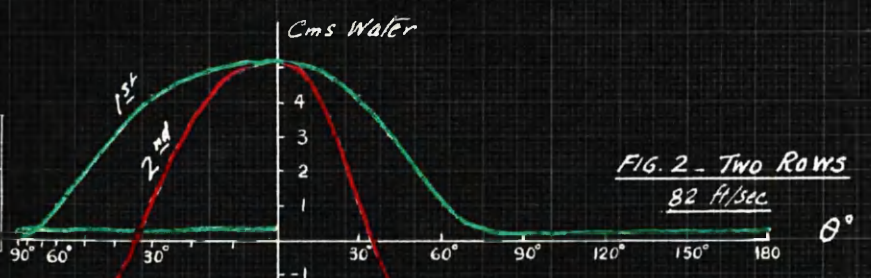
FOUR ROWS

PRESSURE DISTRIBUTION CURVES FOR 5/8" PITCH  
WITH BAFFLE FULLY OPEN  
STAGGERED

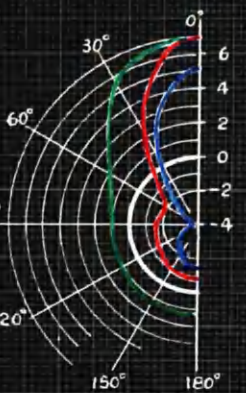
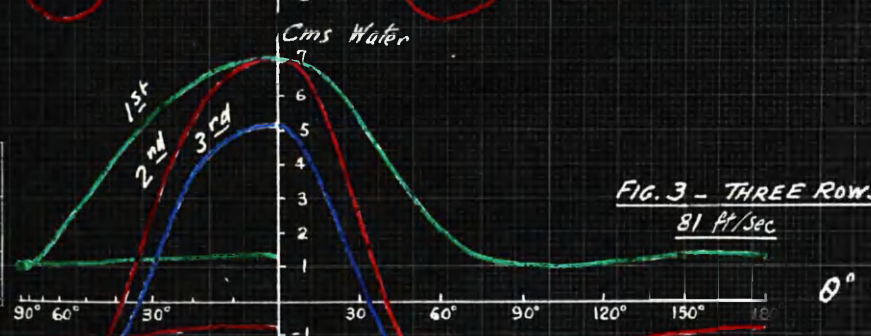
Mean Ord.	Area Cms <sup>2</sup>
3.06	5.9



Mean Ord.	Area Cms <sup>2</sup>
3.01	5.8
2.54	4.9
Av. M.O.	2.77 Cms



Mean Ord.	Area Cms <sup>2</sup>
3.48	6.7
3.11	6.0
2.54	4.9
Av. M.O.	3.04 Cms



Mean Ord.	Area Cms <sup>2</sup>
3.17	6.1
2.96	5.7
1.66	3.2
1.2	3.2
Av. M.O.	2.36 Cms

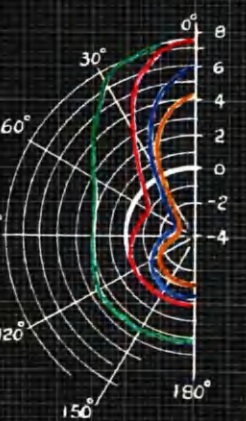
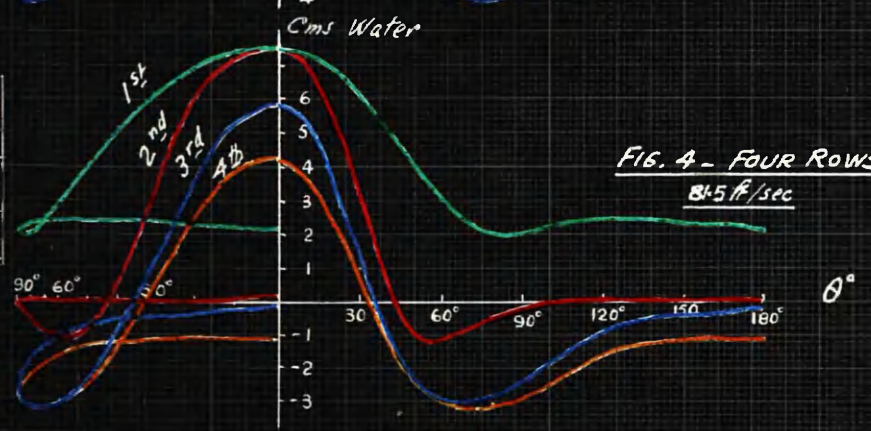


PLATE 39

DEVELOPED PRESSURE DIAGRAMS FOR FOUR ROWS  
CHAIN & STAGGERED ARRANGEMENT  
VARIOUS SPEEDS - PITCHES 1/4" - 5/8"



FIG. 1 - CHAIN P 1/4"

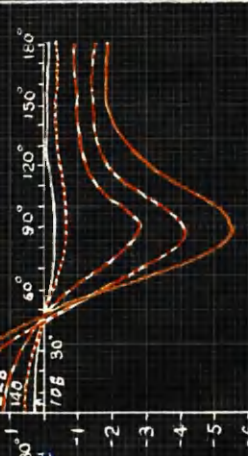


FIG. 2 - CHAIN P 5/8"

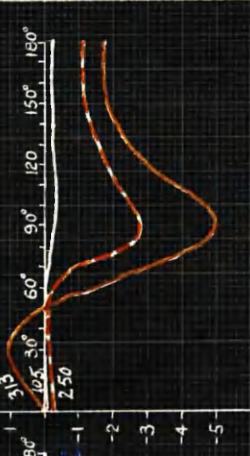
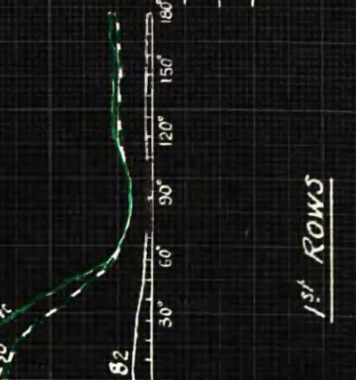
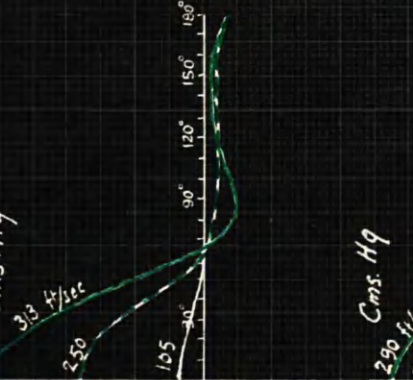
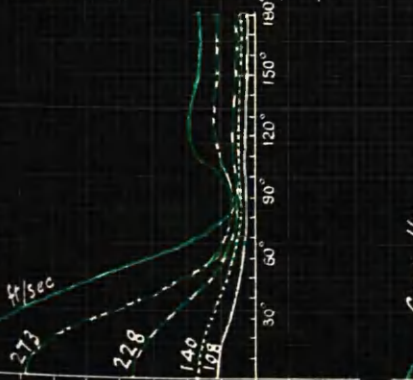
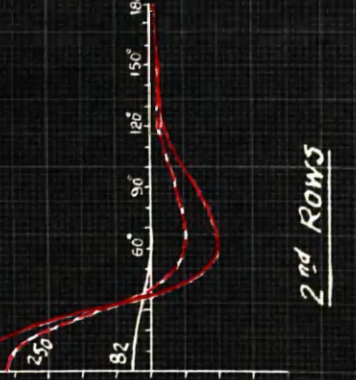
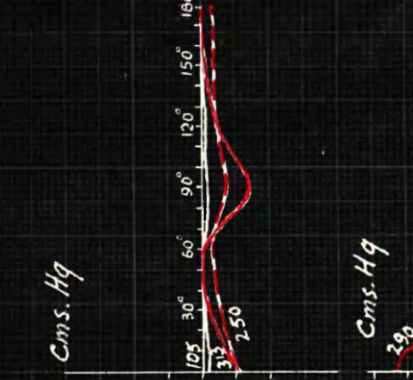
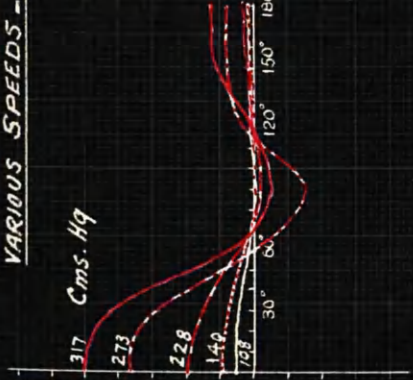
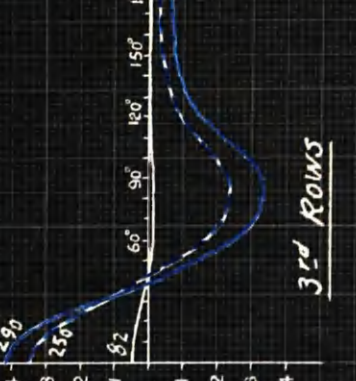
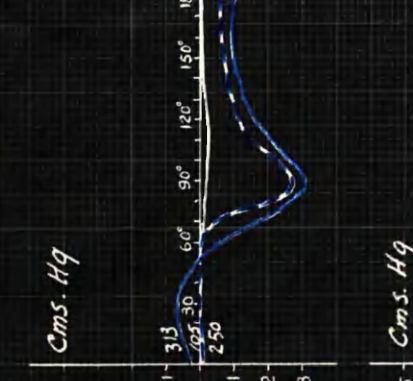
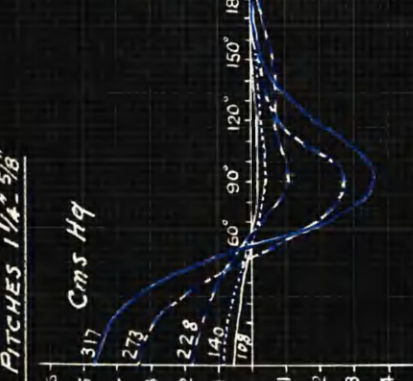
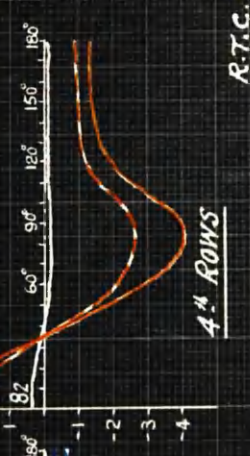


FIG. 3 - STAGGERED P 3/8"



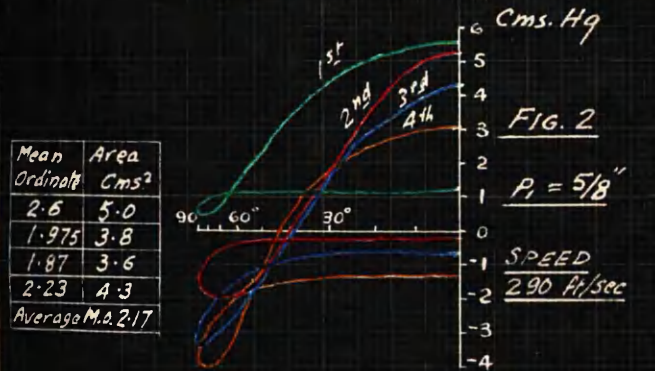
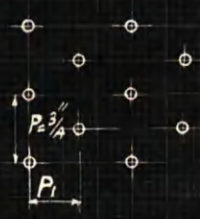
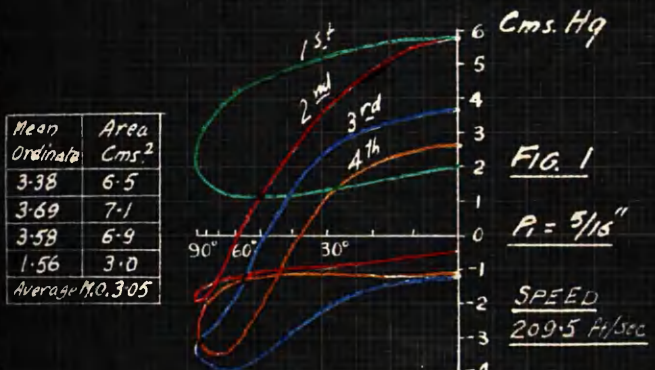
R.T.C.  
1944

FORM DRAG DIAGRAMS - FOUR ROWS

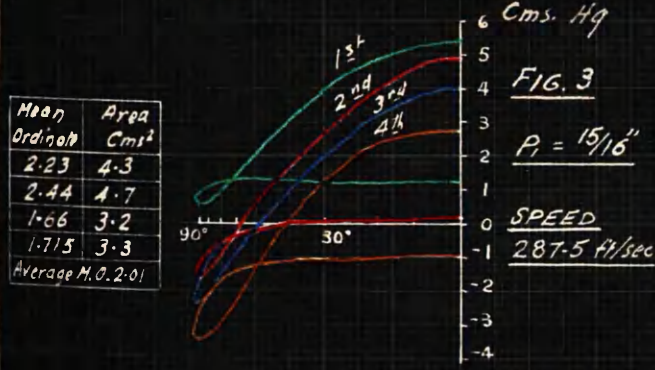
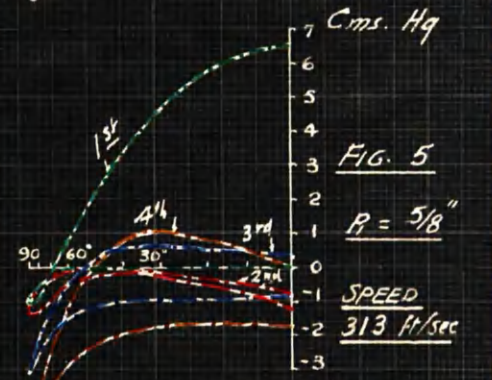
STAGGERED AND CHAIN

FOR

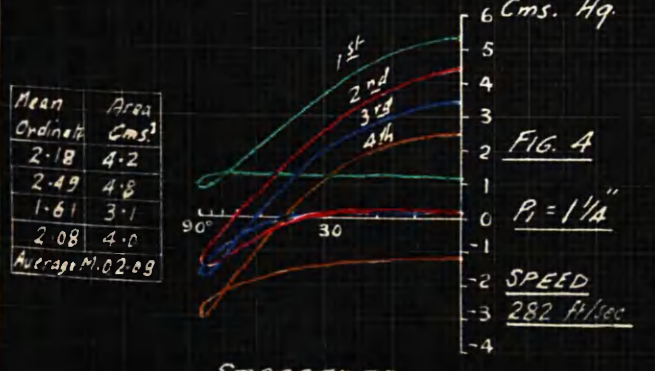
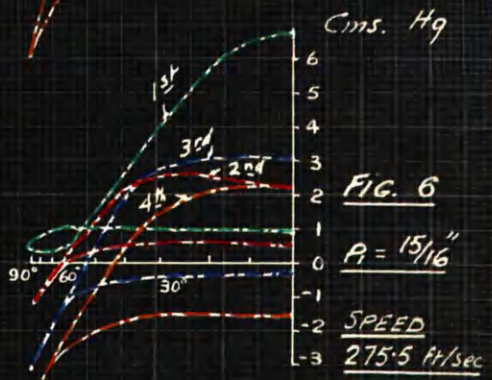
VARIOUS SPEEDS & VARIOUS PITCHES



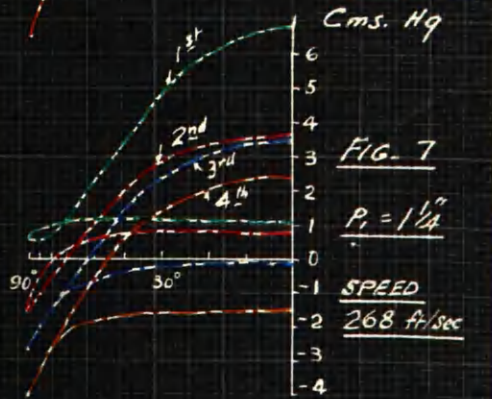
Mean Ordinate	Area Cms. <sup>2</sup>
4.26	8.2
0.104	0.2
1.19	2.3
2.18	4.2
Average M.O. 1.94	



Mean Ordinate	Area Cms. <sup>2</sup>
2.6	5.0
1.4	2.7
1.97	3.8
2.18	4.2
Average M.O. 2.02	



Mean Ordinate	Area Cms. <sup>2</sup>
3.12	6.0
1.4	2.7
2.13	4.1
2.44	4.7
Average M.O. 2.27	



STAGGERED

CHAIN

/the dial showing the 30 degree angular rotation of the single tube had to be carefully considered. This is shown on Plate No.31, Fig.2.

The effect of size of hole had already been investigated by other experimenters (Thom and Warner)<sup>(49)</sup>. These experiments were carried out on vertical tubes with holes drilled perpendicular to the axis of tube. Tests on angled tubes with holes drilled parallel to the flow direction or perpendicular to the axis of the inclined tube, might form a subject for further experiments.

Plate No.41, Fig.2, shows pressure curves for a bank of angled tubes staggered arrangement. Fig. 1 is plotted here for comparison.

Results are tabulated at the appendix of the thesis.

- (e) Smoke Tests : In Plate No.42, Figs.1,2 and 3 the arrangement is shown for a test with smoke introduced into the air flow. Titanium Tetra-Chloride was used to give a dense quantity of white smoke. The box containing the bank of tubes had a glass panel so that photographs could be made. High pressure air was used in these tests along with a stream of air which passed through the nozzle. This is an injector arrangement with a regulating valve. The plan view shows the arrangement of the tubes. The flow of the smoke is spread evenly over the tubes.

The holes in the rose funnel L tube were bored  $3/32$  inch diameter. The ends of the tube were made so that they could be opened for cleaning purposes. It was found that seven holes were necessary to give the right quantity of smoke before approaching the model tubes. The cleaning was carried out after each test. This was done by using warm water as the Titanium left a sticky deposit which reduced the area of the  $3/32$  inch holes.

It was found in these experiments that the smoke tended to return over the top of the test box containing the tubes. It was, therefore, necessary to carry the smoke a fair distance away from the glass panel. This was done by means of an extension attachment, not shown in the sketch plan of the box, which permitted clear photographs to be made.

Plate No.43, Fig.1 shows the tube model arrangement and baffle position. A special tripod was obtained to carry the camera which was fitted with an extra/

FORM DRAG DIAGRAMS FOR ANGLED TUBES

SINGLE AND MULTIPLE

TEST HOLE ON  $\phi$  - WITHOUT BAFFLE

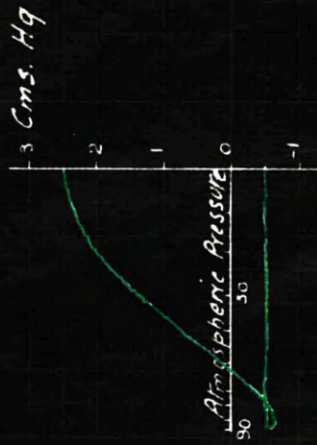


FIG. 1

SINGLE TUBE INCLINED  $45^\circ$

SPEED 255 m/sec

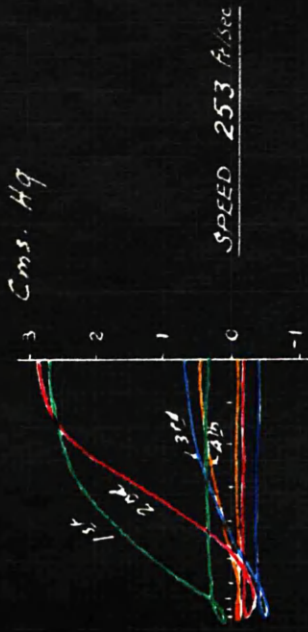


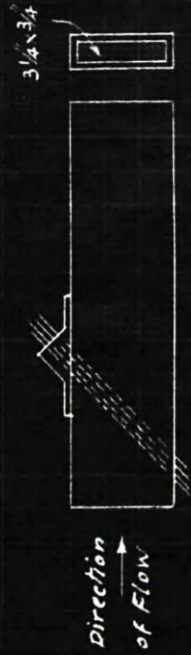
FIG. 2

STAGGERED TUBES - FOUR ROWS

INCLINED  $45^\circ$



BOX FOR SINGLE TUBE  
TUBE DIAM. 1/8"



BOX FOR MULTIPLE TUBE  
TUBE DIAM. 3/16"

ARRANGEMENT  
OF  
SMOKE TEST BOX

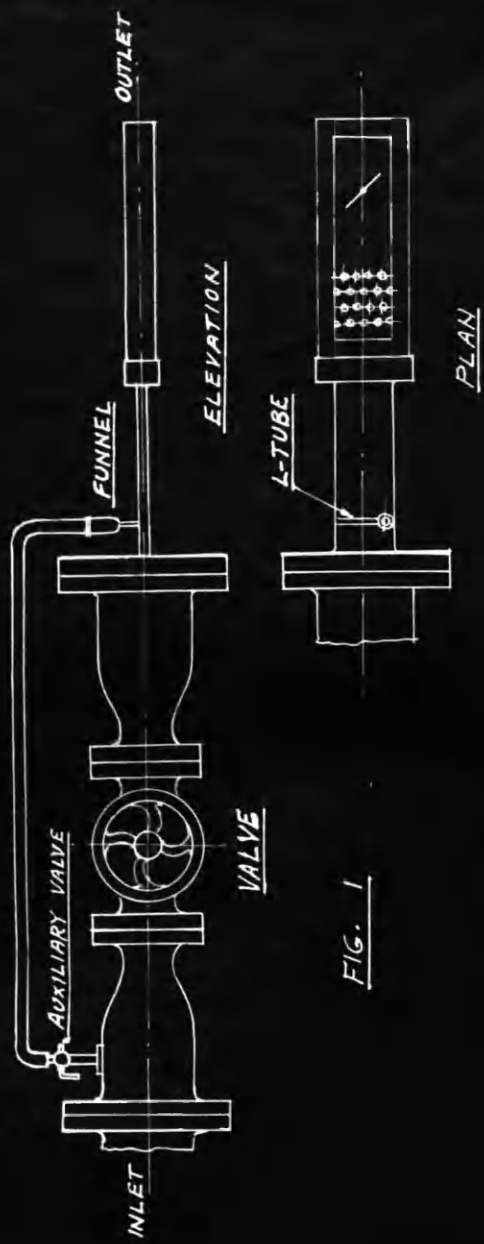


FIG. 1

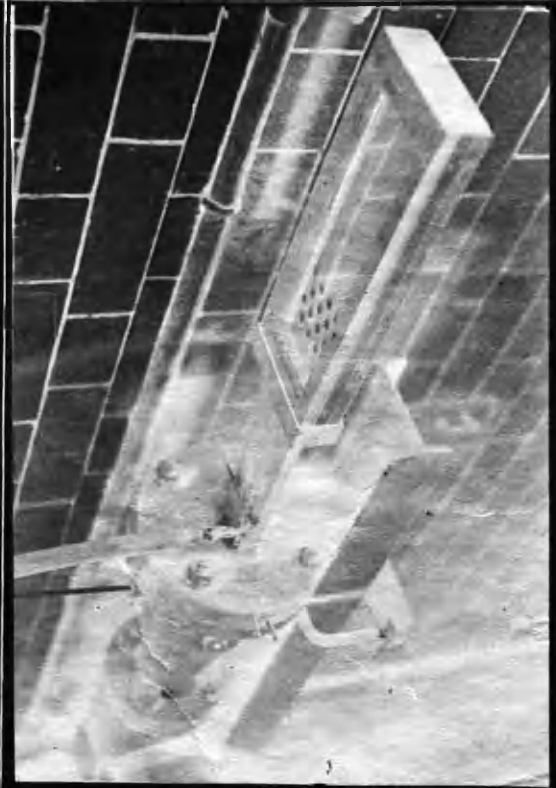


FIG. 2

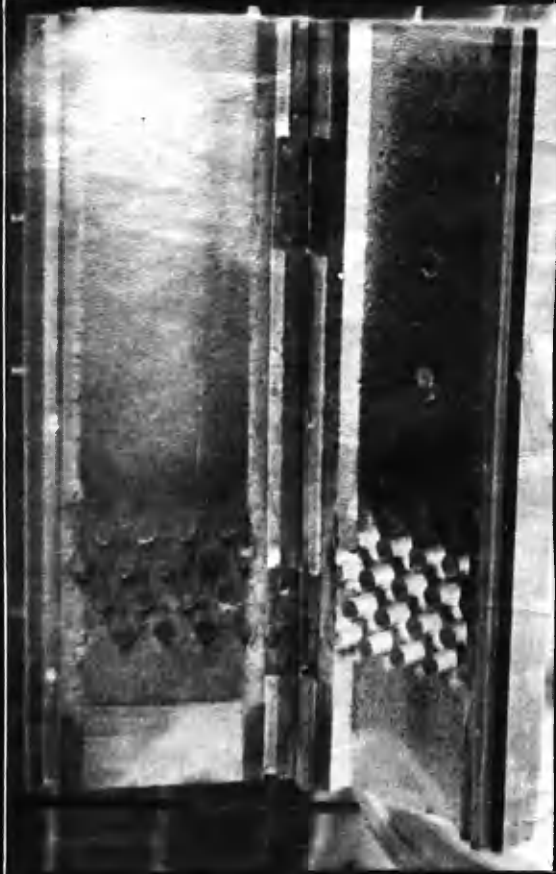


FIG. 3

SMOKE TESTS

DIRECTION OF FLOW →

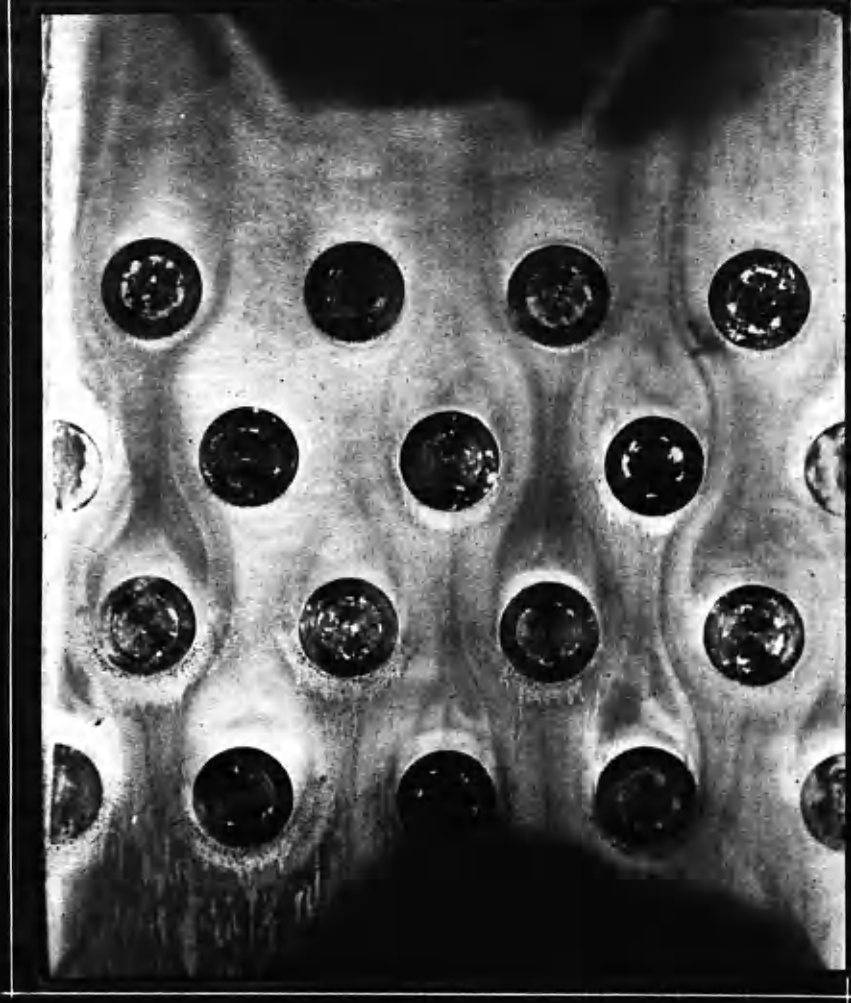


FIG. 3

PLATE-431-

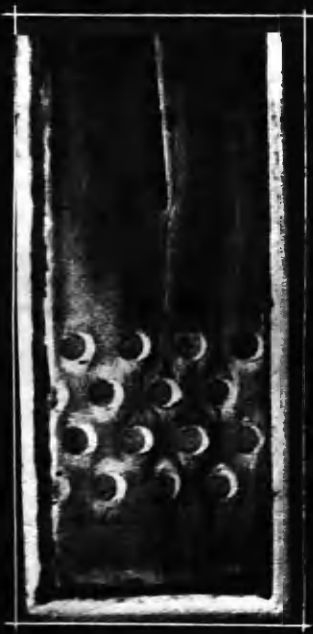


FIG. 1



FIG. 2

/extra lens so that a full size photograph could be made of a portion of the box carrying the tubes. This is clearly shown in Fig. 2. It was, therefore, decided to take another negative to see if further detail of stream line flow could be brought out. Fig.3 shows the enlargement which is  $1\frac{1}{2}$  times full size.

A study of the photograph, Fig.3, shows where the breakaway point of flow takes place in the front and second rows. The picture of the air-smoke stream gives a clear impression of higher velocity round the second row and a much earlier breakaway point. This corresponds to the results obtained by photographs of the water tank experiments.

It may be of interest to record here that a deposit method was also experimented with. In the first experiments air was blown simultaneously through concentrated nitric acid and concentrated ammonia solution. The two clouds met and gave a fume and white deposit on the surface of the model tubes. This experiment was quite successful but required a very long time to give a heavy deposit such as was found on the boiler tubes. In order to obtain the heavy deposit required, a piece of waste was soaked in oil and burnt before the air stream nozzle plate. As previously stated in Section 1, the hard bulge deposits appeared on the sides of the faulty boiler tubes. With this experiment the deposit appeared on the front surface. The deposits were certainly heavier on the second row than on the first row tubes, but, with this oil-smoke experiment, the deposits gathered on the front of the tubes. This is clearly shown on Plate No.42, Fig.3.

- (f) Discussion of Results : The general form of the pressure distribution curves, plotted from the data obtained in the small high speed trunk experiments, is similar to that found at the speed of 100 ft/sec. used in the large Wind Tunnel. Comparison of a single horizontal tube pressure curve with a front row horizontal tube in a four row bank shows clearly the effect of form drag on these tubes, - Plate No.37, Figs.1 and 13.

Average speeds during the tests were kept constant at 250 and 350 ft per second at the test tubes. The pressure distribution curves were taken on a test hole on the middle of tube and at points above and below the centre line of flow. These when plotted show much the same form.

One point should be noted and that/

/that is that change of wake form as shown by photographs, Plates No. 13, 14, 15 and 16, appear on the pressure diagrams. Naturally one would have thought that equal distances above and below the centre line should have given perfectly symmetrical curves of pressure distribution. The curves in Plate No. 35, Fig. 6 show, in nearly all cases, that the top test pressure hole gives slightly higher pressures at the back of tube. The difference is not always constant as slight changes of conditions in room temperature and barometer pressure, affect readings. Instantaneous readings for twelve points around tubes under test could not be made on these small scale experiments. This may cause slight variations, but with the number of tests made on vertical tubes the pressure distribution agrees favourably with other investigators.

The tests with the single tube when inclined at 45 degrees have been made under similar conditions and velocities of 260 to 370 ft per second were used and kept as constant as possible. When the curves of pressure distribution were plotted it was found that much the same characteristics appeared as in the vertical position. The form drag diagram is such that the area of the inclined position and hence the drag mean ordinate, is approximately 50% or as cosine of the angle of inclination, Plate No. 35, Figs. 6 and 7.

Slight differences in the curves for the top and bottom holes appear in both vertical and inclined tubes and give indication of turbulence near the top and bottom wall of the tube box. With a test hole close to the top wall of the box a smaller frontal pressure is noted. For reference these have been plotted on the same base in Plate No. 35, Fig. 4.

Comparison between the short  $\frac{3}{8}$  inch diameter and  $\frac{1}{2}$  inch long vertical tube test and the  $\frac{1}{8}$  inch diameter by 3 inch long tube is shown separately on Plate No. 35, Fig. 5.

These curves have close resemblance to each other. The effect of the closeness of the trunk walls in the case of the  $\frac{1}{2}$  inch long tube with central hole is to raise the back pressure distribution line. This affects the pressures at the loop and the point of breakaway.

The multi tube arrangement test results when examined are in accordance with those already discussed in the large wind tunnel.

The pressure distribution curves, Plates No. 36 and 37, show that the second row is the one which has greatest slope. This holds for vertical and inclined position of the bank of tubes, Plate No. 41.

In the experiments carried out on a two row bank the test results have been plotted for various pitches. For the two row bank staggered and chain arrangement the pressure distribution curves show that the second row curves are steeper than the first and much steeper at small pitches, Plate No.36, Figs.1 and 2. In staggered arrangement the slope of the second row approaches that of first at larger pitches.

Plate No.37 illustrates the various positions in which the baffle plates were used, - (1) closed, (2) 30 degrees open, (3) 60 degrees open and (4) fully open. The pressure curves have been plotted from the readings in such a manner that single row, two row, three row and four row bank is illustrated for baffle closed and 30 degrees position. These have been numbered 1 and 2 on the diagram.

When the baffle was closed it was found that there was no change in the shape or form of the pressure distribution curves. The position of the curves relative to the atmospheric pressure datum line changed for all rows. Take for example the single row. The front and back pressures for baffle closed read 28.5 and 23.8 cms water respectively, while with the baffle opened by 30 degrees these become 21 and 16 cms water respectively. There is no appreciable change in area enclosed in curve with this single row of tube arrangement, Figs. 1,2,3, and 4.

The same holds good for the second row frontal pressure in a bank of two rows. The frontal pressure is 31 cms water and the back pressure is 23.4 cms with baffle closed. When the baffle is opened by 30 degrees the front and back pressure on the second row tubes read 20.6 and 13.2 cms water respectively. Again there is very little change in area and the slopes of the second row curves remain steeper than the first row curves.

The addition of a third row to the two row bank is now examined for alteration to pressure distribution diagrams, Figs.9 and 10. The effect of the third row with baffle closed is to raise frontal and back pressure for the first and second rows. The slope of the second row curve is greater but only slightly. The areas of the enclosed curves remain much the same.

When a fourth row is added to the bank and the baffle positions are again closed and 30 degrees open, there is a distinct difference in the slope of the second row pressure distribution curves, Figs.13 and 14. The frontal pressure at 0 degrees test tube hole is higher, but so also is the pressure at the 180 degree hole. The area of the second

/second row pressure curve is greater than with the two bank arrangement and the slope of the second row curve is also greater. The pressure through the four row bank with baffle closed, Fig.13, is approximately 1.12 times the pressure through the two row bank, Fig.5. When the baffle is opened by 30 degrees much the same differences occur when changing from two to four row bank. It is, however, noticed that the gradient of the second row pressure distribution curve is again steeper with the four bank but to a greater extent than with the baffle closed.

The same treatment was given to one, two, three and four row bank of tubes but with baffle 60 degrees open and fully open. Plate No.37 shows the pressure curves have the same characteristics, but it was noticed that when the fourth row was added to the bank of tubes the negative loop on the third row curve was changed giving an earlier point of break-away in the pressure and consequently a much smaller form drag diagram. The first and second rows were only slightly affected by the addition of the fourth row.

For a low speed test at 82 ft. per sec. the data obtained gave the curves plotted in Plate No.38, Figs. 1, 2, 3 and 4, for one, two, three and four row banks with the baffle fully open. This Plate shows the projected, developed and polar diagrams for the pressure distribution curves. The polar curves were plotted on a zero circle with radius equivalent to 4 cms of water pressure.

The latter type of curve representation was used by Stanton<sup>(43)</sup> for a single vertical tube. Stanton found that the back pressure intersected the zero circle which corresponds to the pressure curves used by the author where the pressure at 180 degrees is below the datum line or negative. Continuing the same method of plotting shows that the presence of the rows behind the first row of further rows makes the back pressure always positive.

The curves plotted in Plate No.38 give areas for the first row, 0 to 180 degrees range, of 5.9, 5.8, 6.7 and 6.1 cm<sup>2</sup> respectively for the four rows shown. The second row areas are 4.9, 6.0 and 5.7 cm<sup>2</sup> respectively. The third row diagrams give 4.9 and 3.2 cm<sup>2</sup>, while that of the fourth row is the same as 3.2 cm<sup>2</sup>, Fig.4. These areas are marked along side the diagrams in Plate No.38.

The gradients of the projected pressure distribution curves when taken from horizontal datum line in a bank of four rows, Fig.4, are in order of magnitude and measured in degrees, -second row 70, third row 64, fourth row 56 and first row 52. The contrast between the second and the/

/the first is surprising. It is also remarkable that the gradient of the second row keeps on increasing as the number of rows in staggered formation is increased.

Developed pressure distribution curves are illustrated in Plate No.39 which compares chain arrangement with staggered. Fig.1 shows the curves for chain arrangement of  $3/8$  inch diameter tube at  $1\frac{1}{4}$  inch pitch. The speeds of air flow range from approximately 100 to 315 ft.per second. All back pressure points, although varying towards atmospheric pressure line, never get below this datum line. In the second row tubes the side and back pressures between 60 and 120 degree angle of turn for the speeds above 200 fall below the atmospheric line and for speeds less than 200 they are close to the datum line. After an angle of 120 degrees turn all the back tube pressures are above atmospheric pressure.

In the third and fourth rows the curves are all below the atmospheric line from 50 to 180 degrees. All the high speed curves give very large side and back pressure, the maximum occurring at 90 degrees. All the tests on chain arrangements show that the frontal pressures in the second, third, and fourth rows are below that of the first row. Comparison with staggered tube arrangement, which is the one considered in the Boiler Tube failures, shows that this is a feature belonging to chain or rectilinear arrangement.

For comparative purposes two high speed curves and one low speed have been plotted for the usual  $5/8$  inch staggered pitch, Plate No.39, Fig.3. It will be noticed that with the chain arrangement the pressure distribution curves become very close and are all under the atmospheric line in the second row. The third and fourth rows show the same tendency to go below datum line but are much opener curves. All the maximum negative pressures are at 90 degree angle of turn.

When the staggered arrangement is considered the front pressures in the second row are equal to the first. The first never gets below atmospheric pressure. For second rows, the negative pressures at high speed becomes a maximum about 63 degrees. The pressure curve at low speed in the staggered arrangement for the first row remains above the atmospheric line. In the second it is above datum line in front but is on the datum from about 63 degrees. In the third and fourth row the curves are part above and part below the datum. It will be noted that the pressures at 90 degrees in the fourth row is greater than that on the frontal area and is equal to that on the front of the third row.

The areas of the pressure curves in staggered and chain arrangement are compared for different/

/different pitches,-Plate No.40,-Figs.1 to 4 are for  $5/16$  inch to  $1\frac{1}{4}$  inch staggered while Figs.5 to 7 are for  $5/8$  inch to  $1\frac{1}{4}$  inch chain. The areas and the average mean ordinate are marked on the various figures.

Consider the areas of the second row curves on Plate No.40. The area for the  $5/16$  inch pitch is greater than for the  $5/8$  inch pitch but the slope of the curve is greater in the latter case. Again for the  $15/16$  inch pitch the area is larger than for  $5/8$  inch and the slope is less.

With the chain arrangement of  $5/8$  inch pitch the area of the second row pressure curve is exceedingly small as the negative loop is about as great as the positive. Opening out the pitch in the chain arrangement to  $15/16$  and  $1\frac{1}{4}$  inch the characteristic features throughout the test recur. The front row pressures are always higher than any of the other rows and do not alter but the second row frontal pressure increases as the pitch increases.

The figures for average mean ordinates marked in Plate No.40 show that as pitches increase up to  $5/8$  inches the pressure on the bank decreases. Further opening of the pitch makes little change to the mean value, but at the value of  $5/8$  inch pitch the slope of the second row diagram has reached the maximum both for row and pitching.

SECTION III.

## SECTION III - HYDRODYNAMIC ANALYSIS.

### PART 1 - INTRODUCTORY.

- (a) Purposes of Analysis : The preceding sections of this Thesis have all shown the special significance of the second row in multi-row arrangement and particularly in the case of staggered row sections. The main points are wholly experimental. However, it seems desirable to examine whether a theoretical treatment on two-dimensional lines would bear out the main features.

With the relatively close spacing of tubes in such boilers as have been considered, the ideal two-dimensional flow problems need not take circulation into account as the effect of this would be slight or negligible. The treatment would, therefore, ignore both circulation and the influences of wake vortices; the former becomes negligible and the latter because it cannot be included in the ideal flow analysis.

Only qualitative results need be considered. The main point is to discover whether ideal flow condition in multi-tube rows would establish special features in the pressure distribution around the second row. Even although the analytical method can only give results of any value for the front half, it still might show an inherent tendency towards steeper pressure gradient in the second row.

If this was the case, then the feature which is being emphasized by these investigations would lie inherent in the ideal theory. If on the other hand this is not the case, which of course is the likely fact, then the conclusion is reached that the wake vortices are responsible for the condition. It would seem to be of value to demonstrate this if possible.

For this purpose ideal flow analysis of single, double, three and four row arrangement have been carried out and the pressure distribution given by these analysis examined with particular regard to second row effects. This section of the thesis is concerned with these calculations and the conclusion they lead to. The formulae are used for staggered row arrangement, but the same formulae could be applied equally well to chain pitching.

(b) Ideal Flow Across Single Tube : In ideal flow the idea of a source, constantly emitting fluid radially in the same plane is important. The streamlines are obviously radial and, if the volume of fluid per unit depth emitted is  $m$  ft<sup>2</sup> per sec., termed the strength of the source, then the radial velocity at radius  $r$  will be  $v = m/2\pi r$ . The flux crossing an arc joining two radial lines subtending an angle  $\theta$  at the origin  $x$  will be

$$\Psi = .m\theta/2\pi \dots\dots\dots (1)$$

where  $\Psi$  is the stream function.

It can be readily shown that  $\Psi =$  constant defines a particular streamline for a given flow.

The source is an outward radial flow and if  $m$  is changed in sign we obtain an inward radial flow which is termed a sink.

When the distance between a source and a sink of equal strength becomes infinitely small and their strengths infinitely great we obtain a combination referred to as a doublet for which the stream function is

$$\Psi = u/2\pi r \sin \theta \dots\dots\dots (2)$$

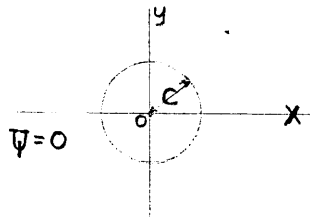
where  $u$  is the strength of the doublet and  $r$  and  $\theta$  are polar co-ordinates.

A doublet of strength  $u$  fixed at the origin together with a uniform flow of  $U$  ft/sec. gives for the combination in the  $xy$  field,

$$\Psi = -Uy + u \sin\theta/2\pi r = -Uy(1-u/2\pi r^2 U) \text{ ft}^2/\text{sec} \dots\dots\dots (3)$$

$$\Psi = -U \sin\theta (r-c^2/r) \text{ ft}^2/\text{sec} \dots\dots\dots (4)$$

where  $c = \sqrt{u/2\pi U}$



For the streamline  $\Psi = 0$  we can select the boundary made up by the circle  $r = c$  and the  $OX$  axis. This obviously gives the flow past a circular cylinder with its longitudinal axis perpendicular to the plane of flow, if we neglect the motion within the cylinder.

The potential function of the irrotational flow is the complex function  $w = \phi + i\Psi$  where  $\phi$  is the velocity - potential of the flow and  $i$  is the operator  $= \sqrt{-1}$ .

In terms of the complex variable  $Z = x + iy$  the potential function of the flow past the circular cylinder in the  $Z$  plane is given by  $w = U (z + c^2/z)$  ft<sup>2</sup>/sec.

It can be readily shown that the relationship between the potential function and the velocity components  $u$  and  $v$  in the direction of OX and OY axis respectively is

$$dw/dZ = u - iv \dots\dots\dots (5)$$

Hence for the flow past the circular cylinder

$$w = U (Z + c^2/Z) \text{ ft}^2/\text{sec.}$$

$$u - iv = dw/dZ = U(1 - c^2/Z^2) \text{ ft/sec.}$$

giving

$$u = U \{1 + c^2(y^2 - x^2) / [y^2 + x^2]^2\} \text{ ft/sec} \dots\dots (6)$$

and

$$v = -U(2xy)c^2/[y^2 + x^2]^2 \text{ ft/sec} \dots\dots\dots (7)$$

The resultant velocity  $V = \sqrt{u^2 + v^2}$  and the pressure  $p$  at any point can be obtained by applying Bernoulli's equation

$$P + \rho U^2/2 = p + \rho V^2/2 \dots\dots\dots (8)$$

The difference between the pressure at any point on the cylinder of radius  $c$  and the pressure  $P$  in the free stream reduces to the standard equation in polar co-ordinates

$$p = P + \rho U^2/2(1 - 4 \sin^2\theta) \text{ lb/ft}^2 \dots\dots (9)$$

If  $P = 0$  then

$$p + \rho V^2/2 = 1 - 4 \sin^2\theta \dots\dots\dots (10)$$

The pressure distribution round a circular cylinder from a paper written by Thom<sup>(4)</sup> is reproduced by the developed curve in Plate No.44, Fig.1. From this curve the projected pressure distribution curve has been plotted. On the same figure the theoretical curve derived from formula No.(10) for a single tube has also been plotted for comparison. It will be seen that the experimental curve follows that derived analytically, but is of smaller amplitude. At the back of the tube Thom's experimental curve follows an almost horizontal line parallel to the datum.

This applies also to the pressure distribution curves on the same Plate, Fig.2 which have been plotted from the author's experimental results on a single tube in the vertical and inclined positions. As previously stated the wake vortices are responsible for this departure and it is obvious that the form drag diagram for the theoretical irrotational flow is zero.

PRESSURE DISTRIBUTION ROUND CIRCULAR

CYLINDER

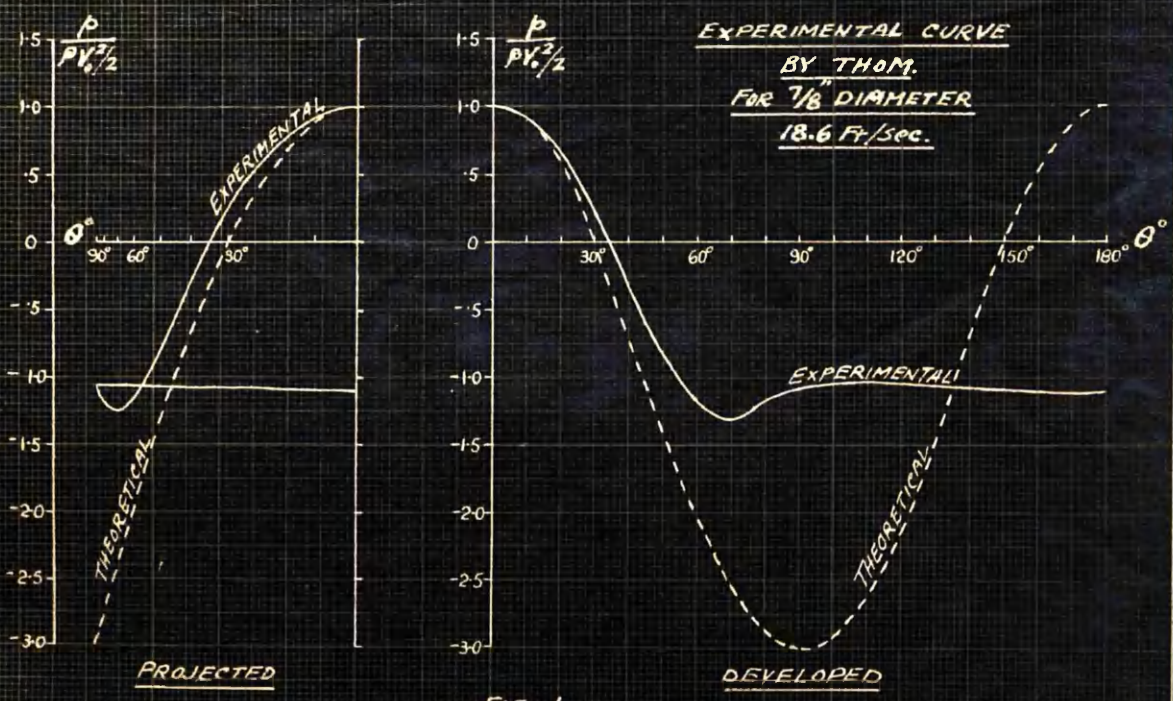


FIG - 1

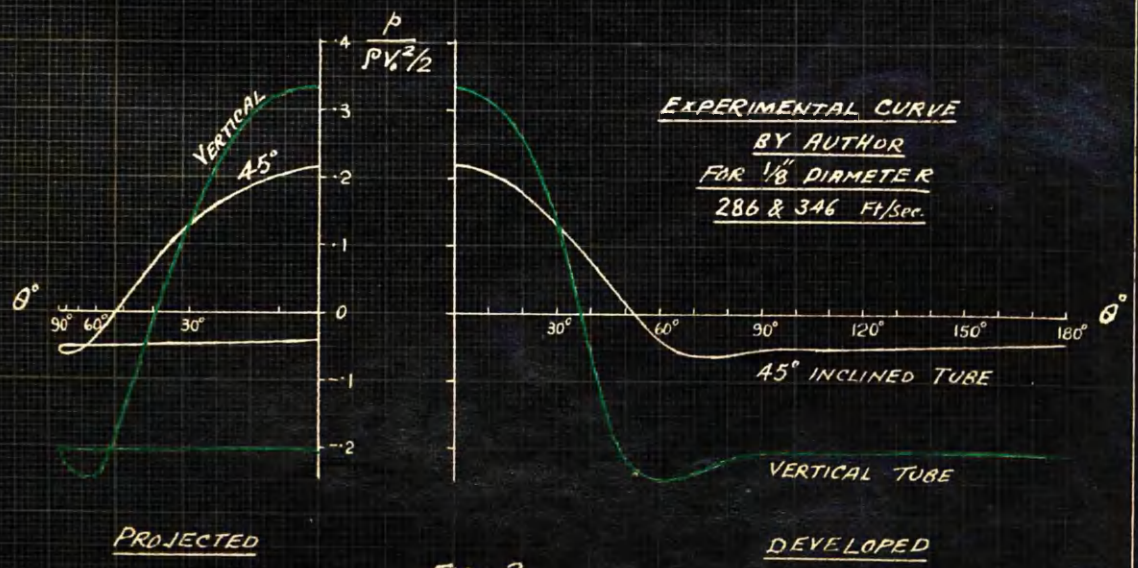


FIG - 2

PART 2 - SINGLE ROW CASE.

- (a) Flow Across Limited Single Row : The potential function for a doublet at the origin of the XY axis combined with a flow U ft/sec parallel to the OX axis was written above in the form:

$$w = U (Z + c^2/Z) \text{ ft}^2/\text{sec.}$$

To displace the doublet a distance "a" above the OX axis the potential functions has to be written in the following form:

$$w = U (Z + c^2/Z-ia) \text{ ft}^2/\text{sec.}$$

This gives the stream function

$$\psi = U \{y - c^2(y-a)/x^2 + (y-a)^2\} \text{ ft}^2/\text{sec} \dots\dots\dots (11)$$

Obviously when  $y = a$  the stream function  $\psi = aU \text{ ft}^2/\text{sec}$  and this value also remains constant round the circle of radius  $c$  and centre at  $(0 - a)$ . Thus the form  $w$  as above gives the required displacement of the doublet.

The potential function for the flow past a row of tubes of limited number can be obtained by writing

$$w = U \{ Z + \{c^2/Z+ina\} \} \text{ ft}^2/\text{sec} \dots\dots\dots (12)$$

where "a" is the tube spacing and n has to be given values depending on the number of tubes involved.

This equation could be considered as an adaption of the form given by Lamb<sup>(56)</sup> for a series of uniform doublets lying in the Y axis together with a streaming velocity U ft/sec. For the series of doublets Lamb gives

$$w = c \text{ Coth } \pi Z/a \text{ ft}^2/\text{sec} \dots\dots\dots (13)$$

where  $c$  is the strength of the doublets.

From these equations the following conditions hold

$$u-iv = dw/dZ = U \left\{ 1 - \frac{c^2 \{x^2 - (y+na)^2 - 2i(y+na)x\}}{[(y+na)^2 + (x)^2]^2} \right\} \text{ ft/sec} \dots\dots (14)$$

and the velocity components are

$$u = U \left\{ 1 + c^2 \frac{(y+na)^2 - x^2}{[(y+na)^2 + x^2]^2} \right\} \dots\dots\dots (15)$$

$$v = -U \left\{ c^2 \left\langle \frac{2x(y + na)}{[(y + na)^2 + x^2]^2} \right\rangle \right\} \dots\dots\dots (16)$$

A single row of five tubes pitched at  $\frac{3}{4}$  inch, which is "a", and the diameter of the tubes  $\frac{3}{8}$  inch, which is "2c" in equations 15-16.

Speeds U of 280 and 82 ft/sec with values of n = 0, +1 +2 have been used in calculation of the various columns in tables lettered A, B etc.

- (b) Calculations and Collected Results : From equations 15 and 16 the calculations using the vertical and horizontal components were made for the range 0 to 180 degrees, by 30 degree increments as shown. The resultants were obtained by calculation and from these the pressures in cms of water and cms Hg were obtained. This gave the values of  $p + \rho V^2/2$  from the single row formulae.

The results have been tabulated in Table A for the centre tube as shown in the sketch. The axis XX was chosen through the centre line of the middle tube as this gave an axis of symmetry.

- (c) Contrast with Experimental Curve : In Plate No.45 the theoretical curves have been drawn for single, double, three and four rows.

Fig.1 is for a single row of five vertical tubes with speed of flow of 82 ft per second. From the calculated values the theoretical curve has been plotted on a sine of angle of turn base, the ordinates being pressure ratios. The curve is symmetrical and, therefore, made for 360 degrees turn.

Fig.2 shows the corresponding experimental data pressure distribution curve for single row, only the points are from 0 to 180 degrees for the same velocity of flow. In this curve the pressures came below the datum level at 60 degrees, remain under and reach the maximum negative pressures of exactly half the value of the frontal pressure.

The theoretical curve Fig.1 is a parabolic curve. In this curve the pressures are 0 at 30, 150, 210 and 330 degrees. Pressures remain negative after 30 degree and reach the maximum negative value of exactly three times the value of the frontal pressure. Then from 90 degrees the curve returns at 180 degrees to the former front positive pressure receding again to 270 degrees and back for the next 90 degree angle of turn. This curve might be compared with that on Plate No.44 which has been plotted from standard equn. in polar co-ordinates. The two curves are almost exactly similar for all pressures above and below datum line. The drag in both cases is zero.

## SINGLE ROW FORMULAE.

$$u = U \left\{ 1 + c^2 \frac{(y+na)^2 - x^2}{[(y+na)^2 + x^2]^2} \right\} \dots (15)$$

WHERE  $n = 0^{\pm} 1 \text{ and } 2$

FLOW SPEED  
U FT./SEC

$$v = -U \left\{ c^2 \frac{2x(y+na)}{[(y+na)^2 + x^2]^2} \right\} \dots (16)$$

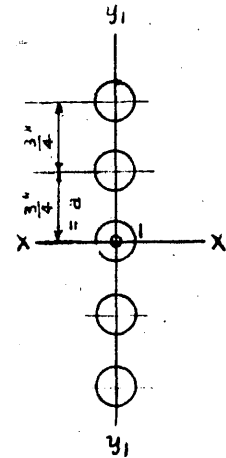


TABLE "A"

### COLLECTED RESULTS FOR SINGLE ROW.

$\theta$	$0^\circ$	$30^\circ$	$60^\circ$	$90^\circ$	$120^\circ$	$150^\circ$	$180^\circ$
$x$	$c$	$\cdot 866c$	$\cdot 5c$	$0$	$\cdot \cdot 5c$	$\cdot \cdot 866c$	$-c$
$y$	$0$	$\cdot 5c$	$\cdot 866c$	$c$	$\cdot 866c$	$\cdot 5c$	$0$
TERM N <sup>o</sup> ①	$\cdot 8654$	$\cdot 3572$	$\cdot 6672$	$1 \cdot 1837$	$\cdot 6672$	$\cdot 3572$	$\cdot 8654$
$u = U \{ 1 + c^2 \text{①} \}$	$\cdot 1346$	$\cdot 6428$	$1 \cdot 6672$	$2 \cdot 1837$	$1 \cdot 6672$	$\cdot 6428$	$\cdot 1346$
TERM N <sup>o</sup> ②	$0$	$\cdot 8465$	$\cdot 8421$	$0$	$\cdot 8188$	$\cdot 8482$	$0$
$v = -U \{ c^2 \text{②} \}$	$0$	$\cdot 8465$	$\cdot 8421$	$0$	$\cdot 8188$	$\cdot 8482$	$0$
$V = U \sqrt{u^2 + v^2}$	$\cdot 1346$	$1 \cdot 060$	$1 \cdot 865$	$2 \cdot 1837$	$1 \cdot 850$	$1 \cdot 063$	$\cdot 1346$
$p$ in lbs/ft <sup>2</sup>	$91 \cdot 2$	$-12 \cdot 0$	$-235 \cdot 0$	$-352 \cdot 0$	$-225 \cdot 0$	$-12 \cdot 1$	$91 \cdot 2$
" " Cms of Water	$44 \cdot 5$	$\cdot 5 \cdot 86$	$-114 \cdot 8$	$-172 \cdot 0$	$-109 \cdot 9$	$\cdot 5 \cdot 9$	$44 \cdot 5$
" " " " Mercury	$3 \cdot 27$	$\cdot 432$	$-8 \cdot 28$	$-12 \cdot 6$	$-8 \cdot 09$	$\cdot 436$	$3 \cdot 27$
$p \div \rho V_0^2 / 2$	$\cdot 982$	$\cdot 123$	$\cdot 2 \cdot 48$	$\cdot 3 \cdot 77$	$\cdot 2 \cdot 42$	$\cdot 130$	$\cdot 982$

NOTE:- To Find  $u, v$  or  $V$  multiply values in Table by  $U$ .

R.T.C  
1944.

PRESSURE DISTRIBUTION DIAGRAMS  
FOR  
SINGLE ROW

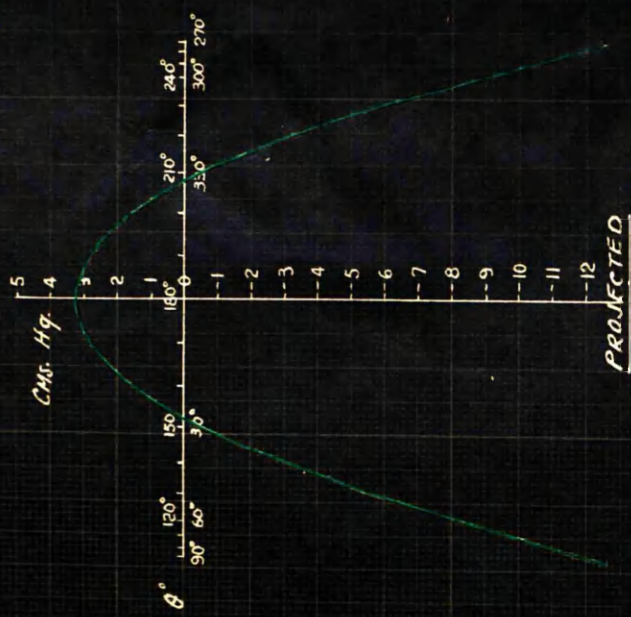
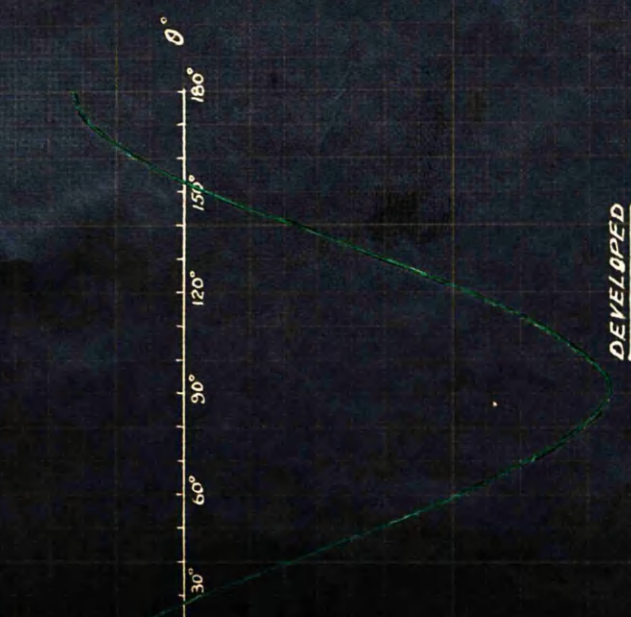
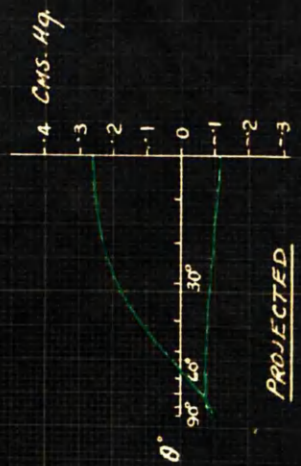


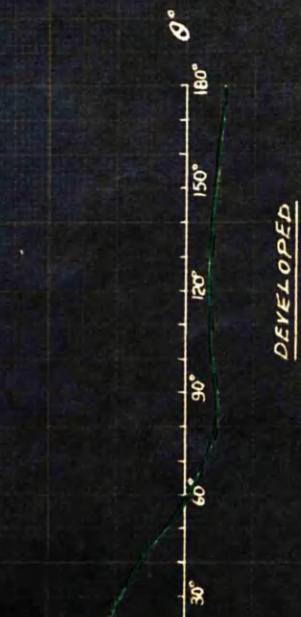
FIG-1  
THEORETICAL



DEVELOPED



PROJECTED



DEVELOPED

FIG-2  
EXPERIMENTAL

PART 3 - DOUBLE ROW CASE.

- (a) Extension of Theory for Two Rows : To obtain the potential function for the flow past a multi-row bank of tubes, it is necessary to modify further the equation used for a single row. By examination of the equation,

$$w = U \{ Z + c^2/Z-b \} \text{ ft/sec.}$$

we find that the doublet is displaced an amount  $b$  from the OY axis.

Hence the flow past a row of tubes pitch " $a$ " and displaced " $b$ " from the OY axis is given by

$$w = U \{ Z + c^2 \sum 1/Z+ina-b \} \text{ ft}^2/\text{sec} \dots\dots\dots (17)$$

where the values of  $n$  specify the number and vertical positions of the tubes.

For two staggered rows of tubes the equations become

$$w = U \{ Z + c^2 \sum 1/Z+ina+imb \} \dots\dots\dots (18)$$

where  $m = 0$  or  $1$  and  $b = 5/8$ " the distance between the rows.  
 $n = 0, \pm 1, \pm 2$  in first row.  
 $n = \pm \frac{1}{2}, \pm \frac{3}{2}$  in second row.

and hence the velocity components  $u$  and  $v$  at any point  $x$  and  $y$  would be as shown in equations 19 to 22 which appear on tables B and C.

- (b) Calculations and Results : In this case the axis have been taken as  $x_1$  and  $y_1$  for first row,  $x_2$  and  $y_2$  for second row in making the calculations and in drawing the pressure distribution curves. These axis are shown in sketch of tube arrangement of double row bank.

Equations 19 and 20 represent the conditions of the first row of the double bank which has now changed by the addition of the second row. The results are given in tabular form for front row and for tube marked (1).

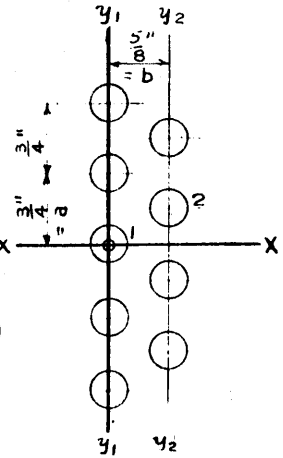
Equations 21 and 22 show the conditions for tube in second row marked (2). The tests were made for 360 degrees by 30 degree increments. The equations have been made for the theoretical values and plotted. From the test/

# TWO ROW FORMULAE.

$$u = U \left\{ 1 + c^2 \frac{(y+na)^2 - x^2}{[(y+na)^2 + x^2]^2} + c^2 \frac{(y+na)^2 - (x-b)^2}{[(y+na)^2 + (x-b)^2]^2} \right\} \dots (19)$$

WHERE  $\pi = 0^\pm 1$  and  $^\pm 2$ .  $\pi = \pm \frac{1}{2}$  and  $^\pm 1\frac{1}{2}$

FLOW SPEED  
U FT/SEC



$$v = -U \left\{ c^2 \frac{2x(y+na)}{[(y+na)^2 + x^2]^2} + c^2 \frac{2(x-b)(y+na)}{[(y+na)^2 + (x-b)^2]^2} \right\} \dots (20)$$

TABLE "B"

## COLLECTED RESULTS FOR 1<sup>ST</sup> ROW.

$\theta$	$0^\circ$	$30^\circ$	$60^\circ$	$90^\circ$	$120^\circ$	$150^\circ$	$180^\circ$
$x$	C	.866C	.5C	0	-.5C	-.866C	-C
$y$	0	.5C	.866C	C	.866C	.5C	0
TERM N <sup>o</sup> ①	-.8654	-.3572	-.6672	1.1837	-.6672	-.3572	-.8654
" " ③	.0032	-.0050	-.0486	-.0531	-.0498	-.0464	-.0556
$u = U \{ 1 + ① \ ③ \}$	.1378	.6378	1.6186	2.1306	1.6174	.5964	.0790
TERM N <sup>o</sup> ②	0	.8465	.8421	0	-.8188	-.8482	0
" " ④	0	.0321	.0248	.0086	.0023	.0018	0
$v = U \{ ② \ ④ \}$	0	-.8786	-.8669	-.0086	.8165	.8500	0
$V = U \sqrt{u^2 + v^2}$	.1378	1.0830	1.8820	2.1300	1.8120	1.0390	.0780
$p$ in lbs/ft <sup>2</sup>	91.3	-16.38	-237	-329.5	-212	-7.16	92.5
" " Cms of Water	44.7	-8.0	-116	-161	-103.8	-3.51	45.3
" " " Mercury	3.28	-.589	-8.53	-11.85	-7.63	-.258	3.33
$p \div \rho v^2 / 2$	.981	-.170	-2.54	-3.53	-2.28	-.080	.994

NOTE:- To Find  $u, v$  or  $V$  multiply values in Table by  $U$ .

R.T.C  
1944.

# TWO ROW FORMULAE.

$$u = U \left\{ 1 + c^2 \left[ \frac{(y+na)^2 - x^2}{[(y+na)^2 + x^2]^2} + c^2 \left\{ \frac{(y+na)^2 - (x+b)^2}{[(y+na)^2 + (x+b)^2]^2} \right\} \right] \right\} \quad \text{---(21)}$$

WHERE  $n = \pm \frac{1}{2}$  and  $\pm \frac{1}{2}$   $n = 0^+ \text{ and } 0^-$

$$v = -U \left\{ c^2 \left[ \frac{2x(y+na)}{[(y+na)^2 + x^2]^2} + c^2 \left\{ \frac{2(x+b)(y+na)}{[(y+na)^2 + (x+b)^2]^2} \right\} \right] \right\} \quad \text{---(22)}$$

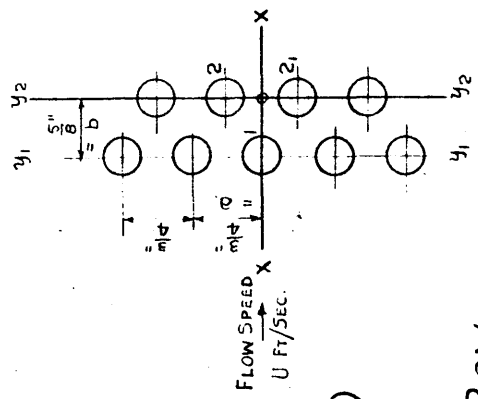
TABLE "C"

COLLECTED RESULTS FOR 2<sup>ND</sup> ROW.

θ	0°	30°	60°	90°	120°	150°	180°	210°	240°	270°	300°	330°	360°
<b>X</b>	C	.866C	5C	0	-.5C	-.866C	-C	-.866C	-.5C	0	.5C	.866C	C
<b>Y</b>	2C	2.5C	2.866C	3C	2.866C	2.5C	2C	1.5C	1.134C	C	1.134C	1.5C	2C
<b>TERM N° ⑤</b>	-.8814	-.3744	.6483	1.1673	.6481	-.3743	-.8815	-.3707	.6547	1.1710	.6546	-.3706	-.8814
<b>" " ⑦</b>	-.0398	-.0208	-.0436	-.0437	-.0420	-.0127	.0119	-.0112	-.0394	-.0476	-.0422	-.0402	-.0398
<b>u = U { + ⑤ ⑦ }</b>	.0788	.6048	1.6047	2.1146	1.6061	.6130	.1304	-.6181	1.6153	2.1234	1.6124	-.6124	.0788
<b>TERM N° ⑥</b>	-.0038	-.8506	.8450	0	-.8450	-.8506	-.0038	-.8428	.8408	0	-.8408	-.8439	-.0038
<b>" " ⑧</b>	-.0061	.0070	.0033	-.0047	-.0206	-.0310	-.0042	.0374	.7002	.0159	.0091	.0419	.0061
<b>v = -U { ⑥ + ⑧ }</b>	-.0099	-.8576	-.8483	.0047	.8656	.8816	-.0004	-.8802	1.5410	-.0159	.8317	.8020	-.0099
<b>V = U √ [u² + v²]</b>	.0788	1.0480	1.8130	2.1170	1.8200	1.0720	.1304	1.0750	2.2300	2.1240	1.8150	.9220	.0788
<b>β in lbs/ft²</b>	92.3	-9.16	-213.5	-32.1	-216.2	-14.05	91.4	-14.5	-371.0	-327.5	-213.0	-1.005	92.3
<b>" Cms of Water</b>	45.0	-4.48	-104.2	-12.1	-105.5	-7.08	44.6	-7.06	-181.0	-159.0	-103.3	-.49	45.0
<b>" " Mercury</b>	3.32	-.329	-7.60	-.11	-7.78	-.505	3.285	-.522	-13.34	-11.78	-7.66	-.0361	3.32
<b>β ÷ PV²/2</b>	.994	-.098	-2.28	-.3	-2.31	-.150	.983	-.155	-3.97	-3.52	-2.29	-.012	.994

**NOTE:-** To Find u, v or V multiply values in Table by U.

R.T.C  
944.



/test data pressure distribution curves have been plotted. This gives comparative results as they are both taken at 82 ft.per second.

- (c) Contrast with Experimental Curves : The comparison of theoretical derived curves for second row with those plotted from experimental data, Plate No.46, Figs.1 & 2, shows that the presence of the second row raises the back pressure in the first. The second and first rows, both for calculated and experimental, have remained at same frontal pressure. The second row curve falls within the first row showing a distinctly higher gradient of pressure from 0 to 90 and from 90 to 180 degrees. The curve of the second then departs from the symmetrical curve from 180 to 240 and the pressure is much steeper. This gives a greater velocity at the back second row tube, but from 240 to 270 degrees it returns to the value of the first row.

From the sketch of tube arrangement it will be seen that tube number (2) in second row is not now in the centre of bank of tubes but is above. Further it will be seen that there is now  $1\frac{1}{2}$  tubes above the centre line of tubes under consideration and, therefore,  $2\frac{1}{2}$  tubes below the tube axis xx for number (2) tube. This accounts for the change from 180 to 360 which forms a loop on the right hand side of the theoretical curve for the second row tube. This loop would have been on left hand side of curve if the tube(2) had been the second row tube considered.

The experimental curves for the second row tube pressure distribution curves, Plate No.46, Fig.2, show also this tendency. The breakaway point of these curves on the left hand side takes place at 30 degrees and on the right hand side at 220 degrees. This gives a steeper gradient on part of the second row tube under consideration. On taking second row tube marked 2 the opposite would be the case. In all second row tubes, however, the pressure gradient is always the greatest in the bank of four tubes.

PRESSURE DISTRIBUTION DIAGRAMS  
FOR  
DOUBLE ROW

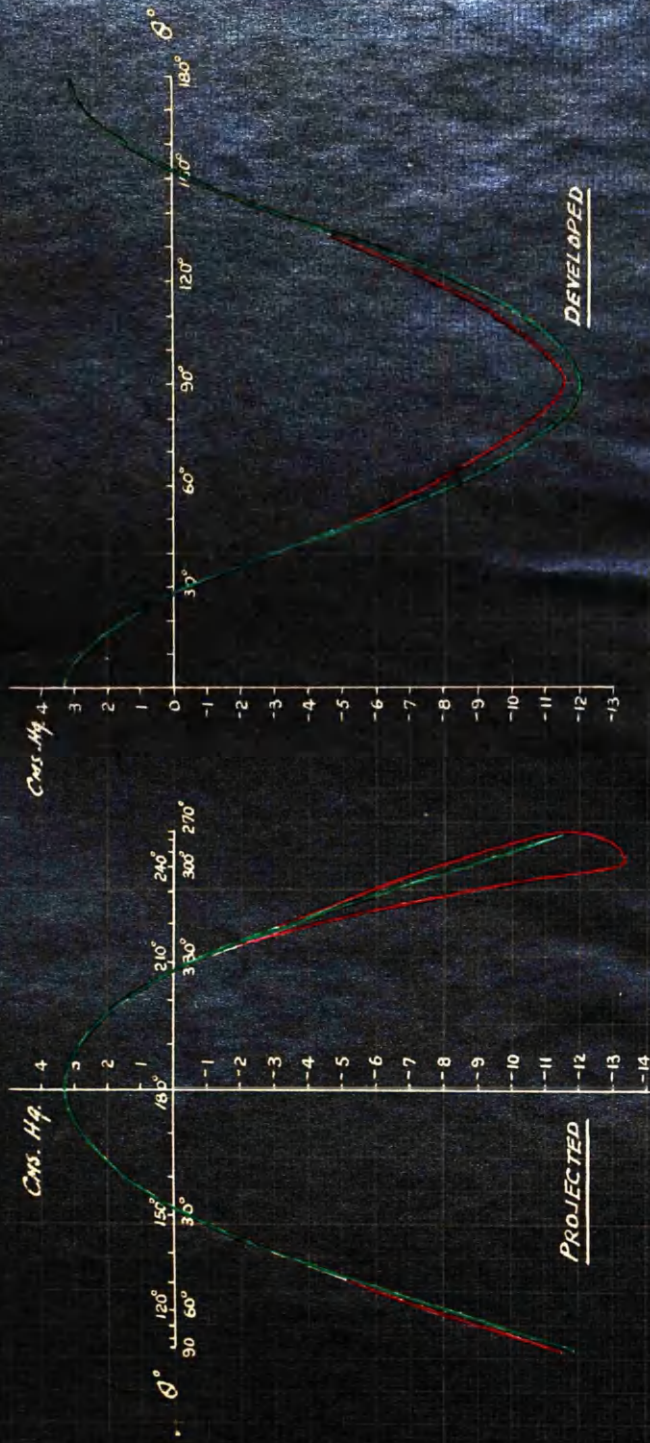


FIG. 1  
THEORETICAL

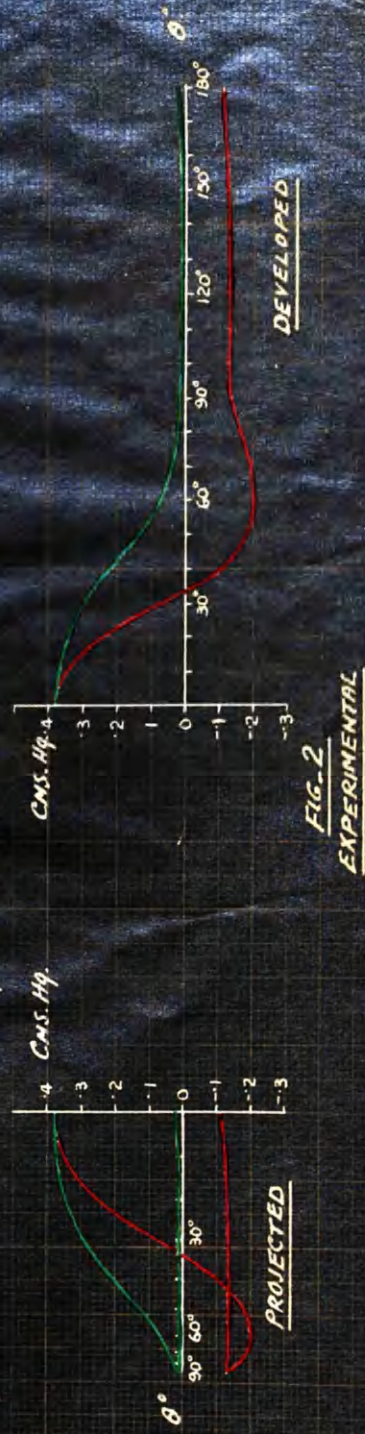


FIG. 2  
EXPERIMENTAL

PART 4 - THREE AND FOUR ROW CASES.

- (a) Further Extension of Formulae : In making the calculations and formulae for the three row bank the axis  $x_1x_1$  and  $y_1y_1$  are taken for the first row and equations 23 and 24 are evolved for tube marked (1), Table D.

For second row the tube marked (2) is used with axis  $x_2x_2$  and  $y_2y_2$  giving equations 25 and 26, Table E. The third row equations 27 and 28, Table F, have been derived using tube marked (3) and axis  $x_3x_3$  and  $y_3y_3$ . The axis and tubes under consideration are shown in sketch and the following tables give the results of calculations for the  $p \div \rho V_0^2/2$  ordinate values of the pressure distribution curves.

The sketch of the arrangement is given on Tables G-L. Here again the axis are  $x_1x_1$ ,  $y_1y_1$ ,  $x_2x_2$ ,  $y_2y_2$ ,  $x_3x_3$ ,  $y_3y_3$  and  $x_4x_4$ ,  $y_4y_4$  for the four row bank of tubes.

In this case the equations used are numbered 29 to 36. The pressure values have been calculated from these equations and plotted for the fourth row tube marked (4) in the four row bank of tubes. Here again the second row curve has been plotted along with that of the fourth, Plate No.47, Fig.4a.

- (b) Calculations and Results : The calculations are similar to those of the two row bank using equations 23 to 28 and the results have been calculated and tabulated. Formulae and tables for three row banks are in separate sheets.

Calculations have also been made for all four rows and the pressure distribution values obtained as a ratio  $p \div \rho V_0^2/2$ . The equations 29 to 36 are given on separate sheets along with table of results.

- (c) Contrast with Experimental Curves : The theoretical values as calculated have been plotted, Plate No.47. It will be seen that there is a further rise of the curve at the 90 degree point, otherwise the pressure curve is similar to that of the first row tube. The front pressure is the same and the curve is symmetrical when plotted from calculated values, Fig.1. With the experimental data when the curves are plotted, Fig.2 they are approximately symmetrical for the third row tube marked (3). The frontal pressure is very much reduced although/

# THREE ROW FORMULAE.

$$u = U \left\{ 1 + c^2 \left\langle \frac{(y+na)^2 - x^2}{[(y+na)^2 + x^2]^2} \right\rangle + c^2 \left\langle \frac{(y+na)^2 - (x-b)^2}{[(y+na)^2 + (x-b)^2]^2} \right\rangle + c^2 \left\langle \frac{(y+na)^2 - (x-2b)^2}{[(y+na)^2 + (x-2b)^2]^2} \right\rangle \right\} \dots (23)$$

WHERE  $n = 0^{\pm} 1$  and  $\pm 2$        $n = \pm \frac{1}{2}$  and  $\pm \frac{1}{2}$        $n = 0^{\pm} 1$  and  $\pm 2$

$$v = -U \left\{ c^2 \left\langle \frac{2x(y+na)}{[(y+na)^2 + x^2]^2} \right\rangle + c^2 \left\langle \frac{2(x-b)(y+na)}{[(y+na)^2 + (x-b)^2]^2} \right\rangle + c^2 \left\langle \frac{2(x-2b)(y+na)}{[(y+na)^2 + (x-2b)^2]^2} \right\rangle \right\} \dots (24)$$

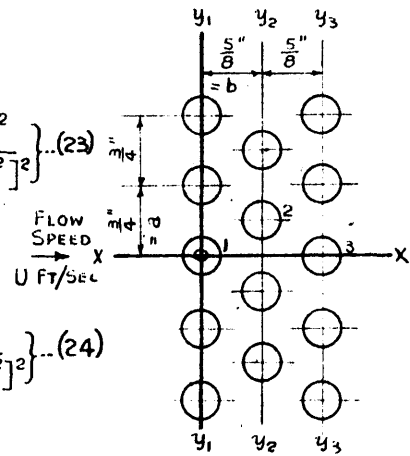


TABLE "D"

## COLLECTED RESULTS FOR 1<sup>ST</sup> ROW.

$\theta$	$0^\circ$	$30^\circ$	$60^\circ$	$90^\circ$	$120^\circ$	$150^\circ$	$180^\circ$
x	c	.866c	.5c	0	-.5c	-.866c	-c
y	0	.5c	.866c	c	.866c	.5c	0
TERM N <sup>o</sup> ①	-.8654	-.3572	.6672	1.1837	.6672	-.3572	-.8654
" " ③	.0632	-.0050	-.0486	-.0531	-.0498	-.0464	-.0556
" " ⑨	-.0382	-.0367	-.0363	-.0336	-.0331	-.0321	-.0317
$u = U \{ ① \ ③ \ ⑨ \}$	.0996	.6011	1.5823	2.0970	1.5843	.5643	.0473
TERM N <sup>o</sup> ②	0	.8465	.8421	0	-.8188	.8482	0
" " ④	0	.0321	.0248	.0086	.0023	-.0018	0
" " ⑩	0	-.0019	-.0028	-.0031	-.0027	-.0062	0
$v = -U \{ ② \ ④ \ ⑩ \}$	0	-.8767	-.8641	-.0055	.8192	.8562	0
$V = U \sqrt{u^2 + v^2}$	.0996	1.0610	1.8040	2.0980	1.7850	1.0250	.0473
$\beta$ in lbs/ft <sup>2</sup>	92.0	12.0	-209.0	-313.5	-203.0	-4.74	92.6
" " Cms of Water	4.5	-5.87	-102.2	-153.2	-99.2	-2.319	45.3
" " - Mercury	3.31	-.432	-7.52	-11.28	-7.3	-.1705	3.34
$\beta \div \rho v_0^2 / 2$	.991	-.123	-2.26	-3.40	-2.18	-.050	.998

NOTE:- To Find u, v or V multiply values in Table by U.

RTC  
1944.



# THREE ROW FORMULAE.

$$u = U \left\{ 1 + C^2 \left\{ \frac{(y+na)^2 - x^2}{[(y+na)^2 + x^2]^2} \right\} + C^2 \left\{ \frac{(y+na)^2 - (x+b)^2}{[(y+na)^2 + (x+b)^2]^2} \right\} + C^2 \left\{ \frac{(y+na)^2 - (x+2b)^2}{[(y+na)^2 + (x+2b)^2]^2} \right\} \right\} \quad (27)$$

WHERE  $n = 0^{\pm 1}$  and  $\pm 2$        $n = \pm \frac{1}{2}$  and  $\pm \frac{1}{2}$        $n = 0^{\pm 1}$  and  $\pm 2$

$$v = -U \left\{ C^2 \left\{ \frac{2x(y+na)}{[(y+na)^2 + x^2]^2} \right\} + C^2 \left\{ \frac{2(x+b)(y+na)}{[(y+na)^2 + (x+b)^2]^2} \right\} + C^2 \left\{ \frac{2(x+2b)(y+na)}{[(y+na)^2 + (x+2b)^2]^2} \right\} \right\} \quad (28)$$

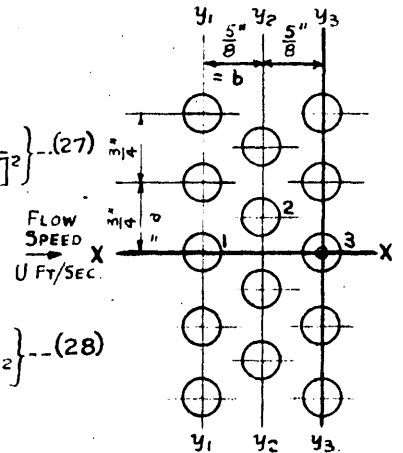


TABLE "F"

## COLLECTED RESULTS FOR 3<sup>RD</sup> ROW.

$\theta$	$0^\circ$	$30^\circ$	$60^\circ$	$90^\circ$	$120^\circ$	$150^\circ$	$180^\circ$
$x$	$c$	$.866c$	$.5c$	$0$	$-.5c$	$-.866c$	$-c$
$y$	$0$	$.5c$	$.866c$	$c$	$.866c$	$.5c$	$0$
TERM N <sup>o</sup> (1)	$-.8654$	$-.3572$	$-.6672$	$1.1837$	$-.6672$	$-.3572$	$-.8654$
" " (13)	$0$	$-.0464$	$-.0497$	$-.0004$	$.0485$	$.0001$	$.0034$
" " (15)	$-.0316$	$-.1076$	$-.0330$	$-.0348$	$-.0362$	$-.0084$	$-.0382$
$u = U \{1 + (1) (13) (15)\}$	$1.030$	$.4688$	$1.5845$	$2.1485$	$1.5805$	$.6344$	$-.0998$
TERM N <sup>o</sup> (2)	$0$	$.8465$	$.8421$	$0$	$-.8188$	$-.8482$	$0$
" " (14)	$0$	$-.0001$	$-.0022$	$-.0085$	$-.0247$	$-.0330$	$0$
" " (16)	$0$	$.0226$	$.0026$	$.0034$	$-.0051$	$-.0013$	$0$
$v = -U \{(2) (14) (16)\}$	$0$	$-.8690$	$-.8425$	$.0051$	$.8486$	$.8799$	$0$
$V = U \sqrt{u^2 + v^2}$	$1.030$	$.9960$	$1.7900$	$2.1485$	$1.7910$	$1.0820$	$.0998$
$\beta$ in lbs/ft <sup>2</sup>	$92.0$	$-.600$	$-.206.0$	$-.336.5$	$-.208.0$	$-.16.2$	$92.1$
" " Cms of Water	$45.0$	$-.2935$	$-.100.8$	$-.164.5$	$-.101.8$	$-.7.92$	$45.1$
" " " Mercury	$3.31$	$-.0216$	$-.7.41$	$-.12.1$	$-.7.49$	$-.582$	$3.32$
$\beta + \rho v^2 / 2$	$.989$	$-.008$	$-.2.20$	$-.3.62$	$-.2.21$	$-.171$	$.990$

NOTE:- To Find  $u, v$  or  $V$  multiply values in Table by  $U$

RTC  
1944.

PRESSURE DISTRIBUTION DIAGRAMS

FOR  
THREE ROWS

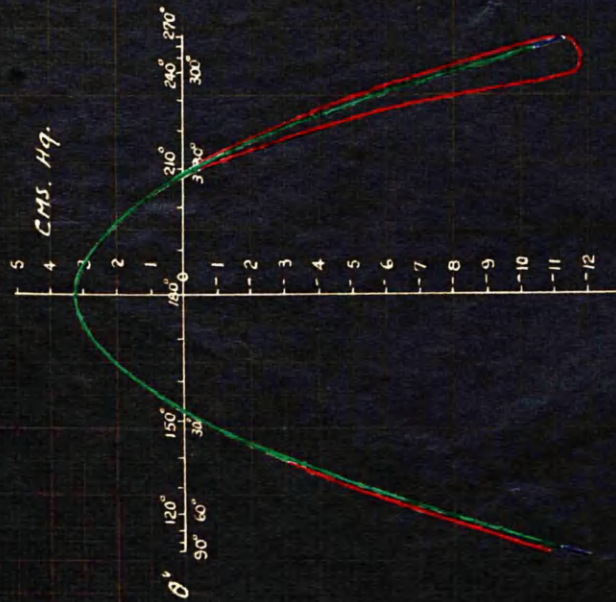


FIG-1 THEORETICAL

FOR  
FOUR ROWS

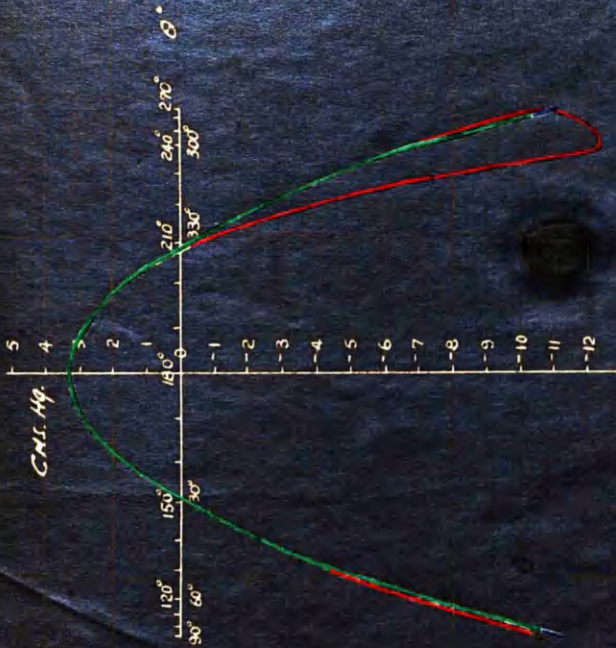


FIG-3 THEORETICAL

CMS. Hq.

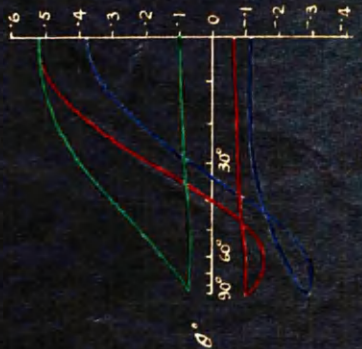


FIG-2 EXPERIMENTAL

CMS. Hq.

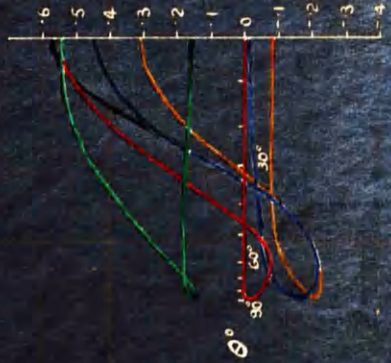
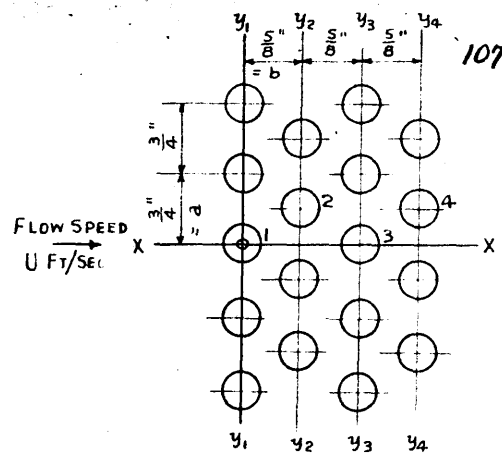


FIG-4 EXPERIMENTAL

# FOUR ROW FORMULAE.



$$u = U \left\{ 1 + C^2 \left[ \frac{(y+na)^2 - x^2}{[(y+na)^2 + x^2]^2} \right] + C^2 \left[ \frac{(y+na)^2 - (x-b)^2}{[(y+na)^2 + (x-b)^2]^2} \right] + C^2 \left[ \frac{(y+na)^2 - (x-2b)^2}{[(y+na)^2 + (x-2b)^2]^2} \right] + C^2 \left[ \frac{(y+na)^2 - (x-3b)^2}{[(y+na)^2 + (x-3b)^2]^2} \right] \right\} \dots (29)$$

WHERE  $n = 0^{\pm 1}$  and  $\pm 2$        $n = \pm \frac{1}{2}$  and  $\pm \frac{1}{2}$        $n = 0^{\pm 1}$  and  $\pm 2$        $n = \pm \frac{1}{2}$  and  $\pm \frac{1}{2}$ .

$$v = -U \left\{ C^2 \left[ \frac{2x(y+na)}{[(y+na)^2 + x^2]^2} \right] + C^2 \left[ \frac{2(x-b)(y+na)}{[(y+na)^2 + (x-b)^2]^2} \right] + C^2 \left[ \frac{2(x-2b)(y+na)}{[(y+na)^2 + (x-2b)^2]^2} \right] + C^2 \left[ \frac{2(x-3b)(y+na)}{[(y+na)^2 + (x-3b)^2]^2} \right] \right\} \dots (30)$$

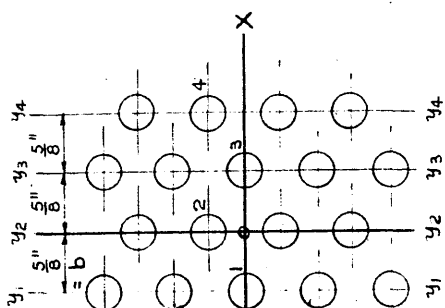
TABLE "G"  
COLLECTED RESULTS FOR 1<sup>ST</sup> ROW.

$\theta$	$0^\circ$	$30^\circ$	$60^\circ$	$90^\circ$	$120^\circ$	$150^\circ$	$180^\circ$
x	c	.866c	.5c	0	-.5c	-.866c	-c
y	0	.5c	.866c	c	.866c	.5c	0
TERM N <sup>o</sup> (1)	-.8654	-.3572	.6672	1.1837	.6672	-.3572	-.8654
" " (3)	.0032	-.0050	-.0486	-.0531	-.0498	-.0464	-.0556
" " (9)	-.0382	-.0367	-.0363	-.0336	-.0331	-.0321	-.0317
" " (17)	-.0279	-.0279	-.0260	-.0245	-.0231	-.0222	-.0218
$u = U \{ (1) (3) (9) (17) \}$	.0717	.5731	1.5563	2.0726	1.5612	.5421	-.0255
TERM N <sup>o</sup> (2)	0	.8465	.8421	0	-.8188	-.8482	0
" " (4)	0	.0321	.0248	.0086	.0023	-.0018	0
" " (10)	0	-.0019	-.0028	-.0031	-.0027	-.0062	0
" " (18)	0	-.0017	-.0028	-.0029	-.0025	-.0013	0
$v = -U \{ (2) (4) (10) (18) \}$	0	-.8750	.8614	-.0026	.8217	.8575	0
$V = U \sqrt{u^2 + v^2}$	.0717	1.0480	1.7800	2.0730	1.7620	1.0120	.0255
p in lbs/ft <sup>2</sup>	92.4	-8.65	-200.7	-305	-195.5	-2.65	92.2
" " Cms of Water	45.2	-4.23	-98.5	-149.2	-95.7	-1.29	45.2
" " " Mercury	3.32	-.311	-7.24	-10.98	-7.04	-.095	3.32
$p \div \rho V_0^2 / 2$	.995	-.100	-2.165	-3.30	-2.10	-.024	.995

NOTE:- To Find u, v or V multiply values in Table by U.

R.T.C.  
1944

# FOUR ROW FORMULAE.



$$u = U \left\{ 1 + c^2 \frac{(y+nd)^2 - x^2}{[(y+nd)^2 + (x+b)^2]^2 + c^2} + c^2 \frac{(y+nd)^2 - (x-b)^2}{[(y+nd)^2 + (x-b)^2]^2 + c^2} \right\} \quad (19)$$

WHERE  $n = \pm \frac{1}{2}$  and  $\pm \frac{1}{2}$   $n = 0, \pm 1$  and  $\pm 2$   $n = \pm \frac{1}{2}$  and  $\pm 1 \frac{1}{2}$ .

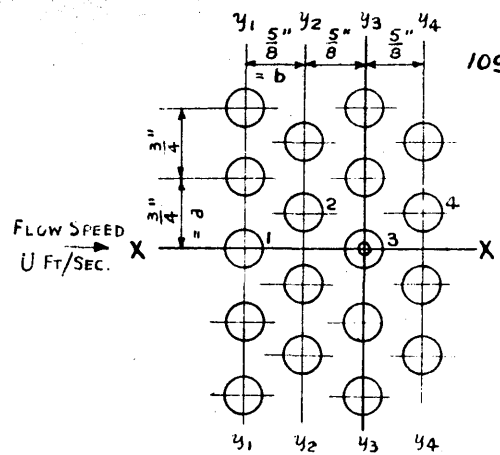
$$v = -U \left\{ c^2 \frac{2x(y+nd)}{[(y+nd)^2 + (x+b)^2]^2 + c^2} + c^2 \frac{2(x-b)(y+nd)}{[(y+nd)^2 + (x-b)^2]^2 + c^2} \right\} \quad (20)$$

TABLE "H" COLLECTED RESULTS FOR 2<sup>ND</sup> ROW.

$\theta^\circ$	$0^\circ$	$30^\circ$	$60^\circ$	$90^\circ$	$120^\circ$	$150^\circ$	$180^\circ$	$210^\circ$	$240^\circ$	$270^\circ$	$300^\circ$	$330^\circ$	$360^\circ$
X	C	.866C	.5C	0	-.5C	-.866C	-C	-.866C	-.5C	0	.5C	.866C	C
Y	2C	2.5C	2.866C	3C	2.866C	2.5C	2C	1.5C	1.34C	C	1.34C	1.5C	2C
TERM N <sup>o</sup> (5)	-.8814	-.3744	.6483	1.1633	.6481	-.3743	-.8815	-.3707	.6547	1.1710	.654C	-.3706	-.8814
" (7)	-.0398	-.0208	-.0436	-.0467	-.0420	-.0127	.0119	-.0112	-.0394	-.0476	-.0422	-.0402	-.0398
" (11)	.0124	-.0126	-.0418	-.0468	-.0440	-.0329	-.0397	-.0403	-.0423	-.0449	-.0398	-.0112	.0124
" (13)	-.0406	-.0407	-.0378	-.0351	-.1065	-.0317	-.0309	-.0330	-.0347	-.0324	-.0377	-.0319	-.0406
$u = U \{ (5) + (7) + (11) + (13) \}$	.0505	.5515	1.5251	2.0347	1.4556	.5483	.0598	.5448	1.5383	2.0461	1.5349	.5461	.0505
TERM N <sup>o</sup> (6)	.0039	.8506	.8450	0	-.8450	-.8506	-.0038	.8428	.8408	0	-.8408	-.8439	.0038
" (8)	.0061	.0070	.0033	-.0047	-.0206	-.0310	.0042	.0374	.7002	.0159	.0091	-.0419	.0061
" (12)	-.0042	.0288	.0206	.0046	-.0044	.0055	.0004	-.0068	-.0094	-.0156	-.0305	-.0375	-.0042
" (20)	-.0098	-.0111	-.0138	-.0139	-.0124	-.0104	-.0081	.0166	-.0050	-.0042	-.0095	-.0067	-.0098
$v = -U \{ (6) + (8) + (12) + (20) \}$	.0041	-.8754	-.8551	.0140	.8824	.8865	.0073	-.8900	-1.5257	.0039	.8716	.8462	.0041
$V = U \sqrt{u^2 + v^2}$	.0506	1.0300	1.7480	2.0350	1.7000	1.0420	.0598	1.0400	2.1610	2.0460	1.7620	1.0050	.0506
p in lbs/ft <sup>2</sup>	92.7	-6.37	-191	-290	-176.0	-8.28	92.6	-8.28	-342	-296	-196.2	-12.10	92.7
" " Cms of Water	45.4	-3.12	-93.4	-142	-86.3	-4.05	45.3	-4.05	-167	-145	-96.1	-5.93	45.4
" " " Mercury	3.33	-.229	-6.87	-10.42	-6.34	-.290	3.33	-.290	-12.3	-10.65	-7.06	-.436	3.33
p ÷ $\rho \sqrt{2}$	.998	-.068	-2.55	-3.12	-1.885	-.069	.995	-.069	-3.68	-3.19	-2.105	-.013	.998

NOTE:- To Find u, v or V multiply values in Table by U.

# FOUR ROW FORMULAE.



$$u = U \left\{ 1 + c^2 \left[ \frac{(y+na)^2 - x^2}{[(y+na)^2 + x^2]^2} \right] + c^2 \left[ \frac{(y+na)^2 - (x+b)^2}{[(y+na)^2 + (x+b)^2]^2} \right] + c^2 \left[ \frac{(y+na)^2 - (x+2b)^2}{[(y+na)^2 + (x+2b)^2]^2} \right] + c^2 \left[ \frac{(y+na)^2 - (x-b)^2}{[(y+na)^2 + (x-b)^2]^2} \right] \right\} \dots (33)$$

WHERE  $n = 0^{\pm} 1$  and  $\pm 2$        $n = \pm \frac{1}{2}$  and  $\pm 1\frac{1}{2}$        $n = 0^{\pm} 1$  and  $\pm 2$        $n = \pm \frac{1}{2}$  and  $\pm 1\frac{1}{2}$

$$v = -U \left\{ c^2 \left[ \frac{2x(y+na)}{[(y+na)^2 + x^2]^2} \right] + c^2 \left[ \frac{2(x+b)(y+na)}{[(y+na)^2 + (x+b)^2]^2} \right] + c^2 \left[ \frac{2(x+2b)(y+na)}{[(y+na)^2 + (x+2b)^2]^2} \right] + c^2 \left[ \frac{2(x-b)(y+na)}{[(y+na)^2 + (x-b)^2]^2} \right] \right\} \dots (34)$$

TABLE "K"

## COLLECTED RESULTS FOR 3<sup>RD</sup> ROW.

$\theta$	$0^\circ$	$30^\circ$	$60^\circ$	$90^\circ$	$120^\circ$	$150^\circ$	$180^\circ$
X	c	.866c	.5c	0	-.5c	-.866c	-c
Y	0	.5c	.866c	c	.866c	.5c	0
TERM N <sup>o</sup> (1)	-.8654	-.3572	.6672	1.1837	.6672	-.3572	-.8654
" " (13)	0	-.0464	-.0497	-.0004	-.0485	.0001	.0034
" " (15)	-.0316	-.1076	-.0030	-.0348	-.0362	-.0084	-.0382
" " (3)	-.0032	-.0050	-.0486	-.0531	-.0498	-.0464	-.0556
$u = U \{ (1) (3) (15) (3) \}$	.1062	.4838	1.5359	2.0954	1.6297	.5880	.0442
TERM N <sup>o</sup> (2)	0	.8465	.8421	0	-.8188	-.8482	0
" " (14)	0	-.0001	-.0022	-.0085	-.0247	-.0330	0
" " (16)	0	.0226	.0026	.0034	-.0051	.0013	0
" " (4)	0	.0321	.0248	.0086	.0023	-.0018	0
$v = -U \{ (2) (14) (16) (3) \}$	c	-.9011	-.8673	-.0035	.8463	.8817	0
$V = U \sqrt{u^2 + v^2}$	.1062	1.0220	1.7600	2.1000	1.8300	1.0600	.0442
$p$ in lbs/ft <sup>2</sup>	91.8	-4.23	-196.3	-314	-218	-11.35	92.7
" " Cms of Water	45.0	-2.07	-96.0	-154	-106.6	-5.55	45.4
" " " Mercury	3.31	-.152	-7.05	-11.3	-7.84	-.408	3.34
$p \div \rho v_0^2 / 2$	.989	-.040	-2.10	-3.14	-2.35	-.124	.998

NOTE:- To Find u, v or V multiply values in Table by U.

RTC  
1944.

# FOUR ROW FORMULAE.

$$u = U \left\{ 1 + c^2 \frac{(y+na)^2 - x^2}{[(y+na)^2 + x^2]^2} + c^2 \frac{(y+na)^2 - (x+b)^2}{[(y+na)^2 + (x+b)^2]^2} + c^2 \frac{(y+na)^2 - (x+3b)^2}{[(y+na)^2 + (x+3b)^2]^2} \right\} \quad (35)$$

WHERE  $n = +\frac{1}{2}$  and  $+\frac{1}{2}$        $n = 0^+ - 1$  and  $-2$

$$v = -U \left\{ c^2 \frac{2x(y+na)}{[(y+na)^2 + x^2]^2} + c^2 \frac{2(x+b)(y+na)}{[(y+na)^2 + (x+b)^2]^2} + c^2 \frac{2(x+3b)(y+na)}{[(y+na)^2 + (x+3b)^2]^2} \right\} \quad (36)$$

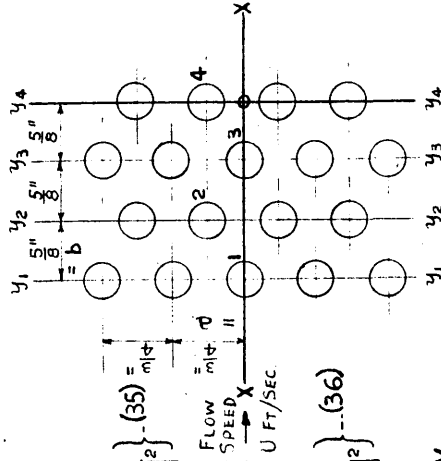


TABLE "L"  
COLLECTED RESULTS FOR 4<sup>th</sup> ROW.

$\theta^\circ$	0°	30°	60°	90°	120°	150°	180°	210°	240°	270°	300°	330°	360°
X	C	.866C	.5C	0	-.5C	-.866C	-C	-.866C	-.5C	0	.5C	.866C	C
Y	2C	2.5C	2.866C	3C	2.866C	2.5C	2C	1.5C	1.134C	C	1.134C	1.5C	2C
TERM No	⑤	-.8814	-.3744	.6483	1.1633	.6481	-.3743	-.8815	-.3707	.6547	1.1710	-.6546	-.8814
"	⑦	-.0398	-.0208	-.0436	-.0467	-.0420	-.0127	.0119	-.0112	-.0394	-.0476	-.0422	-.0398
"	②①	-.0320	-.0320	-.0331	-.0352	-.0408	-.0404	-.0416	-.0409	-.0404	-.0370	-.0348	-.0320
"	②③	-.0224	-.0231	-.0230	-.0241	-.0255	-.0267	-.0274	-.0272	-.0259	-.0251	-.0238	-.0224
$u = U \{ \text{⑤} + \text{⑦} + \text{②①} + \text{②③} \}$	.0244	.5497	1.5486	2.0573	1.5398	.5459	.0376	.5500	1.5490	2.0613	1.5538	.5335	.0244
TERM No	⑥	.0038	.8506	.8450	0	-.8450	-.8506	-.0038	.8428	.8408	0	-.8408	-.8439
"	⑧	.0061	.0070	.0033	-.0047	-.0206	-.0310	.0042	.0374	.7002	.0159	-.0091	-.0419
"	②②	.0302	.0104	.0125	.0139	.0149	.0125	.0098	.0071	-.0277	.0045	.0048	.0063
"	②④	.0045	.0058	.0068	.0075	.0062	.0068	.0055	.0041	.0029	.0025	.0026	.0035
$v = -U \{ \text{⑥} + \text{⑧} + \text{②②} + \text{②④} \}$	-.0446	-.8738	-.8676	-.0167	.8445	.8623	-.0157	-.8914	-1.5162	-.0229	.8243	.7922	-.0446
$V = U \sqrt{u^2 + v^2}$	.0891	1.0310	1.7720	2.0600	1.7510	1.0200	.0197	1.0430	2.1620	2.0600	1.7590	.9540	.0891
P in lbs/ft <sup>2</sup>	92.2	5.9	199	298	192.5	3.82	92.6	344	301	194.2	8.28	92.2	
" " Cms of Water	45.1	2.88	97.5	146	94.1	1.87	45.3	168	147.4	95.2	4.05	45.1	
" " " Mercury	3.32	.212	7.16	10.71	6.92	1.38	3.33	3.25	12.38	10.82	7.0	3.32	
$P = \rho V^2 / 2$	.992	.064	2.14	3.20	2.07	.04	.96	.097	3.69	3.24	2.09	.992	

NOTE: To Find u, v or V multiply values in Table by U.

/although the pressure gradient is as steep as that for the second row.

In order to carry the comparison further the second row curve has been plotted from calculated values and placed on diagram, Fig.1. The gradient of the two curves from 0 to 180 degrees fall closely on the top of each other, but the second row pressure curve from 180 to 240 degrees is much steeper showing an increase of pressure. Then from 240 to 270 degrees the second sways over to the right and from 270 to 360 degrees falls on top of the third row curve.

The second row curve obtained from experimental data when placed with the third row curve shows the third row curve much smaller in area and the mean ordinate  $p/\rho V_0^2/2$  falls below that of the second row curve.

The values found by calculation from equations for the fourth row tube marked (4) have been compared with those of the second row tube marked (2) by plotting on the same base, Fig.3.

The second row 90 degree test point has risen owing to the presence of the third and fourth rows, otherwise the curves are similar.

It will be seen that the fourth row pressure curve has again swayed to the right between 240 and 270 degree angle of turn and does not return along the calculated values for calculated points from 180 to 240 degrees, that is, the fourth row tube marked (4) has the same loop as the second row tube marked (2). If the tube marked (4) had been under consideration the pressure curve loop would have appeared on the left side. The fourth row and the second row curves are un-symmetrical when the central axis is taken as xx in sketch.

The curves derived from the experimental data for the four rows, Fig.4, have been obtained for the speed 82 ft per second. The frontal pressures on first and second rows has again increased due to the addition of the fourth row to the bank. The second row frontal pressure is as great as the first row tube so that any additional change by adding to the bank of two rows has increased the pressure per square inch on the frontal portion from 0 degrees to breakaway point which is 40 degrees for second row tube.

Both experimental and calculated values show that the second row tubes are subjected to the most severe working in the four banks of tubes - staggered arrangement.

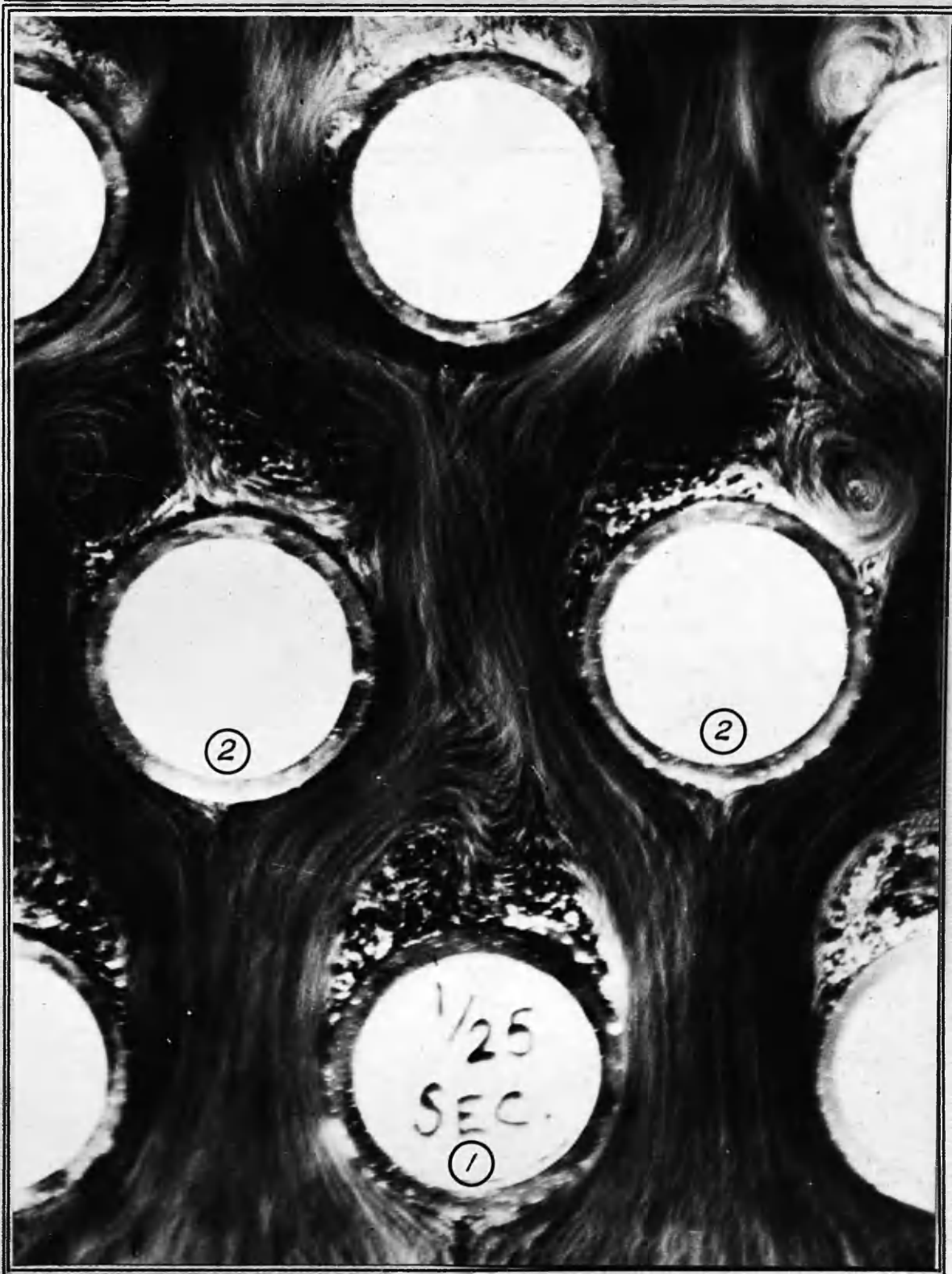
PART 5 - INFLUENCES OF WAKE VORTICES.

- (a) Turbulent Action in Wake Vortices : The theoretical calculations for the pressure distribution diagram for each row in a four row bank of tubes does not bring out the reason for the existence of the extra steep pressure gradient at the front 40 degree positions on the second row tubes which is revealed by experimental results. Owing to the failures of the second row tubes in boiler practice, it seems desirable, in spite of the difficulties, to examine the probable influence in introducing the last three rows into the turbulent wake behind the first row. This is necessary in so far as it effects the front half of the second row.

The single circular tube model in the vertical position has been so well studied that it has now become a simple laboratory experiment. The changes which take place in the wake vortices have been revealed by a film camera, by plotting a field of velocities and by graphical differentiation of experimental pressure distribution diagram velocities. Thom in his investigations remarks that after steady conditions have been attained in the flow stream the wake vortices, although turbulent, remain of a fixed pattern unless altered by baffle plates or approach of side of tunnel to tubes.

The turbulent wake behind the single row of tubes forms two approximately parallel vortex lines referred to as the Kármán Trail. These vortices are staggered as they leave the two sides of the tube alternately and have opposite rotations. Kármán<sup>(23)</sup> was successful in establishing a theory covering the stable formation of vortices behind the single row of tubes in a plane at right angles to the fluid stream. The effect of baffle or guide plates when tubes are inclined to the fluid stream and also the change in the vortices due to the addition of subsequent rows of tubes has brought into the investigation many variables.

Only general deductions from observations and records of the experimental work previously dealt with can be made. On referring to Plate No.14, which has again been introduced at this point, it is clear that a fixed pair of vortices forms in the wake to the rear of each tube. The directions of rotation and positions are similar to the direction of rotation and positions of the initial/



ENLARGEMENT OF SECOND ROW

WAKE VORTICES

/initial vortices in the wake behind a single tube, that is, before the vortices elongate and form the stable Kármán Trail.

- (b) Features of Vortex Pairs : The features of the vortex pairs behind the tubes in the banks brought out during the experiments are such as to clearly demonstrate that the strongest vortices lay between the first and second rows. This agrees with the variation in the pressure drag of the tubes which is greatest for the first row tubes and least for the fourth row tubes. It is highly probable that the strength of a pair of vortices is related to the pressure drag of the tube immediately in front and possibly it will be roughly proportional to the pressure drag.

It will be observed that the effect of the two tubes in the second row which split the stream-line flow from the first row into two parts has caused a backward flow of the stream into the wake behind the first row tube (1). This has the effect of reducing the velocity of flow of the stream at the centre of the second row tubes marked (2).

The velocity at the front of the second row tubes was found to be the same as at the front of tube (1). The velocity at the breakaway point on tube (2) has increased and stream-line flow becomes more like that at the front of the first row as it passes between the second row tubes. Owing to the backward flow into the wake, turbulent flow is seen to replace rotational vortices.

Attention is now drawn to the wake at the back of the second row which has now become very similar to that which would appear behind a single row of tubes. The turbulence in the wake vortices is not nearly so active as that behind the tubes in a front row bank of tubes. The pressure distribution curves for the third row show a frontal pressure less than that on the second row. The area of flow is contracted and remains so, thus giving as steep a gradient as that of the second.

- (c) Change of Strength in Wake Vortices : The change in strength in the vortices may be caused by pitch of tubes or width of rows. In the type of spacing being dealt with, the vortex pair behind the front tube (1) in Plate 14, has a maximum free vortex effect on the flow past the following two tubes marked (2) at approximately 40 degree angular positions. The ratio of the radii from the centres of the cores to this point on one side is about 2 : 3. Since this apparently held good throughout the experiments the circulations of the two vortices oppose each/

/each other and the net induced velocity will be equivalent to at least  $1/3$  of the effect of the nearest vortex alone.

Again the induced velocity tangential to the surface of the second row tube will increase from zero near  $\theta = 0$  to a maximum about 90 degrees. Hence the presence of the strong vortices in the turbulent wake at the rear of the first row tubes explains the comparatively steep pressure gradient at the 40 degree positions on the second row tubes obtained experimentally since a steep velocity gradient means a steep pressure gradient.

With the diminishing strength of the vortices behind the rows following the first, it was, therefore, to be expected that the maximum pressure gradient obtained from test results would also decrease for the rows corresponding with the diminishing vortex strength. The graphical differentiation of the pressure distribution curves, Plate No.30, shows that this is verified by test results. The maximum pressure gradient for the first row tube is outstandingly low. The reason for this is that there are no adjacent vortices as for the subsequent rows.

Plate No.47, Fig.4, for four row bank shows that the pressure at the frontal stagnation point of the second row tube is the same as that on front of the first and there is a drop in frontal pressure at the third and fourth rows. It is safe to assume that the velocity head must be high for the second row tube so as to keep frontal stagnation point pressures equal in first and second rows. It seems probable that the fluid velocity will reach a maximum at some point between the first and second row tubes.

Collectively these deductions indicate the existence of unique velocity and pressure conditions in the region at the front of the second row tubes marked (2) on Plate 14. The breakaway point on the second row tube is clearly seen to take place at about 40 degrees. This gives an opportunity for slag accumulation. As the bulge of slag grows on the second row steam boiler tube further restriction of stream line flow takes place with corresponding higher velocity and reduction of the front already narrow strip of tube surface on the second row.

In conclusion, I wish to acknowledge my indebtedness to Professor William Kerr, Ph.D., A.R.T.C., M.I.Mech.E., for his guiding influence throughout the research, to the Governors of the Royal Technical College for the privilege of using the Wind Tunnel and Air Compressor, and to my own Egyptian Government for giving me the opportunity to conduct this work in Britain.

APPENDIX I.

## APPENDIX I

### WIND TUNNEL EXPERIMENTS FOR LIFT AND DRAG ON BANK OF TUBES.

A model was made of four row bank of staggered tubes  $\frac{3}{8}$  in. diameter, 18 in. long,  $\frac{3}{4}$  in. pitch and  $\frac{5}{8}$  in. between the rows. This model was made of light material, with no side plates. The rows were wired at both ends and spaced evenly by thin wire distance pieces these took the place of the headers in the other models, Plate No.48, Fig.1.

The model was hung in front of the Wind Tunnel between two side plates 4 feet by 6 feet. The model was two feet apart from the nozzle. The weighing apparatus was attached to the model by light steel wires, which permitted of several position of angle of incidence from 0 - 180 degrees.

Three balances were used to measure the Lift and one to measure the Drag. The wire attachment is shown in Plate No.48, Fig.2 and the photograph shows the delicate balances used for measuring the pulls.

Fig.2 shows the arrangement for measuring the position of Change of angle of incidence very accurately. The balances are moved to suit by the aid of locating pins, one of which is seen in the photograph Fig.3. By these special arrangements the drag wire was kept of constant length, and also the angle  $\theta$  which it made with the vertical was kept constant.

The air speeds were 25,35 and 45 feet per second. Readings for these speeds are tabulated in Kilograms and equivalent in pounds pull. From these the coefficients of lift,  $C_L$ , and drag  $C_D$  are calculated for each speed. A fourth table gives the resultant,  $R$ , of Lift and drag. The vector diagram for obtaining resultant  $R$  is shown in Fig.4. Also the values for the angle between the drag line and  $R$ . and the angle  $\gamma$  between the normal to the box and  $R$ . are shown.

In Plate No.49, the curve of drag coefficients is shown for the four row bank plotted from the mean values of the drag coefficients obtained from experiments. On the same base is plotted the corresponding results for an R.A.F.6. Stream line Wing profile and a flat plate. It will be seen that the maximum coefficient of drag occurs at 90 degrees and the curves have similar features. The maximum gradient lying between 20 and 50 degrees angle of incidence.

Plate No.50, shows the curves of lift coefficient on angle of incidence base. The speeds are marked on the corresponding curves. The dotted line for the mean lift coefficient has been shown. In all four curves it will be seen that there are two maximum values  $C_L$ .

PLATE - 48 -

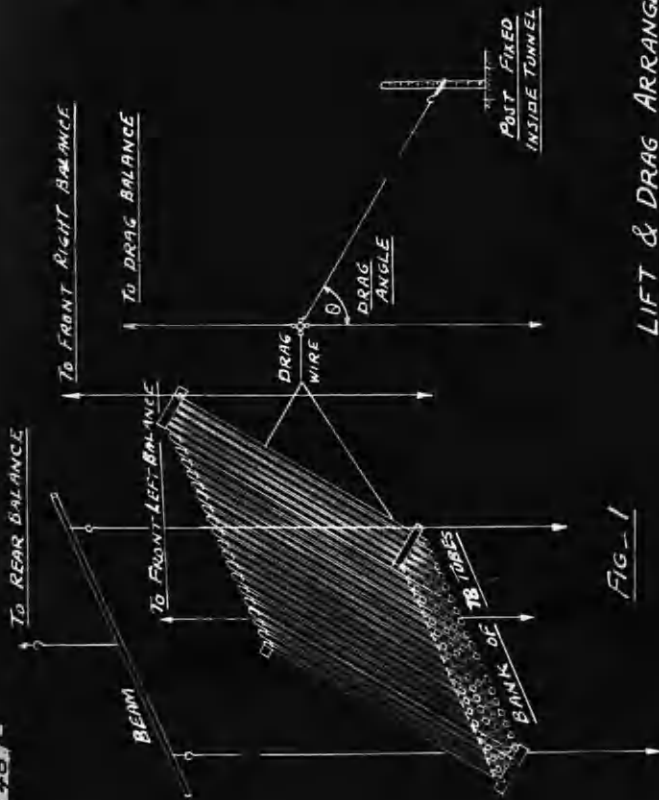


FIG-1

LIFT & DRAG ARRANGEMENT  
FOR BANK OF TB TUBES



FIG-3



FIG. 4

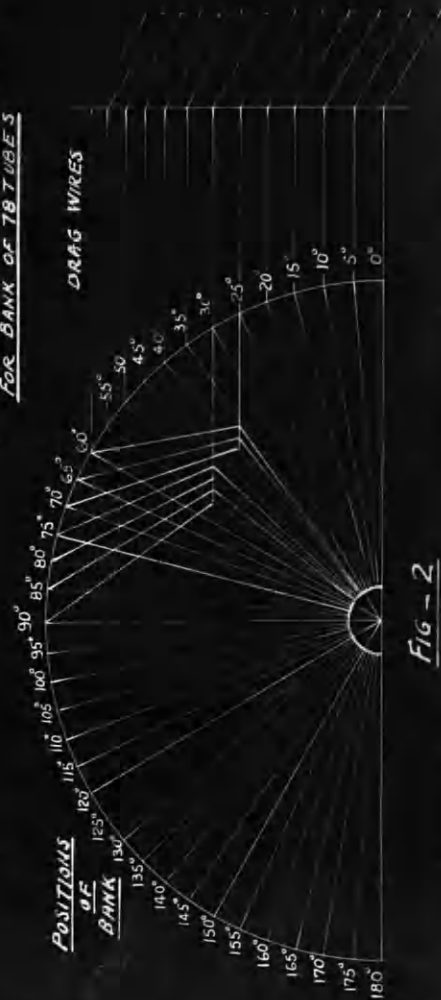
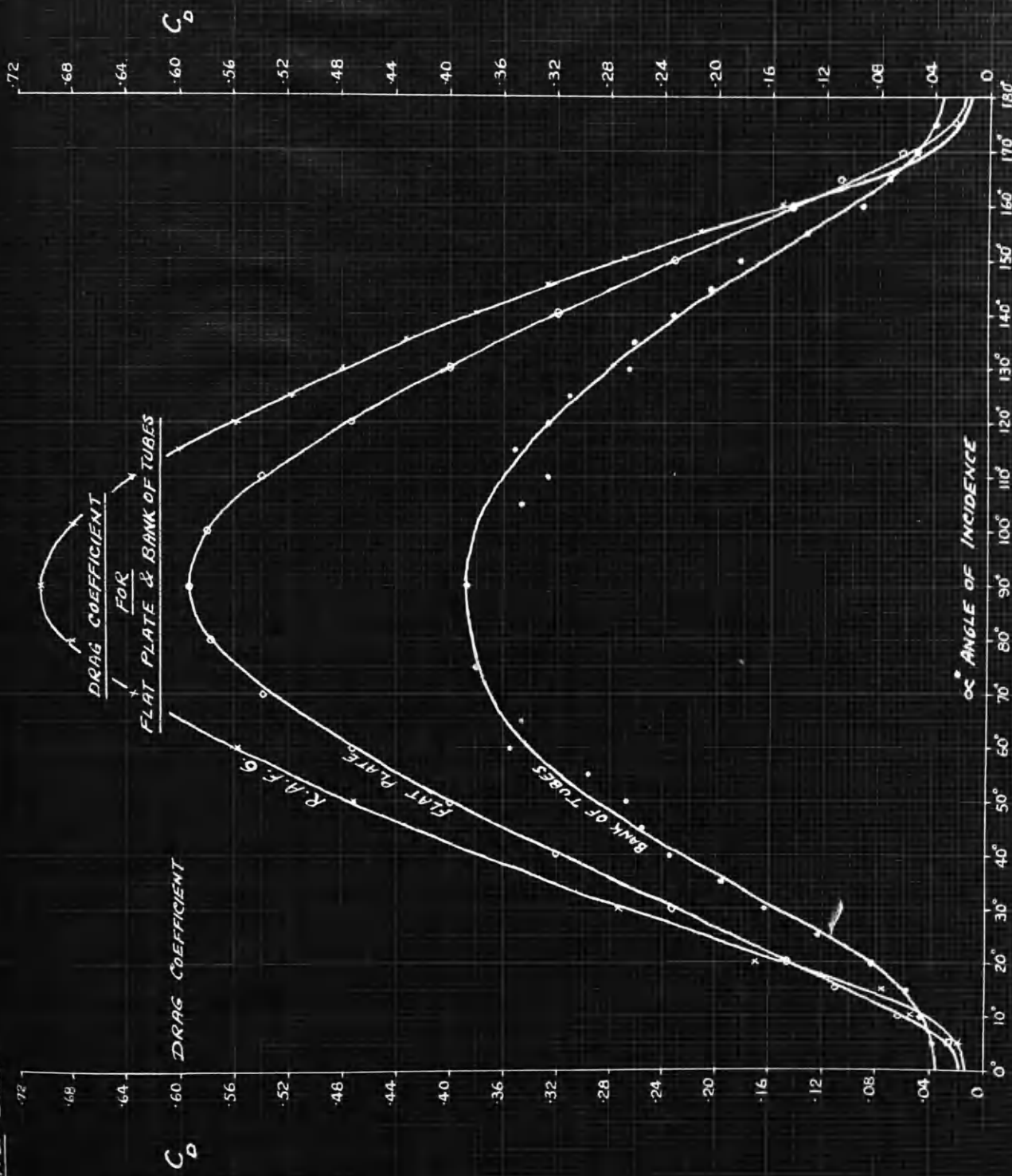
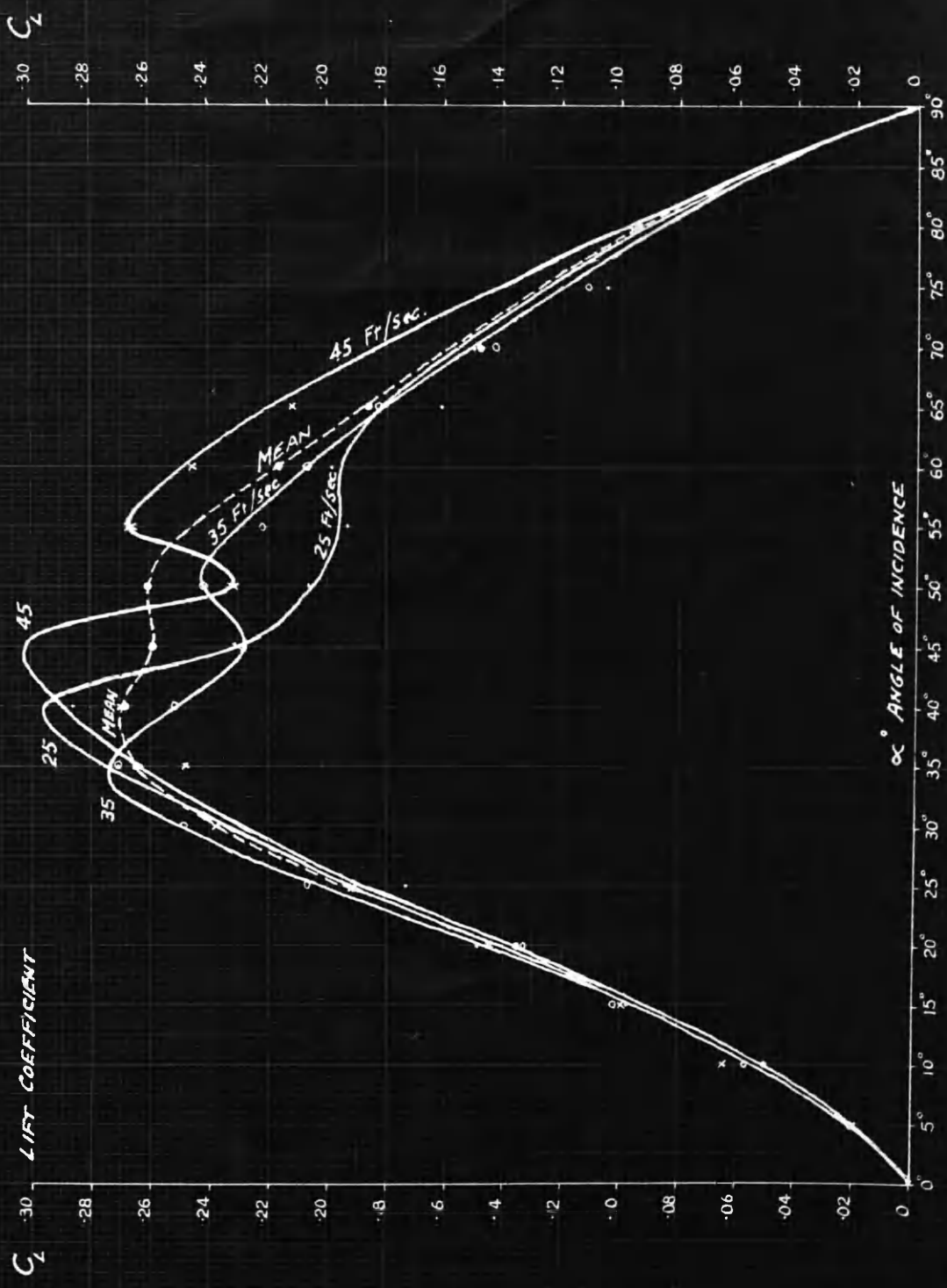


FIG-2



EFFECT OF SPEED ON LIFT COEFFICIENT



This is more pronounced in the 45 feet per second speed, but appears also in the dotted mean curve. The greater of the two maximum values of the coefficient of lift occurs at 40 degrees, and the maximum slope is between 10 and 30 degrees.

Curves for lift coefficient on a base 0 - 180 degree angle of incidence are shown in Plate No.51. These have been marked R.A.F.6. Wing Profile; Flat Plate and Bank of Tubes, and are plotted from mean values.

It will be observed that the three curves have much the same characteristics. The experimental mean points which were obtained for the bank of tubes has not such high maximum values as the stream line flow wing, nor the flat plate and its maximum occurs at 40 degrees angle of incidence.

When ratio  $L/D$  is taken as the ordinates and these plotted on the angle of incidence again the same features appear. The curves on Plate No.52 have been plotted together as it shows the effect of struts or guy ropes if not smoothed over.

Inset diagram is Plate No.53 represents the inclined Bank of Tubes, the angle of incidence or inclination of model bank being  $\alpha$  degrees. This was varied from 0 to 180 degrees, the lift,  $L$  and drag,  $D$ , are shown and the angles to the resultant,  $R$ , are as indicated. The three curves  $R$ ,  $\phi$  and  $\gamma$  are almost symmetrical about the vertical position.

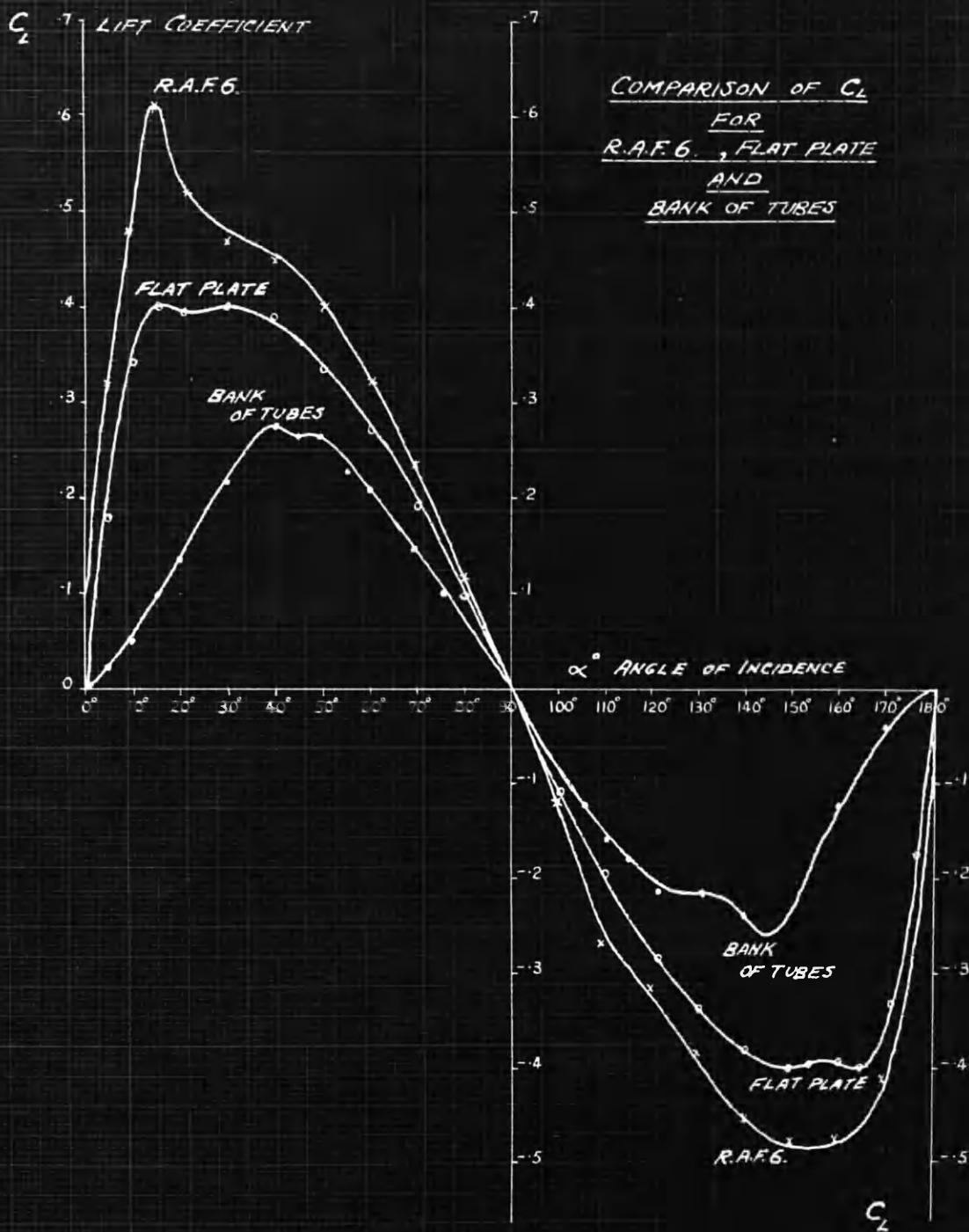
The gradient of the resultant  $R$  curve is greatest between 10 and 40 degrees and has maximum values at 60 degrees. Curve of  $\gamma$  when plotted shows three maximum points one at 0, 90 and 180 degrees. The minimum values are approximately at 15 and 155 degree angle of incidence.

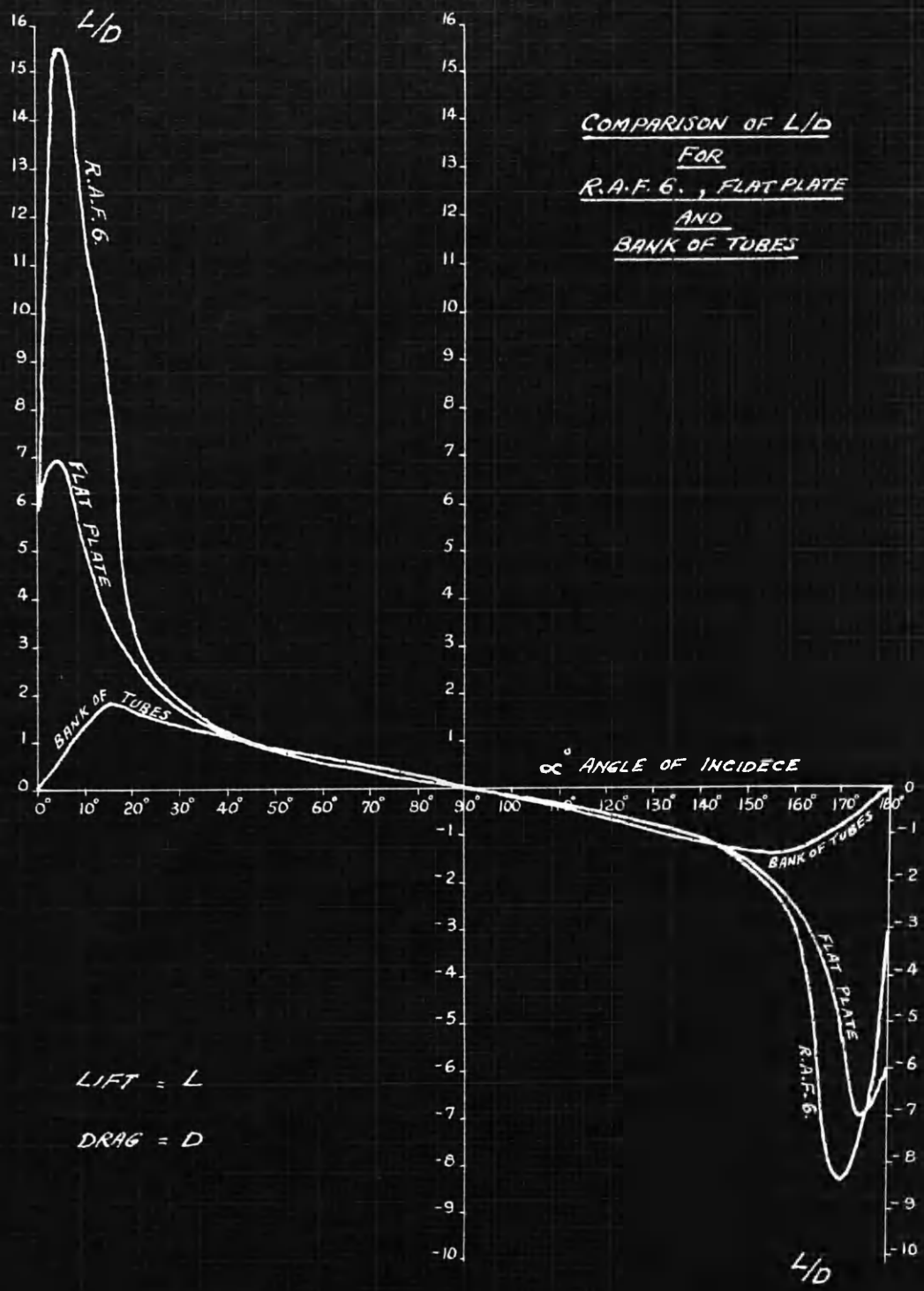
It will be seen that the  $\gamma$  curve has the same maximum value as that of the  $\phi$  curve, but goes below the datum level as the normal goes to the opposite side of  $R$  from that shown on Plate. This is shown in the negative portion of the  $\gamma$  curve which is below the datum from 45 to 90 and again from 90 to 128 degrees, reaching maximum again at 180 degrees.

The curves shown on Plate No.53 could be used for finding the resultant force on the bank at any angle of incidence from which the vertical and tangential component forces on the bank could be obtained.

Results are tabulated for 25, 35 and 45 ft/sec in tables 'a', 'b', 'c' and 'd'.

PLATE - 51 -





LIFT = L  
 DRAG = D

RESULTANT FORCE ON BANK OF TUBES  
IN STAGGERED ARRANGEMENT

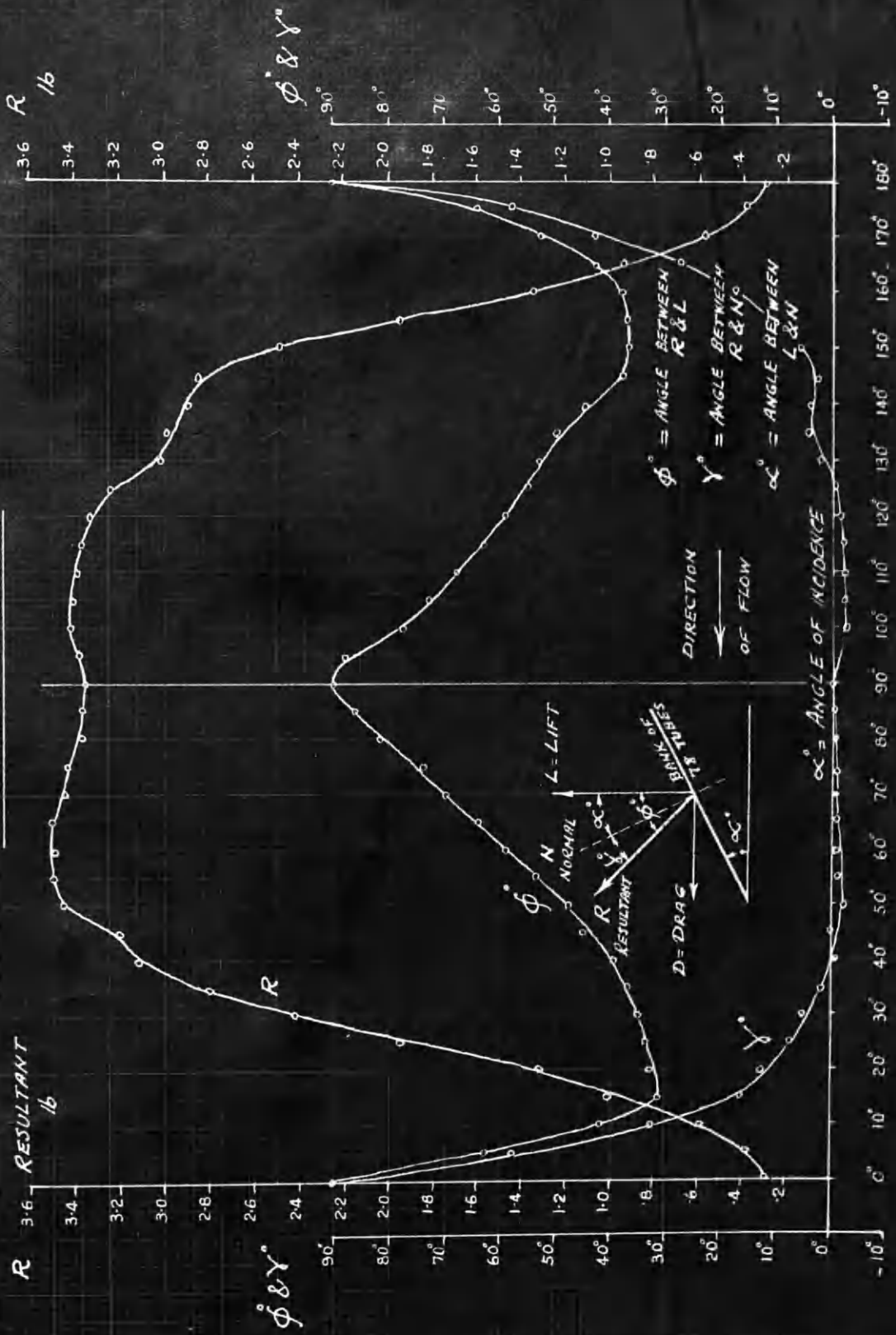


# TABLE "a" FOR

## LIFT AND DRAG TESTS ON BANK OF 78 TUBES

STAGGERED      SPEED 25 FT/SEC.      TUBE DIA  $\frac{3}{8}$ "

ANGLE OF INCIDENCE	DRAG			LIFT			DRAG			LIFT		
	DRAG READING	D IN lb.	COEF OF DRAG CD.	LIFT READING	L IN lb.	COEF OF LIFT CL.	DRAG READING	D IN lb.	COEF OF DRAG CD.	LIFT READING	L IN lb.	COEF OF LIFT CL.
0°	.017	.030	.0299	.001	.0022	.0008	.204	.964	.358	0	0	0
5°	.019	.0896	.0335	.024	.0529	.0198	—	—	—	—	—	—
10°	.025	.118	.0441	.061	.134	.0501	—	—	—	—	—	—
15°	.028	.132	.0493	.119	.262	.098	.184	.868	.321	.157	.346	.128
20°	.045	.212	.0793	.180	.397	.149	.183	.864	.320	.193	.426	.158
25°	.061	.288	.1080	.209	.461	.173	.206	.970	.359	.230	.507	.188
30°	.082	.387	.1510	.260	.373	.145	.164	.774	.286	.215	.474	.175

35°	.105	.495	.193	.315	.635	.271	.181	.854	.316	.273	.603	.223
40°	.127	.600	.234	.332	.732	.286	.130	.612	.226	.275	.406	.225
45°	.122	.576	.224	.269	.593	.231	.150	.707	.252	.312	.688	.256
50°	.120	.566	.221	.239	.527	.206	.126	.594	.226	.276	.608	.225
55°	.122	.576	.224	.224	.494	.193	.108	.509	.189	.266	.586	.217
60°	.196	.925	.344	.243	.536	.199	.100	.472	.175	.285	.608	.232

65°	.178	.640	.312	.196	.432	.161	.072	.340	.126	.231	.510	.189
70°	.218	1.030	.383	.184	.405	.151	.049	.231	.0792	.161	.355	.122
75°	.225	1.060	.394	.124	.273	.1015	.042	.198	.0678	.109	.240	.0822
80°	.185	.873	.325	.117	.258	.0975	.026	.123	.0422	.059	.131	.0449
85°	—	—	—	—	—	—	.014	.066	.0226	.011	.0242	.0083
90°	.204	.964	.358	0	0	0	.017	.0302	.0274	0	0	0

# TABLE "b" FOR

## LIFT AND DRAG TESTS ON BANK OF 78 TUBES.

TUBE DIA  $\frac{3}{8}$ "

SPEED 35 FT/SEC

STAGGERED

ANGLE OF INCIDENCE	DRAG			LIFT		
	DRAG READING IN lb	D (COEF. OF DRAG) CD	DRAG READING IN lb	LIFT READING IN lb	L (COEF. OF LIFT) CL	LIFT
90°	—	—	—	—	—	—
95°	—	—	—	—	—	—
100°	—	—	—	—	—	—
105°	.332	.340	.312	.688	.130	.130
110°	.358	.320	.393	.867	.164	.164
115°	.371	.331	.417	.920	.174	.174
120°	.370	.331	.517	1.140	.216	.216

ANGLE OF INCIDENCE	DRAG			LIFT		
	DRAG READING IN lb	D (COEF. OF DRAG) CD	DRAG READING IN lb	LIFT READING IN lb	L (COEF. OF LIFT) CL	LIFT
0°	.037	.033	.003	.007	.0013	.0013
5°	.048	.041	.049	.108	.0206	.0206
10°	.059	.053	.136	.300	.0573	.0573
15°	.068	.062	.242	.533	.102	.102
20°	.097	.075	.358	.590	.113	.113
25°	.150	.135	.493	1.087	.207	.207
30°	.188	.177	.567	1.250	.249	.249

125°	.331	.295	.547	1.210	.229	.229
130°	.319	.285	.545	1.200	.227	.227
135°	.303	.270	.744	1.640	.310	.310
140°	.270	.240	.605	1.335	.252	.252
145°	.241	.216	.624	1.380	.261	.261
150°	.218	.195	.599	1.320	.250	.250

35°	.223	.209	.616	1.360	.271	.271
40°	.243	.220	.591	1.300	.251	.251
45°	.244	.209	.521	1.150	.229	.229
50°	.308	.208	.552	1.215	.242	.242
55°	.320	.200	.506	1.115	.222	.222
60°	.374	.305	.494	1.090	.207	.207

155°	.160	.132	.482	1.065	.201	.201
160°	.116	.0356	.354	.782	.137	.137
165°	.091	.0752	.255	.562	.0984	.0984
170°	.064	.0528	.134	.296	.0518	.0518
175°	.045	.0371	.045	.0992	.0174	.0174
180°	.046	.038	.0	.0	.0	.0

65°	.398	.357	.436	.965	.1835	.1835
70°	.389	.348	.341	.752	.143	.143
75°	.442	.396	.265	.584	.111	.111
80°	.411	.308	.229	.505	.096	.096
85°	—	—	—	—	—	—
90°	.457	.410	.0	.0	.0	.0

# TABLE "C" FOR

## LIFT AND DRAG TESTS ON BANK OF 78 TUBES

STAGGERED      SPEED 45 FT/SEC.      TUBE DIA 3/8"

ANGLE OF INCIDENCE	DRAG			LIFT		
	DRAG READING IN lb	D	COEF OF DRAG CD	LIFT READING IN lb	L	COEF OF LIFT CL
0°	.071	335	0387	.005	.011	.0013
5°	.074	345	0403	.080	.176	.0203
10°	.096	452	0522	254	.560	.0646
15°	.115	543	0626	387	.853	.0985
20°	.158	746	0861	571	1.260	.1455
25°	.238	1.120	.129	.755	1.660	.192
30°	.288	1.360	.165	.887	1.950	.236

ANGLE OF INCIDENCE	DRAG			LIFT		
	DRAG READING IN lb	D	COEF OF DRAG CD	LIFT READING IN lb	L	COEF OF LIFT CL
90°	—	—	—	—	—	—
95°	—	—	—	—	—	—
100°	—	—	—	—	—	—
105°	.095	3.280	.385	.621	-1.370	-.156
110°	.623	2.940	.335	.815	-1.800	-.205
115°	.696	3.280	.385	.840	-1.850	-.211
120°	.670	3.160	.360	.961	-2.120	-.242

35°	.339	1.600	.134	.929	2.045	.247
40°	.421	1.990	.241	1.011	2.230	.270
45°	.543	2.560	.310	1.182	2.610	.316
50°	.508	2.400	.290	.870	1.920	.232
55°	.640	3.020	.365	1.003	2.240	.267
60°	.731	3.445	.392	.973	2.140	.245

125°	.631	2.980	.340	-1.045	-2.310	-.264
130°	.521	2.460	.280	-.904	-1.990	-.237
135°	.494	2.330	.266	-.577	-1.270	-.145
140°	.446	2.110	.241	-1.054	-2.320	-.264
145°	.398	1.880	.211	-1.217	-2.680	-.306
150°	.335	1.580	.187	-.955	-2.110	-.241

65°	.672	3.165	.361	.834	1.840	.211
70°	—	—	—	—	—	—
75°	.869	4.100	.467	1.057	2.330	.267
80°	—	—	—	—	—	—
85°	—	—	—	—	—	—
90°	—	—	—	—	—	—

155°	.262	1.240	.115	-.925	-1.920	-.208
160°	.201	.949	.101	-.623	-1.375	-.146
165°	.149	.702	.0744	-.399	-.880	-.0933
170°	.130	.613	.065	-.221	-.487	-.0516
175°	.082	.0387	.041	-.074	-.163	-.0173
180°	.076	.0358	.038	0	0	0

# TABLE "d" FOR

## LIFT AND DRAG TESTS ON BANK OF 78 TUBES

### MEAN VALUES OF TABLES NOS 34, 35 & 36.

ANGLE OF INCID <sup>E</sup>	DRAG		LIFT		R = $\sqrt{D^2+L^2}$	L/D	D/L $\frac{D}{\tan \phi}$	$\phi$	$\gamma = \phi - \alpha$
	D IN LB	C <sub>D</sub>	L IN LB	C <sub>L</sub>					
0°	.293	.034	0	0	.293	∞	90	0	90
5°	.339	.039	.174	.020	.341	1.95	62.85	.513	57.85
10°	.391	.045	.435	.050	.585	.90	42.0	1.110	32.0
15°	.522	.060	.870	.100	1.014	.60	31.0	1.670	16.0
20°	.722	.083	1.130	.130	1.340	.64	32.65	1.570	12.65
25°	1.042	.120	1.650	.190	1.950	.63	32.25	1.580	7.25
30°	1.375	.158	2.000	.230	2.420	.688	34.65	1.450	4.65

ANGLE OF INCID <sup>E</sup>	DRAG		LIFT		R = $\sqrt{D^2+L^2}$	L/D	D/L $\frac{D}{\tan \phi}$	$\phi$	$\gamma = \phi - \alpha$
	D IN LB	C <sub>D</sub>	L IN LB	C <sub>L</sub>					
90°	3.370	.388	0	0	3.33	∞	90	0	0
95°	3.350	.385	.435	-.05	3.37	-7.70	88.6	-.13	3.60
100°	3.330	.383	.782	-.09	3.42	-4.26	76.65	-.234	3.35
105°	3.240	.372	1.04	-.12	3.40	-3.12	72.35	-.321	2.65
110°	3.130	.360	1.31	-.15	3.39	-2.39	67.30	-.419	2.7
115°	2.990	.344	1.56	-.18	3.36	-1.92	62.45	-.522	2.55
120°	2.820	.325	1.74	-.20	3.31	-1.62	58.35	-.618	1.65

35°	1.650	.190	2.260	.260	2.800	.73	36.15	1.370	1.15
40°	1.950	.225	2.440	.280	3.120	.80	38.75	1.250	-1.25
45°	2.260	.260	2.260	.260	3.200	1.00	45.0	1.00	0
50°	2.520	.290	2.350	.270	3.450	1.07	47.0	.935	-3.00
55°	2.780	.320	2.090	.240	3.480	1.33	53.1	.750	-1.90
60°	2.980	.342	1.830	.210	3.490	1.63	58.45	.615	-1.55

125°	2.640	.304	1.87	-.215	3.24	-1.41	54.65	-.708	-.35
130°	2.430	.280	1.87	-.215	3.06	-1.30	52.45	-.770	2.45
135°	2.220	.255	1.91	-.220	2.93	-1.16	49.25	-.860	4.25
140°	2.000	.230	2.04	-.235	2.86	-.98	44.45	-1.02	4.45
145°	1.740	.200	2.26	-.260	2.85	-.77	37.60	-1.30	2.60
150°	1.460	.168	2.00	-.230	2.48	-.73	36.15	-1.37	6.15

65°	3.120	.359	1.570	.180	3.490	1.99	63.45	.503	-1.55
70°	3.210	.370	1.220	.140	3.430	2.63	69.25	.370	-.75
75°	3.290	.378	.960	.110	3.420	3.43	73.75	.292	-1.25
80°	3.330	.383	.522	.060	3.370	6.38	81.05	.157	-1.05
85°	3.350	.385	.261	.030	3.360	12.80	85.55	.780	.55
90°	3.370	.388	0	0	3.330	∞	90	0	0

155°	1.160	.134	1.57	-.18	1.95	-.738	36.45	-1.35	11.45
160°	.810	.093	1.04	-.12	1.33	-.780	37.85	-1.285	17.85
165°	.635	.073	.695	-.08	.94	-.913	42.4	-1.095	27.4
170°	.452	.052	.348	-.04	.568	-1.30	52.45	-.77	42.45
175°	.348	.040	.174	-.02	.388	-2.00	63.45	-.50	58.45
180°	.296	.034	0	0	2.96	∞	90	0	0

APPENDIX II.

APPENDIX IIResistance to Stream Flow through Tube Banks and Friction Measurements.

Other investigators have carried out various experiments on flow past single circular cylinders and resistance of flow through nests of tubes in a position at rights angles to the stream. The results have not been very satisfactory for banks of tubes in inclined positions.

Experiments were made with four row bank and the test results for the vertical position were compared with results given by Wallis.<sup>(53)</sup> It was thought desirable, to compare experimental results with those obtained by five formulae given by Chilton and Genereaux.<sup>(5)</sup> The experimental data gave results in agreement with Wallis, but not quite in agreement with those of Chilton.

For the inclined position of tubes the banks would require to be longer to give dependable results, and to get clear comparison with actual boiler conditions. However, the vertical position of the bank tubes Plate 48, Fig.1 shows the arrangement used. Preliminary tests showed that the pitot tube could be kept at a constant distance in front of the tube containing the four row bank. While pressures at the back of box were taken at 48 different positions, 3 inches apart giving 8 rows of 6 readings.

An example is worked from experimental results obtained at 45 feet per second on the four row bank of tubes. Pressure drop has been measured with an Askania Manometer and gave 13.25 m.m. of water which is equal to  $13.25 \times 0.205 = 2.72$  lb.per sq.ft.

Taking the formula as derived by Chilton for the same speed 45 ft.per sec./

$$\Delta p = \frac{1.5 \rho^{.8} u_{\max}^{1.8} \mu^{-.2} N}{g d_s^{.2}} \quad \text{lb/ft}^2$$

where  $\Delta p$  = pressure drop density,  $\rho$  = density  
 $u_{\max}$  = maximum speed, ft/sec.  $\mu$  = Coefficient of friction  
 $N$  = number of rows,  $g$  = gravity  
 $d_s$  = distance between rows of tubes in bank in feet

$$\begin{aligned} \therefore \text{pressure drop} &= \frac{1.5 \times 0.125 \times 950 \times 0.104 \times 4}{32.2 \times 0.5} \\ &= 4.6 \quad \text{lb/ft}^2 \end{aligned}$$

If the constant had been 0.9 in place of 1.5 the pressure drop would have been more in agreement with experimental results for staggered arrangement.

Using the results given by Wallis for a nest of seven rows and the same units as Chilton, the resistance of a four row bank can be obtained thus

$$\begin{aligned} \text{Pressure drop} &= \frac{4}{7} \times \frac{(45)^2}{(130)^2} \times 0.286 \times 144 \\ &= 2.815 \quad \text{lb/ft}^2 \end{aligned}$$

which is in agreement with results obtained by the author.

Another example is worked out from experimental data obtained for Position 1B Section II Part 3 for a bank of tubes supported in the Wind Tunnel at 30 degrees to the direction of stream flow. On graphically integrating the form drag diagrams it was found that the form drag coefficient for first, second, third and fourth rows were 0.416, 0.482, 0.282 and 0.396 respectively. From these values, the total form drag Coefficient for four rows is 1.575 and the average form drag coefficient is 0.394.

The resistance due to the pressure drop, between inlet and outlet of model bank of tubes is 0.465 in the same units as those above. The tangential drag or skin friction is therefore 0.071 or 15 per cent of the total drag and the ratio between form and total drag is 85 per cent.

The results obtained by Wallis for the tangential drag of a staggered nest of vertical tubes is 7 per cent. This again is in agreement with the above 15 per cent for a staggered bank of 30 degree inclined tubes obtained by the author.

A valuable paper "Viscous Layer associated with a Circular Cylinder", R & M No. 1313 by Green<sup>(10)</sup> gives a very complete solution for the single cylinder. In multi-rows of tubes the difficulties of solution are magnified as additional rows are added.

The loss of energy in the stream line flow is dependent on the surface or skin friction of the bank of tubes, but this is only one source of loss. The pressure drag which is due to eddies in the wake vortice must be considerable. These two losses are very different.

Skin friction could be reduced in a model bank of tubes by giving attention to the surface finish of the model as Green did with his aluminum cylinder. The tubes in a steam boiler cannot be expected to retain their initial smooth surface, although the boiler tubes, the failure of which were considered in Section 1 showed a narrow bright frontal area. It may be said then that skin friction may be reduced, but turbulence in the wake vortices cannot be minimized.

In the bank of circular cylindrical tubes no attempt has been made at stream-lining in order to decrease eddy resistance and loss of steam energy. It was also shown by Green working in conjunction with Baristow that there was a distinct rise of velocity through the boundary layer. Consideration is given to boundary layer from 0 to 45 degrees round tubes, from 45 to 67 and from 67 degrees to breakaway point where the opening out rapidly increases from 0.04 to 0.07 inches.

A pressure distribution curve for a second row tube is reproduced in Plate No. 40, Fig. 4 for a velocity,  $V=82$  ft/sec; diameter of tube in bank,  $d=3/8$ "; Kinematic Viscosity for air  $\nu=.000159$ , which give  $R=Vd/\nu=1.64 \times 10^5$  and  $S$  = distance round cylinder in degrees. The theoretical determination of the pressure distribution is difficult owing to turbulence outside the boundary layer, both in the initial stream, in the space between the first and second row, and after the breakaway point in first and second row in bank of tubes. The second has been split up into its different harmonics by the "Rungé" method and the following obtained.

$$p \div \frac{\rho V^2}{2} = -0.7 + 1.6 \cos \theta + 1.6 \cos 2\theta + 1.25 \cos 3\theta + 0.6 \cos 4\theta + 0.05 \cos 5\theta$$

then by differentiation,

$$\frac{\delta}{\delta s} \left( p \div \frac{\rho V^2}{2} \right) = 1.6 \sin \theta - 3.2 \sin 2\theta + 3.75 \sin 3\theta - 2.4 \sin 4\theta - 0.25 \sin 5\theta$$

= value of function  $\frac{2}{R} f_1$

$$\frac{\delta^2}{\delta s^2} \left( p \div \frac{\rho V^2}{2} \right) = -1.6 \cos \theta - 6.4 \cos 2\theta - 11.25 \cos 3\theta - 9.6 \cos 4\theta - 1.15 \cos 5\theta$$

= value of function  $\frac{2}{R^2} f_1'$

$$\frac{\delta^3}{85} \left( p = \rho \frac{V^2}{Z} \right) = 1.6 \sin \theta + 19.8 \sin 2\theta + 33.75 \sin 3\theta + 30.4 \sin 4\theta + 5.75 \sin 5\theta$$

= Value of function  $\frac{2}{R} f''$

$$f_0 = \text{skin friction}, f_1 = \frac{R^2}{2} \frac{\partial^2 p}{\partial s^2}$$

It is required to evaluate the  $f$  functions at various positions round the cylinder. Again using a tabular method the value of  $f_1$ ,  $f_1'$  and  $f_1''$  are obtained for  $R = 1.64 \times 10^5$ .

As shown by Green the value of the limiting Velocity just outside the boundary layer can be obtained experimentally and by calculation. A curve of Skin Friction similar to that shown in Green's paper, Fig 6 could be obtained. The author puts this section forward as it might help any other investigation on Viscous drag and skin friction.

APPENDIX III.

APPENDIX IIITabulated Results of Wind Tunnel Experiments.

Collected results and calculations are tabulated in seventeen tables, 1 to 17. These have been put in this Appendix to avoid discontinuity in the main work of Thesis. The tables selected are only representative of the many readings taken, and the method of obtaining calculated results can easily be followed.

-----

# TABLE NO. I.

POSITION No. 1A.

BAROMETER 29.9 IN. HG.

VELOCITY 100 FT/SEC

HOLE No. 4

TEMPERATURE 65°F

WT INLET 5.8 CMS OF WATER

POSITION OF HOLE.	1 <sup>st</sup> ROW		2 <sup>nd</sup> ROW		3 <sup>rd</sup> ROW		4 <sup>th</sup> ROW.	
	CMS. OF WATER	$\frac{p}{\rho V_0^2/2}$	CMS. OF WATER	$\frac{p}{\rho V_0^2/2}$	CMS. OF WATER	$\frac{p}{\rho V_0^2/2}$	CMS. OF WATER	$\frac{p}{\rho V_0^2/2}$
0°	4.7	.824	4.8	.842	4.0	.702	3.0	.526
10°	4.6	.806	4.3	.754	3.8	.666	2.8	.490
20°	4.6	.806	3.1	.544	2.8	.490	1.8	.316
30°	4.1	.718	1.9	.334	1.3	.228	.8	.140
40°	3.6	.634	.5	.086	.1	.016	-.3	-.052
50°	2.9	.508	-.2	-.034	-.6	-.104	-1.1	-.192
60°	2.1	.368	-.2	-.034	-1.1	-.192	-1.8	-.316
70°	1.3	.228	-.5	-.086	-1.6	-.280	-2.2	-.386
80°	1.0	.174	-.3	-.052	-1.4	-.246	-2.0	-.350
90°	1.0	.174	-.2	-.034	-1.3	-.228	-2.0	-.350
100°	1.1	.192	-.2	-.034	-1.0	-.174	-2.0	-.350
110°	1.2	.210	-.3	-.052	-.4	-.070	-1.7	-.298
120°	1.2	.210	-.4	-.070	-.1	-.016	-1.2	-.210
130°	1.2	.210	-.4	-.070	0	0	-1.1	-.192
140°	1.2	.210	-.3	-.052	0	0	-1.0	-.174
150°	1.2	.210	-.2	-.034	-.1	-.016	-.9	-.156
160°	1.2	.210	-.1	.016	-.1	-.016	-.9	-.156
170°	1.2	.210	-.1	.016	-.1	-.016	-.9	-.156
180°	1.2	.210	.2	.034	.1	.016	-.8	-.140
190°	1.2	.210	.3	.052	.1	.016	-.8	-.140
200°	1.2	.210	.3	.052	.1	.016	-.8	-.140
210°	1.2	.210	.3	.052	.1	.016	-.8	-.140
220°	1.5	.262	.3	.052	.1	.016	-.9	-.156
230°	1.5	.262	.4	.070	0	0	-1.0	-.174
240°	1.6	.280	.6	.104	-.1	-.016	-1.1	-.192
250°	1.7	.298	.8	.140	-.3	-.052	-1.4	-.246
260°	1.7	.298	.8	.140	-.6	-.104	-1.8	-.316
270°	1.6	.280	.8	.140	-1.0	-.174	-1.9	-.332
280°	1.4	.246	.8	.140	-1.2	-.210	-2.0	-.350
290°	1.6	.280	.4	.070	-1.5	-.262	-2.0	-.350
300°	2.0	.350	.4	.070	-1.3	-.228	-2.0	-.350
310°	2.1	.368	.8	.140	-.5	-.086	-1.5	-.262
320°	2.5	.438	1.7	.298	.9	.158	-.4	-.070
330°	3.1	.544	2.5	.438	1.9	.332	.9	.156
340°	3.8	.666	4.0	.702	3.3	.578	2.1	.368
350°	4.4	.770	4.8	.842	4.0	.702	3.0	.526
360°	4.7	.824	4.8	.842	4.0	.702	3.0	.526

# TABLE No 2.

POSITION No. 1A.

BAROMETER 29.2 IN. Hg.,

VELOCITY 100 FT/SEC.

HOLE No. 2

TEMPERATURE 63°F.

W.T. INLET 5.8 CMS OF WATER.

POSITION OF HOLE	1 <sup>st</sup> Row.		2 <sup>nd</sup> Row.		3 <sup>rd</sup> Row.		4 <sup>th</sup> Row.	
	CMS. OF WATER	$\frac{p}{\rho V^2/2}$	CMS. OF WATER.	$\frac{p}{\rho V^2/2}$	CMS. OF WATER.	$\frac{p}{\rho V^2/2}$	CMS. OF WATER	$\frac{p}{\rho V^2/2}$
0°	5.3	.944	5.4	.962	4.4	.784	3.4	.606
10°	5.0	.892	4.9	.872	4.0	.712	3.2	.570
20°	4.7	.836	3.9	.696	3.0	.534	2.7	.482
30°	4.1	.730	2.5	.446	1.5	.268	1.5	.268
40°	3.4	.606	.7	.124	0	0	0	0
50°	2.6	.464	0	0	-1.3	-.232	-1.2	-.214
60°	1.9	.338	-.6	-.126	-2.0	-.356	-2.0	-.356
70°	1.3	.232	-1.0	-.178	-2.2	-.392	-2.6	-.464
80°	1.2	.214	-1.0	-.178	-2.2	-.392	-2.8	-.498
90°	1.4	.250	-.8	-.142	-2.0	-.356	-2.5	-.446
100°	1.6	.286	-.8	-.142	-1.6	-.286	-2.1	-.374
110°	1.7	.302	-.8	-.142	-1.0	-.178	-1.7	-.304
120°	1.7	.302	-.7	-.124	-.6	-.106	-1.3	-.232
130°	1.9	.338	-.2	-.034	-.2	-.034	-1.0	-.178
140°	1.9	.338	.2	.034	0	0	-.9	-.160
150°	1.9	.338	.5	.088	.2	.034	-.8	-.142
160°	1.9	.338	.7	.130	.3	.052	-.7	-.124
170°	1.8	.320	.8	.142	.3	.052	-.6	-.106
180°	1.8	.320	.8	.142	.3	.052	-.7	-.124
190°	1.8	.320	.8	.142	.3	.052	-.7	-.124
200°	1.8	.320	.7	.142	.2	.034	-.7	-.124
210°	1.7	.302	.5	.088	.2	.034	-.7	-.124
220°	1.7	.302	.5	.088	.3	.052	-.8	-.142
230°	1.7	.302	.2	.034	0	0	-.9	-.160
240°	1.7	.302	0	0	-.6	-.106	-1.0	-.178
250°	1.7	.302	-.2	-.034	-1.0	-.178	-1.2	-.214
260°	1.4	.250	-.4	-.070	-1.7	-.302	-1.8	-.320
270°	1.1	.196	-.6	-.106	-2.0	-.356	-2.0	-.356
280°	1.1	.196	-.7	-.124	-2.1	-.374	-2.4	-.428
290°	1.4	.250	-.8	-.142	-2.1	-.374	-2.5	-.446
300°	2.0	.356	-.7	-.124	-2.0	-.356	-2.2	-.392
310°	2.7	.484	-.4	-.070	-1.7	-.302	-1.8	-.320
320°	3.5	.624	.5	.088	-1.1	-.196	-1.0	-.178
330°	4.2	.748	1.9	.338	1.6	.286	.5	.088
340°	4.6	.820	2.6	.464	2.6	.464	1.7	.304
350°	4.9	.874	4.6	.820	3.5	.624	2.8	.498
360°	5.3	.944	5.4	.962	4.4	.784	3.4	.606

R.T.C.  
1944.

# TABLE No 3.

138

POSITION No 1B.

BAROMETER 30.4 IN. HG.

VELOCITY 100 FT/SEC.

HOLE No. 2

TEMPERATURE 66°F.

W.T INLET 5.9 CMS OF WATER

POSITION OF HOLE.	1 <sup>st</sup> Row		2 <sup>nd</sup> Row.		3 <sup>rd</sup> Row		4 <sup>th</sup> Row.	
	CMS. OF WATER.	$\frac{P}{PV_0^2/2}$	CMS. OF WATER	$\frac{P}{PV_0^2/2}$	CMS. OF WATER.	$\frac{P}{PV_0^2/2}$	CMS. OF WATER	$\frac{P}{PV_0^2/2}$
0°	5.5	.948	5.5	.948	4.3	.740	3.2	.556
10°	5.3	.912	4.7	.808	4.1	.706	2.8	.522
20°	5.0	.862	3.9	.672	3.4	.586	2.6	.448
30°	4.2	.724	2.0	.344	1.9	.326	1.7	.292
40°	3.9	.672	.8	.138	0	0	.7	.120
50°	3.0	.516	-1.0	-.172	-1.4	-.242	-.9	-.154
60°	2.4	.414	-1.6	-.276	-2.6	-.448	-1.8	-.310
70°	1.9	.326	-1.7	-.292	-3.0	-.516	-2.5	-.430
80°	1.0	.172	-1.9	-.326	-3.7	-.636	-3.4	-.586
90°	.9	.154	-1.5	-.258	-3.6	-.620	-3.5	-.602
100°	1.0	.172	-1.4	-.242	-3.0	-.516	-3.4	-.586
110°	1.1	.188	-1.4	-.242	-2.6	-.448	-3.3	-.568
120°	1.1	.188	-1.4	-.242	-1.9	-.326	-2.5	-.430
130°	1.2	.206	-1.3	-.224	-1.4	-.242	-2.0	-.344
140°	1.2	.206	-.9	-.154	-1.0	-.172	-1.9	-.326
150°	1.2	.206	-.8	-.138	-.6	-.102	-1.7	-.292
160°	1.2	.206	-.7	-.120	-.5	-.086	-1.7	-.292
170°	1.2	.206	-.5	-.086	-.3	-.052	-1.6	-.276
180°	1.1	.188	-.2	-.034	-.2	-.034	-1.5	-.258
190°	1.1	.188	-.5	-.086	-.2	-.034	-1.6	-.276
200°	1.1	.188	-.7	-.120	-.3	-.052	-1.6	-.276
210°	1.1	.188	-.8	-.138	-.5	-.086	-1.6	-.276
220°	1.1	.188	-.9	-.154	-.7	-.120	-1.9	-.326
230°	1.0	.172	-1.5	-.258	-1.2	-.206	-2.0	-.344
240°	1.0	.172	-1.5	-.258	-1.9	-.326	-2.5	-.430
250°	1.0	.172	-1.7	-.292	-2.4	-.412	-2.8	-.482
260°	1.0	.172	-1.7	-.292	-2.6	-.448	-3.0	-.516
270°	1.0	.172	-1.7	-.292	-3.0	-.516	-3.5	-.602
280°	1.0	.172	-2.0	-.344	-3.0	-.516	-3.5	-.602
290°	.8	.138	-2.5	-.430	-3.0	-.516	-3.6	-.620
300°	2.0	.344	-2.4	-.412	-2.6	-.448	-3.0	-.516
310°	2.2	.378	-2.4	-.412	-2.2	-.378	-2.5	-.430
320°	3.9	.672	-1.7	-.292	-1.6	-.276	-1.6	-.276
330°	4.2	.724	.7	.120	1.0	.172	-.3	-.052
340°	5.0	.862	3.0	.516	3.0	.516	1.2	.206
350°	5.3	.912	4.7	.808	4.1	.706	2.5	.430
360°	5.5	.948	5.5	.948	4.3	.740	3.1	.534

R.T.C  
1944.

# TABLE No 4.

POSITION No. 1B.

BAROMETER 30.4 IN HG.

VELOCITY 100 FT/SEC.

HOLE No 4

TEMPERATURE 66° F.

W.T. INLET 5.9 CMS OF WATER.

POSITION OF HOLE.	1 <sup>st</sup> Row.		2 <sup>nd</sup> Row.		3 <sup>rd</sup> Row.		4 <sup>th</sup> Row.	
	CMS. OF WATER	$\frac{p}{PV^2/2}$	CMS. OF WATER.	$\frac{p}{PV^2/2}$	CMS. OF WATER.	$\frac{p}{PV^2/2}$	CMS. OF WATER	$\frac{p}{PV^2/2}$
0°	5.3	.912	5.3	.912	4.3	.740	2.9	.500
10°	5.1	.878	5.0	.862	3.9	.672	2.6	.448
20°	5.0	.862	3.4	.586	2.8	.482	2.3	.396
30°	4.1	.706	2.4	.412	.9	.154	1.6	.276
40°	3.7	.636	.5	.086	-1.4	-.242	.5	.086
50°	3.0	.516	-1.7	-.292	-2.5	-.430	-1.4	-.242
60°	1.7	.292	-2.2	-.378	-3.8	-.656	-2.5	-.430
70°	1.0	.172	-2.2	-.378	-3.8	-.656	-3.0	-.516
80°	.6	.122	-2.3	-.396	-3.8	-.656	-3.5	-.604
90°	.6	.122	-2.1	-.362	-3.6	-.620	-3.6	-.620
100°	.8	.138	-2.0	-.344	-3.0	-.516	-3.5	-.604
110°	.9	.154	-1.8	-.310	-2.6	-.448	-3.5	-.604
120°	.9	.154	-1.7	-.292	-2.0	-.344	-3.0	-.516
130°	.9	.154	-1.5	-.258	-1.4	-.242	-2.2	-.378
140°	.9	.154	-.9	-.154	-1.3	-.224	-2.0	-.344
150°	.9	.154	-.5	-.086	-.6	-.102	-1.8	-.310
160°	.9	.154	0	0	-.6	-.102	-1.7	-.292
170°	.8	.138	0	0	-.3	-.050	-1.7	-.292
180°	.8	.138	0	0	-.3	-.050	-1.7	-.292
190°	.8	.138	0	0	-.3	-.050	-1.7	-.292
200°	.8	.138	-.3	-.050	-.5	-.086	-1.6	-.276
210°	.8	.138	-.5	-.086	-.6	-.102	-1.6	-.276
220°	.8	.138	-.8	-.138	-.9	-.154	-1.6	-.276
230°	.8	.138	-1.3	-.224	-1.2	-.206	-1.4	-.242
240°	.8	.138	-1.6	-.276	-1.5	-.258	-2.0	-.344
250°	.8	.138	-1.8	-.310	-1.9	-.326	-2.7	-.464
260°	.8	.138	-2.0	-.344	-2.3	-.396	-3.0	-.516
270°	.8	.138	-2.0	-.344	-3.0	-.516	-3.4	-.586
280°	.8	.138	-2.1	-.362	-3.2	-.552	-3.2	-.552
290°	.5	.086	-2.2	-.378	-3.4	-.586	-3.2	-.552
300°	1.2	.206	-1.7	-.292	-2.9	-.500	-2.9	-.500
310°	1.8	.310	-1.4	-.242	-2.4	-.412	-2.0	-.344
320°	3.2	.552	.5	.086	-1.4	-.242	-1.4	-.242
330°	4.1	.706	1.9	.328	.9	.154	.3	.050
340°	4.3	.740	3.4	.586	2.8	.482	2.3	.396
350°	5.1	.878	5.0	.862	3.9	.672	2.6	.448
360°	5.3	.912	5.3	.912	4.3	.740	2.9	.500

R.T.C.  
1944.

# TABLE No 5.

POSITION No 1 B.

BAROMETER 30.5 IN. Hg.

VELOCITY 100 FT./SEC.

HOLE No 6

TEMPERATURE 68°F.

W.T. INLET 5.8 CMS. OF WATER.

POSITION OF HOLE.	1 <sup>st</sup> Row		2 <sup>nd</sup> Row		3 <sup>rd</sup> Row		4 <sup>th</sup> Row	
	CMS. OF WATER.	$\frac{P}{PV_0^2/2}$	CMS. OF WATER	$\frac{P}{PV_0^2/2}$	CMS. OF WATER	$\frac{P}{PV_0^2/2}$	CMS. OF WATER	$\frac{P}{PV_0^2/2}$
0°	4.9	.848	5.1	.884	4.3	.744	2.8	.484
10°	4.6	.796	4.9	.848	4.0	.692	2.6	.470
20°	4.1	.710	3.8	.658	3.0	.518	1.9	.330
30°	3.3	.572	1.9	.330	2.0	.346	1.7	.120
40°	2.7	.468	-.2	-.034	-.8	-.138	-.9	-.156
50°	2.5	.432	-1.4	-.244	-2.4	-.416	-1.5	-.260
60°	1.8	.312	-2.1	-.364	-3.1	-.536	-3.3	-.572
70°	.7	.120	-2.1	-.364	-3.3	-.572	-3.3	-.572
80°	.5	.086	-2.0	-.346	-3.3	-.572	-3.6	-.624
90°	.7	.120	-1.9	-.330	-3.3	-.572	-3.5	-.606
100°	.9	.156	-1.7	-.294	-3.0	-.518	-3.1	-.536
110°	.9	.156	-1.5	-.260	-2.1	-.364	-2.6	-.450
120°	.9	.156	-1.3	-.226	-1.5	-.26	-2.2	-.382
130°	.9	.156	-1.1	-.190	-1.1	-.190	-1.8	-.312
140°	.8	.138	-.9	-.156	-.7	-.120	-1.7	-.294
150°	.8	.138	-.4	-.068	-.5	-.086	-1.5	-.260
160°	.8	.138	-.1	-.016	-.3	-.052	-1.4	-.242
170°	.7	.120	-.3	-.052	-.4	-.068	-1.4	-.242
180°	.8	.138	-.1	-.016	-.2	-.034	-1.4	-.242
190°	.8	.138	-.2	-.034	-.3	-.052	-1.4	-.242
200°	.7	.120	-.6	-.104	-.5	-.086	-1.5	-.260
210°	.7	.120	-.8	-.138	-.7	-.120	-1.6	-.276
220°	.7	.120	-1.0	-.172	-1.1	-.190	-1.7	-.294
230°	.8	.138	-1.2	-.208	-1.5	-.260	-1.8	-.312
240°	.7	.120	-1.6	-.276	-2.1	-.364	-2.3	-.398
250°	.7	.120	-2.0	-.346	-2.7	-.468	-2.8	-.484
260°	.7	.120	-2.0	-.346	-3.0	-.518	-3.3	-.572
270°	.5	.086	-2.3	-.398	-3.2	-.554	-3.8	-.658
280°	.7	.120	-2.3	-.398	-3.2	-.554	-3.6	-.624
290°	.8	.138	-2.5	-.432	-3.0	-.518	-3.3	-.572
300°	1.8	.312	-1.7	-.294	-3.0	-.518	-3.3	-.572
310°	2.4	.416	-1.7	-.294	-2.2	-.382	-1.5	-.260
320°	3.3	.572	-.2	-.034	-1.3	-.226	.5	-.086
330°	4.4	.762	1.5	.260	.8	.138	1.4	.242
340°	4.6	.796	3.8	.658	2.5	.432	2.1	.364
350°	4.8	.832	4.4	.762	4.0	.692	2.6	.450
360°	4.9	.848	5.1	.884	4.3	.744	2.8	.484

R.T.C.  
1944.

# TABLE NO. 6.

POSITION No 2A.

BAROMETER 29.2 IN. HG.

VELOCITY 100 FT/SEC.

HOLE No 1

TEMPERATURE 63°F.

W.T. INLET 5.9 CMS OF WATER.

POSITION OF HOLE.	1 <sup>st</sup> Row		2 <sup>nd</sup> Row.		3 <sup>rd</sup> Row.		4 <sup>th</sup> Row.	
	CMS. OF WATER	$\frac{P}{\rho V_0^2/2}$	CMS. OF WATER.	$\frac{P}{\rho V_0^2/2}$	CMS. OF WATER.	$\frac{P}{\rho V_0^2/2}$	CMS. OF WATER	$\frac{P}{\rho V_0^2/2}$
0°	5.7	1.016	5.7	1.016	4.8	.854	3.8	.676
10°	5.7	1.016	5.4	.962	4.5	.802	3.8	.676
20°	5.5	.980	4.3	.766	3.8	.676	3.2	.570
30°	5.1	.908	3.1	.552	2.5	.446	1.8	.320
40°	4.6	.820	2.1	.374	1.0	.178	.6	.106
50°	4.1	.730	1.2	.214	.2	.034	.8	.142
60°	3.6	.642	1.0	.178	.6	.106	1.4	.250
70°	3.2	.570	1.0	.178	.6	.106	1.5	.268
80°	3.0	.534	1.3	.232	.2	.034	1.2	.214
90°	3.1	.552	1.4	.250	0	0	1.0	.178
100°	3.3	.588	1.4	.250	.2	.034	.7	.124
110°	3.3	.588	1.4	.250	.5	.088	.5	.088
120°	3.3	.588	1.3	.232	.6	.106	.4	.070
130°	3.3	.588	1.2	.214	.7	.124	.3	.052
140°	3.2	.570	1.2	.214	.8	.142	.3	.052
150°	3.2	.570	1.3	.232	.9	.160	.2	.034
160°	3.2	.570	1.4	.250	.9	.160	.2	.034
170°	3.3	.588	1.7	.302	1.0	.178	.1	.016
180°	3.3	.588	1.7	.302	1.0	.178	.1	.016
190°	3.6	.642	1.7	.302	1.0	.178	.2	.034
200°	3.4	.606	1.5	.268	.9	.160	.2	.034
210°	3.3	.588	1.4	.230	.8	.142	.4	.070
220°	3.5	.624	1.3	.232	.7	.124	.4	.070
230°	3.5	.624	1.3	.232	.4	.070	.5	.088
240°	3.3	.588	1.3	.232	0	0	.6	.106
250°	3.6	.642	1.4	.230	.3	.052	0	0
260°	3.6	.642	1.4	.230	.5	.088	1.3	.232
270°	3.2	.570	1.1	.196	.6	.106	1.5	.268
280°	3.3	.588	1.0	.178	.8	.142	1.6	.284
290°	3.4	.606	1.1	.196	.8	.142	1.4	.250
300°	3.5	.624	1.3	.232	.4	.070	.7	.124
310°	4.1	.730	2.3	.410	0	0	.3	.052
320°	4.6	.820	3.2	.570	.6	.106	.2	.034
330°	4.9	.874	4.2	.748	2.0	.356	1.2	.214
340°	5.6	.998	5.4	.962	3.6	.642	2.8	.500
350°	5.7	1.016	5.7	1.016	4.8	.854	3.8	.676
360°	5.7	1.016	5.7	1.014	4.8	.854	3.8	.676

# TABLE No 7.

POSITION No 2A.

BAROMETER 29.15 IN. Hg

VELOCITY 100 FT/SEC.

HOLE No 2

TEMPERATURE 62°F

W.T. INLET 6.0 CMS OF WATER.

POSITION OF HOLE.	1 <sup>st</sup> Row.		2 <sup>nd</sup> Row.		3 <sup>rd</sup> Row.		4 <sup>th</sup> Row.	
	CMS. OF WATER.	$\frac{p}{PV^2/2}$						
0°	5.5	.986	5.5	.986	5.0	.896	4.3	.770
10°	5.4	.968	5.3	.948	4.8	.858	4.3	.770
20°	5.2	.932	4.8	.858	4.1	.734	3.9	.698
30°	4.8	.858	4.0	.716	3.2	.574	3.1	.556
40°	4.5	.806	3.2	.574	2.4	.430	2.4	.430
50°	3.9	.698	2.5	.448	1.7	.304	1.5	.268
60°	3.6	.644	2.2	.394	1.6	.286	1.2	.214
70°	3.4	.608	2.2	.394	1.5	.268	1.1	.196
80°	3.3	.592	2.3	.412	1.7	.304	1.2	.214
90°	3.4	.608	2.3	.412	1.7	.304	1.4	.250
100°	3.6	.644	2.3	.412	1.8	.322	1.5	.268
110°	3.6	.644	2.2	.394	1.9	.340	1.5	.268
120°	3.6	.644	2.5	.448	2.0	.358	1.8	.322
130°	3.7	.662	2.7	.484	2.2	.394	1.8	.322
140°	3.6	.644	2.8	.502	2.4	.430	1.8	.322
150°	3.6	.644	2.9	.520	2.5	.448	1.9	.340
160°	3.6	.644	3.0	.538	2.6	.466	1.9	.340
170°	3.7	.662	3.0	.538	2.7	.484	1.9	.340
180°	3.7	.662	3.0	.538	2.6	.466	1.9	.340
190°	3.6	.644	2.9	.520	2.6	.466	1.9	.340
200°	3.6	.644	2.8	.502	2.5	.448	1.9	.340
210°	3.6	.644	2.6	.466	2.5	.448	1.8	.322
220°	3.5	.626	2.5	.448	2.2	.394	1.7	.304
230°	3.5	.626	2.5	.448	2.1	.376	1.7	.304
240°	3.5	.626	2.5	.448	1.9	.340	1.7	.304
250°	3.6	.644	2.5	.448	1.8	.322	1.6	.286
260°	3.5	.626	2.4	.430	1.6	.286	1.5	.268
270°	3.3	.592	2.3	.412	1.6	.286	1.3	.232
280°	3.3	.592	2.3	.412	1.4	.250	1.1	.196
290°	3.6	.644	2.3	.412	1.5	.268	1.3	.232
300°	3.7	.662	2.6	.466	1.5	.268	1.3	.232
310°	4.1	.734	3.0	.538	1.8	.322	1.6	.286
320°	4.7	.842	3.8	.680	2.6	.466	2.0	.358
330°	5.0	.894	4.7	.842	3.4	.610	2.7	.484
340°	5.4	.964	5.0	.894	4.3	.770	3.5	.628
350°	5.5	.986	5.2	.932	4.9	.878	4.0	.716
360°	5.5	.986	5.5	.986	5.0	.896	4.3	.770

# TABLE No 8.

POSITION No 2A

BAROMETER 29.9 IN. HG

VELOCITY 100 FT./SEC.

HOLE No 4

TEMPERATURE 65°F

W.T. INLET 5.9 CMS. OF WATER

POSITION OF HOLE	1 <sup>st</sup> Row.		2 <sup>nd</sup> Row.		3 <sup>rd</sup> Row.		4 <sup>th</sup> Row.	
	CMS. OF WATER	$\frac{P}{PV_0^2/2}$						
0°	5.3	.928	5.4	.946	5.1	.892	4.9	.858
10°	5.0	.876	5.2	.912	5.0	.876	4.8	.842
20°	5.0	.876	5.1	.892	4.8	.842	4.6	.806
30°	4.8	.842	4.8	.842	4.4	.770	4.3	.754
40°	4.5	.788	4.4	.770	4.0	.700	3.8	.666
50°	4.4	.770	4.0	.700	3.7	.648	3.5	.612
60°	4.3	.754	4.0	.700	3.6	.630	3.5	.612
70°	4.2	.736	3.9	.684	3.6	.630	3.4	.596
80°	4.1	.718	3.9	.684	3.6	.630	3.4	.596
90°	4.0	.700	4.0	.700	3.6	.630	3.5	.612
100°	4.2	.736	4.0	.700	3.7	.648	3.6	.630
110°	4.3	.754	4.0	.700	3.7	.648	3.6	.630
120°	4.1	.718	4.0	.700	3.7	.648	3.7	.648
130°	4.0	.700	4.0	.700	3.8	.666	3.7	.648
140°	4.0	.700	4.0	.700	3.8	.666	3.8	.666
150°	4.1	.718	4.0	.700	3.8	.666	3.7	.648
160°	4.2	.736	4.0	.700	3.8	.666	3.7	.648
170°	4.2	.736	4.0	.700	3.9	.684	3.7	.648
180°	4.2	.736	4.0	.700	3.9	.684	3.8	.666
190°	4.1	.718	4.0	.700	3.9	.684	3.8	.666
200°	4.2	.736	4.0	.700	3.9	.684	3.8	.666
210°	4.2	.736	4.0	.700	3.8	.666	3.7	.648
220°	4.2	.736	3.9	.684	3.8	.666	3.7	.648
230°	4.2	.736	3.9	.684	3.8	.666	3.7	.648
240°	4.3	.754	4.0	.700	3.8	.666	3.7	.648
250°	4.2	.736	4.0	.700	3.7	.648	3.7	.648
260°	4.2	.736	3.9	.684	3.6	.630	3.5	.612
270°	4.1	.718	3.9	.684	3.6	.630	3.5	.612
280°	4.1	.718	3.9	.684	3.6	.630	3.5	.612
290°	4.4	.770	3.9	.684	3.6	.630	3.5	.612
300°	4.7	.824	3.9	.684	3.6	.630	3.5	.612
310°	4.8	.842	4.0	.700	3.7	.648	3.7	.648
320°	4.9	.858	4.1	.718	3.9	.684	3.9	.684
330°	5.0	.876	4.5	.788	4.2	.736	4.2	.736
340°	5.1	.892	4.7	.824	4.4	.770	4.3	.754
350°	5.1	.892	5.1	.892	4.9	.858	4.7	.824
360°	5.3	.928	5.4	.946	5.1	.892	4.9	.858

R.T.C.  
1944

# TABLE No 9.

144

POSITION No 2A

BAROMETER 28.9 IN Hg

VELOCITY 100 FT/SEC.

HOLE No 6

TEMPERATURE 56.2°F

W.T. INLET 5.9 CMS OF WATER.

POSITION OF HOLE.	1 <sup>st</sup> Row.		2 <sup>nd</sup> Row.		3 <sup>rd</sup> Row.		4 <sup>th</sup> Row.	
	CMS. OF WATER	$\frac{p}{\rho V_0^2/2}$	CMS. OF WATER	$\frac{p}{\rho V_0^2/2}$	CMS. OF WATER.	$\frac{p}{\rho V_0^2/2}$	CMS. OF WATER.	$\frac{p}{\rho V_0^2/2}$
0°	5.2	.922	5.3	.940	5.0	.888	4.6	.816
10°	5.2	.922	5.2	.922	4.9	.870	4.6	.816
20°	5.1	.904	4.7	.834	4.5	.798	4.4	.780
30°	5.0	.888	4.4	.780	4.2	.746	4.0	.710
40°	4.7	.834	3.9	.692	3.7	.656	3.8	.674
50°	4.6	.816	3.7	.656	3.7	.656	3.8	.674
60°	4.3	.764	3.7	.656	3.6	.638	3.8	.674
70°	4.1	.728	3.6	.638	3.5	.620	3.7	.656
80°	3.9	.692	3.7	.656	3.5	.620	3.7	.656
90°	3.9	.692	3.8	.674	3.6	.638	3.7	.656
100°	4.1	.728	3.7	.656	3.6	.638	3.8	.674
110°	3.9	.692	3.7	.656	3.5	.620	3.7	.656
120°	4.0	.710	3.8	.674	3.7	.656	3.7	.656
130°	4.1	.728	3.8	.674	3.8	.674	3.7	.656
140°	4.1	.728	3.9	.692	3.9	.692	3.8	.674
150°	4.2	.746	3.9	.692	3.9	.692	3.8	.674
160°	4.1	.728	4.0	.710	3.9	.692	3.8	.674
170°	4.1	.728	4.0	.710	3.9	.692	3.8	.674
180°	4.0	.710	3.9	.692	3.9	.692	3.8	.674
190°	4.2	.746	4.0	.710	3.8	.674	3.7	.656
200°	4.0	.710	3.9	.692	3.9	.692	3.8	.674
210°	4.1	.728	4.1	.728	3.9	.692	3.8	.674
220°	4.1	.728	3.9	.692	3.9	.692	3.8	.674
230°	4.2	.746	3.9	.692	3.8	.674	3.7	.656
240°	4.0	.710	3.8	.674	3.8	.674	3.7	.656
250°	4.2	.746	3.9	.692	3.7	.656	3.7	.656
260°	4.0	.710	3.8	.674	3.6	.638	3.6	.638
270°	4.0	.710	3.7	.656	3.6	.638	3.6	.638
280°	4.0	.710	3.8	.674	3.6	.638	3.6	.638
290°	4.2	.746	3.6	.638	3.5	.620	3.6	.638
300°	4.2	.746	3.7	.656	3.6	.638	3.6	.638
310°	4.4	.780	3.7	.656	3.6	.638	3.8	.674
320°	4.5	.798	3.8	.674	3.7	.656	3.9	.692
330°	4.8	.852	4.5	.798	3.9	.692	4.0	.710
340°	5.1	.904	4.9	.870	4.5	.798	4.4	.780
350°	5.2	.922	5.2	.922	4.9	.870	4.6	.816
360°	5.2	.922	5.3	.940	5.0	.888	4.6	.816

R.T.C.  
1944.

# TABLE No 10.

POSITION No 2B

BAROMETER 29.73 IN. HG

VELOCITY 100 FT/SEC

HOLE No 2

TEMPERATURE 68°F

W.T. INLET 6.0 CMS. OF WATER

POSITION OF HOLE.	1 <sup>st</sup> Row.		2 <sup>nd</sup> Row.		3 <sup>rd</sup> Row.		4 <sup>th</sup> Row.	
	CMS. OF WATER.	$\frac{P}{PV_0^2/2}$						
0°	5.7	1.012	5.7	1.012	5.0	.888	4.0	.710
10°	5.6	.994	5.5	.976	4.8	.852	3.4	.604
20°	5.3	.940	4.9	.868	3.8	.674	2.5	.444
30°	4.8	.852	3.8	.674	2.5	.444	1.2	.214
40°	4.2	.746	2.2	.390	1.5	.266	.5	.088
50°	3.4	.604	1.3	.230	- .1	-.016	- .1	-.016
60°	2.9	.514	.9	.158	- .2	-.034	- .5	-.088
70°	2.5	.444	.9	.158	0	0	- .7	-.124
80°	2.5	.444	.9	.158	.2	.034	- .5	-.088
90°	2.8	.496	1.0	.176	.4	.070	- .3	-.052
100°	2.9	.514	1.0	.176	.7	.124	- .2	-.034
110°	2.9	.514	1.0	.176	.9	.158	0	0
120°	2.9	.514	1.0	.176	1.0	.176	.3	.052
130°	2.9	.514	1.2	.214	1.2	.214	.4	.070
140°	2.9	.514	1.6	.284	1.5	.266	.5	.088
150°	2.8	.496	1.7	.302	1.5	.266	.5	.088
160°	2.8	.496	1.9	.336	1.5	.266	.5	.088
170°	2.8	.496	1.9	.336	1.5	.266	.5	.088
180°	2.8	.496	1.9	.336	1.6	.284	.6	.106
190°	2.9	.514	2.0	.354	1.5	.266	.7	.124
200°	2.9	.514	1.9	.336	1.4	.248	.6	.106
210°	2.9	.514	1.8	.320	1.1	.194	.6	.106
220°	2.8	.496	1.6	.284	1.0	.176	.5	.088
230°	2.8	.496	1.3	.230	.8	.142	.5	.088
240°	2.8	.496	1.2	.214	.5	.088	0	0
250°	2.7	.478	1.1	.194	0	0	- .1	-.016
260°	2.6	.467	1.0	.176	0	0	- .2	-.034
270°	2.4	.426	.9	.158	- .1	-.016	- .6	-.106
280°	2.4	.426	.8	.142	- .1	-.016	- .7	-.124
290°	2.7	.478	.7	.124	- .1	-.016	- .7	-.124
300°	3.1	.550	.9	.158	.5	.088	- .5	-.088
310°	3.7	.650	1.2	.214	.9	.158	- .1	-.016
320°	4.4	.780	2.0	.354	2.9	.514	.8	.142
330°	5.1	.904	3.5	.620	4.3	.744	2.3	.408
340°	5.4	.958	4.8	.852	4.8	.852	3.4	.604
350°	5.6	.994	5.5	.976	4.9	.868	3.8	.674
360°	5.7	1.012	5.7	1.012	5.0	.888	4.0	.710

# TABLE NO II.

POSITION No 2 B.

BAROMETER 29.67 IN HG.

VELOCITY 100 FT/SEC.

HOLE No 4

TEMPERATURE 67°F

W.T INLET 5.8 CMS. OF WATER

POSITION OF HOLE	1 <sup>st</sup> Row.		2 <sup>nd</sup> Row.		3 <sup>rd</sup> Row		4 <sup>th</sup> Row.	
	CMS. OF WATER	$\frac{p}{\rho V^2/2}$	CMS. OF WATER.	$\frac{p}{\rho V^2/2}$	CMS. OF WATER.	$\frac{p}{\rho V^2/2}$	CMS. OF WATER	$\frac{p}{\rho V^2/2}$
0°	5.4	.958	5.3	.940	5.1	.916	4.5	.798
10°	5.2	.922	5.1	.906	5.0	.888	4.4	.780
20°	5.0	.888	4.9	.868	4.7	.834	4.2	.744
30°	4.8	.852	4.3	.762	3.9	.692	3.8	.674
40°	4.5	.798	3.7	.656	3.3	.586	3.4	.604
50°	4.3	.762	3.3	.586	2.9	.514	3.1	.550
60°	3.8	.674	2.9	.514	2.5	.444	2.8	.496
70°	3.7	.656	2.8	.496	2.5	.444	2.6	.462
80°	3.7	.656	2.8	.496	2.5	.444	2.6	.462
90°	3.7	.656	2.9	.514	2.5	.444	2.5	.444
100°	3.8	.674	2.9	.514	2.7	.480	2.5	.444
110°	3.9	.692	3.0	.532	2.7	.480	2.5	.444
120°	3.8	.674	3.1	.550	2.9	.514	2.7	.480
130°	3.9	.692	3.2	.568	3.0	.532	2.8	.496
140°	3.8	.674	3.3	.586	3.1	.550	2.8	.496
150°	3.8	.674	3.4	.604	3.2	.568	2.8	.496
160°	3.8	.674	3.5	.620	3.2	.568	2.8	.496
170°	3.7	.656	3.5	.620	3.2	.568	2.8	.496
180°	3.7	.656	3.5	.620	3.3	.586	2.9	.514
190°	3.8	.674	3.6	.638	3.4	.604	2.9	.514
200°	3.8	.674	3.6	.638	3.5	.620	2.9	.514
210°	3.7	.656	3.4	.604	3.2	.568	2.9	.514
220°	3.8	.674	3.4	.604	3.2	.568	2.9	.514
230°	3.7	.656	3.1	.550	2.9	.514	2.9	.514
240°	3.7	.656	3.0	.532	2.8	.496	2.9	.514
250°	3.7	.656	2.9	.514	2.7	.480	2.8	.496
260°	3.6	.638	2.9	.514	2.6	.462	2.8	.496
270°	3.6	.638	2.8	.496	2.6	.462	2.8	.496
280°	3.5	.620	2.7	.480	2.5	.444	2.8	.496
290°	3.7	.656	2.6	.462	2.5	.444	2.7	.480
300°	4.3	.762	2.7	.480	2.6	.462	2.8	.496
310°	4.5	.798	2.8	.496	2.7	.480	2.9	.514
320°	4.7	.834	3.3	.586	2.9	.514	3.4	.604
330°	4.8	.852	4.1	.728	3.5	.620	3.8	.674
340°	4.9	.868	4.6	.814	4.0	.710	4.0	.710
350°	5.2	.922	5.2	.922	4.9	.868	4.4	.780
360°	5.4	.958	5.3	.940	5.1	.916	4.5	.798

R.T. C  
1944.

# TABLE NO 12.

147

POSITION No 2B

BAROMETER 29.7 IN. HG

VELOCITY 100 FT./SEC

HOLE No 6

TEMPERATURE 68°F

W.T INLET 5.9 CMS OF WATER

POSITION OF HOLE.	1 <sup>st</sup> Row		2 <sup>nd</sup> Row		3 <sup>rd</sup> Row		4 <sup>th</sup> Row.	
	CMS. OF WATER	$\frac{p}{\rho V_0^2/2}$	CMS. OF WATER	$\frac{p}{\rho V_0^2/2}$	CMS. OF WATER.	$\frac{p}{\rho V_0^2/2}$	CMS. OF WATER	$\frac{p}{\rho V_0^2/2}$
0°	5.6	.994	5.6	.994	5.4	.956	4.9	.868
10°	5.5	.976	5.5	.976	5.3	.940	4.8	.852
20°	5.4	.956	5.2	.922	5.0	.888	4.7	.834
30°	5.3	.940	4.8	.852	4.7	.834	4.6	.798
40°	5.1	.904	4.2	.746	4.0	.710	4.0	.710
50°	4.9	.868	3.7	.656	3.5	.620	3.8	.674
60°	4.5	.798	3.5	.620	3.3	.586	3.4	.604
70°	4.3	.762	3.5	.620	3.3	.586	3.4	.604
80°	4.2	.746	3.5	.620	3.3	.586	3.3	.586
90°	4.2	.746	3.6	.638	3.3	.586	3.4	.604
100°	4.3	.762	3.7	.656	3.5	.620	3.4	.604
110°	4.3	.762	3.5	.620	3.4	.604	3.3	.586
120°	4.3	.762	3.6	.638	3.5	.620	3.5	.620
130°	4.3	.762	3.6	.674	3.7	.656	3.6	.638
140°	4.3	.762	3.9	.692	3.8	.674	3.6	.638
150°	4.3	.762	3.9	.692	3.8	.674	3.6	.638
160°	4.3	.762	4.0	.710	3.8	.674	3.7	.656
170°	4.3	.762	4.0	.710	3.8	.674	3.7	.656
180°	4.3	.762	4.0	.710	3.9	.692	3.7	.656
190°	4.3	.762	4.0	.710	3.9	.692	3.7	.656
200°	4.3	.762	4.0	.710	3.8	.674	3.7	.656
210°	4.3	.762	3.9	.692	3.8	.674	3.7	.656
220°	4.3	.762	3.9	.692	3.7	.656	3.7	.656
230°	4.4	.780	3.8	.674	3.6	.638	3.7	.656
240°	4.3	.762	3.7	.656	3.4	.604	3.6	.638
250°	4.3	.762	3.6	.638	3.3	.586	3.5	.620
260°	4.3	.762	3.6	.638	3.2	.568	3.5	.620
270°	4.2	.746	3.5	.620	3.2	.568	3.4	.604
280°	4.3	.762	3.5	.620	3.2	.568	3.3	.586
290°	4.5	.798	3.4	.604	3.1	.550	3.4	.604
300°	4.6	.816	3.3	.586	3.1	.550	3.6	.638
310°	4.8	.852	3.5	.620	3.2	.568	3.8	.674
320°	5.1	.904	3.7	.656	3.5	.620	4.0	.710
330°	5.3	.940	4.3	.762	4.6	.816	4.5	.798
340°	5.4	.956	4.9	.868	5.0	.888	4.7	.834
350°	5.5	.976	5.3	.940	5.3	.940	4.8	.852
360°	5.6	.994	5.6	.994	5.4	.956	4.9	.868

R.T.C  
1944

# TABLE No 13.

148

POSITION No. 2c

BAROMETER 29.2 IN. HG

VELOCITY 100 FT/SEC.

HOLE No 1

TEMPERATURE 63°F

W.T. INLET 5.9 CMS. OF WATER.

POSITION OF HOLE	1 <sup>st</sup> Row.		2 <sup>nd</sup> Row.		3 <sup>rd</sup> Row.		4 <sup>th</sup> Row.	
	CMS. OF WATER	$\frac{P}{\rho V_0^2/2}$						
0°	5.7	1.016	5.7	1.016	4.7	.836	3.8	.676
10°	5.6	.998	5.2	.926	4.5	.802	3.7	.660
20°	5.5	.980	4.5	.802	3.8	.676	3.2	.570
30°	5.1	.908	3.1	.552	2.5	.446	1.8	.320
40°	4.6	.820	2.1	.574	1.0	.178	.6	.106
50°	4.1	.730	1.2	.214	-.2	-.034	-.8	-.142
60°	3.6	.642	1.0	.178	-.6	-.106	-1.4	-.250
70°	3.2	.570	1.0	.178	-.6	-.106	-1.5	-.268
80°	3.0	.534	1.3	.232	-.2	-.034	-1.2	-.214
90°	3.1	.552	1.4	.250	0	0	-1.0	-.178
100°	3.3	.588	1.4	.250	.2	.034	-.7	-.124
110°	3.3	.588	1.4	.250	.5	.088	-.5	-.088
120°	3.3	.588	1.3	.232	.6	.106	-.4	-.070
130°	3.3	.588	1.2	.214	.7	.124	-.3	-.052
140°	3.2	.570	1.2	.214	.8	.142	-.3	-.052
150°	3.2	.570	1.3	.232	.9	.160	-.2	-.034
160°	3.2	.570	1.4	.250	.9	.160	-.2	-.034
170°	3.3	.588	1.7	.302	1.0	.178	-.1	-.018
180°	3.3	.588	1.7	.302	1.0	.178	-.1	-.018
190°	3.6	.642	1.7	.302	1.0	.178	-.2	-.034
200°	3.4	.606	1.5	.268	.9	.160	-.2	-.034
210°	3.4	.606	1.4	.230	.8	.142	-.4	-.070
220°	3.5	.624	1.3	.232	.7	.124	-.4	-.070
230°	3.5	.624	1.3	.232	.4	.070	-.5	-.088
240°	3.3	.588	1.3	.232	0	0	-.6	-.106
250°	3.6	.642	1.4	.250	-.3	-.052	0	0
260°	3.6	.642	1.1	.196	-.5	-.088	-1.3	-.232
270°	3.2	.570	1.0	.178	-.6	-.106	-1.5	-.268
280°	3.3	.588	1.1	.196	-.8	-.142	-1.6	-.284
290°	3.4	.606	1.3	.232	-.8	-.142	-1.4	-.250
300°	3.5	.624	2.3	.410	-.4	-.070	-.7	-.124
310°	4.1	.730	3.2	.570	0	0	-.3	-.052
320°	4.6	.820	4.0	.710	.6	.106	.2	.034
330°	4.9	.874	4.3	.766	2.0	.356	1.2	.214
340°	5.4	.962	5.4	.908	3.6	.642	2.8	.500
350°	5.6	.998	5.4	.962	4.5	.802	3.2	.570
360°	5.7	1.016	5.7	1.016	4.7	.836	3.8	.676

R.T.C.  
1944.

TABLE NO. 14.

POSITION No 2C

BAROMETER 30.54 Hg.

VELOCITY 100 Ft./Sec.

HOLE No. 2

TEMPERATURE 66°F

W.T. INLET 5.9 CMS. OF WATER.

POSITION OF HOLE	1 <sup>st</sup> Row.		2 <sup>nd</sup> Row.		3 <sup>rd</sup> Row.		4 <sup>th</sup> Row.	
	CMS. OF WATER.	$\frac{p}{\rho V_0^2/2}$						
0°	5.6	.964	5.6	.964	5.0	.862	3.9	.672
10°	5.5	.948	5.4	.930	4.6	.792	3.6	.620
20°	5.3	.912	4.5	.776	3.4	.586	2.8	.482
30°	4.9	.844	3.4	.586	2.4	.414	1.7	.292
40°	4.7	.810	2.2	.378	0.8	.138	1.2	.206
50°	4.2	.724	1.4	.242	0.1	.016	.3	.050
60°	3.8	.654	1.2	.206	0	0	.1	.016
70°	3.1	.534	1.0	.172	-.2	-.034	-.2	-.034
80°	2.6	.448	1.1	.190	0	0	-.2	-.034
90°	2.6	.448	1.3	.224	.1	.016	0	0
100°	2.6	.448	1.3	.224	.1	.016	.1	.016
110°	2.6	.448	1.3	.224	.2	.034	.3	.050
120°	2.7	.464	1.2	.206	.7	.120	.4	.068
130°	2.7	.464	1.3	.224	.7	.120	.4	.068
140°	2.7	.464	1.4	.242	.8	.138	.4	.068
150°	2.7	.464	1.6	.276	1.3	.224	.6	.102
160°	2.7	.464	1.6	.276	1.3	.224	.6	.102
170°	2.7	.464	1.6	.276	1.3	.224	.6	.102
180°	2.6	.448	1.7	.327	1.5	.258	.6	.102
190°	2.6	.448	1.7	.328	1.5	.258	.6	.102
200°	2.6	.448	1.7	.328	1.5	.258	.6	.102
210°	2.6	.448	1.7	.328	1.5	.258	.6	.102
220°	2.6	.448	1.6	.276	1.5	.258	.6	.102
230°	2.6	.448	1.4	.242	1.5	.258	.6	.102
240°	2.6	.448	1.1	.190	.8	.138	.4	.068
250°	2.6	.448	1.1	.190	.8	.138	.3	.050
260°	2.6	.448	1.1	.190	.7	.120	.1	.016
270°	2.5	.430	1.2	.206	.2	.034	-.2	-.034
280°	2.5	.430	1.2	.206	.2	.034	-.2	-.034
290°	2.5	.430	1.1	.190	.2	.034	-.2	-.034
300°	2.6	.448	1.1	.190	.2	.034	-.3	-.050
310°	3.1	.534	1.2	.206	.7	.120	.1	.016
320°	3.8	.654	2.2	.378	.8	.138	.4	.068
330°	4.3	.740	3.2	.551	2.6	.448	2.3	.396
340°	4.9	.844	4.5	.776	3.4	.586	2.8	.482
350°	5.5	.948	5.4	.930	4.6	.792	3.6	.620
360°	5.6	.964	5.6	.964	5.0	.862	3.9	.672

R.T.C  
1944.

# TABLE No. 15.

POSITION No. 2C

BAROMETER 35 IN HG.

VELOCITY 100 FT/SEC.

HOLE No. 4

TEMPERATURE 66°F

W.T. INLET 5.8 CMS OF WATER

POSITION OF HOLE	1 <sup>st</sup> ROW.		2 <sup>nd</sup> ROW.		3 <sup>rd</sup> ROW.		4 <sup>th</sup> ROW.	
	CMS. OF WATER.	$\frac{p}{\rho V^2/2}$						
0°	5.5	.822	5.3	.792	5.2	.778	4.6	.688
10°	5.4	.808	5.2	.778	5.1	.762	4.5	.672
20°	5.3	.792	5.0	.748	4.6	.688	4.3	.644
30°	5.0	.748	4.4	.658	3.9	.584	3.9	.584
40°	4.6	.688	3.7	.554	3.4	.508	3.2	.480
50°	4.4	.658	3.3	.494	2.8	.420	2.9	.434
60°	4.1	.614	3.1	.464	2.7	.404	2.7	.404
70°	4.0	.598	3.0	.448	2.7	.404	2.6	.390
80°	3.9	.584	3.0	.448	2.6	.390	2.6	.390
90°	3.8	.568	3.1	.464	2.7	.404	2.6	.390
100°	3.9	.584	3.1	.464	2.8	.420	2.7	.404
110°	4.0	.598	3.3	.494	3.1	.464	2.8	.420
120°	4.1	.614	3.3	.494	3.2	.480	2.8	.420
130°	4.0	.598	3.4	.508	3.3	.494	2.9	.434
140°	4.0	.598	3.5	.524	3.3	.494	2.9	.434
150°	4.0	.598	3.6	.538	3.4	.508	2.9	.434
160°	4.0	.598	3.7	.554	3.5	.524	3.0	.448
170°	4.0	.598	3.7	.554	3.6	.538	3.0	.448
180°	4.0	.598	3.7	.554	3.5	.524	3.0	.448
190°	4.0	.598	3.7	.554	3.6	.538	3.0	.448
200°	4.0	.598	3.7	.554	3.6	.538	3.0	.448
210°	4.0	.598	3.6	.538	3.5	.524	3.1	.464
220°	4.0	.598	3.6	.538	3.5	.524	3.1	.464
230°	4.0	.598	3.5	.524	3.4	.508	3.1	.464
240°	4.0	.598	3.4	.508	3.2	.480	3.1	.464
250°	4.0	.598	3.3	.494	3.1	.464	3.1	.464
260°	4.0	.598	3.2	.480	2.9	.434	3.0	.448
270°	3.9	.584	3.2	.480	2.9	.434	2.9	.434
280°	3.8	.568	3.0	.448	2.9	.434	2.7	.404
290°	3.8	.568	2.9	.434	2.9	.434	2.7	.404
300°	4.1	.614	2.9	.434	3.0	.448	2.8	.420
310°	4.3	.644	3.0	.448	3.0	.448	2.9	.434
320°	4.6	.688	3.3	.494	3.4	.508	2.9	.434
330°	4.9	.732	3.9	.584	3.8	.568	3.3	.494
340°	5.3	.792	4.6	.688	4.6	.688	3.9	.584
350°	5.4	.808	5.2	.778	5.1	.762	4.4	.658
360°	5.5	.822	5.3	.792	5.2	.778	4.6	.688

R.T.C.  
1944.

# TABLE No 16

POSITION No 2C.

BAROMETER 30.5 IN.HG.

VELOCITY 100 FT/SEC

HOLE No 6

TEMPERATURE 68°F.

W.T. INLET 5.8 CMS OF WATER.

POSITION OF HOLE.	1 <sup>st</sup> Row		2 <sup>nd</sup> Row.		3 <sup>rd</sup> Row.		4 <sup>th</sup> Row.	
	CMS. OF WATER	$\frac{p}{\rho V_0^2/2}$	CMS. OF WATER	$\frac{p}{\rho V_0^2/2}$	CMS. OF WATER	$\frac{p}{\rho V_0^2/2}$	CMS. OF WATER	$\frac{p}{\rho V_0^2/2}$
0°	5.4	.934	5.4	.934	5.2	.900	4.8	.830
10°	5.3	.930	5.3	.920	5.2	.890	4.7	.820
20°	5.2	.910	5.1	.880	5.0	.860	4.6	.800
30°	4.9	.848	4.7	.812	4.6	.796	4.3	.774
40°	4.7	.820	4.4	.760	4.3	.750	4.3	.740
50°	4.5	.780	4.0	.700	4.0	.690	4.0	.700
60°	4.3	.744	3.9	.674	3.7	.640	3.8	.658
70°	4.2	.730	3.8	.660	3.7	.630	3.7	.640
80°	4.2	.730	3.8	.660	3.7	.630	3.7	.640
90°	4.3	.744	3.9	.674	3.6	.622	3.7	.640
100°	4.3	.744	3.9	.674	3.6	.622	3.7	.640
110°	4.3	.744	3.9	.674	3.7	.630	3.7	.640
120°	4.3	.744	3.9	.674	3.8	.658	3.6	.622
130°	4.3	.744	3.9	.674	3.8	.658	3.6	.622
140°	4.3	.744	4.0	.700	3.8	.658	3.7	.640
150°	4.3	.744	4.1	.710	3.9	.674	3.8	.658
160°	4.3	.744	4.1	.710	3.9	.674	3.8	.658
170°	4.3	.744	4.1	.710	4.0	.690	3.8	.658
180°	4.3	.744	4.2	.726	4.1	.710	3.8	.658
190°	4.3	.744	4.2	.726	4.1	.710	3.8	.658
200°	4.3	.744	4.1	.710	4.0	.690	3.8	.658
210°	4.2	.726	4.0	.692	3.9	.674	3.8	.658
220°	4.2	.726	4.0	.692	3.9	.674	3.8	.658
230°	4.2	.726	4.0	.692	3.8	.658	3.7	.640
240°	4.2	.726	3.9	.674	3.7	.640	3.6	.622
250°	4.2	.726	3.9	.674	3.7	.640	3.6	.622
260°	4.2	.726	3.9	.674	3.7	.640	3.6	.622
270°	4.1	.710	3.9	.674	3.6	.622	3.6	.622
280°	4.2	.730	3.9	.674	3.6	.622	3.6	.622
290°	4.3	.744	3.9	.674	3.6	.622	3.6	.622
300°	4.6	.796	3.8	.658	3.7	.640	3.6	.622
310°	4.7	.820	4.0	.700	4.0	.700	4.0	.700
320°	4.9	.848	4.3	.744	4.2	.730	4.2	.730
330°	5.2	.900	4.5	.778	4.5	.778	4.5	.778
340°	5.2	.900	5.1	.880	4.7	.812	4.6	.800
350°	5.3	.930	5.2	.910	4.9	.848	4.7	.820
360°	5.4	.934	5.4	.934	5.2	.900	4.8	.830

R.T.C.  
1944.

# TABLE NO 17.

POSITION No 3B — VELOCITY 100 FT/SEC.

HOLE No 2.

TEMPERATURE 63° F.

BAROMETER 30.4 IN HG.

POSITION OF HOLE.	1 <sup>st</sup> ROW		2 <sup>nd</sup> ROW		3 <sup>rd</sup> ROW		4 <sup>th</sup> ROW	
	CMS. OF WATER	$\frac{p}{\rho V_0^2/2}$	CMS. OF WATER	$\frac{p}{\rho V_0^2/2}$	CMS. OF WATER.	$\frac{p}{\rho V_0^2/2}$	CMS. OF WATER	$\frac{p}{\rho V_0^2/2}$
0°	5.6	.960	5.6	.960	5.5	.944	5.5	.944
30°	5.4	.926	5.3	.908	5.5	.944	5.4	.926
60°	5.0	.856	5.1	.874	5.2	.892	5.3	.908
90°	5.0	.856	5.1	.874	5.2	.892	5.2	.892
120°	5.0	.856	5.1	.874	5.1	.874	5.3	.908
150°	4.9	.840	5.1	.874	5.1	.874	5.3	.908
180°	5.1	.874	5.1	.874	5.1	.874	5.3	.908
210°	4.8	.824	5.0	.856	5.1	.874	5.1	.874
240°	5.0	.856	5.1	.874	5.1	.874	5.2	.892
270°	4.8	.824	5.0	.856	5.0	.856	5.0	.856
300°	4.8	.824	4.9	.840	5.0	.856	5.2	.892
330°	5.0	.856	5.3	.908	5.2	.892	5.2	.892
360°	5.6	.960	5.6	.960	5.5	.944	5.5	.944

HOLE No 4

TEMPERATURE 65° F

BAROMETER 29.9 IN HG.

0°	5.9	1.032	5.9	1.032	5.9	1.032	5.8	1.016
30°	5.8	1.016	5.7	.998	5.6	.980	5.5	.962
60°	5.5	.962	5.5	.962	5.5	.962	5.4	.944
90°	5.6	.980	5.6	.980	5.5	.962	5.5	.962
120°	5.6	.980	5.6	.980	5.6	.980	5.6	.980
150°	5.7	.998	5.7	.998	5.7	.998	5.7	.998
180°	5.6	.980	5.6	.980	5.6	.980	5.6	.980
210°	5.7	.998	5.7	.998	5.7	.998	5.7	.998
240°	5.7	.998	5.6	.980	5.5	.962	5.5	.962
270°	5.7	.998	5.7	.998	5.6	.980	5.6	.980
300°	5.6	.980	5.6	.980	5.6	.980	5.5	.962
330°	5.8	1.016	5.8	1.016	5.7	.998	5.7	.998
360°	5.9	1.032	5.9	1.032	5.9	1.032	5.8	1.016

HOLE No 6.

TEMPERATURE 69° F.

BAROMETER 29.8 IN HG.

0°	5.5	.972	5.5	.972	5.5	.972	5.5	.972
30°	5.4	.954	5.3	.936	5.4	.954	5.3	.936
60°	5.5	.972	5.5	.972	5.5	.972	5.5	.972
90°	5.3	.936	5.3	.936	5.5	.972	5.4	.954
120°	5.3	.936	5.3	.936	5.3	.936	5.3	.936
150°	5.3	.936	5.2	.918	5.3	.936	5.2	.918
180°	5.3	.936	5.3	.936	5.3	.936	5.3	.936
210°	5.2	.918	5.3	.936	5.3	.936	5.2	.918
240°	5.3	.936	5.2	.918	5.4	.954	5.3	.936
270°	5.4	.954	5.3	.936	5.3	.936	5.3	.936
300°	5.4	.954	5.3	.936	5.4	.954	5.4	.954
330°	5.3	.936	5.3	.936	5.4	.954	5.3	.936
360°	5.5	.972	5.5	.972	5.5	.972	5.5	.972

R.T.C.  
1944.

APPENDIX IV.

APPENDIX IVTabulated Results of Small High Speed Trunk Tests.

Readings for various pitches and speeds are tabulated in sixteen tables, 18 to 33. References for the different tests on single, double, three and four banks of tubes are indicated on the tables. The angle of turn in these tests is from 0 to 180 degrees by 30 degree increments.

-----

# TABLE N° 18.

TEST ON SINGLE TUBE

BARM 78.0 CMS HG.

GAUGE CMS HG.

VERTICAL

WITHOUT PAFFLE.

TUBE DIA 1/8"

TEST HOLE 1.4" ABOVE €

HOLE POSITION	NOZZLE		SINGLE ROW	TEMP DEG. F.	SPEED FT/SEC
	IN	OUT			
0°	10.0	-1.1	4.3	92.7	340
30°	"	"	3.7	"	"
60°	"	"	-1.1	"	"
90°	"	"	-4.0	"	"
120°	"	"	-3.0	"	"
150°	"	"	-3.1	"	"
180°	"	"	-3.3	"	"

TEST HOLE ON €

HOLE POSITION	NOZZLE		I ROW	TEMP DEG. F.	SPEED FT/SEC
	IN	OUT			
0°	10.0	-1.0	6.5	75.15	338
30°	"	"	3.0	"	"
60°	"	"	-5.5	"	"
90°	"	"	-5.25	"	"
120°	"	"	-4.7	"	"
150°	"	"	-4.6	"	"
180°	"	"	-4.7	"	"

TEST HOLE 1" ABOVE €

0°	10.0	-1.1	5.1	83.1	334
30°	"	"	0.85	"	"
60°	"	"	-4.7	"	"
90°	"	"	-3.2	"	"
120°	"	"	-3.2	"	"
150°	"	"	-3.0	"	"
180°	"	"	-3.3	"	"

TEST HOLE 1" BELOW €

0°	10.0	-1.15	5.7	87.5	339
30°	"	"	-0.5	"	"
60°	"	"	-5.85	"	"
90°	"	"	-4.3	"	"
120°	"	"	-4.3	"	"
150°	"	"	-4.0	"	"
180°	"	"	-4.0	"	"

TEST ON SINGLE TUBE

BARM 78.0 CMS HG

GAUGE CMS HG.

HORIZONTAL

WITHOUT BAFFLE

TUBE DIA 3/8"

TEST HOLE ON €

HOLE POSITION	NOZZLE		SINGLE ROW	TEMP DEG. F.	SPEED FT/SEC
	IN	CUT			
0°	10.0	-2.1	6.25	89.0	371
30°	"	"	1.7	"	"
60°	"	"	-4.5	"	"
90°	"	"	-4.2	"	"
120°	"	"	-2.1	"	"
150°	"	"	-2.4	"	"
180°	"	"	-2.2	"	"

# TABLE N° 19.

TEST ON SINGLE TUBE

BARM 77.5 CMS. HG

GAUGE CMS HG.

VERTICAL

WITHOUT BAFFLE.

TUBE DIA  $\frac{1}{8}$ "

HOLE POSITION	NOZZLE		SINGLE TUBE	TEMP. DEG. F	SPEED FT/SEC
	IN	OUT			
0°	10.0	-0.9	5.7	82.3	332
30°	"	"	2.5	"	"
60°	"	"	-3.0	"	"
90°	"	"	-2.8	"	"
120°	"	"	-2.8	"	"
150°	"	"	-2.8	"	"
180°	"	"	-2.75	"	"

TEST HOLE 1" ABOVE  $\epsilon$

HOLE POSITION	NOZZLE		SINGLE TUBE	TEMP. DEG. F	SPEED FT/SEC
	IN	OUT			
0°	5.0	-0.4	2.8	76.9	232.5
30°	"	"	1.15	"	"
60°	"	"	-1.5	"	"
90°	"	"	-1.5	"	"
120°	"	"	-1.5	"	"
150°	"	"	-1.5	"	"
180°	"	"	-1.5	"	"

0°	10.0	-0.7	6.4	76.3	286
30°	"	"	2.9	"	"
60°	"	"	-4.3	"	"
90°	"	"	-4.0	"	"
120°	"	"	-3.3	"	"
150°	"	"	-3.4	"	"
180°	"	"	-3.35	"	"

TEST HOLE ON  $\epsilon$

0°	5.0	-0.4	3.4	81.7	232.5
30°	"	"	1.5	"	"
60°	"	"	-1.9	"	"
90°	"	"	-1.85	"	"
120°	"	"	-1.8	"	"
150°	"	"	-1.8	"	"
180°	"	"	-1.8	"	"

0°	10.0	-1.0	5.4	87.5	345
30°	"	"	2.8	"	"
60°	"	"	-3.3	"	"
90°	"	"	-4.2	"	"
120°	"	"	-3.7	"	"
150°	"	"	-3.8	"	"
180°	"	"	-3.8	"	"

TEST HOLE 1" BELOW  $\epsilon$

0°	5.0	-0.4	2.8	82.5	237
30°	"	"	1.7	"	"
60°	"	"	-1.3	"	"
90°	"	"	-1.6	"	"
120°	"	"	-1.7	"	"
150°	"	"	-1.8	"	"
180°	"	"	-1.8	"	"

TEST ON FOUR ROWS

BARM 75.63 CMS HG.

P.  $\frac{3}{8}$ "

STAGGERED

GAUGE CMS HG.

P.  $\frac{5}{16}$ "

HOLE POSITION	NOZZLE		1 <sup>ST</sup> ROW	2 <sup>ND</sup> ROW	3 <sup>RD</sup> ROW	4 <sup>TH</sup> ROW	TEMP. DEG. F	SPEED FT/SEC
	IN	CUT						
0°	4.5	0.8	0.8	0.8	0.5	0.2	110.0	181.5
30°	"	"	0.75	0.1	0.45	0.1	"	"
60°	"	"	0.4	0	-0.2	0.1	"	"
90°	"	"	0.1	-0.1	-0.4	0	"	"
120°	"	"	0.1	-0.1	-0.4	0	"	"
150°	"	"	0.1	-0.1	-0.4	0	"	"
180°	"	"	0.1	-0.1	-0.4	0	"	"

TUBE DIA  $\frac{3}{16}$ " VERTICAL

WITHOUT BAFFLE PLATE.

RTC  
1944.

# TABLE N<sup>o</sup>20.

TEST ON SINGLE TUBE

BARM 77.5 CMS.HG.

GAUGE CMS. HG.

ANGLED (45°)

WITHOUT BAFFLE.

TUBE DIA 1/8".

HOLE POSITION	NOZZLE		SINGLE TUBE	TEMP DEG. F.	SPEED FT/SEC
	IN	OUT			
0°	10.0	-1.3	2.65	86.3	341
30°	"	"	2.35	"	"
60°	"	"	-0.2	"	"
90°	"	"	-0.6	"	"
120°	"	"	-0.6	"	"
150°	"	"	-0.5	"	"
180°	"	"	-0.5	"	"

TEST HOLE 1" ABOVE  $\phi$

HOLE POSITION	NOZZLE		SINGLE TUBE	TEMP DEG. F.	SPEED FT/SEC
	IN	OUT			
0°	5.0	-0.85	1.7	70.8	241
30°	"	"	0.9	"	"
60°	"	"	-0.4	"	"
90°	"	"	-0.6	"	"
120°	"	"	-0.6	"	"
150°	"	"	-0.6	"	"
180°	"	"	-0.6	"	"

0°	10.0	-1.5	3.9	92.6	346
30°	"	"	2.0	"	"
60°	"	"	-0.9	"	"
90°	"	"	-0.5	"	"
120°	"	"	-0.5	"	"
150°	"	"	-0.8	"	"
180°	"	"	-1.5	"	"

TEST HOLE ON  $\phi$

0°	5.0	-0.8	1.9	87.9	244
30°	"	"	1.0	"	"
60°	"	"	-0.45	"	"
90°	"	"	-0.3	"	"
120°	"	"	-0.3	"	"
150°	"	"	-0.35	"	"
180°	"	"	-0.8	"	"

0°	10.0	-1.0	3.4	67.5	334
30°	"	"	2.75	"	"
60°	"	"	-0.7	"	"
90°	"	"	-1.0	"	"
120°	"	"	-0.9	"	"
150°	"	"	-1.0	"	"
180°	"	"	-0.9	"	"

TEST HOLE 1" BELOW  $\phi$

0°	5.0	-0.6	1.5	74.7	237
30°	"	"	1.0	"	"
60°	"	"	0	"	"
90°	"	"	-0.2	"	"
120°	"	"	-0.2	"	"
150°	"	"	-0.2	"	"
180°	"	"	-0.2	"	"

TEST ON FOUR ROWS

BARM 75.44 CMS HG.

P 3/8"

STAGGERED

GAUGE CMS HG.

P 5/16"

HOLE POSITION	NOZZLE		1 <sup>ST</sup> ROW	2 <sup>ND</sup> ROW	3 <sup>RD</sup> ROW	4 <sup>TH</sup> ROW	TEMP DEG. F.	SPEED FT/SEC
	IN	OUT						
0°	4.9	0.8	2.7	2.9	0.7	0.4	74.5	253
30°	"	"	2.2	1.3	0.3	0.2	"	"
60°	"	"	0.7	-0.3	-0.3	-0.1	"	"
90°	"	"	0.1	-0.2	-0.5	-0.1	"	"
120°	"	"	0.3	-0.2	-0.5	-0.1	"	"
150°	"	"	0.3	-0.2	-0.4	-0.1	"	"
180°	"	"	0.3	-0.2	-0.4	-0.1	"	"

TUBE DIA 3/16" ANGLED (45°) WITHOUT BAFFLE PLATE.

RTC  
1944.

TABLE N° 21.

TABLE N° 22.

TEST ON TWO ROWS BARM. 76.5 CMS. HG P 3/4"  
 STAGGERED GAUGE CMS. WATER. P<sub>1</sub> 5/16"

TEST ON TWO ROWS BARM. 76.5 CMS. HG P 3/4"  
 STAGGERED GAUGE CMS. WATER. P<sub>1</sub> 5/16"

HOLE POSITION	NOZZLE		1 <sup>ST</sup> ROW	2 <sup>ND</sup> ROW	TEMP DEG. F.	SPEED FT/SEC	BAFFLE POSITION
	IN	OUT					
0°	31.5	29.0	29.8	29.8	70	63.4	CLOSED ↑
30°	"	"	28.7	26.8	"	"	
60°	"	"	27.5	23.0	"	"	
90°	"	"	26.0	23.8	"	"	
120°	"	"	24.9	23.6	"	"	
150°	"	"	25.3	23.6	"	"	
180°	"	"	25.3	23.7	"	"	

HOLE POSITION	NOZZLE		1 <sup>ST</sup> ROW	2 <sup>ND</sup> ROW	TEMP DEG. F.	SPEED FT/SEC	BAFFLE POSITION
	IN	OUT					
0°	17.0	14.5	16.2	16.2	67	63.7	CLOSED ↑
30°	"	"	15.4	14.2	"	"	
60°	"	"	13.8	12.1	"	"	
90°	"	"	13.6	12.6	"	"	
120°	"	"	13.8	12.7	"	"	
150°	"	"	13.7	12.6	"	"	
180°	"	"	13.7	12.8	"	"	

0°	15.8	13.3	14.9	14.9	70	63.8	30° ↑
30°	"	"	13.9	11.8	"	"	
60°	"	"	11.9	7.3	"	"	
90°	"	"	10.0	8.0	"	"	
120°	"	"	9.6	8.0	"	"	
150°	"	"	9.8	8.1	"	"	
180°	"	"	9.8	8.3	"	"	

0°	12.5	10.0	11.8	11.8	67	63.7	30° ↑
30°	"	"	11.0	9.9	"	"	
60°	"	"	9.5	7.8	"	"	
90°	"	"	9.1	8.1	"	"	
120°	"	"	9.2	8.1	"	"	
150°	"	"	9.2	8.1	"	"	
180°	"	"	9.3	8.2	"	"	

0°	7.3	4.8	6.2	6.2	70	64.2	60° ↑
30°	"	"	5.1	3.2	"	"	
60°	"	"	3.1	-1.5	"	"	
90°	"	"	1.7	-0.8	"	"	
120°	"	"	0.9	-0.7	"	"	
150°	"	"	1.1	-0.8	"	"	
180°	"	"	1.1	-0.5	"	"	

0°	5.0	2.5	4.1	4.1	67	64.2	60° ↑
30°	"	"	3.6	2.8	"	"	
60°	"	"	1.9	0.2	"	"	
90°	"	"	1.5	0.2	"	"	
120°	"	"	1.5	0.2	"	"	
150°	"	"	1.5	0.2	"	"	
180°	"	"	1.5	0.2	"	"	

0°	5.6	3.1	4.6	4.6	70	64.2	FULLY ↑
30°	"	"	3.9	2.0	"	"	
60°	"	"	2.3	-3.0	"	"	
90°	"	"	0.9	-2.3	"	"	
120°	"	"	0.9	-2.1	"	"	
150°	"	"	-0.6	-2.1	"	"	
180°	"	"	-0.3	-2.2	"	"	

0°	3.7	1.2	2.9	2.9	67	64.2	FULLY ↑
30°	"	"	2.1	0.7	"	"	
60°	"	"	0.6	-1.5	"	"	
90°	"	"	0.2	-1.2	"	"	
120°	"	"	0.2	-1.2	"	"	
150°	"	"	0.2	-1.2	"	"	
180°	"	"	0.2	-1.2	"	"	

TUBE DIA 3/8" HORIZONTAL WITH BAFFLE PLATE.

TABLE N<sup>o</sup> 23.

TABLE N<sup>o</sup> 24.

TEST ON TWO ROWS BARM. 76 CMS. HG P 3/4"

TEST ON TWO ROWS BARM 76 CMS HG. P 3/4"

STAGGERED GAUGE CMS WATER P<sub>i</sub> 15/16"

STAGGERED GAUGE CMS WATER P<sub>i</sub> 1/4"

HOLE POSITION	NOZZLE		1 <sup>ST</sup> ROW	2 <sup>ND</sup> ROW	TEMP DEG. F.	SPEED FT/SEC	BAFFLE POSITION
	IN	OUT					
0°	26.5	24.0	25.6	25.6	70	66.3	CLOSED ↓ //////////
30°	"	"	24.5	23.6	"	"	
60°	"	"	23.3	22.1	"	"	
90°	"	"	23.4	21.8	"	"	
120°	"	"	23.5	22.2	"	"	
150°	"	"	23.5	22.2	"	"	
180°	"	"	23.4	23.2	"	"	

HOLE POSITION	NOZZLE		1 <sup>ST</sup> ROW	2 <sup>ND</sup> ROW	TEMP DEG. F.	SPEED FT/SEC	BAFFLE POSITION
	IN	OUT					
0°	26.0	23.5	25.0	24.8	63	63.4	CLOSED ↓ //////////
30°	"	"	24.3	23.7	"	"	
60°	"	"	23.8	21.9	"	"	
90°	"	"	22.7	21.3	"	"	
120°	"	"	23.0	21.7	"	"	
150°	"	"	22.8	21.8	"	"	
180°	"	"	22.8	21.8	"	"	

0°	23.3	20.8	22.2	22.4	70	66.3	30° ////////// ↗ ////////// OPEN
30°	"	"	21.3	20.6	"	"	
60°	"	"	19.7	18.5	"	"	
90°	"	"	19.7	18.2	"	"	
120°	"	"	19.8	18.6	"	"	
150°	"	"	19.9	18.7	"	"	
180°	"	"	19.9	18.8	"	"	

0°	13.2	10.7	12.0	11.7	63	63.7	30° ////////// ↗ ////////// OPEN
30°	"	"	11.3	10.6	"	"	
60°	"	"	9.9	9.0	"	"	
90°	"	"	9.9	8.4	"	"	
120°	"	"	9.9	8.5	"	"	
150°	"	"	9.8	8.6	"	"	
180°	"	"	9.8	8.6	"	"	

0°	9.9	7.4	9.0	9.0	70	67.1	60° ////////// ↗ ////////// OPEN
30°	"	"	8.2	7.8	"	"	
60°	"	"	6.7	5.6	"	"	
90°	"	"	6.8	5.6	"	"	
120°	"	"	6.9	5.8	"	"	
150°	"	"	6.9	5.7	"	"	
180°	"	"	6.9	5.7	"	"	

0°	8.2	5.7	7.4	7.0	63	64.1	60° ////////// ↗ ////////// OPEN
30°	"	"	6.4	5.9	"	"	
60°	"	"	5.0	4.0	"	"	
90°	"	"	5.0	3.1	"	"	
120°	"	"	5.0	3.2	"	"	
150°	"	"	4.9	3.2	"	"	
180°	"	"	4.9	3.6	"	"	

0°	3.7	1.2	2.8	2.8	70	67.2	FULLY ////////// ↔ ////////// OPEN
30°	"	"	1.9	1.0	"	"	
60°	"	"	0.5	-1.0	"	"	
90°	"	"	0.5	-1.0	"	"	
120°	"	"	0.5	-1.0	"	"	
150°	"	"	0.5	-0.9	"	"	
180°	"	"	0.6	-0.8	"	"	

0°	3.7	1.2	2.7	2.2	63	64.2	FULLY ////////// ↔ ////////// OPEN
30°	"	"	1.8	1.2	"	"	
60°	"	"	0.5	-0.3	"	"	
90°	"	"	0.4	-1.5	"	"	
120°	"	"	0.4	-1.3	"	"	
150°	"	"	0.3	-1.2	"	"	
180°	"	"	0.3	-1.1	"	"	

TUBE DIA. 3/8" HORIZONTAL WITH BAFFLE PLATE.

# TABLE N<sup>o</sup> 25.

TEST ON TWO ROWS

BARM 75.6 CMS 116

P  $\frac{3}{4}$ "

CHAIN

GAUGE CMS WATER

P<sub>1</sub>  $\frac{5}{8}$ "

HOLE POSITION	NOZZLE		1 <sup>ST</sup> ROW	2 <sup>ND</sup> ROW	TEMP DEG. F.	SPEED FT/SEC.
	IN	OUT				
0°	5.0	0.9	3.5	-1.3	60.5	82
30°	"	"	2.0	-1.3	"	"
60°	"	"	0.15	0	"	"
90°	"	"	-2.0	-2.4	"	"
120°	"	"	-1.5	-1.3	"	"
150°	"	"	-1.6	-1.0	"	"
180°	"	"	-1.3	-1.0	"	"

P<sub>1</sub>  $\frac{1}{4}$ "

0°		1.1	3.8	2.0	61.5	77
30°	"	"	2.5	1.5	"	"
60°	"	"	-0.3	-1.3	"	"
90°	"	"	-1.2	-3.2	"	"
120°	"	"	-0.3	-2.1	"	"
150°	"	"	-0.3	-1.7	"	"
180°	"	"	-0.3	-1.6	"	"

P<sub>1</sub>  $\frac{1}{8}$ "

0°	4.9	0.9	3.5	1.5	66.5	81.5
30°	"	"	1.35	0.85	"	"
60°	"	"	1.35	-1.35	"	"
90°	"	"	-1.5	-2.4	"	"
120°	"	"	-0.7	-1.2	"	"
150°	"	"	-0.7	-0.8	"	"
180°	"	"	-0.65	-0.75	"	"

P<sub>1</sub>  $2\frac{1}{2}$ "

0°	4.85	0.75	3.45	1.6	68.0	82.7
30°	"	"	1.9	0.9	"	"
60°	"	"	-0.9	-0.9	"	"
90°	"	"	-1.45	-2.0	"	"
120°	"	"	-0.85	-1.35	"	"
150°	"	"	-0.9	-0.9	"	"
180°	"	"	-0.9	-0.8	"	"

TUBE DIA  $\frac{3}{8}$ " HORIZONTAL

WITHOUT BAFFLE PLATE

RTC  
1944.

TABLE N<sup>o</sup>26.

TABLE N<sup>o</sup>27.

TEST ON ONE ROW BARM 75.49 CMS HG. P 3/4"

TEST ON TWO ROWS BARM 75.49 CMS HG. P 3/4"

GAUGE CMS WATER.

STAGGERED

GAUGE CMS WATER.

Pi 5/8"

HOLE POSITION	NOZZLE		SINGLE ROW.	TEMP DEG. F	SPEED FT/SEC	BAFFLE POSITION
	IN	OUT				
0°	30.0	26.0	28.5	73.0	81.0	CLOSED ↓ OPEN
30°	"	"	27.5	"	"	
60°	"	"	24.3	"	"	
90°	"	"	24.0	"	"	
120°	"	"	23.8	"	"	
150°	"	"	23.8	"	"	
180°	"	"	23.8	"	"	

HOLE POSITION	NOZZLE		1 <sup>ST</sup> ROW	2 <sup>ND</sup> ROW	TEMP DEG. F	SPEED FT/SEC	BAFFLE POSITION
	IN	OUT					
0°	31.7	27.7	31.0	31.0	73.0	80.4	CLOSED ↓ OPEN
30°	"	"	29.6	27.1	"	"	
60°	"	"	26.3	22.6	"	"	
90°	"	"	25.2	23.4	"	"	
120°	"	"	25.4	23.4	"	"	
150°	"	"	25.3	23.3	"	"	
180°	"	"	25.3	23.4	"	"	

0°	22.7	18.7	21.0	73.0	81.5	30° ↓ OPEN
30°	"	"	19.2	"	"	
60°	"	"	15.9	"	"	
90°	"	"	15.6	"	"	
120°	"	"	16.0	"	"	
150°	"	"	16.0	"	"	
180°	"	"	16.1	"	"	

0°	21.0	17.0	20.7	20.7	73.0	80.1	30° ↓ OPEN
30°	"	"	19.4	16.9	"	"	
60°	"	"	16.1	12.6	"	"	
90°	"	"	15.0	13.3	"	"	
120°	"	"	15.1	13.2	"	"	
150°	"	"	15.1	13.2	"	"	
180°	"	"	15.1	13.3	"	"	

0°	6.8	2.8	5.5	73.0	82.0	60° ↓ OPEN
30°	"	"	4.1	"	"	
60°	"	"	0.9	"	"	
90°	"	"	0.6	"	"	
120°	"	"	0.3	"	"	
150°	"	"	0.2	"	"	
180°	"	"	0.2	"	"	

0°	9.1	5.1	7.8	7.8	73.0	81.8	60° ↓ OPEN
30°	"	"	7.0	3.9	"	"	
60°	"	"	3.8	-0.3	"	"	
90°	"	"	2.8	0.6	"	"	
120°	"	"	2.9	0.5	"	"	
150°	"	"	2.9	0.6	"	"	
180°	"	"	3.0	0.9	"	"	

0°	5.2	1.2	3.5	73.0	82.0	FULLY ↓ OPEN.
30°	"	"	2.6	"	"	
60°	"	"	-0.3	"	"	
90°	"	"	-1.3	"	"	
120°	"	"	-1.0	"	"	
150°	"	"	-1.2	"	"	
180°	"	"	-1.5	"	"	

0°	6.5	2.5	5.2	5.2	73.0	82.0	FULLY ↓ OPEN.
30°	"	"	4.2	1.0	"	"	
60°	"	"	1.0	-2.8	"	"	
90°	"	"	0.2	-1.8	"	"	
120°	"	"	0.2	-1.8	"	"	
150°	"	"	0.2	-1.8	"	"	
180°	"	"	0.3	-1.5	"	"	

TUBE DIA. 3/8" HORIZONTAL WITH BAFFLE PLATE.

# TABLE No 28.

TEST ON THREE ROWS

BARM 75.49 CMS. HG.

P 3/4"

STAGGERED

GAUGE CMS WATER.

P 5/8"

HOLE POSITION	NOZZLE		1 <sup>ST</sup>	2 <sup>ND</sup>	3 <sup>RD</sup>	TEMP	SPEED	BAFFLE POSITION
	IN	OUT	Row	Row	Row	DEG F	FT/SEC	
0°	33.0	29.0	32.5	32.5	30.8	73.5	81.0	CLOSED 
30°	"	"	30.9	28.5	26.8	"	"	
60°	"	"	27.7	24.0	22.1	"	"	
90°	"	"	26.5	24.6	22.0	"	"	
120°	"	"	26.6	24.6	23.0	"	"	
150°	"	"	26.4	24.3	23.7	"	"	
180°	"	"	26.4	24.4	23.8	"	"	

0°	22.0	18.0	20.5	20.5	18.8	73.5	81.5	30° 
30°	"	"	19.3	16.6	15.1	"	"	
60°	"	"	16.5	12.7	11.1	"	"	
90°	"	"	15.6	13.6	11.1	"	"	
120°	"	"	15.8	13.5	12.1	"	"	
150°	"	"	15.8	13.7	13.1	"	"	
180°	"	"	15.8	13.7	13.1	"	"	

0°	11.3	7.2	9.8	9.8	8.1	73.5	81.7	60° 
30°	"	"	8.8	5.5	3.5	"	"	
60°	"	"	5.7	1.1	-0.9	"	"	
90°	"	"	4.5	1.9	-0.9	"	"	
120°	"	"	4.6	1.9	0.9	"	"	
150°	"	"	4.6	1.9	1.3	"	"	
180°	"	"	4.8	2.4	1.6	"	"	

0°	7.7	3.7	7.1	7.1	5.2	73.5	82.2	FULLY 
30°	"	"	5.4	2.6	0.8	"	"	
60°	"	"	2.0	-2.1	-3.8	"	"	
90°	"	"	1.0	-1.4	-3.9	"	"	
120°	"	"	1.0	-1.4	-2.9	"	"	
150°	"	"	1.2	-1.0	-1.7	"	"	
180°	"	"	1.3	-0.8	-1.5	"	"	

TUBE DIA 3/8" HORIZONTAL WITH BAFFLE PLATE.

RTC  
1944.

# TABLE N° 29.

TEST ON FOUR ROWS

BARM. 75.49 Cms Hg.

P. 3/4"

STAGGERED

GAUGE Cms WATER

P. 5/8"

HOLE POSITION	NOZZLE		1 <sup>ST</sup> Row	2 <sup>ND</sup> Row	3 <sup>RD</sup> Row	4 <sup>TH</sup> Row	TEMP DEG F	SPEED FT/SEC	BAFFLE POSITION
	IN	OUT							
0°	28.5	24.5	39.3	39.3	37.6	36.2	69.0	81.0	CLOSED 
30°	"	"	38.0	36.5	34.0	32.0	"	"	
60°	"	"	35.0	30.8	28.8	28.7	"	"	
90°	"	"	33.8	31.7	29.4	28.7	"	"	
120°	"	"	34.1	31.6	30.7	30.0	"	"	
150°	"	"	33.6	31.3	31.0	30.0	"	"	
180°	"	"	33.6	31.4	31.0	30.0	"	"	

0°	27.0	23.0	26.0	26.0	24.4	22.9	70.0	81.0	30° 
30°	"	"	24.9	22.0	19.6	19.1	"	"	
60°	"	"	21.2	17.3	15.4	15.3	"	"	
90°	"	"	20.6	18.1	15.9	15.4	"	"	
120°	"	"	20.5	18.1	17.2	16.8	"	"	
150°	"	"	20.6	18.2	17.9	17.0	"	"	
180°	"	"	20.6	18.4	18.0	17.0	"	"	

0°	10.4	6.6	9.3	9.3	8.8	6.1	70.5	81.8	60° 
30°	"	"	8.0	5.0	3.5	2.8	"	"	
60°	"	"	5.0	1.0	-0.9	-1.0	"	"	
90°	"	"	4.1	1.9	-0.3	-0.9	"	"	
120°	"	"	4.3	2.0	1.1	0.6	"	"	
150°	"	"	4.3	2.0	1.7	0.9	"	"	
180°	"	"	4.4	2.3	2.0	1.0	"	"	

0°	8.5	4.5	7.5	7.5	5.8	4.2	70.1	82.0	FULLY. 
30°	"	"	6.2	3.3	1.0	0.6	"	"	
60°	"	"	3.0	-1.1	-3.0	-3.0	"	"	
90°	"	"	2.0	-0.2	-2.4	-3.0	"	"	
120°	"	"	2.4	0	-0.9	-1.6	"	"	
150°	"	"	2.3	0	-0.4	-1.2	"	"	
180°	"	"	2.1	0.1	-0.2	-1.2	"	"	

TUBE DIA 3/8" HORIZONTAL WITH BAFFLE PLATE.

RTC  
1944.

# TABLE N<sup>o</sup> 30.

TEST ON FOUR ROWS

BARM 75.16 CMS. HG.

P 3/4"

CHAIN.

GAUGE CMS. HG.

P<sub>1</sub> 1/4"

HOLE POSITION	NOZZLE		1 <sup>ST</sup>	2 <sup>ND</sup>	3 <sup>RD</sup>	4 <sup>TH</sup>	TEMP	SPEED
	IN	OUT	Row	Row	Row	Row	DEG F	FT/SEC
0°	11.0	6.15	9.2	5.0	4.7	3.2	58.0	317
30°	"	"	7.2	4.2	3.7	2.0	"	"
60°	"	"	3.1	0.6	-0.4	-2.0	"	"
90°	"	"	0.65	-0.19	-3.5	-5.5	"	"
120°	"	"	2.0	0	-1.8	-3.15	"	"
150°	"	"	1.65	1.15	-0.2	-1.9	"	"
180°	"	"	1.6	1.2	-0.15	-1.9	"	"

BARM 75.16 CMS. HG.

GAUGE CMS. HG.

0°	8.0	4.5	6.8	3.65	3.4	2.4	60.0	273
30°	"	"	4.7	2.9	2.4	1.5	"	"
60°	"	"	1.15	0	-1.0	-1.9	"	"
90°	"	"	0.6	-1.5	-2.7	-4.15	"	"
120°	"	"	1.15	0.4	-0.8	-1.9	"	"
150°	"	"	1.1	0.8	-0.2	-1.5	"	"
180°	"	"	1.1	0.8	-0.15	-1.5	"	"

BARM 74.92 CMS. HG.

GAUGE CMS. HG.

0°	4.5	2.25	3.65	1.9	1.8	1.2	60.5	228
30°	"	"	2.5	1.5	1.2	0.7	"	"
60°	"	"	0.85	0.4	0.2	-0.8	"	"
90°	"	"	0.55	-0.5	-1.2	-2.85	"	"
120°	"	"	0.7	0	-0.75	-1.25	"	"
150°	"	"	0.55	0.25	-0.75	-1.0	"	"
180°	"	"	0.5	0.3	-0.2	-0.95	"	"

BARM 75.16 CMS. HG.

GAUGE CMS. WATER.

0°	26.7	14.8	23.0	12.8	11.5	7.3	64.0	140
30°	"	"	16.4	10.0	8.0	3.5	"	"
60°	"	"	6.0	2.7	0	-4.9	"	"
90°	"	"	4.15	-2.0	-6.3	-10.8	"	"
120°	"	"	5.3	1.9	-2.3	-6.1	"	"
150°	"	"	4.6	3.0	-0.4	-4.9	"	"
180°	"	"	4.6	3.3	0	-4.5	"	"

TUBE DIA 3/8" HORIZONTAL WITHOUT BAFFLE PLATE.

RTC  
1944.

# TABLE No 31.

TEST ON FOUR ROWS

BARM 75.16 CMS HG

P. 3/4"

CHAIN

GAUGE CMS WATER.

P. 1/4"

HOLE POSITION	NOZZLE		1 <sup>ST</sup>	2 <sup>ND</sup>	3 <sup>RD</sup>	4 <sup>TH</sup>	TEMP	SPEED
	IN	OUT	ROW	ROW	ROW	ROW	DEG F.	FT/SEC
0°	16.0	9.0	13.8	8.0	7.0	4.3	64.5	108
30°	"	"	10.5	6.7	4.8	3.0	"	"
60°	"	"	4.0	1.5	-0.8	-2.8	"	"
90°	"	"	3.0	-0.5	-3.2	-5.8	"	"
120°	"	"	3.6	1.4	-1.1	-3.8	"	"
150°	"	"	3.2	1.8	-0.3	-3.0	"	"
180°	"	"	3.0	2.0	0	-3.0	"	"

BARM 75.16 CMS HG.

GAUGE CMS HG.

P. 5/8"

0°	8.0	3.5	6.5	-1.2	0.3	0	71.0	313
30°	"	"	4.6	-0.3	0.65	1.05	"	"
60°	"	"	0.7	-0.15	-0.5	-1.2	"	"
90°	"	"	-1.0	-1.5	-3.1	-5.0	"	"
120°	"	"	-0.25	-0.5	-1.5	-2.8	"	"
150°	"	"	-0.2	-0.15	-1.0	-1.85	"	"
180°	"	"	-0.8	0	-1.0	-1.75	"	"

BARM 74.92 CMS HG.

GAUGE CMS HG.

P. 5/8"

0°	4.5	1.65	3.6	-1.1	-0.1	-0.3	60.5	250
30°	"	"	2.5	-0.5	0	-0.15	"	"
60°	"	"	0.15	-0.3	0	-0.25	"	"
90°	"	"	-0.45	-0.8	-2.75	-2.8	"	"
120°	"	"	-0.4	-0.5	-1.0	-1.85	"	"
150°	"	"	-0.4	-0.4	-0.7	-1.2	"	"
180°	"	"	-0.8	-0.3	-0.65	-1.15	"	"

STAGGERED. BARM. 70.5 CMS HG.

GAUGE CMS HG.

P. 5/8"

0°	5.0	2.3	4.3	4.2	3.5	2.35	58.0	250
30°	"	"	3.3	1.35	1.3	0.5	"	"
60°	"	"	1.2	1.15	-1.75	-2.15	"	"
90°	"	"	0.65	-0.75	-2.3	-2.65	"	"
120°	"	"	0.1	-0.35	-1.0	-1.2	"	"
150°	"	"	0.95	-0.3	-0.4	-1.0	"	"
180°	"	"	1.0	-0.15	-0.35	-0.95	"	"

TUBE DIA 3/8" HORIZONTAL

WITHOUT BAFFLE PLATE.

RTC  
1944.

# TABLE No 32.

TEST ON FOUR ROWS

BARM. 70.5 CMS HG.

P  $\frac{3}{4}$ "

STAGGERED

GAUGE CMS HG.

P  $\frac{5}{16}$ "

HOLE POSITION	NOZZLE		1 <sup>ST</sup> Row	2 <sup>ND</sup> Row	3 <sup>RD</sup> Row	4 <sup>TH</sup> Row	TEMP DEG F.	SPEED FT/SEC.
	IN	OUT						
0°	6.4	4.5	5.8	5.8	3.75	2.6	73.0	209.5
30°	"	"	5.2	3.5	2.5	1.2	"	"
60°	"	"	4.2	-0.15	-1.9	-3.3	"	"
90°	"	"	2.0	-1.9	-3.4	-2.9	"	"
120°	"	"	1.2	-1.25	-3.9	-1.1	"	"
150°	"	"	1.35	-1.0	-1.9	-1.1	"	"
180°	"	"	2.0	-0.5	-1.35	-1.1	"	"

P  $\frac{5}{8}$ "

0°	6.6	3.0	5.5	5.5	4.2	3.0	69.0	290
30°	"	"	5.4	1.7	1.6	0.8	"	"
60°	"	"	1.3	-1.3	-2.45	-3.0	"	"
90°	"	"	0.6	-1.5	-3.3	-4.0	"	"
120°	"	"	1.1	-0.45	-1.5	-1.9	"	"
150°	"	"	1.1	-0.35	-0.65	-1.3	"	"
180°	"	"	1.2	-0.25	-0.65	-1.3	"	"

P  $\frac{15}{16}$ "

0°	6.5	3.0	5.4	4.95	4.0	2.75	73.0	287.5
30°	"	"	4.0	2.8	2.1	1.5	"	"
60°	"	"	1.5	-0.2	-0.85	-2.25	"	"
90°	"	"	0.6	-1.65	-2.4	-3.5	"	"
120°	"	"	1.3	-0.3	-0.2	-1.3	"	"
150°	"	"	1.25	0.1	0.1	-1.0	"	"
180°	"	"	1.25	0.25	0.15	-1.0	"	"

P  $1\frac{1}{4}$ "

0°	6.2	2.8	5.35	4.4	3.4	2.5	69.0	282
30°	"	"	3.7	2.7	2.1	1.25	"	"
60°	"	"	1.65	0.1	0.55	-1.5	"	"
90°	"	"	0.95	-1.4	-1.7	-3.0	"	"
120°	"	"	1.25	-0.9	-0.5	-2.0	"	"
150°	"	"	1.25	0.1	0.1	-1.3	"	"
180°	"	"	1.2	0.2	0.1	-1.2	"	"

TUBE DIA  $\frac{3}{8}$ " HORIZONTAL

WITHOUT BAFFLE PLATE.

RTC  
1944.

# TABLE No 33.

TEST ON FOUR ROWS

BARM 75.16 CMS HG

P  $\frac{3}{4}$ "

CHAIN

GAUGE CMS WATER.

P<sub>i</sub>  $\frac{5}{8}$ "

HOLE POSITION	NOZZLE		1 <sup>ST</sup>	2 <sup>ND</sup>	3 <sup>RD</sup>	4 <sup>TH</sup>	TEMP	SPEED
	IN	OUT	ROW	ROW	ROW	ROW	DEG F	FT/SEC
0°	10.5	4.0	8.3	-2.4	-1.0	-1.2	72.0	105
30°	"	"	5.2	-1.0	0.5	0.1	"	"
60°	"	"	-0.5	-1.3	0.1	0	"	"
90°	"	"	-0.7	-2.4	-3.0	-4.4	"	"
120°	"	"	-0.6	-1.7	-2.0	-3.3	"	"
150°	"	"	-0.5	-1.2	-1.8	-2.8	"	"
180°	"	"	-1.4	-1.0	-1.5	-2.6	"	"

GAUGE CMS HG

P<sub>i</sub>  $\frac{15}{16}$ "

0°	11.0	6.5	9.0	3.5	4.25	2.7	69.5	300
30°	"	"	6.2	3.7	3.5	1.7	"	"
60°	"	"	2.5	2.15	0.15	-0.9	"	"
90°	"	"	-0.4	-0.9	-2.9	-4.35	"	"
120°	"	"	1.7	-0.35	-2.2	-3.6	"	"
150°	"	"	1.3	0.5	-0.55	-2.1	"	"
180°	"	"	0.8	0.2	-0.7	-2.1	"	"

GAUGE CMS HG

P<sub>i</sub>  $\frac{15}{16}$ "

0°	8.0	4.5	6.7	2.1	3.1	2.2	71.5	275.5
30°	"	"	4.0	2.6	2.8	1.6	"	"
60°	"	"	0.4	0.3	-1.1	-2.2	"	"
90°	"	"	0.5	-1.2	-3.2	-4.5	"	"
120°	"	"	1.0	0.1	-1.0	-2.25	"	"
150°	"	"	1.0	0.6	-0.4	-1.6	"	"
180°	"	"	0.9	0.5	-0.35	-1.5	"	"

GAUGE CMS HG.

P<sub>i</sub>  $\frac{1}{4}$ "

0°	8.0	4.5	6.8	3.65	3.4	2.4	60.0	268
30°	"	"	4.7	2.9	2.4	1.5	"	"
60°	"	"	1.15	0	-1.0	-1.9	"	"
90°	"	"	0.6	-1.5	-2.7	-4.15	"	"
120°	"	"	1.15	0.4	-0.8	-1.9	"	"
150°	"	"	1.1	0.8	-0.2	-1.5	"	"
180°	"	"	1.1	0.8	-0.15	-1.5	"	"

TUBE DIA  $\frac{3}{8}$ " HORIZONTAL WITHOUT BAFFLE PLATE

RTC  
1944.

- | No.  | AUTHOR.                            | TITLE, ETC.  |
|------|------------------------------------|--|
| 1.   | Addison, H.                        | Hydraulic Measurements.  |
| 2.   | Bailey, A., and Woods, S.A.        | Conversion of the Stanton 3 inch high speed wind tunnel to the open jet type (with an appendix on an approximate graphical construction for the profile of a nozzle to give a parallel jet with a speed greater than that of sound). 1937. Vol.135, p.445. |
| 3.   | Bairstow, L.                       | Skin friction, Jour.Roy.Aero.Soc.1925.   |
| 4.   | Bairstow, L.                       | The boundary layer and recent development. Jour.Roy.Aero.Soc.1936.   |
| 5.   | Chilton, T.H., and Genereaux, R.P. | Pressure drop across tube banks. Contribution No.127 from the Experimental Station E.1, du Pont de Nemours & Co.   |
| 6.   | Clark, K.W.                        | Methods of visualising air flow, R&M. 1552, 1933.  |
| 7.   | Cope, W.F.                         | Friction and heat transmission coefficients, 1937, Vol.137, p.165, and Proc. 1941, vol.145 146.  |
| 8.   | Dryden, H.L.                       | Air flow in the boundary layer near a plate. N.A.C.A. Report 562, 1936.  |
| 9.   | Fage, A.                           | Determination of the pressure distribution round a cylinder. R&M.106, 1913-14.   |
| 10.  | Fage, A., and Johansen, F.C.       | The structure of vortex sheets. Phil.Mag. 1928, Vol.5.   |
| 11.  | Fage, A.                           | The Air-flow around a circular cylinder in the region where the boundary layer separates from the surface, R&M. 1179.  |
| 12.  | Fage A. and Warsap, J.H.           | The effects of turbulence and surface roughness on the drag of a circular cylinder. R & M. 1283. 1929.   |
| 13./ |                                    |  |

- | No.  | AUTHOR.                     | TITLE, ETC.   |
|------|-----------------------------|---|
| 13.  | Fage, A., and Falkner, V.M. | An experimental determination of the intensity of friction on the surface of an aerofoil. R & M. 1315. 1930.  |
| 14.  | Fage, A.                    | Drag of circular cylinders and spheres. R & M. 1370. 1930.  |
| 15.  | Fage, A.                    | Frictional drag of flat plates below the critical reynolds number. R & M. 1580. 1933.   |
| 16.  | Farren, W.S.                | Experiments in which air flow is made visible with the white smoke from titanium tetrachloride. Jour.Roy.Aero. Soc.1932.  |
| 17.  | Glauert, H.                 | The characteristics of a Karman vortex street in a channel of finite breadth. R & M. 1151, 1928-29. Vol.1.  |
| 18.  | Green, J.J.                 | Viscous layer associated with a circular cylinder. R & M. 1313. 1930.   |
| 19.  | Green, J.J.                 | Breakaway of boundary layer on a cylinder and an aerofoil, R & M. 1396. 1930.   |
| 20.  | Grimson, E.D.               | Correlation and utilization of new data on flow resistance and heat transfers for cross flow of gases over tube banks. A.S.M.E. (Trans.)1937?                                   |
| 21.  | Howarth, L.                 | Steady flow in the boundary layer near the surface of a cylinder in a stream. R & M. 1632, 1934.  |
| 22.  | Huge, E.C.                  | Experimental investigation of effects of equipment size on convection heat transfer and flow resistance in cross flow of gases over tube banks. A.S.M.E. (Trans.) 1937, Vol.59. |
| 23./ |                             |   |

- | No. | AUTHOR.                             | TITLE, ETC.   |
|-----|-------------------------------------|---|
| 23. | Karman, Th.V.,                      | Turbulence and skin friction.<br>Jour. Ac. Sc. Vol.1. 1934.   |
| 24. | Lander, C.H.,                       | Review of recent progress in heat<br>transfer. Proc. 1942. Vol.148.<br>p.81.  |
| 25. | McIntyre, J.I.,                     | Heat transmission in surface feed<br>heaters. Journal of the R.T.C.,<br>Vol. 2, Part 2, 1930.   |
| 26. | Mathieson, R.,                      | Experimental lift distribution<br>across the span of a stalled<br>rectangular aerofoil.   |
| 27. | Morley, T.B.,                       | Flow of air through nozzles.<br>1916. P.51.   |
| 28. | Nisi, H., and<br>Porter, A.W.,      | On eddies in air. Phil.Mag. Vol.49.<br>1923.  |
| 29. | Ower, E., and<br>Johansen, F.C.,    | The design of Pitot-static tubes.<br>R & M. 981. 1925.  |
| 30. | Parr, H.L.,                         | Fluid-flow analyzer. A.S.M.E. 1937.<br>Vol. 59.   |
| 31. | Piercy, N.A.V.,                     | Aerodynamics. 1937.   |
| 32. | Pierson, O.L.,                      | Experimental investigation of the<br>influence of tube arrangement on<br>convection heat transfer and flow<br>resistance in cross flow of gases<br>over tube banks. A.S.M.E. (Trans.).<br>1937. Vol.59. |
| 33. | Powell, W.,                         | Mechanics of Liquids.   |
| 34. | Prandtl, L., and<br>Tietjens, O.G., | Applied Hydro and Aeromechanics,<br>1934.   |
| 35. | Reynolds, O.,                       | Colour bands in water. Phil.Trans.A.<br>Roy.Soc. 1883.  |
| 36. | Schack, Goldschmidt,<br>Partridge.  | Industrial heat transfer.   |

- | No. | AUTHOR.                           | TITLE, ETC.  |
|-----|-----------------------------------|--|
| 37. | Schaub, Von Otto                  | New aspects of the theory of liquid streams. (Zur Theorie der Flüssigkeitsströmungen) Biel. 1943.                            |
| 38. | Simmons, L.F.G., & Dewey, N.S.,   | Wind tunnel experiments with circular discs. R & M. 1334, 1930.  |
| 39. | Simmons, L.F.G., & Dewey, N.S.,   | Smoke photographs of turbulent flow in boundary layer. R & M. 1335. 1930-31.   |
| 40. | Simmons, L.F.G., & Brown, A.F.C., | Experimental investigation of boundary layer flow. R & M. 1547. 1934.  |
| 41. | Small, J.,                        | Heat transmission rates round a tube in a transverse current of fluid. Engineering, Vol.132. 1931.                           |
| 42. | Squire, H.B., and Young, A.D.,    | The calculation of the profile drag of aerofoils. R & M. 1838. 1937.   |
| 43. | Stanton, T.E.,                    | On the effect of air compression on drag and pressure distribution in cylinders of infinite aspect ratio. R & M. 1210. 1928. |
| 44. | Taylor, G.I.,                     | On the dissipation of eddies R & M. 598. 1918-19.  |
| 45. | Taylor, G.I.,                     | The flow of air at high speeds past curved surfaces. R & M. 1381. 1930.  |
| 46. | Thom, A.,                         | The boundary layer of the front portion of a cylinder. R & M. 1176. 1928.  |

47/

No.	AUTHOR.	TITLES, ETC.
47.	Thom, A.	An investigation of fluid flow in two dimensions. R & M. 1194.1928-29.
48.	Thom, A.	The pressure on the front generator of a cylinder. R & M. 1389. 1930.
49.	Thom, A.	Flow past circular cylinders at low speeds. R & M. 1539. 1932.
50.	Tomotika, S.	The laminar boundary layer on the surface of a sphere in a uniform stream. R & M. 1678. 1935.
51.	Townend, H.C.H.	On rendering air flow visible by means of hot wires. R & M. 1349.
52.	Wallis, R.P.	Photographic study of fluid flow between banks of tubes. Proc.1939. Vol.142, p.379.
53.	Wallis, R.P., & White, C.M.	Resistance to Flow through rests of tubes. Engineering, Vol.146, 1938.
54.	Webb, H.A.	The decay of eddies. R & M. 609. 1918-19.
55.	White, C.M.	Fluid friction and its relation to heat transfer. Inst.Chem. Eng. 1932. Vol.10.
56.	Whittaker & Robinson.	The calculus of observations.
57.	Ahlborn, F.	Abhandlungen aus dem Gebit der Naturwissenschaften. Vol.17. 1902.
58.	Lamb, H.	Hydrodynamics.